The hydraulics of steep streams

Lee, A. J.
University of Sheffield

submitted for the degree of Doctor of Philosophy
September 1998

CONTAINS PULLOUT

Acknowledgements

This thesis could not have been completed with the help of many people. I am especially grateful to:

My supervisor, Rob Ferguson, for help and guidance at every stage of the research,

David Knighton for his useful comments during the research design stage,

Michele Dimes, my A-Level Geography teacher, for interesting me enough in Physical Geography for me to want to study it further,

Marcus Crabbe, for proof-reading this thesis, and providing encouragement,

My parents, for giving me indirect support at every stage.

I was assisted with the fieldwork part of the research by Charlotte Bennett, Rachael Dils, Andrew Hodkinson and Adrian Lane. I am very grateful to them for all their help, patience and muscles.

I am also grateful to the following landowners for allowing me access to the fieldsites: The Forestry Commission, Severn Trent Water, The Natural Trust and Mr. Andrew Crichlow.

Abstract

This thesis describes research carried out to study steep streams. Step-pool sequences, a typical feature of such streams, were found to occur on every steep stream studied in the field. The most important control on the spacing of the steps was width. Flume experiments produced steps (at an average Froude number of 0.88), and showed that the presence of steps increased resistance to flow at lower than step-forming flow and decreased resistance at above step-forming flows. In the field, flow resistance was found to be controlled by sediment characteristics and the amount of step protrusion. The hydraulic geometry of the steep streams was also studied, and was found to differ considerably from hydraulic geometry characteristics of lowland streams.

The formation of steps and pools was not found to be related to antidune processes; rather they were built up individually as large particles captured other large particles that had been entrained by the near critical flow. It was concluded that it is not the absolute values of slope and discharge that determines whether steps form. Near critical flow and high relative roughness appear to be the only requirements necessary.

Previous equations were generally found to perform poorly when used with the experimental data, and an attempt to model the velocity profile using sediment characteristics and considering stresses on the flow also produced poor correlation with the actual field data. Modifications to these were made with some success, especially in the ability to predict friction factor based on relative roughness using D_{84}. Flume velocity profiles identified characteristic velocity profiles at different locations within the step-pool sequence and the presence 'S-shaped' profiles downstream of the step.

Table of contents

Appendices

Notation

Symbols used frequently during the course of the thesis are simply defined; where a symbol is used mainly for a specific equation or section in the thesis, this location is noted.

a	intercept for hydraulic geometry discharge/width relationship (Section 2.7.3)
A	coefficient used for 'law of the wall' equation (Section 2.5.2)
A_F	frontal cross section of object (Equation 2.20)
A_{bed}	area of the bed (Equation 2.21)
A_{TA}	bed-parallel, planar area affected by an object (Equation 10.5)
b	exponent for hydraulic geometry discharge/width relationship (Section 2.7.3)
B	value representing boundary condition for 'law of the wall' equation (Equation 2.13)
B_S	step width (Equation 2.22)
c	intercept for hydraulic geometry discharge/depth relationship (Section 2.7.3)
c_b	maximum concentration of sediment on the bed (Section 10.3.2)
c_m	proportion of sediment fraction *m* in the sediment distribution (Section 10.3.1)
C_r	measure of channel roughness characteristics (Equation 2.15)
C	Chezy resistance coefficient (Equation 2.11)
C_1	constant (Equation 2.1)
C_2	constant (Equation 2.1)
C_D	drag coefficient
d	flow depth
d_{bl}	boundary layer thickness (Equation 2.14)
D	effective roughness height of bed material
D_F	drag force (Equation 2.20)
D_{FS}	drag force created by a step (Equation 2.22)
D_m	sediment of size *m*
D_n	size of the bed material (median axis) which is larger than *n*% of the material
D_x	sediment size in direction of x axis
D_y	sediment size in direction of y axis
D_z	sediment size in direction of z axis
e	roughness spacing measure (Section 2.7.2)
E	energy (Equation 10.1)
f	Darcy Weisbach resistance coefficient (Equation 2.9)
F_D	drag force on an object

Fr	Froude number (Equation 2.4)
g	gravitational acceleration
h	step height (Equation 2.22)
i	smallest size sediment present at height z
i_S	sediment size (z axis) equal to the water depth
j	exponent for hydraulic geometry discharge/depth relationship
k	1. intercept for hydraulic geometry discharge/velocity relationship 2. object height (used for calculation of Reynolds number - Equation 2.25)
kd	Wave number
k_S	roughness height (Section 2.5.1)
K	representative measure of bed element height (Equation 2.1)
$K(z)$	eddy viscosity (Section 10.4.1)
L	step spacing
L_a	antidune spacing
L_e	length scale (eddy mixing length)
$L_{\min}$	predicted minimum antidune spacing
m	1. exponent for hydraulic geometry discharge/velocity relationship 2. component (size fraction) m of the sediment distribution (Equation 10.5)
M	largest sized sediment present at height z (Equation 10.5)
N	Manning resistance coefficient (Equation 2.10)
p	intercept for hydraulic geometry discharge/friction factor relationship
r	exponent for hydraulic geometry discharge/friction factor relationship
q_{cr}	critical unit discharge (Sections 2.7.6 and 9.3.4)
q_{cr*}	dimensionless critical unit discharge (Section 9.3.4)
Q	discharge
R	hydraulic radius
Re	Reynold number (Equation 2.25)
R_S	ratio of mean spacing to mean step height (Equation 2.3)
S	bed slope
S_f	energy / friction slope
S_w	water slope
u_*	shear velocity
u^*	dimensionless shear velocity
$\overline{U}$	mean velocity
U_s	freestream velocity
u,v	velocity at a point in velocity profile
u(i)	velocity at point i in profile
v_{*f}	local shear velocity (Section 10.4.1)
V	velocity
w	width
W	wake function (Equation 2.14)
y	vertical point in profile

z	point in flow profile
z_m	height in flow profile equal to z-axis of sediment size m.
z_S	surface of flow in profile
z_0	theoretical bottom of the flow
ϕ_m	sediment of size m expressed in phi units (Equation 10.8)
ψ	proportion of the channel reach containing steps (Equation10.27)
γ	kinematic viscosity (approximately equal to 1 x 10^{-3} N s m^{-2} at typical stream water temperature)
κ	von Karman constant
λ	roughness spacing / concentration (Section 2.6.1)
Λ_e	effective roughness concentration (Equation 2.26)
θ_s	local bed angle
ρ	water density (1000kg m^{-3})
ρ_s	sediment density (taken as 2650 kg m^{-3})
σ	standard deviation of the sediment distribution in ϕ units (Equation 10.9)
τ	bed shear stress
τ_{cr}	critical bed shear stress – shear stress needed to move the largest particle in the flow
τ_{cr*}	dimensionless critical bed shear stress
τ_{cr50*}	dimensionless critical bed shear stress – shear stress needed to move the D_{50} sized sediment in the flow
τ_D	drag stress associated with the form drag produced by flow around the roughness elements (Equation 10.5)
$(\tau_D)_S$	drag stress from any sediment protruding through the surface of the flow
τ_f	fluid stress
τ_r	run average bed shear stress
τ_T	total shear stress (sum of fluid and drag stress)
τ^*	dimensionless shear stress ($\frac{\tau_r}{\tau_{cr}}$)
Ω	streampower (Equation 3.3)

Explanation of selected hydraulic concepts and terms

1. Flow classification

Steady flow

Defined as where the parameters describing the flow (e.g. velocity, discharge, depth) do not vary with time. Unsteady flow is where the opposite is true. It is rare for open channel flow to be truly steady. However, equations developed for use in steady flow are often applied to unsteady flows. If the changes occur slowly, steady flow equations give reasonable results (Chadwick and Morfett, 1993).

Uniform flow

Where parameters describing the flow do not vary along the path of the flow and the flow cross-section is of constant area, i.e. flow is constant (not accelerating nor decelerating), and the cross-section perpendicular to the direction of flow is constant. This state is, therefore, not typical of river channels. However, equations developed for use in uniform flow are commonly applied to non-uniform channel flow.

2. Reynolds Number

Reynolds number (*Re*) is the ratio of the inertial and viscous forces in the flow. Equation 1 below shows how it is calculated, where k is the object height and γ is kinematic viscosity (approximately equal to 1 x 10^{-6} $m^2 s^{-1}$ at typical stream water temperature);

$$Re = \frac{\overline{U}k}{\gamma} \qquad [1]$$

Laminar flow is defined as flow where $Re < 500$. Transitional flow is where $500 < Re < 2000$, with turbulent flow defined as flow with $Re > 2000$. This is considered further in Chapter 2, especially in relation to drag forces.

Hydraulically rough / smooth flow

Hydraulically smooth flow is where the surface irregularities are non-existent (e.g. a flume with no sediment) or negligible (very fine sediment). This enables a laminar sub-layer to develop near the bed, above which the bed roughness has no effect. Rough (turbulent) flow is characteristic of the channels considered in this research, i.e. where the sediment in the channel is of a significant size and protrudes through the laminar sub-layer into the turbulent boundary layer.

3. Types of flow interaction for flow over rough surfaces

Isolated-roughness flow

The roughness elements are located far enough away from each other that there is no interference between the elements. The wake and vortex associated with a particular roughness element are completely developed and dissipated before the next roughness element is reached.

Wake-interference flow

The roughness elements are close enough together that the wake and vortex associated with the element will interfere with those of the next element, leading to turbulent mixing.

Skimming (or Quasi-smooth) flow

The roughness elements are so close together that the flow 'skims' over the tops of the elements. Dead zones (containing stable eddies) exist between the roughness elements. The skimming of the flow means that it is effectively hydraulically smooth. A higher friction factor exists as the eddies between the roughness elements consume energy.

4. Froude number

The most common equation used to define Froude number for a channel with a rectangular cross-section is shown below in Equation 2. Froude number represents the ratio of inertial forces to gravitational forces. Flow with a Froude number of unity is defined as being 'critical'. Sub-critical flow is where the Froude number is less than critical, with super-critical flow being the converse. This classification is valid for all channels (Chadwick and Morfett, 1993).

$$Fr = \frac{\overline{U}}{\sqrt{gd}} \qquad [2]$$

Froude number also represents the ratio of water velocity to wave velocity, and is, therefore, a very useful parameter as defines the regime of the flow. In super-critical flow, the water velocity is faster than the wave velocity, meaning that flow disturbances can only travel downstream (as can be seen by e.g. throwing a pebble into a river with super-critical flow). In sub-critical flow such disturbances can travel upstream as well as downstream, as the wave velocity is greater than the water velocity. One of the implications for this in open channel flow is that as the Froude number approaches unity (critical flow), flow conditions become unstable, resulting in wave formations.

5. Hydraulic jumps

A hydraulic jump occurs where a super-critical flow meets a sub-critical flow. In the context of this research this would occur over a step or large roughness element. The greater the difference in terms of Froude number between the two flows determines the amount of energy lost through turbulent dissipation over the jump. This is considered further in Chapter 8.

6. Tumbling flow

This is a non-standard term used by e.g. Chin, 1989 and Beltaos, 1983. It is basically a qualitative term used to describe the flow over step-pool sequences i.e. the fact that it 'tumbles' over the steps into the pools.

7. Slope definitions

Energy gradient (or friction slope), S_f, is the line representing the gradient of the elevation of the total head of flow for gradually varied flow (i.e. where geometry changes only gradually downstream). For rapidly varying flow, friction is considered unimportant over short distances in which there are large changes in other things (Chadwick and Morfett, 1993).

In gradually varied flow it is assumed that the change in energy total energy is needed to overcome friction, where $S_f = \frac{dH}{dx}$ H (energy head) can be defined as:

$$H = d + z + \alpha \frac{\overline{U}^2}{2g} \qquad [3]$$

where d is flow depth, z is bed elevation, $\overline{U}$ is mean velocity, and α is a coefficient usually assumed to be unity (Chadwick and Morfitt, 1993).

Chapter 1

Introduction

1.1 Backgound

Why study steep streams? In many countries, there has been increased human activity in mountainous regions, leading to a need for further understanding of mountain streams (generally considered as channels with >0.05 gradient) in order to help with, for example, flood control and prediction. Flood depths and velocities have been incorrectly predicted in the past because of a lack of knowledge concerning sediment transport and friction in high flows in these streams.

Increased knowledge of the hydraulics of steep streams would also help understand how pollutants are dispersed in such streams, where there are typically dead zones and very fast 'tumbling flow' (Beltaos, 1982) as the flow travels over large roughness elements. As they have different hydraulic and geomorphological features from lowland rivers, their study produces a new range of problems, as equations developed for lowland rivers usually cannot be applied to steep streams. As a result of these problems there has been relatively little previous work carried out on high-gradient streams, and much about them is either unknown or misunderstood.

In steep streams, the sediment is generally larger and more poorly sorted than in lowland streams, meaning that the sediment is of the same order of magnitude as the flow depth. The presence of steep slopes and fast flows means that stream power is much greater than in lowland environments. Steep streams are, therefore, high energy environments, and the flow and bedform features reflect this. The main bedform features found in steep streams are steps and pools (described by e.g. Chin (1989)), where the steps are generally made up of the coarser sediment in the stream and the flow is faster; the pools are deeper and the flow is slower.

Step-pool sequences are stable bedforms as they are generally thought to form at high flow (Whittaker and Jaeggi, 1982), which makes them very important in affecting the flow of steep streams. Their main purpose appears to be to dissipate energy (from hydraulic jumps and from the form drag of the large clasts); in high gradient channels there is a vast amount of energy, which if not dissipated would result in considerable erosion and channel degradation (Heede, 1981). Grant (1997) suggests that steps are necessary to produce hydraulic jumps, which act to dissipate energy in these high energy streams. As the channels are narrow, energy cannot be dissipated by braiding or meandering.

El Khashab (1986) stated that the 'best way of dissipating energy in steep streams and weirs is to lead flow over a series of steps'. This is because of the increased resistance to flow as a result of form drag from the large clasts in the streams. Whilst there has been considerable work carried out investigating the effect of isolated large clasts / uniformly spaced artificial elements on flow resistance (e.g. Flammer et al, 1970; Nowell and Church, 1979), little work has been carried out on the effects of steps.

This report describes research that was carried out to investigate high-gradient hydraulics, and is organised as follows:

Chapter 2 considers the previous work carried out on the subject, and describes theories that can be applied to steep streams. It concludes with a description of the main aims of this research. The fieldwork is described in Chapters 3 to 5; Chapter 3 describes the initial reconnaissance fieldwork survey that was carried out, Chapter 4 describes the sediment and channel characteristics found during the main fieldwork stage of the research, and Chapter 5 describes the salt dilution gauging in terms of theory, methodology and logistics. The flume methodology is discussed in Chapter 6. Chapter 7 considers the flow data obtained from the salt dilution gauging in terms of the sediment and channel features described in Chapter 4. Chapter 8 considers the effects the steps have on hydraulic geometry and flow resistance, and Chapter 9 attempts to provide theories for step formation based on flume experiments. Velocity profiles measured in the flume and modelling of the velocity distribution using Visual Basic computer model are described in Chapter 10. Final conclusions are offered in Chapter 11.

1.2 Research aims

It was decided that steps and pools would be particularly focused on, as well as the presence of large sediment in steep streams in general. Field studies were considered the most useful approach to adopt, backed up by flume work to produce steps and pools and compare flow conditions before and after the steps were formed. The main areas of research identified were:

1. Investigate the hydraulic conditions of step-pool formation;
2. Determine the hydraulic effects of large clasts and steps / pools in steep streams.

These main research areas are described in more detail in the following sections.

1.2.1 Hydraulic conditions of step-pool formation

This was considered best studied by flume experiments (as one is unlikely to witness step formation in the field), backed up by field studies of step characteristics to determine whether bedrock and alluvial steps are the same and investigate what controls step spacing. The aims identified for this research area are:

Aim 1a: Determine the conditions necessary for step-pool formation.

The flumework carried out by Grant (1994) and Whittaker and Jaeggi (1982) provided guidelines for these conditions in terms of hydraulic conditions, sediment size distribution, and channel geometry. A series of flume runs were carried out, where the run is characterised by discharge, slope, and sediment size based on the conditions used in these previous studies, as well as information from the initial reconnaissance field study carried out at the start of the research. From these experiments the range of conditions necessary to enable step formation were obtainable.

Aim 1b: Study the hydraulic conditions leading to the formation of steps in order to understand more fully the processes leading to their creation.

Detailed study of the flume runs that produced steps and pools provided insight into the mechanism of step formation, enabling a theory for their formation to be produced and the sequence of events that leads to their formation clarified. Information regarding the flow conditions necessary for step formation and observation of the particles that form the steps was considered necessary to achieve this aim, therefore, it was considered desirable to be able to easily recognise the larger sized sediment, which would most likely comprise the steps. The relationship between standing waves and the step bedforms was also considered important as standing waves / antidunes have been claimed by Grant (1994) to be the main control of step formation. Therefore, this was also studied in the flume by taking a series of water height measurements and observations of the step forming process.

1.2.2 Hydraulic effects of steps and large clasts

Study of this research area was planned to involve a combination of fieldwork, flume studies, and computing. The main aims identified comprising this research area are:

Aim 2a: Study the effect of steps and large elements on flow resistance.

Whilst plenty of work has been carried out looking at the effect large clasts or artificial elements have on flow resistance (Judd and Peterson, 1969; Flammer et al, 1970; Bayazit, 1975; Nowell and Church, 1979), less work has been carried out on the effects of steps. Use of the Darcy-Weisbach equation (Equation 2.33, and described in Section 2.4.1) enabled flow resistance (*f*) to be estimated from measurements of channel slope (S_f), hydraulic radius (R) and average reach velocity ($\overline{U}$).

$$f = \frac{8gRS_f}{\overline{U}^2} \qquad [1.1]$$

Average velocity was determined in the field by measuring salt tracer travel time (as part of salt dilution gauging; described in Elder et al, 1990) and channel slope by detailed surveying of the study reaches. Hydraulic radius was harder to measure as a result of the highly variable width and depth in steep streams, therefore, detailed error analysis was carried out prior to the fieldwork to establish the most accurate method to estimate these values.

The relationship between discharge and flow resistance was then studied for the field sites and the flume. Flume experiments enabled comparison of flow resistance before and after steps were formed, therefore, it was possible to directly investigate the effects of the steps. Theoretical and empirical equations were also tested to determine their accuracy in determining the relationship between friction factor and discharge based on sediment and channel characteristics.

Aim 2b: Accurately determine the velocity profile in a steep stream with large roughness elements

Whilst velocity profiles could not be obtained from the fieldsites, they were obtained for step-pool sequences in the flume by using a miniature current meter. Study of these profiles over a step-pool sequence provided information concerning the effect of the steps on the flow, as detailed sediment profiles were also taken over the sequence. Therefore, it was possible to establish how the characteristics of the velocity profile are related to the sediment profile.

The Wiberg and Smith (1991) model for calculating the average velocity profile was tested using the data collected during the research, and the model adapted to attempt to account for the effect from the steps. The aim of doing this was to be able to model the 'S-shaped' profiles considered characteristic of steep streams with poorly-sorted sediment (Bathurst, 1993; Wiberg and Smith, 1991) under various conditions. If the profiles can be modelled accurately then, theoretically, it should be possible to accurately determine the flow resistance in a channel based on sediment and channel characteristics of a site.

Chapter 2

Background to the research

This chapter will describe the previous research that has been carried out in the area of steep stream hydraulics and geomorphology. The geomorphic and hydraulic features of these channels, the available equations applicable for high gradients, and the fieldwork, flume studies, and modelling that have been undertaken to date will be considered. The aim of reviewing previous work is to identify research areas where there is uncertainty, disagreement, and/or a complete lack of knowledge. This will enable detailed research objectives to be defined within the general aims.

2.1 Geomorphic features of steep streams

2.1.1 General description of steep streams

The main difference between high and low gradient channels is that steeper streams have larger sediment and shallower flows. This means that there is sediment present in the channel of a comparable magnitude to flow depth, which can protrude through the flow. This appears to lead to step-pool sequences (illustrated in Figure 2.1), which are 'an ubiquitous feature of high-gradient channels' (Wohl and Grodek, 1994), and are described in detail by many workers (Bowman, 1977; Newson and Harrison, 1978; Whittaker and Jaeggi, 1982; Chin, 1989; Grant et al, 1990; Wohl and Grodek, 1994). The presence of step-pool sequences is often associated with an alternation between sub-critical and super-critical flow over the steps, which causes hydraulic jumps to occur (described in Chadwick and Morfett, 1986).

The gradient of the step is considerably greater than the pool part of the sequence, as shown in Figure 2.1; there can even be a slight upward slope in the pools caused by scour at the base of the step. This causes the flow in pools to be very slow compared to the plunging flow of water over steps. The steps are usually transverse to the flow direction, although they may be oblique with a 70-80° angle to the flow (Grant et al, 1990); or they can form a 'V' pointing upstream (Bowman, 1977). On gentler gradients the steps may only partially extend across the channel. Steps and pools usually occur as a regularly spaced sequence (Judd, 1964; Chin, 1989; Heede, 1981; Whittaker, 1987a; Grant et al, 1990). Factors affecting this spacing are discussed in the following section.

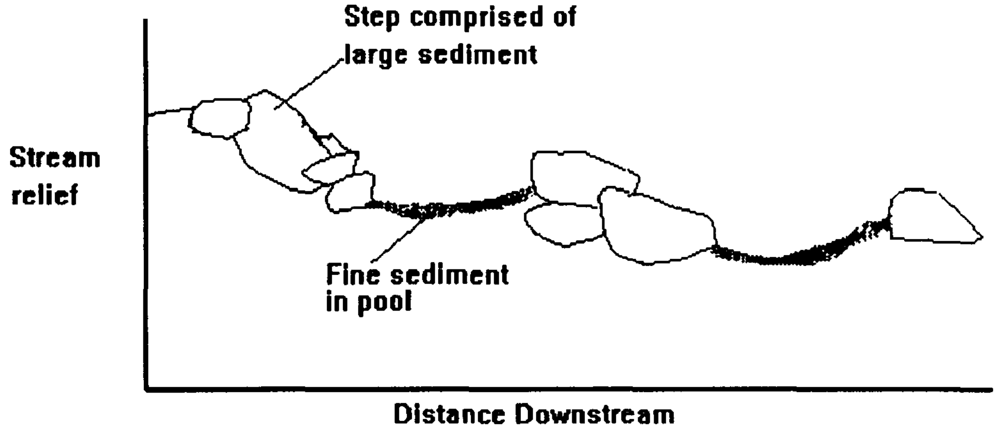

Figure 2.1. Typical step-pool sequence (adapted from Chin, 1989)

2.1.2 Factors controlling the spacing of steps

It has been found that the step spacing, which is typically a distance of one to two channel widths, becomes more regular as slope increases (Judd, 1964; Heede, 1981; Whittaker, 1987b; Grant et al, 1990). Of these previous studies carried out, all have found a correlation with channel width (see Table 2.1 for this relationship, and also the range of slope and width studied), although Grant et al (1990), Chin (1989), Whittaker (1987b) and Judd (1964) claim that spacing correlates better with slope. Judd (1964) suggested that an equation of the form of Equation 2.1 relates these two variables. Whittaker (1987b) proposed Equation 2.2;

$$L = \frac{K}{C_1 S^{C_2}} \qquad [2.1]$$

$$L = \frac{0.3113}{S^{1.188}} \qquad [2.2]$$

where L is the length between steps, S is the slope of the channel, K is a representative measure of bed element height, and C_1 and C_2 are constants. However, Billi et al

(1995) and Montgomery et al (1995) found that slope was not a control on step spacing. Whilst a wide range of slopes (0.07-0.19) was studied by Billi et al (1995), a wide enough range to identify any relationship with slope, they only looked at one stream.

Wohl and Grodek (1994) studied semi-arid streams in the Negev desert, Israel. They looked at the ratio, R_s, of mean step spacing to mean step height, and found an inverse relationship between this and channel slope

$$R_s = \frac{4.5}{S^{0.42}}. \qquad [2.3]$$

Step height and channel slope correlated, with height increasing as slope increases; although this author considers that this could be caused by larger boulders being available and so larger steps possible. This relationship between step height and slope was found to be significant at the $p<0.01$ level (where p is the probability level). Their study contained many data points (over 100) from 4 streams, with a slope range of 0.07-0.67, and a width range of 0.1-2.4 m, the widest range of any of the studies undertaken. They also found the same inverse relationship between step spacing and slope as previously noted, but found that it remained fairly constant when the slope exceeded 0.2. At such high gradients, the step height alone varied. However, for this to happen there needed to be boulders large enough for the step height to increase further. If this was not the case, then the spacing continued to decrease at higher slopes. They found no correlation between step geometry and channel width, nor was spacing affected by whether the step was alluvial or bedrock.

From these previous studies, the two that studied the largest range of slope and had the most data points and streams (Whittaker, 1987b and Wohl and Grodek, 1994) both found a better relationship between step spacing and slope than with width. However, width does appear to have some control over step spacing.

Table 2.1. Relationships found between step spacing and channel width

Workers	slope range (m/m)	width range (m)	step spacing (in channel widths)	data points // number of streams
Field studies				
Billi et al (1995)	0.07-0.19	4.76-6.59	0.99	8 // 1
Montgomery et al (1995)	0.002-0.085	2.7-38.1	0.6 - 1.3	46 // 11
Wohl and Grodek (1994)	0.07 - 0.39	0.1-2.4		>100 // 4
Grant et al (1990)	0.01-0.08	18.1 average	0.4 - 0.8	8 // 2
Chin (1989)	0.04-0.09		1.68 - 2.18	1 stream
Whittaker (1987b)	0.05-0.18		2.7	24 // 3
Bowman (1977)			1.4	
Flume studies				
Grant (1994)	0.04	0.25 / 0.5		2 flumes
Whittaker and Jaeggi (1982)	0.0977-0.2410	0.132		1 flume

2.1.3 Step composition

Steps are generally comprised of loose, alluvial sediment (found by Grant et al, 1990 to be the 90th percentile or coarser sediment), or are carved into the bedrock (Grant et al, 1990; Wohl and Grodek, 1994; Chin 1989). There appears to be no difference between the two in terms of step height, spacing and pool characteristics (Wohl and Grodek, 1994). A sequence of steps and pools may be just bedrock steps, or may alternate between bedrock and alluvial steps. Bedrock steps appear to be more common on steeper slopes (Wohl and Grodek, 1994; Grant et al, 1990).

Steps made up of logs have been observed by Wohl et al (1997), Heede (1981) and Montgomery et al (1995). It was concluded by Wohl et al (1997) that the logs were immobile as live roots were found, and the size of the logs was considered too large to be moved by the flow. Any immobile log steps are incorporated into an alluvial step sequence. Where there is smaller woody debris in the channel, this can form part of an alluvial step.

2.1.4 Similarities with other bedforms

Most fluvial channels have regular bedforms of some type, depending on the flow conditions and sediment in the channel. For example, ripples are only found in sandy channels, pools and riffles are only found in gravel channels, and steps and pools are only found in high energy flows where there is large sediment relative to the flow depth. The similarities and distinctions between steps and pools, and other selected bedforms (those requiring similar sediment and flow conditions), especially those sometimes confused with steps and pools in the literature, will be considered in this sub-section.

Transverse ribs

These features, illustrated in Figure 2.2, have been studied extensively by McDonald and Banerjee (1971), Gustavson (1974) and Koster (1978). They consist of coarse 'ribs', analogous to steps which are separated by areas containing fines. They have a similar spacing to step and pool spacing, which appears to be controlled by clast size, slope and width (McDonald and Banerjee, 1971; Koster, 1978). Closer spaced ribs were found on steeper slopes with narrower widths and smaller sediment. A comparison of Figure 2.1 and Figure 2.2 shows the similarity between transverse ribs and step-pool sequences. The ribs are about two clasts high (and so are much smaller in amplitude than steps), and several clasts wide. They are formed in high flow and in moderately steep (often proglacial) areas with flow near super-critical. Like steps and pools, they are stable features, require poorly sorted sediment, and have similar spacing and controls on spacing of width and slope. Therefore, it is possible that they are formed by similar flow processes to those that form steps and pools, although there are differences in the slope and sediment size. Also, transverse ribs are depositional bedforms, whereas steps and pools appear to be a result of deposition and scour.

Transverse ribs appear to have an upper slope limit of 0.05 (Gustavson; 1974, Koster; 1978) to 0.068 (McDonald and Banerjee, 1971), which is considerably lower than slopes on which steps and pools have been observed (see Table 2.1 for the range of slopes on which steps and pools have been observed). The maximum size of the sediment in transverse ribs is also considerably smaller than that of steps and pools;

Koster (1978) found 24 cm to be the largest sediment present, and McDonald and Banerjee (1971) found sediment up to 32.7 cm. In contrast, sediment over 90 cm has been found in step-pool sequences (Grant et al, 1990). Also, the ribs extend across the flow for a distance several times their wavelength (Allen, 1984) which is generally not the case with steps (where the wavelength is generally greater than the width, as seen in Table 2.1).

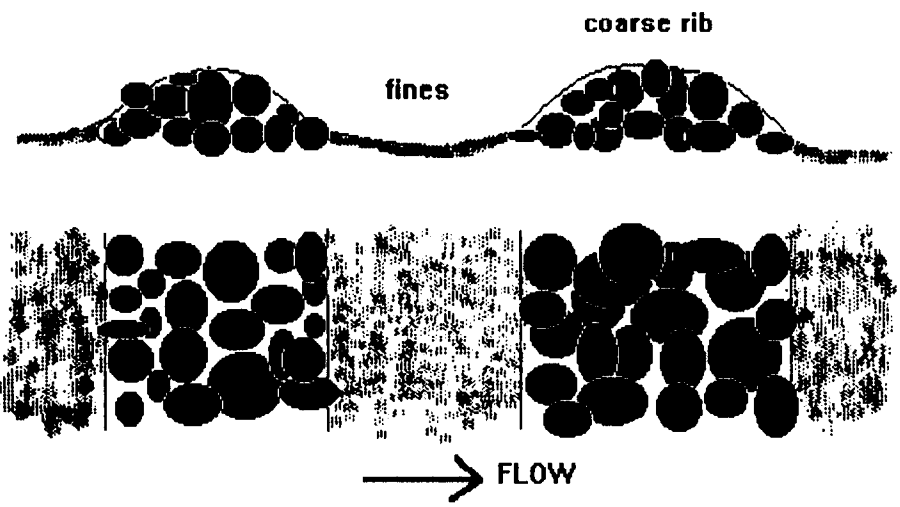

Figure 2.2 Transverse ribs (adapted by McDonald and Banerjee, 1971)

Antidunes

These sediment features, which are accompanied by stationary surface waves, have been described by Kennedy (1963), Middleton (1965), Shaw and Kellerhals (1977) and Allen (1984). Their presence is defined by a limited range of flow conditions, as shown in the phase diagram in Figure 2.3, which considers the flow Froude number (calculated using Equation 2.4) and a value *kd* defined by Equation 2.5 necessary for antidune formation. This term kd is named wave number by e.g. Kennedy, 1963 and Whittaker and Jaeggi, 1982. In Equations 2.4 and 2.5, d is the average flow depth, $\overline{U}$ is the mean velocity, g is the gravitational constant and L_a is the spacing between antidunes.

$$Fr = \frac{\overline{U}}{\sqrt{gd}} \qquad [2.4]$$

$$kd = \frac{2\pi d}{L_a} \quad [2.5]$$

As can be seen from the phase diagram, high Froude number values are required to form antidunes, suggesting an environment with steep slopes. Minimum antidune wavelength can be estimated using $L_{\min}$ (originally proposed by Kennedy, 1963 following his research on antidunes), as shown in Equation 2.6;

$$L_{\min} = \frac{2\pi \overline{U}^2}{g} \quad [2.6]$$

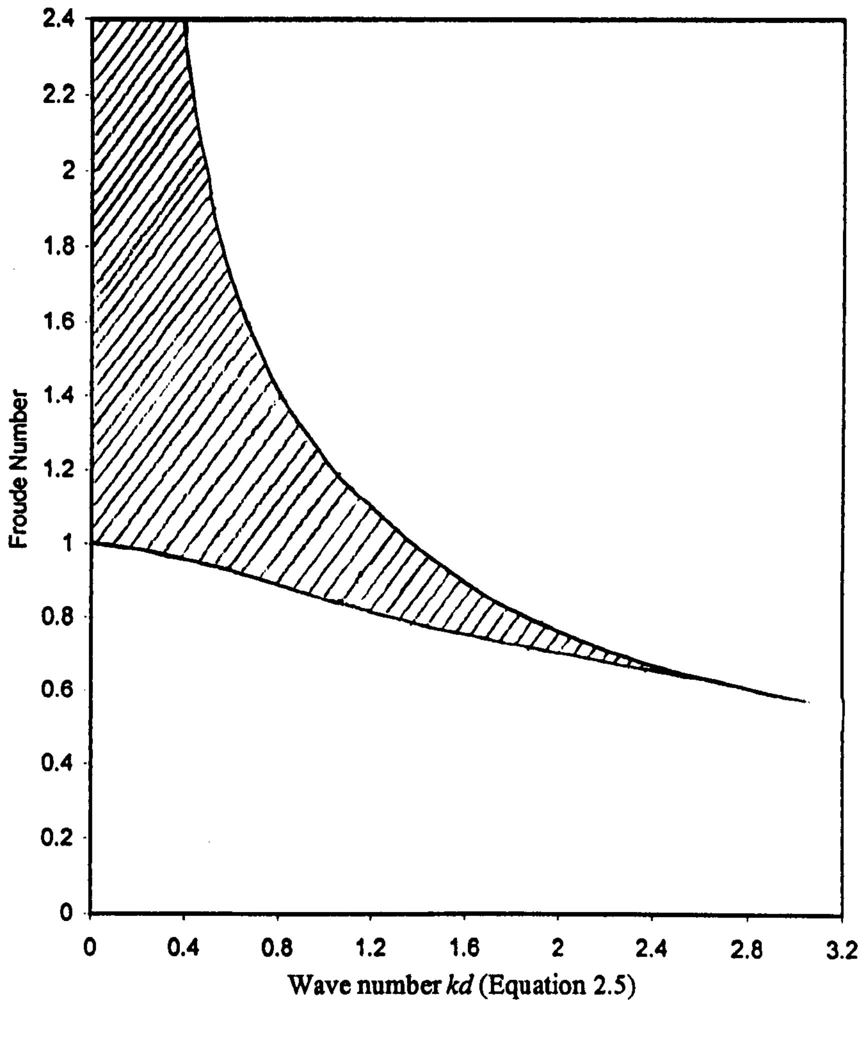

Figure 2.3. Phase diagram showing conditions for antidune formation

Bedload sheets

These features form in low-gradient channels with sand and gravel, and consist of very low amplitude 'sheets' of gravel and sand clusters (Whiting et al; 1988; Iseya and Ikeda, 1987). They are very different features to steps and pools as bedload sheets form in environments with a reasonably high sediment transport rate, whereas steps form in environments with low sediment transport rate (Grant, 1994). The sediment range is smaller than in steps and pools and step-sized particles are not present in bedload sheets. As bedload sheets are smaller, mesoscale, mobile structures, whereas steps and pools are immobile, macroscale bedforms, it can be concluded that these two bedforms are unrelated.

Pools and riffles

It is possible that pools and riffles have a similar effect on the flow as steps and pools (i.e. increasing resistance to flow), but occur on shallower gradients where the sediment range is not large enough to produce steps and pools (Bathurst, 1993 claims they occur on slopes up to about 0.005). However, the spacing is very different (pool and riffle spacing is traditionally quoted as being 5-7 channel widths, although there is much variation), indicating that their formation is not related to that of steps and pools. Steps are usually only one clast high, whereas riffles are many clasts thick. Apart from small amounts of super-critical flow around some of the larger clasts in the riffles, flow is sub-critical, unlike steps and pools where there is a significant amount of supercritical flow.

2.2 Conditions necessary for step-pool formation

Previous field and flume studies carried out to study steps and pools were collated to determine probable flow and sediment conditions necessary for step-pool formation. These conditions are considered in this section.

2.2.1 Climatic conditions

Generally studies have been carried out in mountainous regions in North America (Grant et al, 1990; Chin, 1989) and Europe (Billi et al, 1995). However, the study by Wohl and Grodek (1994) was carried out in an ultra-arid area in Israel where the streams are often dry, and bedrock steps and pools have been observed by the author in underground channels in North England. This suggests that there is no climatic control on their formation.

2.2.2 Slope

The lower limit for steps to form appears to be about 0.02-0.05 (Chin, 1989; Grant et al, 1990); although Whittaker and Jaeggi (1982) found (in the flume) that a slope of 0.075 formed the division between antidunes and steps and pools. Below 0.075 they found only regular antidunes formed; above 0.075 steps and pools predominated. However, Grant (1994) found steps and pools developed on a slope of 0.04. Steps can occur on slopes with gradients as steep as 0.67 (Wohl and Grodek, 1994), so there may not actually be an upper limit for their formation. Generally steps are more defined on steeper slopes (Heede, 1981; Whittaker, 1987a; Grant et al, 1990).

It is, therefore, postulated that the actual value of slope is not important; rather it is the flow conditions and sediment characteristics that determine whether steps and pools form or not, and these are controlled to some extent by slope. For example, the differences found between the slope necessary for step formation by Whittaker and Jaeggi (1982) and Grant (1994) are possibly a reflection of differences between the flumes and the sediment distributions used in their studies.

2.2.3 Froude Number

The discussion in the previous sub-section concerning slope suggests that Froude number (Equation 2.4) is a very important factor in determining whether steps form. It provides a dimensionless measure of the flow conditions by relating the inertial and gravitational forces. For flume runs producing steps and pools, Whittaker and Jaeggi (1982) found a range of $0.6<Fr<1.45$, Grant (1994) found $0.7<Fr<1.0$ for step forming conditions; and Ashida et al (1984) found values of $1.2<Fr<1.8$. The values calculated by Ashida et al (1984) seem very high when considering that one of the features of step-pool sequences is an alternation between sub- and super-critical flow, suggesting that the reach average Froude number would be less than unity as most of the length of the channel is sub-critical pool flow. Grant (1994) questions the method by which

Ashida et al (1984) calculated Froude number (they used a shear velocity measure), and suggests that their results are in question. The values found by Whittaker and Jaeggi (1982) are also questionable as they calculated initial flow conditions rather than measuring them directly.

2.2.4 Shear stress

Grant (1994), using Equations 2.7 and 2.8, considered the ratio of average bed shear stress for the run (τ_r) to the bed shear stress needed to move the largest grain size in the sediment mix (τ_{cr}), where ρ is water density (1000 kg m^{-3}) and θ_S is the local bed angle. He defined this ratio as τ*.

$$\tau_r = \rho g d \sin\theta_s \qquad [2.7]$$

$$\tau^* = \frac{\tau_r}{\tau_{cr}} \qquad [2.8]$$

He found $0.5<\tau^*\leq 1.0$, which is perhaps too wide a range to be considered useful, but shows that only a limited amount of sediment transport can occur for steps and pools to form.

2.2.5 Transport rate

Lisle (1987) stated that for step-pool sequences to form, low rates of transport of large clasts are needed. It was also shown by Grant (1994) in the flume that a high sediment transport rate inhibits the formation of steps - this was attributed to the fact that there would be many grain to grain collisions, meaning that the particles would not be stationary for long periods. This prevents armouring, and conditions necessary for hydraulic jump (and therefore step) formation occur infrequently. He also found that bedload sheets are formed in high sediment transport runs, which also inhibited step formation. The coarse areas had many grain to grain collisions, and the fine areas mobilised any large particles as they protrude more into the flow, thus they were prevented from stopping. Steps that were present in the flume were destroyed at high sediment transport rates because of the increase in collisions (Grant, 1994).

2.2.6 Discharge

It is generally considered that peak flows form steps and pools (Whittaker and Jaeggi, 1982), and evidence from Wohl and Grodek (1994) from a very arid area, where only the peak flows submerge the largest particles, supports this. However, Hasegawa et al (1990) claimed that steps and pools are formed at half peak flow (which they showed was within the antidune forming flow domain), and not at peak flow (which was not). Also, Grant (1994) in his flume experiment used a discharge which was capable of only limited sediment movement.

2.2.7 Sediment characteristics

Both field and flume studies have shown that very poorly sorted sediment is necessary for step-pool formation, with relative roughness (i.e. the ratio of particle size to flow depth) near unity, so that the particles protrude enough for hydraulic jumps to form at low flows. Also, there needs to be a sufficient disparity in entrainment thresholds and bed roughness so that larger grains are able to trap smaller ones (Grant, 1994 from flume experiments).

2.3 Formation of step-pool sequences

Flume experiments conducted by Whittaker and Jaeggi (1982) and Grant (1994) have created step-pool sequences, and have, therefore, provided an opportunity to study the formation of steps, which is not possible in the field as they are formed by very low frequency flows. These studies, along with the field study of Wohl and Grodek (1994), will be described in detail, and then overall conclusions from all three studies considered.

2.3.1 Whittaker and Jaeggi (1982)

Whittaker and Jaeggi (1982) were the first to propose theories for the development of steps, although the theories had originally been developed for transverse ribs, and pools and riffles. The three theories considered by them were:

- Dispersion and sorting theory,
- Velocity reversal theory,
- Antidune theory.

The first two theories were developed for pools and riffles and were discounted by Whittaker and Jaeggi (1982). They proposed the antidune theory (which is the same as was originally suggested to explain the formation of transverse ribs) as an explanation for the formation of steps and pools, which was also proposed by Hasegawa et al (1990) from field studies. The theory is based on the similarity between step-pool sequences and transverse ribs (McDonald and Banerjee, 1971), which has led to speculation that they are formed by a similar process (although transverse ribs have more uniform sediment than steps and pools and do not contain imbricated particles). The theory suggests that steps are relict antidune features formed by standing waves (described in Leeder, 1982: p.92), and/or hydraulic jumps. However, this theory does not explain how the particles come to rest under the antidune crest, nor does it explain the occurrence of bedrock steps.

2.3.2 Grant (1994)

Grant (1994) found the process of step formation to be as follows, and took less than 20 minutes (illustrated in Figure 2.4):

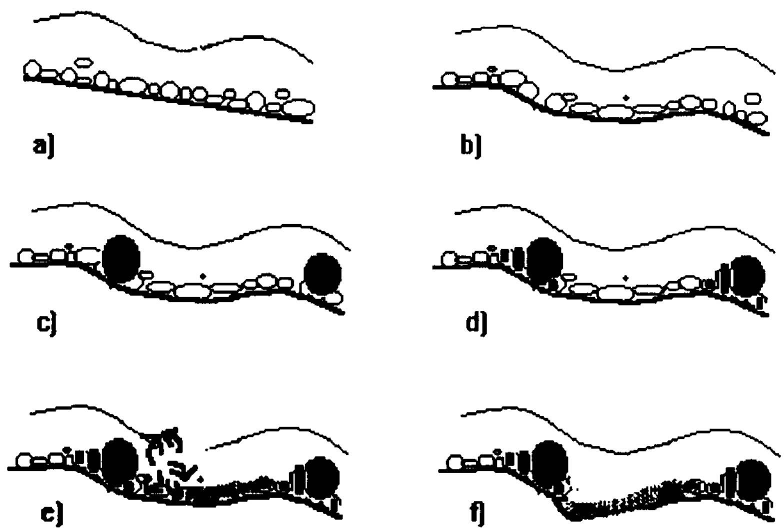

Figure 2.4 Formation of steps and pools described by Grant (1994)

1. Rolling, sliding, and saltation of grains occurs (providing the discharge is high enough for this to be possible for the larger sediment in the flume);
2. Regular antidunes form on the water surface, with bed deformation in phase with the water surface (Figure 2.4a and 2.4b);
3. As the bed deforms, individual, large particles would intermittently come to rest immediately downstream of the antidune crest (Figure 2.4c);
4. These larger particles trap other particles, leading to a cluster of imbricated grains (Figure 2.4d). This was also proposed by McDonald and Day (1978) following flume studies of transverse ribs);
5. The presence of the cluster leads to a hydraulic jump in the antidune trough because of flow depth changes (Figure 2.4e);
6. Turbulence from the jump scours the bed immediately downstream of the stalled grains, which accentuates the relief of the step (Figure 2.4f);

Armouring occurs simultaneously; and more step-forming sediment is trapped by the clasts already deposited in the step because of an abrupt decrease in velocity near a jump. Grant (1994) found a significant relationship (p<0.01) between step spacing and minimum antidune wavelength $L_{\min}$ (Equation 2.6), and from this he concluded that steps and pools are related to antidunes. Figure 2.4, as with the theory proposed by

Whittaker and Jaeggi (1982), does not explain how the particles initially come to rest under the antidune crest. It may be that the slope changes as a result of bed deformation and hence leads to a lower shear stress and so large particles are deposited; chance stalling of particles does not explain the apparent regular spacing of steps.

2.3.3 Wohl and Grodek (1994)

Whilst no flume experiments were carried out in their study, their field study provided some important considerations for step-pool formation, as they investigated bedrock steps and very steep slopes. They tested the theory that bedrock steps are formed by lithology or resistance variations (believed to be a probable cause of bedrock steps by Chin, 1989). Measuring resistance using a Schmidt hammer, they found that there was no constant correlation between lithology and bed-step characteristics. Therefore, they concluded that they must be formed by a fluvial process. Considering that the characteristics of bedrock steps are similar to those of alluvial steps in terms of spacing, height and relationship with gradient (Wohl and Grodek, 1994), it is logical to assume that they are formed by a similar process to the one forming alluvial steps.

It could be that bedrock steps are formed if there is enough alluvial material over a bedrock channel for the processes described in Figure 2.4 to occur, and the turbulence from the hydraulic jump eroded the bedrock to form bedrock steps. The presence of bedrock steps also suggests that the formation of steps is not an iterative one (which would mean that steps are created and destroyed until the optimum spacing is achieved). Any acceptable theory for step formation, therefore, needs to account for the presence of bedrock steps, and also the apparent relationships between spacing and channel gradient, and spacing and width.

2.3.4 Conclusions

Overall, the literature suggests that steps and pools are formed under the same range of flow conditions as those necessary to produce antidunes (concluded by the position of flume run plots on the phase diagram in Figure 2.3 (Grant, 1994; Whittaker and Jaeggi, 1982)). These workers have, therefore, concluded that the same process that forms antidunes (involving standing waves) is responsible for the formation of steps and pools. There do, however, appear to be problems with this theory, as it does not explain the presence of bedrock steps and their similarity with alluvial steps. The fact that steps and pools have been observed in bedrock channels suggests that it is more likely that the hydraulics of the flow that are responsible for their formation, as opposed to them simply being a depositional feature. However, the alluvial steps described in the literature would seem to have similarities with other bedforms (described in the next section), suggesting that they are in fact depositional structures.

2.4 Calculation of flow resistance

Field and flume studies have been carried out to determine the hydraulic effects of steps and pools (and the wide range of sediment found in such channels). Most have concentrated on resistance to flow. Resistance is a very important aspect of fluvial geomorphology and thus controls the amount of water a channel can carry as a result of its effect on velocity and depth (Bathurst, 1993). The resistance to flow in steep streams is considerably different to that of lowland streams (as well as being considerably greater); in lowland rivers most of the resistance is from the bedforms in the channel, whereas in steep streams it is mainly from the large boulders in the channel. This section will consider equations for calculating resistance to flow and the components of flow resistance.

2.4.1 Equations for calculation of flow resistance

The traditional equations for calculating resistance are the Darcy-Weisbach equation (2.9), Manning's equation (2.10) and the Chezy equation (2.11), where f, n and c are the resistance coefficients for each, respectively. R is hydraulic geometry, equal to $\frac{wd}{w+2d}$ for a rectangular cross-section, where w is channel width, S_f is the slope of the energy gradient and $\overline{U}$ is mean velocity. For channels with uniform flow S_f can be replaced with S, which is easier to measure.

$$f = \frac{8gRS_f}{\overline{U}^2} \qquad [2.9]$$

$$n = \frac{R^{2/3} S_f^{\ 1/2}}{\overline{U}} \quad [2.10]$$

$$c = \frac{\overline{U}}{(RS_f)^{1/2}} \quad [2.11]$$

The Darcy-Weisbach equation is most commonly used, as it has the strongest scientific foundation out of the three, and is non-dimensional. As will be discussed later, determining velocity (which is required for all three equations) is usually hard to do in steep streams. Therefore, providing the resistance coefficient and channel geometry can be determined, these equations can be useful in calculating velocity and hence discharge (by use of the continuity equation $Q = wd\overline{U}$, where Q is discharge in m^3 s^{-1}).

According to (Hey, 1979; Jarrett, 1984; Knighton, 1984; Bathurst, 1993), the components of flow resistance can be summarised as:

1. Boundary resistance - comprised of grain roughness and form roughness,
2. Channel resistance,
3. Free surface resistance.

2.4.2 Boundary resistance

This is from the friction/drag of bed material (grain roughness) and bedforms (form roughness), and provides the most resistance in all types of flow.

Grain roughness

Grain roughness is a function of relative roughness, R_r, which is defined by Equation 2.12:

$$R_r = \frac{d}{D_{84}} \quad [2.12]$$

where D_{84} is the size of the median axis of the bed material which is larger than 84% of the material (D_{50} is sometimes used instead). Ergenzinger (1992) offered an alternative to using sediment size - he developed the *K3* value to determine form and grain roughness from height differences on the riverbed. Using a Tausendfüssler device (which gives a very detailed cross-sectional profile), vertical differences in sediment height are measured to quantify the roughness. It has mainly been used to look at roughness changes over a flood; it was found from looking at the *K3* value that during a flood the spaces between large boulders are filled with fines, which reduces the *K3* value indicating roughness is decreased. Ergenzinger (1992) also suggested a variation on the ratios in Equation 2.12; i.e. that relative roughness can be expressed by the ratio of flow depth to the *K3* value.

Form roughness

Form roughness is determined by features in the bed material. For a sand bedded channels these can be plane beds, which offer least resistance to flow, or dunes, with the greatest resistance to flow. In steep streams, the individual boulders make up most of the form roughness, although this may decrease to grain roughness during high flows, when the boulders are drowned out (Ergenzinger, 1992). Bathurst (1985) developed the following categories of relative submergence:

- $\frac{d}{D_{84}} < 1$ represents large-scale roughness,
- $\frac{d}{D_{84}} > 4$ represents small-scale roughness,
- $1 < \frac{d}{D_{84}} < 4$ represents intermediate-scale roughness.

Flow resistance in channels with large-scale roughness depends mainly on the form drag of the boulders / roughness elements, whilst resistance in channels with small-scale roughness is dominated by grain roughness (Bathurst, 1978; Bathurst, 1982a; Li and Simons, 1982; Bathurst, 1985). About 95% of resistance from form drag in steep streams is from individual particles, mainly the largest ones (Nowell and Church, 1979, from flume studies of 'lego' bricks on 'lego' baseboards; El Khashab, 1986, from flume studies simulating steps by two-dimensional triangular elements). The majority of resistance in steep streams is from form drag (Bathurst, 1993). Therefore, it follows that the sediment making up the steps controls the resistance to flow as this is where the large sediment accumulates.

It appears very difficult to distinguish between resistance from steps and that from large sediment because, in channels with large-scale roughness, both are considered to be form roughness. However, it appears that the spacing of the steps has an added effect on the flow resistance due to their regular nature. This is discussed further later in this chapter (Section 2.7).

2.4.3 Channel and free surface resistance

Channel resistance is a result of the effects of the channel cross-section shape, and longitudinal non-uniformities in bed slope, water surface slope and channel plan form. These all cause energy losses which leads to an increase in resistance to flow. Free surface resistance considers energy losses at the surface caused by features such as hydraulic jumps in pools and eddy currents generated behind the boulders which increase resistance. This, and channel resistance are not significant in steep streams when compared to the effects from form drag.

The large amount of form drag needs be considered for any equation attempting to estimate flow resistance in steep streams. There are two main approaches that have been used; an empirical approach modifying boundary layer theory equations (Section 2.5), and consideration of the individual drag forces from the large sediment in the channel (Section 2.6).

2.5 Boundary layer theory

2.5.1 'Law of the wall'

The 'law of the wall' (Schlichting, 1979; Yalin, 1992; Bathurst, 1993) uses the relationship between shear stress and velocity gradient in the bottom 10-20% of the flow, where the channel bed (the wall) affects the flow. The 'law of the wall', which can be used to calculate velocity, v, at a height z in the velocity profile, is defined by Equation 2.13. Shear velocity u_* is equal to $\left(\frac{\tau}{\rho}\right)^{1/2}$, where τ is bed shear stress, κ is von Karman's constant (equal to 0.41), k_S is a measure of the roughness height of the sediment (sometimes termed equivalent sand roughness height), B is a value representing the boundary conditions (equal to 8.5 for rough, turbulent flow) and log is to base 10;

$$\frac{v}{u_*} = \frac{2.303}{\kappa}\log\left(\frac{z}{k_s}\right) + B \qquad \textbf{[2.13]}$$

For the rest of the flow (i.e. the upper 80-90%), the velocity profile can be described by Equation 2.14, known as the velocity-defect law (Schlichting, 1979),

$$\frac{v - U_s}{u_*} = \frac{2.303}{\kappa}\log\left(\frac{z}{d_{bl}}\right) + W \qquad \textbf{[2.14]}$$

where U_S is the freestream velocity, d_{bl} is boundary layer thickness and W is a wake function which accounts for the divergence of the velocity profile from the semi-logarithmic line, which depends on the flow conditions. Combination of Equations 2.13 and 2.14, and converting to mean velocity, $\overline{U}$, produces Equation 2.15, which can be used to determine mean velocity in the velocity profile;

$$\frac{\overline{U}}{u_*} = \frac{2.303}{\kappa}\log\left(\frac{d}{k_s}\right) + C_r \qquad \textbf{[2.15]}$$

where C_r is a value representing the roughness characteristics of the channel and the value of W in Equation 2.14.

2.5.2 Resistance equations based on the 'law of the wall'

The use of mean flow velocity in Equation 2.15 enables this equation to be combined with the Darcy-Weisbach equation and, therefore, the development of resistance equations based on boundary layer theory. By use of the fact that (assuming the profile is logarithmic throughout the whole flow depth) the average velocity is equal to velocity at the dimensionless level z/d = 0.368 (e^{-1}), equations can be written of the form of Equation 2.16. In this equation, coefficient a is equal to $e^{\kappa C-1}$, which represents channel characteristics (Bathurst, 1985; Bathurst, 1993), and D is the effective roughness height of the bed material. Equation 2.16 is a simplification of part of the Colebrook-White equation (described by Hey, 1979); the only difference between this and the Keulegan equation (Keulegan, 1938; Bathurst, 1993) is that k_S rather than D is used for the latter.

$$\left(\frac{8}{f}\right)^{1/2} = 5.62\log\left(\frac{aR}{D}\right) \qquad [2.16]$$

Whilst the equations in the previous sub-section (2.5.1) and Equation 2.16 have been developed for channels where there is low relative roughness, the equations can be modified and constants added to attempt to account for the variation caused by the presence of large sediment in steep streams. Hey (1979) discovered empirically that D is equivalent to 3.5 D_{84} in channels with non-uniform sediment, and modified Equation 2.16 to produce Equation 2.17 for gravel-bed rivers with pool-riffle sequences. Equations similar to his have also been found by Bray (1979) and Griffiths (1981).

$$\left(\frac{8}{f}\right)^{1/2} = 5.62\log\left(\frac{aR}{3.5D_{84}}\right) \qquad [2.17]$$

Theoretically, resistance equations based on the 'law of the wall' cannot be applied to steep streams with large sediment disrupting the flow. Therefore, there are two main approaches to estimating average velocity in steep streams, empirical modifications of equations of the type of Equation 2.17 (discussed in 2.5.3), and consideration of the drag forces acting on the flow (discussed in 2.6).

2.5.3 Empirical modifications to 'law of the wall' resistance equations

Bathurst (1985) tested 2.17 using field data from steep streams. It was found that resistance was underestimated quite considerably - actual resistance could be up to 66% greater than predicted. However, for steep streams with intermediate-scale roughness, the predicted values were closer to the actual values. Bathurst (1985) suggested an empirical modification to 2.17 which fitted the data better. This is shown by Equation 2.18:

$$\left(\frac{8}{f}\right)^{1/2} = 5.62\log\left(\frac{d}{D_{84}}\right) + 4 \qquad \textbf{[2.18]}$$

This equation was also developed by Graf et al (1983) from flume data. However, errors of up to ±35% are associated with it (tested with data from slopes of 0.4 to 4% and relative submergence $d/D_{84}<10$).

Thompson and Campbell (1979) modified Nikuradse's resistance equation to produce Equation 2.19. This equation has been shown to work well for a range of relative roughnesses (Church et al, 1990). It was developed after study of an artificial channel (with 0.052 slope) built for a hydro-electric power station with artificial steps;

$$\left(\frac{8}{f}\right)^{1/2} = 5.62\left(1-\frac{0.1k_s}{R}\right)\log\left(\frac{12R}{k_s}\right) \qquad \textbf{[2.19]}$$

Other empirical resistance equations for use in steep streams with large sediment have been developed by Bathurst (1978), based on work by Judd and Peterson (1969), for channels with intermediate-scale roughness, considering only the most significant boulders. However, it only considers step spacing and relative submergence, and the function is poorly defined. Bathurst et al (1981) and Bathurst (1982a) developed empirical equations from flume experiments based on the influence of the various factors influencing the drag coefficient; and Smart and Jaeggi (1983) developed an equation for use in channels with very high sediment transport rates. However, this type of equation is not considered useful for this research as they depend on empirical coefficients and constants, meaning that they are only applicable to the flows in which they were developed.

2.6 Drag force theory

2.6.1 Equations based on drag force theory

These equations consider the combined drag on the flow caused by the largest sized particles in the flow. As flow is forced around the boulders, a drag force is exerted on the clast which produces resistance to the flow caused by a decrease in momentum (Wiberg and Smith, 1991). This drag force, D_F, on an object (e.g. a boulder) in a flow of uniform velocity, $\overline{U}$, is given in Equation 2.20 below (Bathurst, 1993; Wiberg and Smith, 1991):

$$D_F = \frac{\rho}{2} A_F \overline{U}^2 C_D \qquad \textbf{[2.20]}$$

where A_F is the frontal cross-sectional area of the object, and C_D is the drag coefficient (factors affecting it are considered later in this section). Therefore, the resistive stress on a flow, τ, caused by n isolated, identical elements on an area of bed A_{bed} is given by Equation 2.21 (Bathurst, 1993):

$$\tau = \frac{\sum_1^n D_F}{A_{bed}} = \frac{\rho}{2} \lambda \overline{U}^2 C_D \qquad \textbf{[2.21]}$$

where λ, the roughness spacing / concentration is equal to $\frac{\sum_1^n A_F}{A_{bed}}$.

El Khashab (1986) produced a similar set of equations for the drag force (D_{FS}) created by a step. These are shown in Equations 2.22 and 2.23.

$$D_{FS} = \frac{\rho}{2} h B_S \overline{U}^2 C_D \qquad [2.22]$$

where h is the step height, and B_S is the step width (similar to A_F in Equation 2.20). The resistive stress, τ, like Equation 2.21, is given by the drag force from the step divided by the bed area. This is shown in Equation 2.23, where L is the spacing between steps, so the product of this and step width gives the area of bed occupied by one step-pool sequence:

$$\tau = \frac{D_{FS}}{LB_S} = \frac{\rho h}{2L} \overline{U}^2 C_D \qquad [2.23]$$

There is potential in using these equations to determine velocity by combining equations of the type of 2.21 and 2.23 with equations relating velocity and shear stress. This has been studied by Wiberg and Smith (1987; 1991) with good agreement with field data. This approach is very promising as it is not empirical. Rather, it considers the actual sediment in the stream in question; therefore, it can be applied to any stream where the effect of the boulders in terms of drag force can be estimated. This approach is considered further in Chapter 10. The rest of this section will consider the factors affecting the value of C_D, the drag coefficient.

2.6.2 Factors affecting roughness

Equation 2.24 has been used by several workers (Bathurst et al, 1981; Bathurst, 1982a; Noori, 1984; El Khashab, 1986) to study the effects of various variables on the value of the drag coefficent, C_D.

$$C_D = \frac{2gR}{\overline{U}^2 \cos\theta} \qquad [2.24]$$

where θ is the angle in degrees between the channel bed and horizontal. This equation assumes that the drag force accounts for all of the resistance to flow. El Khashab (1986) stated that at least 92-98% of resistance in steep streams with large-scale roughness was from form drag, so use of this equation would seem to be reasonable. It was found that the following were important controls of C_D and therefore resistance:

- Reynolds number,
- Froude number,
- Roughness geometry,
- Channel geometry,
- Bed material movement.

Reynolds number and Froude number affect the drag coefficient of each individual element; the others affect the overall resistance. Each will be considered separately in the rest of this section.

2.6.3 Reynolds number

Equation 2.25 defines Reynolds number (*Re*), which is the ratio of the inertial and viscous forces in the flow. k is the object height and γ is kinematic viscosity (approximately equal to $1 \times 10^{-6}\ m^2 s^{-1}$ at typical stream water temperature);

$$Re = \frac{\overline{U}k}{\gamma} \qquad [2.25]$$

Laminar flow ($Re < 500$) produces the highest drag, which is constant except at extreme values. For transitional flow ($500 < Re < 2000$), an increase in Reynolds number leads to a decrease in drag (also found by El Khashab, 1986), until the flow is turbulent ($Re > 2000$), where again the drag is constant except at extreme values. The critical value for laminar to transitional flow is dependent on the roughness of the element and the state of the external flow; the rougher the element surface and the more turbulence in the external flow, the lower this critical value.

2.6.4 Froude number

Froude number affects the development of hydraulic jumps and the generation of drag from distortions of the free surface (if the element protrudes through or nearly through the free surface). Flammer et al (1970), using Equation 2.4 to calculate Froude number (*Fr*), found the following during a study of isolated hemispheres:

- For a given relative submergence, an increase in *Fr* leads to an increase in free surface drag, until it reaches a peak when any further rise in *Fr* causes drag to decrease.
- For relative submergence greater than 0.8 this peak occurs at $0.5<Fr<0.6$, whereas for relative submergences of less than 0.5 the peak occurs at approximately critical flow (i.e. $Fr=1$). This difference is caused by the differential formation of hydraulic jumps (Bathurst, 1982a).

El Khashab (1986) and Noori (1984) found an almost perfect relationship between *Fr* and drag, however, their work was looking at very high *Fr* values (>2) and artificial sediment. Generally, an increase in *Fr* causes a decrease in drag as it is usually associated with an increase in relative submergence. This decreases the number of elements affecting the free surface, and so decreases drag. However, initially an increase in *Fr* causes an increase in drag because of the formation of localised super-critical flow around the elements and the formation of hydraulic jumps.

2.6.5 Roughness geometry

This considers the combined effect of the elements on flow resistance, which depends on:

- the proportion of the bed material which contributes significantly to form drag;
- the amount to which each of these elements affects the flow.

These two factors are determined by the geometry and arrangement of the elements; i.e. the relative submergence and concentration of the elements. Not all the elements on the bed need to be considered - only those projecting significantly into the flow (Bathurst, 1978; Nowell and Church, 1979; Bathurst et al, 1981; Bathurst, 1982a). These *n* significant elements comprise the effective roughness concentration Λ_e:

$$\Lambda_e = \frac{\sum_{1}^{n} A_F}{A_{bed}} \qquad [2.26]$$

Depth, and therefore relative submergence, is very important. An increase in depth decreases the number of significant elements, which leads to a decrease in effective roughness concentration and resistance (illustrated in Figure 2.5). A wide range of bed material sizes leads to a slower rate of change of roughness with change in depth, as there are always some significant elements affecting the flow.

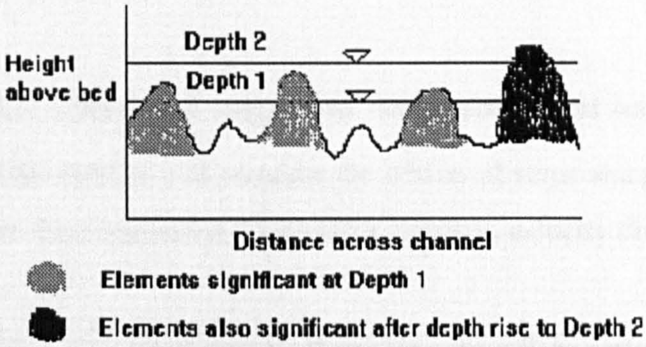

Figure 2.5 Effective roughness concentration after rise in water depth

The spacing of the elements is important as closer spaced elements increase the drag force per unit area more than ones spaced wider. However, if they are so close that the elements become influenced by the wake of neighbouring elements, resistance decreases with closer spacing (Bathurst, 1993).

2.6.6 Channel geometry

This affects the area A_{bed} in Equation 2.26, and therefore effective roughness concentration and relative roughness area (i.e. the proportion of the total cross-sectional area occupied by projecting boulders). Relative roughness area is important for resistance as it affects the degree to which the flow is funnelled between elements (Bathurst, 1985). Slope also appears to be an important measure; work carried out by

Noori (1984) and El Khashab (1986) showed that relationships found between C_D and Reynolds number and relative roughness, for example, plotted on different lines for different slope values.

2.6.7 Bed material movement

Initially sediment movement decreases resistance, as fines fill in the gaps between roughness elements leading to a smoothing effect (Bathurst, 1982a). Increasing transport further, however, makes it possible for sediment to bounce up into the flow which increases resistance as momentum is extracted from the flow. Also, if increased transport leads to an uneven bed, resistance will be increased.

2.7 Effects of steps and large sediment on flow

This section will consider the effects of steps and pools (and large roughness elements) on flow resistance, hydraulic geometry, velocity distribution, and sediment transport.

2.7.1 Effects of step-pool sequences on flow resistance

Step-pool sequences dissipate energy and prevent erosion in the following ways:

- **Bed armouring** - the coarsest sediment is at the surface, which increases form resistance to flow and protects the bed from erosion (Heede, 1981).
- **Step-pool bedform sequence** - leads to an increase in bed form roughness. This will be considered further in 2.7.2.
- **Turbulent mixing** - the flow plunges into pools below steps, where hydraulic jumps cause energy to be dissipated by roller eddies (Whittaker, 1987a). 95% of the *potential* stream energy at the step is dissipated by turbulent mixing (Hayward, 1980). With closely spaced steps the flow becomes very turbulent with intensive and continuous energy dissipation (Chin, 1989).

2.7.2 Step spacing and resistance to flow

It has been suggested by Davies (1980) that the spacing of the steps corresponds to maximum resistance to flow; this has been supported by field studies carried out by

Chin (1989) and Wohl and Grodek (1994). The effect that step spacing has on the resistance to flow (from form roughness) may be a factor in explaining the spacing characteristics of steps and pools and its relationship with gradient and width. It has been suggested by workers such as Davies (1980) and Davies and Sutherland (1980) and Ergenzinger (1992) that rivers adjust in order to maximise resistance to flow, which means that the spacing of bedforms will reflect this tendency.

Davies (1980), from flume studies, showed that resistance increases as the ratio of spacing to height decreases (i.e. as spacing becomes closer and the steps higher), reaching a maximum value of resistance which indicates the spacing that bedforms will preferentially have. However, a further decrease in the ratio from this point leads to a decrease in resistance. Bathurst (1993) suggests that this could be caused by flow becoming affected by the wake from a neighbouring object, although this was a study with isolated objects on a smooth surface as opposed to steps.

In the case of steps, it has been found that spacing *does* tend to correspond to maximum resistance to flow. Whittaker and Jaeggi (1982), from flume experiments creating step-pool sequences used the concept of 'roughness spacing', *e*, as a measure of resistance. This roughness spacing is equal to the sum of the heights of all the significant roughness elements divided by the length of the sample reach. They found that, for a slope range of 1 to 24%, the step spacing was that which should produce maximum resistance to flow. Wohl and Grodek (1994) found that *e* increased with increasing channel slope, reflecting closer spacing and higher steps at steeper slopes.

There is obviously some discrepancy between studies of roughness spacing, as found by Wohl and Grodek (1994) when they compared their results with those of Rouse (1965) and Davies (1980). They (Wohl and Grodek) found that using Rouse's result (that 0.15-0.25 represented maximum *e*) suggested maximum resistance to flow would occur at slopes of 12-50%. However, using Davies' theory that maximum resistance to flow occurs at a spacing to height ratio of 10-20, would mean that maximum resistance to flow would occur on gradients of 3-10%. This spacing to height ratio seems acceptable, as Chin (1989) found a value of 11.

A similar approach by Abrahams et al (1995) suggests that the spacing of steps and pools is adjusted in order to maximise resistance to flow, and that $1 \leq \left(\frac{\overline{H}}{\overline{L}S}\right) \leq 2$. They also showed that evenly spaced steps create the greatest resistance to flow. This seems to go a considerable way to explaining the spacing of steps - i.e. spacing reflects maximum resistance to flow, and at steeper gradients there is more energy, so resistance to flow must increase (shown by Whittaker and Jaeggi, 1982 to occur).

2.7.3 Hydraulic geometry

The effect of the sediment on the flow means that hydraulic geometry relationships are different to those found in lowland streams. An overall hydraulic description of any reach can be obtained from the relationships between discharge and velocity, width and depth, as discharge varies over time (i.e. the at-a-point hydraulic geometry of the sites). Studying these relationships provides information about how the flow in the stream is affected by the sediment and to what extent. Hydraulic geometry can be defined by the following equations:

$$w = aQ^b \quad \textbf{[2.27]}$$

$$d = cQ^j \quad \textbf{[2.28]}$$

$$\overline{U} = kQ^m \quad \textbf{[2.29]}$$

Q is discharge, w is channel width, d is channel depth and $\overline{U}$ is mean velocity. From continuity (i.e. $Q=wd\overline{U}$), the sum of the exponents and the product of the intercepts equal unity, i.e. $b+j+m=1$ and $ack=1$. The values of the exponents reflect the channel characteristics (as they show the relative rates of increase of velocity, depth and velocity with discharge), and hence different values exist for lowland streams and steep streams. Typical values for the exponents are shown in Table 2.2. It is clear that the type of channel has a very pronounced effect on the value of the exponent, in particular the value of the velocity exponent, m. The values of the intercepts have not been given much attention in the literature for any type of stream.

Table 2.2 At a point hydraulic geometry exponents for different channel types.

Exponent	Sand	Gravel	Boulder (no steps and pools)	Boulder (steps and pools)
Velocity (m)	0.34	0.49	0.51	0.69
Width (b)	0.26	0.12	0.10	0.13
Depth (j)	0.40	0.39	0.39	0.19
Data source	Leopold and Maddock (1953)	Bathurst (1993)	Bathurst (1993)	Lisle (1986)

Velocity at a given discharge is lower in steep streams with large sediment because of the increased resistance. However, the rate of increase of velocity with discharge is higher as the effects from the roughness elements become significantly reduced at higher discharges and increased submergences. The channels are usually more confined than lowland channels because of the upland environment, which affects the relationship between discharge and depth.

There are significant problems determining hydraulic geometry relationships in steep streams because of fieldwork problems involved in obtaining measurements. Determining velocity is difficult because of the nature of steep streams. For at-a-point velocity, current meters are hard to use as the bed is very uneven, air bubbles are present in the flow, and the channels are often shallow. Jarrett (1988) claims that some types of current meter tend to overestimate velocity. Therefore, obtaining a reach average using salt dilution gauging is a popular method (Kellerhals, 1970; Kellerhals, 1972; Day, 1976; Beven et al, 1979; Elder et al, 1990; Kite, 1993), which is based on the principle of mass conservation of a chemical tracer before and after dilution by a flowing stream. Estimating width and depth is also more difficult than in lowland streams because of the large variation in these variables as a result of the sediment present in the channel.

2.7.4 Velocity distribution

The most obvious velocity characteristic is that flow over the steps is considerably faster than flow in the pools (because of energy dissipation); and is often super-critical over steps, whilst sub-critical in pools. This leads to a cyclic pattern of acceleration and deceleration of flow (Peterson and Mohanty, 1960). In a lowland stream, the velocity profile can be divided into two parts, the lower part (bottom 10-20% of the flow) where boundary layer theory is used ('law of the wall'), and the upper 80-90% of the flow, where the velocity defect law can be used to describe the velocity profile. However, in steep streams the presence of large clasts (and low ratios of depth to sediment size) causes the velocity profile to deviate from the logarithmic velocity profile characteristic of lowland streams (Wiberg and Smith, 1987; Jarrett, 1988; Wiberg and Smith, 1991; Bathurst, 1993). This is caused by the following (Bathurst, 1993):

- Flow below the tops of the large boulders causes the velocity to be reduced because of drag from the elements reducing the momentum of the flow. This leads to a lower velocity in the lower part of the profile.
- Flow above the boulders is not impeded by drag from the boulders, so high velocities can develop. The point at which this occurs is unclear - the boulders will still affect the flow when they are just topped; when their influence is no longer present is not known. Hey (1979) suggested that this roughness height is equivalent to $3.5D_{84}$ (as used in Equation 2.26).

These two factors lead to a 'S-shaped' profile (if roughness is large- or intermediate-scale). Therefore, if a logarithmic velocity law (law of the wall, velocity defect law) is used to represent the velocity in a steep stream, mean velocity will tend to be underestimated, and hence resistance overestimated (Bathurst, 1993). Figure 2.6 shows the difference between a logarithmic velocity profile and a S-shaped profile (from Bathurst, 1993). Figure 2.6a is from a steep stream; Figure 2.6b is from a flume experiment. As can be seen from the data associated with each graph, the differences are because of variations in sediment size and sorting; not from gradient or relative submergence differences. With smaller sized, uniform sediment there is not space for flow between particles, i.e. most of the flow is above the sediment, so the S-shaped profile cannot develop. At low flow, the boulders protrude through the flow, so only the low velocity zone between the boulders forms. At high flow, the boulders are submerged, leading to the development of the upper zone of the S-shaped profile. This leads to a decrease in boulder form drag as their effect is drowned out, and, therefore, increased velocity results.

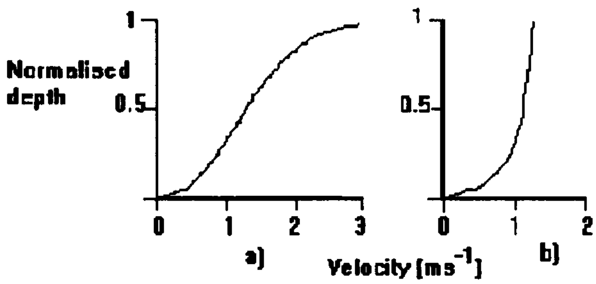

a) slope=0.035, D_{84}=223mm, D_{84}/D_{50}=2.05, d/D_{84}=2.46

b) slope=0.03, D_{84}=28.8mm, D_{84}/D_{50}=1.3, d/D_{84}=1.74

Figure 2.6 Comparison between a) 'S-shaped' velocity profile and b) logarithmic velocity profile.

2.7.5 Sediment transport

In steep streams, it is important to consider that there is a wide range of sediment sizes. This means that transport is affected by armouring and packing, and hiding and protrusion effects are considerable (Lisle, 1987). Also, sediment sources vary temporally and spatially; typical sources are landslides, bank collapses, and debris flows, meaning that sediment transport is non-uniform and unsteady (Bathurst, 1987b). Warburton (1992) proposed a three phase model of bedload transport for steep, coarse-bedded streams with heterogeneous bed material to describe the break up of bed features:

1. Flushing out of fines which were deposited in the channel during low flows (particularly in pools).
2. With a higher discharge, the armour layer is broken meaning that larger sediment can be transported and more sediment is available for transport.
3. Further sediment transportation results in the destruction of the step-pool structure and clusters.

There will also be differences in transport rate between steps and pools because of the differences in shear stress. Tracer experiments (Schmidt and Ergenzinger, 1992) have shown that pools are the most active part of the river bed in terms of the bedload budget; they are favoured sites of deposition, and are important sources of sediment.

2.7.6 Initial movement of sediment

The amount of sediment that a channel can move depends on the shear stress, τ, acting on the bed of the channel (Equation 2.30). The classical equation for defining initial sediment movement is that of Shields (1936), who developed the theory of selective entrainment, i.e. that smaller sediment will be entrained at a lower shear stress than necessary for larger sediment. He showed, by force-balance analysis, that for a bed of uniform sediment, the critical shear stress necessary to move sediment of size D, τ_{cr}, depends purely on the absolute size of the sediment particle. This is shown in Equation 2.31. His laboratory experiments gave a constant value of 0.06 for dimensionless critical shear stress, τ_{cr*}, for uniform sediment greater than 1 mm in size in rough, turbulent flow.

$$\tau = \rho g R S \qquad [2.30]$$

$$\tau_{cr*} = \frac{\tau_{cr}}{(\rho_s - \rho) g D} \qquad [2.31]$$

However, work by Fenton and Abbott (1977), Parker and Klingeman (1982), Andrews (1983), and Andrews and Parker (1987) has illustrated that in poorly sorted sediment, the effects of hiding and protrusion mean that it is *relative* not absolute sediment size that is most important. Sediment smaller than the D_{50} grainsize is hidden by relatively larger sediment, whereas larger sediment protrudes into the flow and is relatively easier to entrain. Therefore, near-equal mobility of all grain sizes exists as a result of these effects. Andrews (1983) developed Equation 2.32, where a value of between 0.65 and 1 for W has been offered (Ferguson, 1994);

$$\tau_{cr*} = \tau_{cr50*} \left(\frac{D_i}{D_{50}} \right)^{-W} \qquad [2.32]$$

For use in steep streams, it has been suggested that the value of τ_{cr*} increases to >0.1 as slopes increase to greater than 1%, and relative submergence decreases to less than 10 (because of the non-logarithmic velocity profile (Bathurst, 1987b)). Wiberg and Smith (1987) suggested that a value of as high as 9.5 may be necessary to move small, hidden sediment (*D/d*=0.02) on a slope of 0.035 (based on theoretical velocity profile modelling to determine the velocity gradient and associated shear stress). Ashida et al (1981) suggested a value of 0.46 for the same slope and that the value of τ_{cr*} is a function of channel slope.

An approach using critical unit discharge (q_{cr}) has been attempted by several workers as is considered more applicable to steep streams (Schoklitsch, 1962; Billi et al, 1995; Whittaker, 1987; Ferguson, 1994; Smart, 1984 and Smart and Jaeggi, 1983). This is because of difficulties with determining shear stress in steep streams as a result of the non-logarithmic velocity profile structure and difficulties in calculating depth. However, there are still problems with applying this approach, as considered by Ferguson (1994).

2.8 Conclusions

The following were concluded from the study of the literature:

- The processes leading to the formation of steps and pools are unclear, and bedrock steps have not been considered in formation theories.
- There are few theoretical equations available for steps and pools; generally equations developed for lowland streams are not acceptable for steep streams because of the non-logarithmic velocity profile and the presence of large roughness elements.
- Fieldwork in such environments is complicated, and techniques such as current metering are not advised for steep streams.
- The controls on step spacing are not completely understood, and the effect of the steps on resistance remains unclear.
- There is considerable scope for research in this area.

Overall, it appears that there is a lack of knowledge concerning resistance in steep streams, and also a lack of accurate equations with a scientific basis; especially ones that can be applied to high flows. Generally, equations developed for lowland rivers with small-scale roughness cannot be applied to high gradient channels as they do not account for the huge effect of large sediment.

Chapter 3

Initial reconnaissance survey and choice of fieldsites

3.1 Introduction and aims of the survey

Before starting the fieldwork part of the research it was considered necessary to carry out an initial reconnaissance survey of potential fieldsites in order to identify what features are actually representative of steep streams, to begin learning about the processes at work in steep streams, and to become familiar with conducting fieldwork in such environments.

Therefore, the aims of this survey were:

- Determine how common streams with step-pool sequences are in the Peak District - are there step and pool sequences in every steep stream? What is the range of channel width, slope, and sediment size within which steps and pools are found to form? Is there a random element also involved, or do all streams within a certain range of conditions always produce step and pool sequences?
- Investigate the geometry of the step-pool sequences found, and their relationship with variables such as slope and channel width. From this is may be possible to learn something about their formation and help select representative sites for the detailed fieldwork;
- Identify any other features typical of steep streams (e.g. dead zones) and consider any implications these might have for future fieldwork;
- Practise and develop fieldwork techniques associated with carrying out fieldwork in steep streams, and identify potential problems;
- Identify a number of study sites to be used for the detailed fieldwork later, making sure that a representative range of stream variables are included.

It was important to ensure that a wide range of streams were studied in order to 'see the whole picture' as far as steps and pools are concerned. Therefore, a range of slopes, bedrock type and stream size were included in the study. A map of the Peak District was studied to identify areas that should be visited in order to achieve these aims. The map in Appendix 1 shows the locations of the streams studied during the survey.

3.2 Fieldwork methodology

The first visit to streams in the Peak District was just to observe what types of features occur, what the streams are actually like, and get an idea of how common step and pool sequences are. With this information it was then possible to design a fieldwork survey sheet for the reconnaissance survey.

The survey sheet used is in Appendix 2. Explanation of this, and in particular how the measurements were carried out, will be discussed in this section. The fieldwork methodology had to achieve the aims of the survey, but the methods needed to be quick, and practical for only one person to carry out. The main consideration was the choice of reach to obtain the measurements from. It was decided that to avoid choosing 'good' reaches, and in order to have a continuous survey, a reach would consist of 20 steps and pools. Therefore, there was no fixed length of reach, rather a fixed number of steps. To cover a number of streams and a number of reaches in the same stream, detailed measurements were only carried out on the 19th, 20th and 21st steps and pools (where the 21st sequence is the first step and pool of the next reach in the survey).

The following were also studied during the survey:

- step characteristics in the reach;
- reach geometry (length, width and slope);
- step-pool sequence characteristics.

3.2.1 Step characteristics in the reach

Firstly, the type of step was recorded, i.e. whether it completely or only partially crossed the channel, whether it crossed the channel at right angles to the bank or obliquely, and whether the step was bedrock or alluvial (to determine whether there is any relationship between the frequency of alluvial and bedrock steps and factors such as slope). An estimate of the length of channel taken up by waterfalls and rapids was also recorded in order to assist the calculation of average distance between steps. If this is not taken into account then the result may suggest that the steps are more widely spaced than they actually are, as a considerable part of the reach will not contain steps and pools if there are waterfalls and rapids instead.

3.2.2 Reach geometry

The length of the reach was measured using a tape measure along one bank, swapping bank at intervals to avoid inaccuracies as a result of meanders etc. Obviously there will be some error associated with this, as it was not possible to keep the tape measure at the same level due to bank undulations etc. This was not a significant error as the length of the reaches was usually over 100 m, and the value was only used to estimate average step spacing.

An estimate of the average reach channel width was needed in order to study the relationships between channel with, step spacing and slope, and to give a measure of the overall channel size for that reach. In order to get a reasonable average but ensure that the survey did not become too time consuming, the average width of the channel at the 19th, 20th and 21st steps was used. A metre rule was used to measure the distance between the banks - this was easier to use than a 30 m tape measure for one person. One possible problem with this is if there is a difference in width between steps and pools (i.e. if the width of the channel is generally greater at pools), then the method described above will consistently underestimate the width. This did not appear to be the case from the streams visited prior to the survey so it was decided that this method, whilst not ideal, was adequate to achieve the aims of the survey, and ensure that the survey did not become too time consuming.

A clinometer was used to estimate the slope of the reach. Whilst not providing as accurate a measure of slope as using the EDM would, it was the only option considering the survey was planned to be carried out with only one person. As the reaches were usually around 100 m in length, it was impossible to obtain an average for the entire reach. Therefore, the slope readings are an indication of the slope of the last 10-20 m (depending on how much of the channel was in view) of the reach up to the 20th step. One measurement was taken sighting upstream and another sighting downstream, and the average of these values used. Obtaining channel slope from an Ordnance Survey map proved useless as the reaches were too short to cross enough contours on the map to get an accurate measure of gradient.

3.2.3 Step-pool sequence characteristics

At the 20th step, the maximum water depth over the step and in the pool was measured with a metre rule. This was to aid with planning the next fieldwork stage, as it was important to determine whether the water was generally deep enough for current meter measurements. Also, it was considered interesting to compare the step water depth with the pool water depth. It was decided that only maximum water depth would be measured as this was relatively easy to estimate quickly. Determining average water depth would have been very time consuming considering the large variation of depth in steep streams.

It was also considered useful to estimate the size of the largest sediment, in order to study any relationships between this and the other variables measured, and also to ensure that the fieldsites chosen for the detailed fieldwork included a wide range of sediment size. The largest particle present (from either the 19th, 20th or 21st step) was identified (D_{max}) and measured with the metre rule. The size class that this fits into (see Appendix 2 for the classes used) could then be recorded. As with water depth, maximum sediment size only was recorded as this was easier to measure than obtaining an average value, and was adequate for achieving the aims of the survey. The D_{max} particle was usually too large to move, and was usually partially hidden by other clasts in the step. Therefore, it was impossible to ensure that the b-axis was measured for each clast.

An attempt was also made to measure the height of the step so that this value could be related to slope. The initial visit made to steep streams prior to performing the reconnaissance survey appeared to show that as channel slope increases, so does the height of the step. However, it was very hard to decide at which part of the step to take the measurement at as the step height was not uniform across its width. To avoid taking many measurements (which was not the idea of the reconnaissance survey) the highest point of the step was used, with step height being the vertical distance from this point to the bed of the pool.

Using the 30 m tape rule, the distances between the 19th and 20th step, and the 20th and 21st step were measured. These distances were generally measured along the bank, however, if the bank was very undulating the metre rule was used in the channel itself. This provided one measure of step spacing. It was also possible to use the length of the reach and the number of steps in the reach to obtain another value for average step spacing. To avoid overestimating step spacing the length of the reach taken up by waterfalls, rapids and pools and riffles (where no steps were present) was subtracted from the length of the reach.

3.2.4 Problems carrying out the survey

Distinguishing between bedrock steps and waterfalls was thought to be a potential problem. In order to establish whether they are generically the same feature it was considered important to be able to distinguish between the two and so identify the range of conditions necessary for their occurrence. Whilst they may appear to be very similar, and both features dissipate energy in steep streams, if they are generically the same feature then there would be alluvial steps with the same geometry as waterfalls, whereas the waterfalls observed were comprised only of bedrock. It was, therefore, considered likely that steps and waterfalls are different features. The upper limit for the height of alluvial steps was approximately the width of the step, so it was decided that this was also likely to be the upper limit for bedrock step height. Hence, if the drop was greater than the width, the feature was classified as a waterfall. In practise, however, it was not hard to distinguish between these features as the waterfalls were usually much higher than the steps, also backing up the theory that they are basically different features.

Carrying out the survey showed that fieldwork in steep streams is considerably harder than in lowland streams because of the high variability of width, depth etc. and the presence of many large boulders, meaning that many of the measurements were harder to obtain than was thought prior to the survey. In particular, the slope over the reach appeared to be very variable, but the only measurement of slope that was taken was the slope at the very end of the reach. If this slope is not representative of the entire reach this will lead to problems with the data analysis, as some of the variables (e.g. reach average step spacing and the number of waterfalls, rapids, alluvial steps and bedrock steps) are for the entire reach. The same was true for the channel width measurements. It was, therefore, important to consider this fact when analysing the data from the survey, and to ensure that this was not a problem with the detailed fieldwork.

3.3 Results and observations

In total, 30 reaches were studied (at seven different streams). Full results are in Appendix 3, and the range of conditions observed at these streams is summarised in Table 3.1.

3.3.1 Presence of steps and pools

All the streams visited during the survey had step-pool sequences. This is, perhaps, not surprising considering that the streams visited were chosen because it was thought likely that they would contain steps and pools (based on information obtained from the literature on steps and pools). The study confirms that step pool sequences are 'ubiquitous features of steep streams' (as was suggested by Chin, 1989 and Wohl and Grodek, 1994), and are found within a wide range of channel conditions. However, there did appear to be a random element involved as some stretches of the streams had no steps and pools, even though the channel characteristics were within the range expected to produce such features.

Generally, steps and pools occurred where the channel gradient was between about 0.026 and 0.176. Below 0.026 (e.g. at the lower part of Burbage Brook and Ashop) pools and riffles occurred, and above 0.176 (e.g. Fairbrook and Grindsbrook) waterfalls and rapids tended to occur. It was seen that the stream could alternate between these features depending on the channel gradient i.e. if the channel became steeper than 0.176 waterfalls and rapids would be present, and if the channel returned to less than this gradient further upstream then steps and pools would return (and likewise for pools and riffles at gentler slopes).

Table 3.1. Range of variables measured during the reconnaissance survey

Channel property	**Minimum**	**Maximum**
Reach length (m)	85	362
Width (m)	0.85	4.78
Channel gradient	0.026	0.176
Average reach step spacing (m)	3.2	19.1
Maximum sediment size (cm)	50	175
Waterfalls and rapids (%)	0	47
Pools and riffles (%)	0	4

The proportion of bedrock steps appeared to increase at higher gradients. These steps appeared to dissipate more energy as they had larger pools, larger hydraulic jumps, more white water and were often higher than alluvial steps. This would seem logical if the idea that steps and pools keep a channel at equilibrium by dissipating energy is true, as at steeper slopes the stream has more energy. On these high gradient slopes the steps were more pronounced and generally seemed to be higher than steps on lower gradients. Also, some of the streams studied were more prone to producing bedrock steps, e.g. on the Burbage and Ashop reaches bedrock steps were rare, whereas on the Fairbrook and Grindsbrook reaches they were more common. This might be related to sediment supply - if there is no shortage of sediment alluvial steps are, perhaps, more likely to be formed.

3.3.2 Other features observed

All of the streams contained dead zones; their presence presumably because of the variability in channel width and in particular because of the low flow conditions at the time of the survey. When the sites were visited during high flow there were fewer dead zones, and some of the reaches did not contain any. Some of the reaches contained meanders, and it appeared that on the lower slopes the meandering parts of the reach did not contain step and pool sequences, whereas on the steeper slopes they did. One possible explanation is that meandering parts are not preferred sites for steps and pools (because of the flow paths in a meander), but at steep slopes there is so much energy to be dissipated that all possible parts of the channel need to form steps and pools. Most of the pools and riffles observed during the survey were on River Ashop on a lower gradient to that on which steps and pools were observed (and so did not actually form part of the reconnaissance survey).

The length of stream taken up by waterfalls and rapids varied considerably; the amount appeared to depend on the stream rather than any other channel variable. Some streams seemed to be more likely to produce waterfalls and rapids, for example there were no waterfalls observed on River Ashop, Doctors Gate and Burbage (although rapids were observed on the River Ashop and Burbage), whilst the Fairbrook reaches seemed most prone to waterfalls. Whilst Upper Seal Clough (a tributary of Fairbrook) had 47% of the channel taken up by waterfalls and rapids, at this site only one short reach was studied as the stream was very narrow and very steep - further upstream the channel was comprised almost completely of waterfalls.

If a site was more likely to produce waterfalls it was also more likely to produce rapids and bedrock steps. This tendency to have waterfalls and rapids was independent of other factors such as slope and width, i.e. at a given slope waterfalls may form on the Fairbrook reaches but not on reaches in other streams. The reason for this tendency is not known, but it might be associated with sediment supply as bedrock steps, rapids and waterfalls do not have loose alluvial sediment, suggesting that these features are more common where there is a shortage of sediment. The survey also indicated that waterfalls are separate features to steps as they were found on higher gradients, and the height was much greater than the height of steps; if they were the same feature, then there would be a gradual change from steps to waterfalls.

3.3.3 Nature of the steps

Twenty-one reaches contained at least one oblique step, whilst only nine contained partial steps. This indicates that in the streams surveyed, and therefore steep streams in general, oblique steps are common (possibly caused when the flow direction is not perpendicular to the banks, for example, because of boulders further upstream deflecting the flow). However, partial steps were not so common. This is understandable, as for steps to be effective they need to slow down the flow all the way across the channel, not just across a part of the channel. Where there were partial steps, the part of the stream without the step tended to be a slower flowing part of the stream (e.g. a dead zone). This would appear to confirm the idea that steps form in order to keep the stream at equilibrium - in these locations it is not necessary to slow the flow down.

3.3.4 Quantification of step spacing

The measurement that was considered to be the most interesting, and therefore the one that was studied most in terms of relationships with other variables, was step spacing. This is because step spacing determines how much energy is dissipated and so understanding what controls step spacing may help to understand why steps and pools form. Also, this is the parameter that has been most studied by other workers, so it was considered of interest to compare results from this study with the others that have been carried out.

As mentioned earlier, there were two methods used to calculate step spacing. The first used the average of the spacing between the 19th and 20th, and the 20th and 21st steps. The second method calculated a reach average step spacing by dividing the total length of the reach (subtracting the distance estimated to have been taken up by waterfalls, rapids and meanders) by the number of steps in the reach. When looking at the relationships with other stream characteristics, using the data obtained by this latter method provided the best results. Therefore, this is the data that was used for the analysis, despite the fact that the other measurements taken (i.e. width and slope) were generally not a reach average, but were obtained from measurements taken only at the end of the reach.

Step spacing ranged from 3.2 to 19.1 m. In terms of channel width, an average of 2.98 $\pm$ 0.42 was found. This is generally a larger value than that found by other workers (Grant et al, 1990; Chin, 1989). These values were shown in Table 2.1. Whittaker (1987b) found a value of 2.7, which is close to the value determined from this survey.

The difference between this value and those found from other studies is not just a result of the way in which reach average step spacing was measured, as using the values obtained from averaging the spacing between the 20th and 19th, and the 20th and 21st steps results in a value of 2.5, still considerably different from the values found by other workers.

3.3.5 Relationship between step spacing and channel geometry

The relationships between spacing and width, and spacing and gradient were studied as these have both previously produced significant relationships (Grant et al, 1990; Chin, 1989; Whittaker, 1987b). When considering all the data points, there was a slightly better relationship between spacing and gradient than spacing and width, as seen in Figures 3.1 and 3.2. The relationship between spacing and width was a positive linear one (r=0.57; p<0.01), whereas the relationship with gradient was a negative power one (r=-0.61; p<0.01).

Multiple regression analysis showed that considering gradient and width accounted for most of the variation in step spacing (R^2=0.44, with both predictors significant at p<0.01 level). This is as expected, as at steeper slopes the streams are smaller and narrower, and there is more energy to be dissipated. Another explanation could be that width is the controlling factor for creation of steps and pools, and so this also means there is a strong relationship between width and slope. This relationship is shown in Figure 3.3. As expected, there is mainly a negative relationship, i.e. as slope decreases width increases. It was unexpected that at very high slopes (greater than 0.125) this relationship became positive, i.e. steeper slopes have wider widths. The data for this relationship is from a number of the streams studied, so it is not just a feature of a single site. One explanation for this could be associated with the way in which the width measurements were taken, i.e. being the average of the width of three of the steps. At steeper slopes the sediment size is generally larger, which could lead to wider steps at steeper slopes.

To attempt to remove some of the scatter obscuring the relationships, the data was grouped and averaged (into slope and width groups). This illustrated the relationships better, as Figures 3.4 and 3.5 show. When the data was compared with that found by other workers, a good comparison was found. Figure 3.6 shows the average data for the relationship between gradient (S) and step spacing (L) from this study, and data from Whittaker (1987b), Grant et al (1990) and Billi et al (1995). As can be seen, this matches well. However, when the equation devised by Whittaker (1987b) was used to predict step spacing (Equation 3.1), spacing is overestimated for low gradients and underestimated for high gradients (Figure 3.7):

$$L = \frac{0.3113}{S^{1.188}} \qquad \textbf{[3.1]}$$

Also interesting is that in this study there appeared to be a slight increase in spacing at high gradients, occurring at a gradient of about 0.13. Study of Figure 3.6 also shows this increase in the data of Whittaker (1987b) and Billi (1995). The data from the study carried out by Grant et al (1990) does not show this increase as they did not study gradients above 0.13. This is associated with the observed increase in channel width (Figure 3.3), possibly as a result of larger sediment at steeper slopes.

3.3.6 Other relationships

The value obtained for maximum sediment size was not as easily explainable as was originally thought. There was no relationship found between this and step spacing, gradient or channel width, even though this might be expected, because at steeper slopes the sediment is larger. These relationships are shown in Figures 3.8a-c. When multiple regression analysis was carried out relating step spacing to other channel characteristics, sediment size had no effect on the analysis. The fact that no relationships were found could possibly be attributed to the way that the sediment size was estimated, being simply a measure of the size of the largest particle from the 19th, 20th or 21st step. This is not a very accurate method and it only provides a record of one of the particles rather than an average. However, this was considered adequate for this survey as the aim was just to determine what range of maximum sediment size existed to aid with choosing fieldsites. The largest sized sediment was observed at the Burbage site (175 cm).

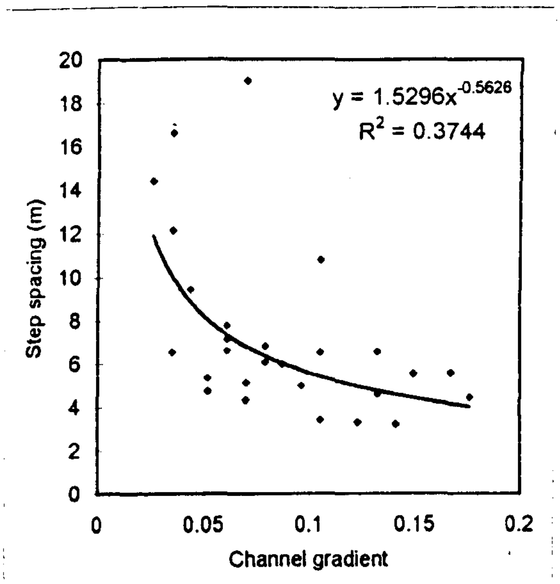

Figure 3.1 Power relationship between gradient and step spacing

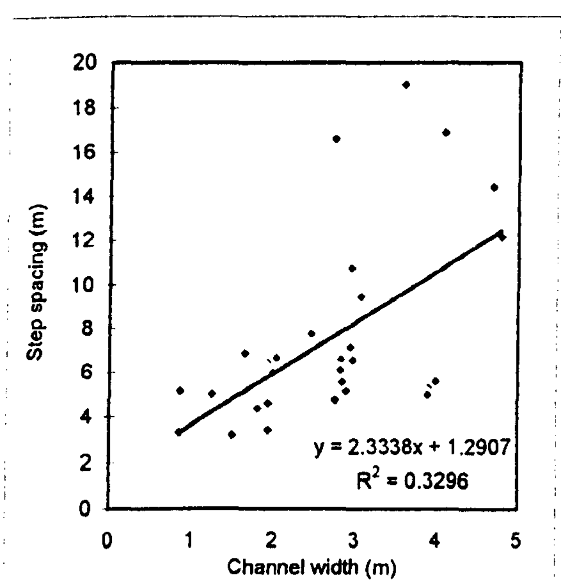

Figure 3.2 Relationship between channel width and step spacing

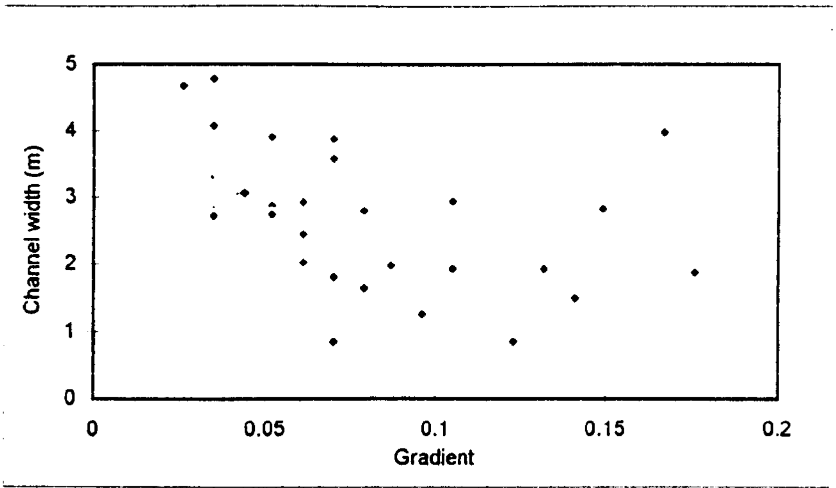

Figure 3.3 Relationship between channel gradient and width

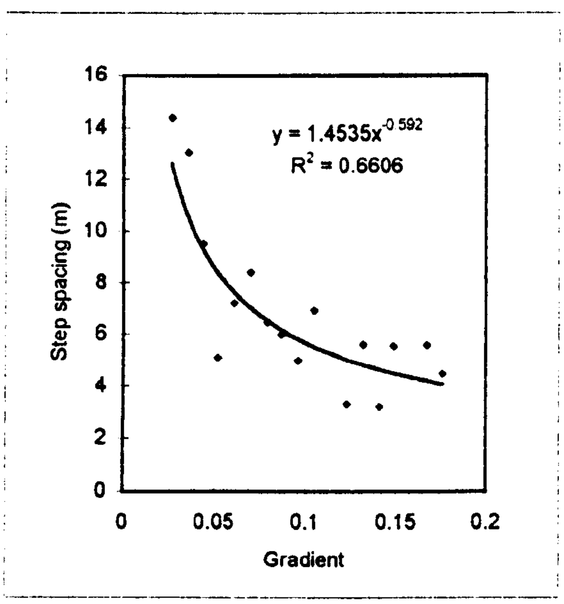

Figure 3.4 Power relationship between gradient and step spacing using grouped data.

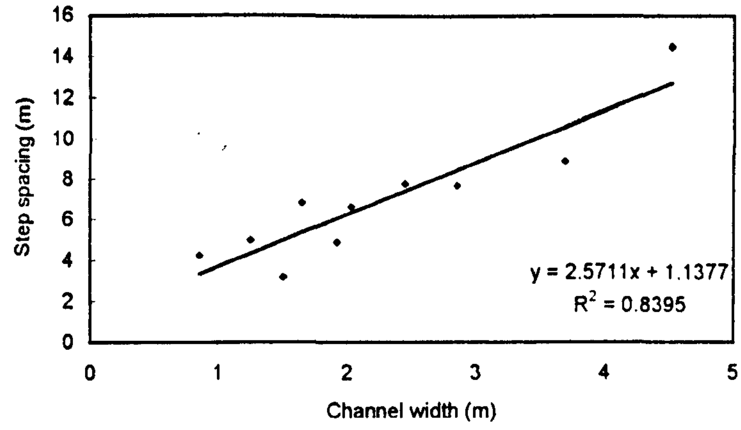

Figure 3.5 Relationship between channel width and step spacing using grouped data.

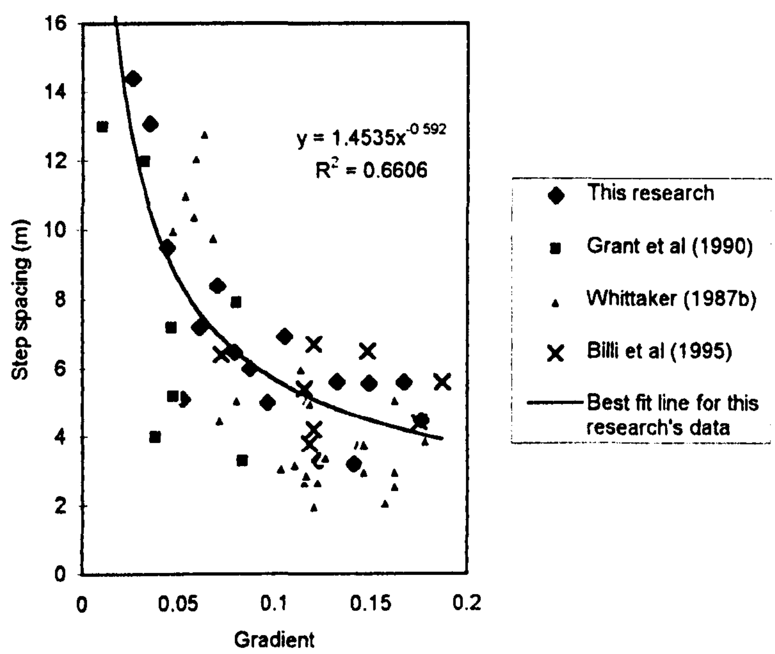

Figure 3.6 Composite plot showing gradient and step spacing data for this research compared with that obtained by previous workers.

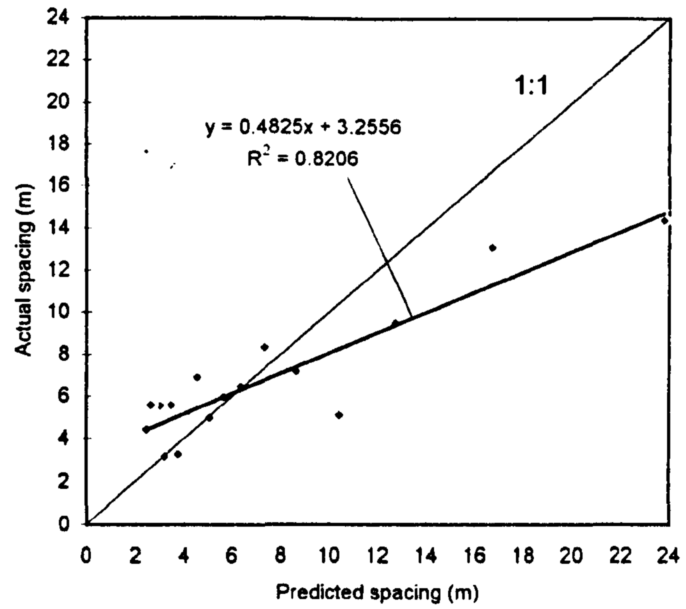

Figure 3.7 Relationship between predicted spacing using Equation 3.1 (Whittaker, 1987b) and actual spacing.

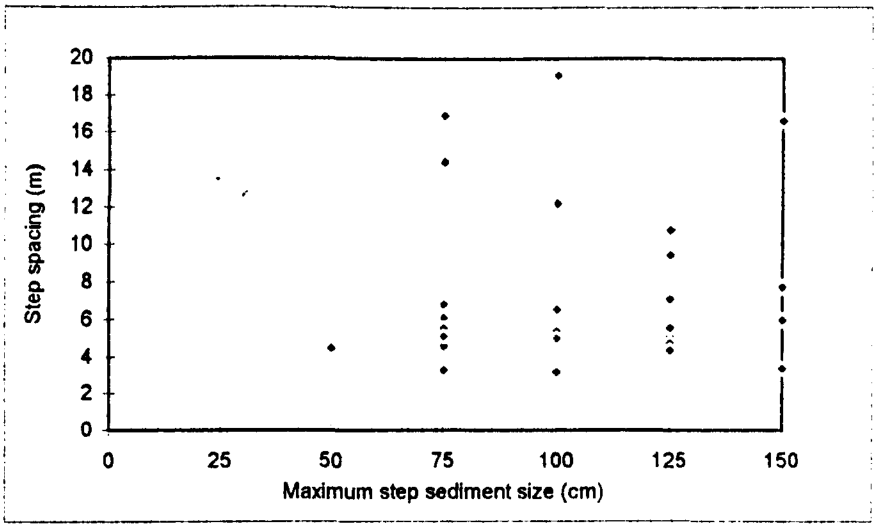

Figure 3.8a.

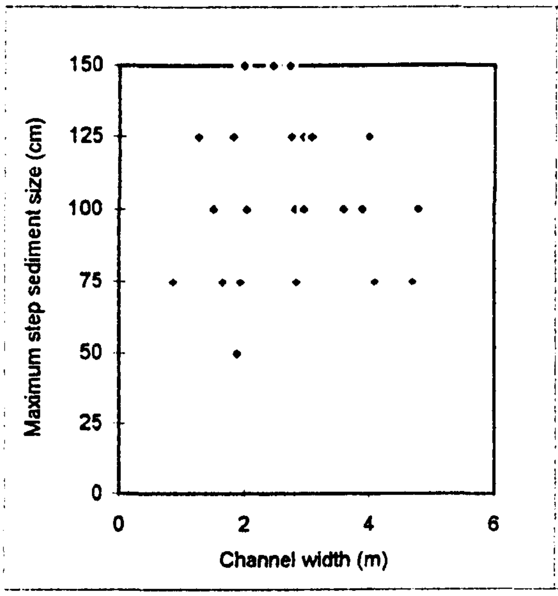

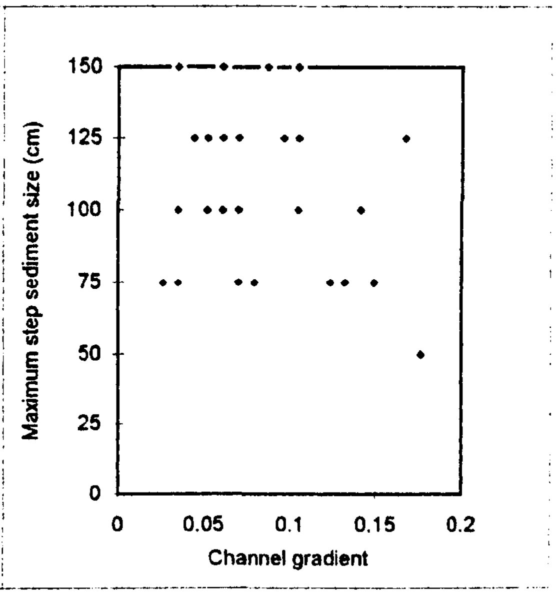

Figure 3.8b

Figure 3.8c.

Figure 3.8. Relationship between maximum step sediment size and a) step spacing, b) channel width and c) channel gradient.

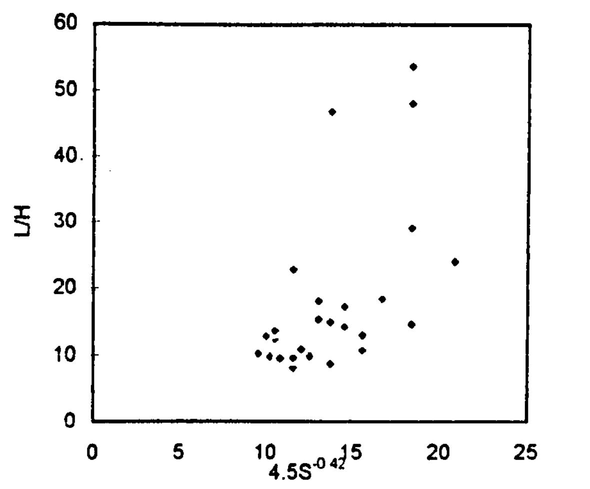

Figure 3.9. Relationship between channel slope (S) and step spacing (L) and step height (H) using Equation 3.2 (Wohl and Grodek, 1994).

Two proposed relationships between average step height (H), spacing (L) and channel gradient (S) were studied; one suggested by Wohl and Grodek (1994), the other by Abrahams et al (1995). The equation proposed by Wohl and Grodek is Equation 3.2, shown graphically in Figure 3.9 using data from this survey.

$$\frac{L}{H} = 4.5S^{-0.42} \qquad [3.2]$$

Abrahams et al (1995) suggested that the inequality $1 \leq \left(\frac{\overline{H}}{\overline{LS}} \right) \leq 2$ describes maximisation to flow resistance. This survey found this inequality was valid at only 12 of the 30 reaches. This suggests that either the values obtained for step height were inaccurate (which is possible considering it was very hard to determine step height because of the high variability), or for some reason flow resistance is not maximised at most of the sites.

3.3.7 Implications for research and fieldwork aims

The survey was very useful for two main reasons. Firstly, for finding out about steep streams and starting to understand what factors are important (and so what would be worth studying further). Secondly, a lot was learnt about the logistics of carrying out fieldwork in steep streams, and what methods are impractical or would produce very inaccurate results. These points needed to be considered when designing the fieldwork methodology for the main fieldwork stage of the research.

The survey suggested that the effect of step spacing on resistance is worthy of further study. The results indicated that in parts of the stream where there is more energy, e.g. if the stream is very steep, the step spacing decreases, meaning that more energy is dissipated. The effect this has on the velocity of the stream would be interesting to study, in particular the variation with sediment submergence as a result of change in discharge. Study of the relationships between step spacing and the other parameters measured showed that channel width and slope are important. However, more detailed measurements were considered necessary in order to establish whether slope or width is the most important factor. If it is slope that is most important then this backs up the theory that steps are necessary in steep streams to dissipate energy, and, therefore, the steeper the slope, the closer together the steps will be. Equation 3.3 can be used to define stream power (rate of dissipation of energy) Ω, in W m^{-1}, showing that slope is a component of power.

$$\Omega = \rho g Q S \qquad [3.3]$$

As far as fieldwork techniques are concerned, the reconnaissance survey highlighted the fact there are many potential problems associated with carrying out fieldwork in steep streams, and, therefore, methods need to be developed to ensure accurate data collection during the main part of the fieldwork. The following were identified as points to consider when carrying out the detailed fieldwork part of the research:

- The data collected should be from the same part of the stream, e.g. for slope and step spacing measurements. This suggests that the best way to carry out the detailed fieldwork is by having short reaches, over which distance average values for all the parameters can be obtained.
- The various parameters studied varied between step and pool, e.g. sediment size, water depth and possibly channel width. Therefore, steps and pools need be treated separately in that measurements should be taken from both in order to obtain a step average, a pool average, and an overall reach average.
- The only accurate way to obtain some of the data is by using the EDM. For example it proved impossible to obtain a value for step height during the reconnaissance survey. Therefore, EDM surveys of all of the sites was considered necessary to obtain slope, step geometry etc.

3.4 Selection of fieldsites for the detailed fieldwork

It was decided that six sites would be used for the detailed fieldwork. This number was considered large enough to include a wide range of sites, yet small enough to be manageable bearing in mind the time available for the detailed fieldwork, and the fact that a number of visits would be necessary to each site.

3.4.1 Rationale for stream selection

In order to understand fully the processes at work, reaches with a range of channel gradient, width, sediment size and tendency to produce waterfalls, rapids and bedrock steps were selected. Before selecting the specific reaches, the results of the reconnaissance survey were studied to determine the variability observed during the course of the survey. How far the site is from convenient parking, and how easy it is to get to the site were considered important factors. This is because heavy equipment was required at the site, and also the time factor. Whether permission could be obtained to carry out fieldwork at the proposed site was also a consideration, although in practise this was not a problem.

It was decided that one site would be on the River Ashop. This is where the lowest gradient was observed, pools and riffles as well as step-pool sequences were present, and it was the widest stream studied (>5 m). Doctor's Gate was the narrowest stream studied (<1 m), therefore a site was desirable on this stream. Including a narrow stream should also allow some study of the effect (if any) of bank roughness. Burbage Brook was also considered interesting as the sediment size was larger at this site than at any of the others observed during the reconnaissance survey, and it also contained steep reaches. The upper reaches of Grindsbrook had some waterfalls and rapids, so this site was also considered interesting. A high gradient (>0.176) study site was planned for this river. A second study site on Grindsbrook was also planned as this part of the river showed the most 'classical' step and pool sequences observed, with alluvial steps dominating. Fairbrook contained many bedrock steps, waterfalls and rapids at moderate gradients, making further study of this stream also desirable.

3.4.2 Reach selection

The streams chosen for the detailed fieldwork were visited again, and reaches with characteristics as close as possible to those outlined in Section 3.4.1 were selected, bearing in mind accessibility and the sites' suitability for salt dilution gauging. To be suitable for salt dilution gauging a reach should have no tributaries and no significant dead zones. As the study reaches were planned to be only about 20 m long, the salt needed to be injected some way upstream in order to ensure complete mixing (a distance of about 20 times the channel width was needed). Therefore, some consideration of the channel upstream of the reach was needed; tributaries and dead zones should be avoided in this part of the stream upstream of the study reach.

In order to ensure that any relationships observed are due to slope, width and step geometry variations and not due to other factors like the number of dead zones and meanders it was important to keep the sites as uniform as possible for all parameters other than those to be studied. Therefore, it was also considered important to choose sites that were as free as possible from dead zones for this reason, and that each site should contain an uninterrupted sequence of, ideally, five steps and pools. However, the reach should be typical of streams at that gradient, therefore a low gradient reach need not contain an uninterrupted sequence of steps and pools as at <0.035 often there are pools and riffles interspersed with the steps and pools.

3.4.3 Description of the study reaches

The sites selected are described in Table 3.2, using data determined from the EDM survey of the site to calculate reach average slope and width (note that this is bankfull width). The location of the sites can be seen in Appendix 1 (shown in more detail in Figure 4.4g in the next chapter), and photographs of the individual sites are Figures 3.10a - f.

Table 3.2. Description of the main characteristics of the sites used for the detailed fieldwork

Site	Gradient	Width (m)	Number of steps and pools
River Ashop	0.0266	5.12	3
Burbage Brook	0.0971	2.76	5
Doctor's Gate	0.0582	1.40	6
Fairbrook	0.0662	3.08	4
Grinds Brook A	0.1254	3.37	4
Grinds Brook B	0.1838	2.59	4

3.4.4 Detailed fieldwork

Bearing in mind the results of the reconnaissance survey, the following was carried out at each of the sites:

- Detailed surveying using an EDM of the channel and in particular the steps and pools in order to obtain step geometry, channel width, slope and roughness. Sediment size and distribution data was obtained from a sediment survey of the reach. This was carried out during Summer 1996, where the flow levels were generally very low, and is described in Chapter 4.
- Salt dilution gauging to determine discharge and velocity, carried out at a variety of discharges, to determine how velocity changes with discharge. The runs were done between Spring 1996 and Spring 1997, during which time there was a wide range of flow conditions. Also, flow resistance (calculated using the Darcy-Weisbach equation) can be determined by using the velocity value from the salt dilution gauging, gradient from the EDM surveying, and width from measurements taken at the time of the salt dilution gauging. This is covered in Chapter 5.
- Chapter 7 will then combine the results obtained from the surveying and the salt dilution gauging in order to try to explain the relationships found at the different sites. The variation of velocity with discharge is mainly a result of the resistance, which can be quantified in terms of the channel geometry and sediment characteristics described in Chapter 4.

Figure 3.10a River Ashop

Figure 3.10b Burbage

Figure 3.10c Doctors Gate

Figure 3.10d Fairbrook

Figure 3.10e Grindsbrook A

Figure 3.10f Grindsbrook B

Chapter 4

Field methods I - Site and sediment characteristics

4.1 Introduction

This chapter will discuss how the overall site geometry and sediment characteristics were determined. It was considered necessary to determine these characteristics in order to:

- further investigate the features that are characteristic of streams with steps and pools;
- determine whether the characteristics are also related to the degree of development of the step-pool sequences;
- enable comparison with the results found by other workers who have studied step-pool sequences in the field;
- identify any features or oddities that would affect the stream in terms of velocity increase with increasing discharge, i.e. any features that would be useful in explaining the salt dilution gauging fieldwork (described in Chapter 7);
- compare the characteristics of the steps with those in the pools, and comparison between the sites.

It was important to have the following information about each of the sites to achieve these described aims:

- channel slope,
- step spacing,
- channel width,
- sediment distribution,
- relative roughness,
- a measure of the development of the step-pool sequences.

To obtain these data, i.e. to characterise each site in terms of general geometry and features, at each of the six study reaches the site was first marked out with wooden pegs to identify the steps. Then, the site was surveyed using an Electronic Distance Meter (EDM), paying particular interest to the banks, water edges, steps and pools, and large boulders to plot up an accurate diagrammatic representation of the site and obtain, for example, step spacing and slope values. Also, photographs were taken at low and high flow as a visual record of the site, and to enable comparison of the amount of sediment protrusion at the different flow levels, and to determine whether there had been any changes in the steps after a very high flow event.

To quantify the sediment characteristics of the study reaches in terms of sediment size and relative roughness, a modified 'Wolman type' count was carried out to obtain a site average value for the sediment in the steps and pools. This can be used to compare the sediment characteristics of the different sites. Detailed transects across the steps and pools were surveyed using the EDM in order to quantify the roughness for each site, and also to study the amount of protrusion at different flow depths.

The methodology of how these studies were carried out and the results found are discussed in more detail in the following sections.

4.2 Sediment size distribution

An estimation of the D_{50} and D_{84} values is useful for comparison of the sediment between the steps and pools, and also between sites. These values can also be compared with the channel depth to obtain a measure of relative roughness. As a result of the nature of streams with step and pool sequences, it was necessary to determine a separate value for the steps and pools, as the sediment making up the steps was expected to be significantly larger than the sediment in the pools. However, to accurately compare the results between the two, the method employed needed to be similar. Wohl et al (1996) reviewed methods available for sampling in coarse sediment channels. The method employed for this research was devised following study of their review and consideration of the field situation.

4.2.1 Methodology

In order to sample the whole reach, sediment from each step and pool was studied. If the reach had 4 steps and pools, then 25 particles from each step and pool were measured to provide 100 measurements from the step sediment and 100 from the pools. If it was not possible to reach this number, as many measurements as possible were taken (for example if the step is a bedrock step there were usually only a few particles). In this situation more particles were sampled from the other steps in that reach.

It was decided that a random-pacing selection method was not practical as it was important to keep the step sediment separate from the pool sediment, and since the steps were relatively narrow it would be impossible to randomly pace-sample from them. Since it was important to use the same sampling method for the steps and pools this meant the method could not be used for either. The original intention was to have two transects for each step and pool (marked out using a tape measure), and to measure the size of the particle directly under the tape measure every e.g. 20 cm in order to get 12 or 13 measurements from each transect.

However, at the first reach visited it became clear that this was not practical, and would not provide a representative value for sediment size as sometimes a step transect would only consist of a few large boulders. Therefore, the method was altered so that for the steps the first 25 particles making up the step (starting from one side of the stream and working across the step) were measured. Gravel trapped between boulders was ignored, and only sediment larger than 8 mm was measured. For the pools, the transect method was feasible since the sediment was generally significantly smaller (gravel was again ignored). Whilst this meant that the methods used to measure the sediment in the steps and pools were not identical, this was believed to be the best methodology to employ. As there were no natural sediment variations with periodicies matching the sampling interval, the methods used provide a controlled, quasi-random sampling approach.

A metre rule was used to measure the size of the sediment. This is because most of the sediment was too large for a template, and a lot of it was immovable, especially in the steps. This meant that it was sometimes hard to obtain an accurate measurement of the b-axis (which was the axis measured where possible) as in the steps, where several particles may be packed together, it was often impossible to see exactly where the *b*-axis went to and from. In these situations, if it was considered impossible to estimate the length of the *b*-axis, that particle was ignored. Smaller sediment that could be moved was measured using a template and replaced once that step-pool sequence had been finished with to avoid measuring the same particle more than once.

4.2.2 Results

The graphs in Figure 4.1 show the sediment distribution from the field sites. As expected, the size of the sediment in the steps is larger than the sediment in the pools. The step sediment is also more variable - the total range of sizes for the step sediment, when considering all the sites, is greater than for the pool sediment. For D_{84} the range of step sediment varies from 296 mm (Doctor's Gate) to 781 mm (Grindsbrook B), whereas for pool sediment this range is 152 mm (Doctor's Gate) to 225 mm (Burbage). However, the magnitude of the difference varies considerably, as seen in Table 4.1. For all the sites other than the two Grindsbrook sites the step D_{50} values are between 75% and 107% higher than the pool D_{50} values. However, at Grindsbrook A this value is 495%, and at Grindsbrook B is 390%.

At Grindsbrook A the step D_{84} is 277% higher than the pool D_{84}, and at Grindsbrook B it is 346% higher. The other sites have values for step D_{84} between 59% and 113% higher than the pool D_{84} values. This indicates that the two Grindsbrook sites have a considerably different sediment distribution than the other four sites. This is a reflection of the fact that the sediment at Grindsbrook is considerably coarser than the others, and the fact that this large sediment accumulates in the steps as a result of step formation. Whilst Burbage has a larger D_{max} than Grindsbrook A, the D_{84} values are higher for Grindsbrook A, suggesting that whilst Burbage contains some exceptionally large sediment, generally Grindsbrook has a larger proportion of larger sediment, and the variation between the steps and the pools is therefore higher.

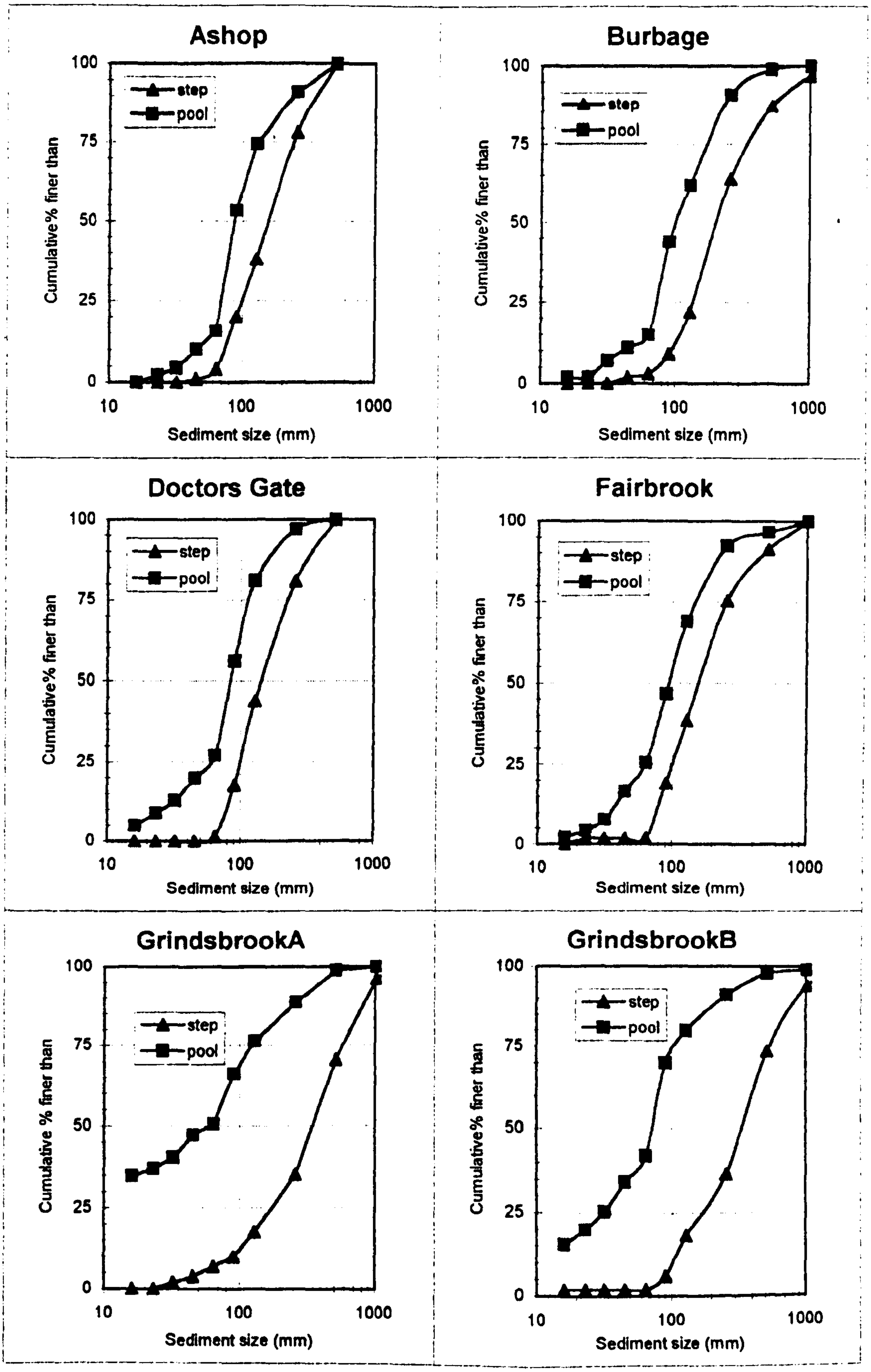

Figure 4.1. Sediment size distributions at each of the fieldsites

Table 4.1. Results from the sediment distribution analysis. The percentages in parentheses are the increase in step values over the pool values.

Site	Step D_{50} (mm)	Pool D_{50} (mm)	Step D_{84} (mm)	Pool D_{84} (mm)	Step D_{84}/D_{50}	Pool D_{84}/D_{50}	Step D_{max} (mm)	Pool D_{max} (mm)
Ashop	166 (89%)	88	320 (59%)	201	1.93	2.28	490 (11%)	440
Burbage	213 (107%)	103	479 (113%)	225	2.25	2.18	1700 (113%)	800
Doctor's Gate	149 (75%)	85	296 (95%)	152	1.99	1.79	500 (56%)	320
Fairbrook	168 (75%)	96	395 (87%)	211	2.35	2.20	790 (23%)	640
Grindsbrook A	363 (495%)	61	781 (277%)	207	2.15	3.39	1140 (104%)	560
Grindsbrook B	348 (390%)	71	776 (346%)	174	2.23	2.45	2600 (145%)	1060

The D_{max} values reflect the fact that at Ashop and Doctor's Gate the steps are less pronounced, and so the difference between step and pool D_{max} is not as great as at the other sites. However, at Fairbrook the steps were very pronounced, yet the step D_{max} is not much larger than pool D_{max}. This highlights one of the limitations of this sediment survey; Fairbrook contains more bedrock in the steps than any of the other sites, however, this was ignored in the sediment survey.

The variability of the sediment within the steps and pools at each site can be determined by the ratio D_{84}/D_{50}. The site with the lowest sorting ratio was Doctor's Gate, a reflection of the fact that this was the narrowest site and had, overall, the smallest step sediment. It is, perhaps, surprising that the largest ratios were found for the pool sediment for Grindsbrook B (3.39) and Grindsbrook A (2.45). It is postulated that at Grindsbrook there is a large supply of step-sized sediment, all of which cannot be accommodated in the steps and, therefore, some is present in the pools, leading to a large sorting ratio for the pool sediment. This could also be the case at Ashop, where the pool sorting ratio (2.28) is also greater than the step sorting ratio (1.93).

4.2.3 Relative roughness

This concept was discussed in more detail in Chapter 2, along with the concept of relative submergence. Relative roughness is the ratio of the sediment size to the flow depth; relative submergence is the ratio of flow depth to sediment size. In this study relative roughness is generally used. It is more useful than absolute size for quantifying the effect of the sediment on the flow, since it looks at the sediment size in relation to the depth of the flow. If a stream has a large relative roughness, then the sediment will considerably resist the flow of the water (and hence the flow will have a higher friction factor), whereas a stream with a smaller relative roughness will have less of an effect on the flow.

To estimate relative roughness at different flow depths, the equation relating discharge and depth (determined from the salt dilution gauging data) was used to estimate depth at a range of discharges. All the sites were surveyed during a very dry summer (within the same week, during which there was no rainfall), meaning it is likely that the lowest discharge that occurred during the course of the fieldwork was measured at each of the sites during this period. This flow level can, therefore, be used to relate the sites to each other. From the depth-discharge equation the predicted depth (d_{min}) at this lowest discharge (Q_{min}) was found, and also the predicted depth at this base discharge multiplied by a range of values (up to 100 times the base discharge, where the depth is termed d_{100}). The relative roughness for each of these depths was then determined, and could be compared with the other sites. This is not ideal as the estimate of depth is a reach average, but the sediment measure is either from just the steps or just the pools.

Figure 4.2 shows graphs for the calculated relative roughness in the steps and the pools. These show that most of the variation in relative roughness occurs at discharges up to 20 times the base discharge, indicating that it is this range of discharge where the effect of the sediment on the flow is highest. It can also be seen that at Burbage, Doctor's Gate and Grindsbrook A the range of relative roughness is highest, again suggesting that the sediment effect on the flow velocity is greatest at these sites.

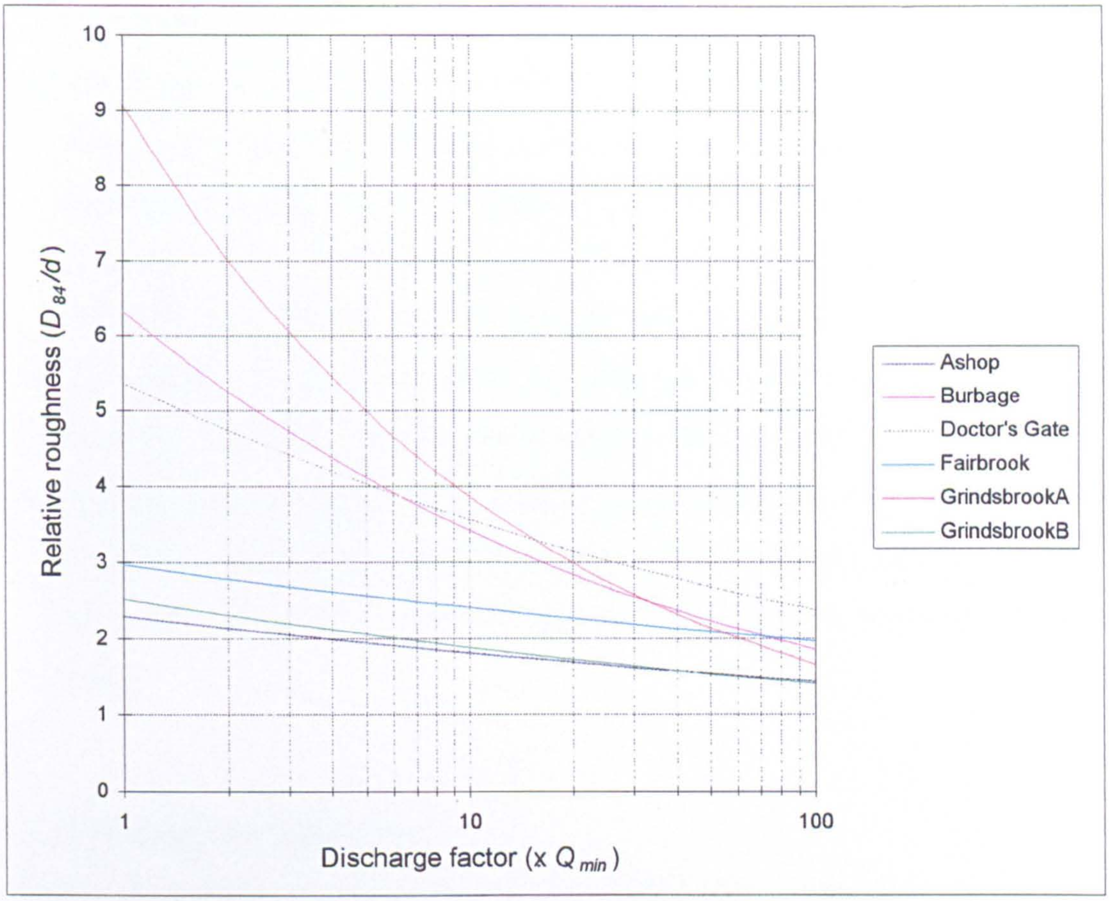

Figure 4.2a. Step.

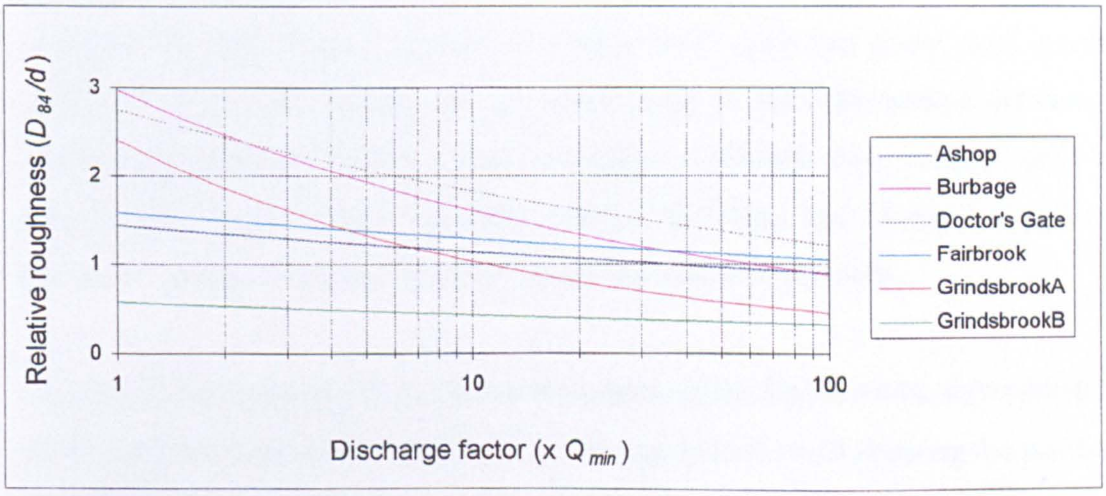

Figure 4.2b. Pool.

Figure 4.2. Calculated relative roughnesses using D_{84} for a) steps and b) pools

4.2.4 Conclusions

The following can be concluded from the sediment distribution study:

- There is a significant difference in the sediment size between steps and pools, indicating that step - pool formation causes larger sediment to accumulate in the steps. Sites with more visually pronounced steps and pools generally had a greater difference in the sediment size between the steps and pools.
- The sediment size survey carried out does not account for sites with significant quantities of bedrock making up the steps (for example, Fairbrook).
- Burbage, Doctor's Gate and Grindsbrook A are expected to be affected most by the sediment in the channel as they have a large range of relative roughness, especially at flows up to 20 times the lowest (base) discharge observed during the salt dilution study.

4.3 Overall site geometry

Using the EDM, a detailed survey of each of the study reaches was carried out, with particular attention paid to the steps and pools. Three to four hundred points were surveyed at each of the sites. The aim of the surveying was to plot detailed site diagrams, identify features typical of reaches with steps and pools, and determine values for slope, step spacing etc. to enable study of the relationships between step spacing and channel geometry. Also, surveying would have been carried out if there was a large flood event to identify whether the steps had changed morphology. However, such an event did not occur during the period of the study.

The surveying is also useful in order to have an accurate diagrammatic representation of all the sites. A longitudinal profile and a plan map of each reach showing the position of the steps and pools as well as all the major boulders were plotted. These survey maps are shown in Figures 4.3 (longitudinal profiles) and 4.4a to f (plan maps). Figure 4.4g shows a map of the Peak District with the location of the study sites.

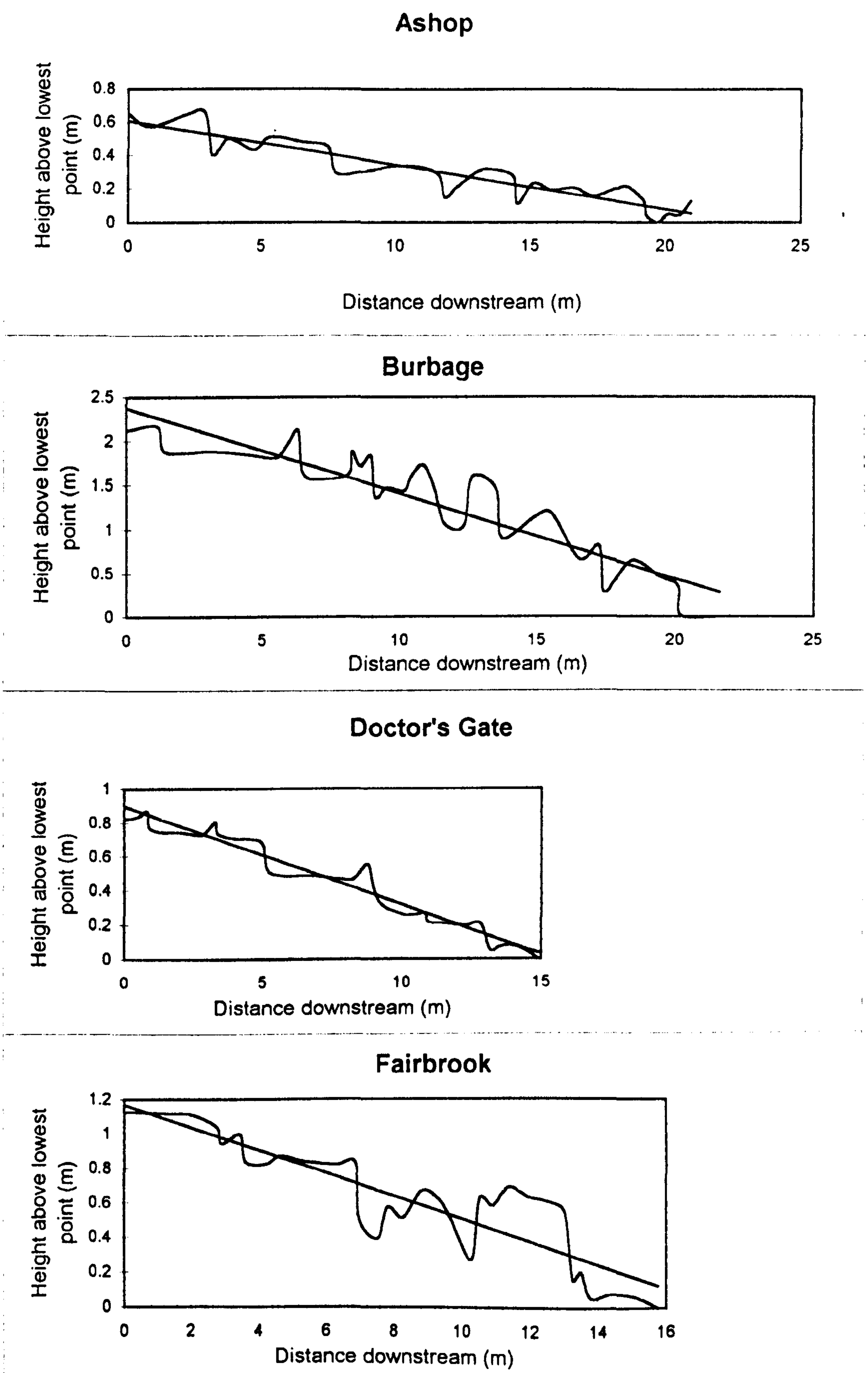

Figure 4.3. Longitudinal profiles for the fieldsites. Note the use of different y axis scales for the Burbage and Grindsbrook sites.

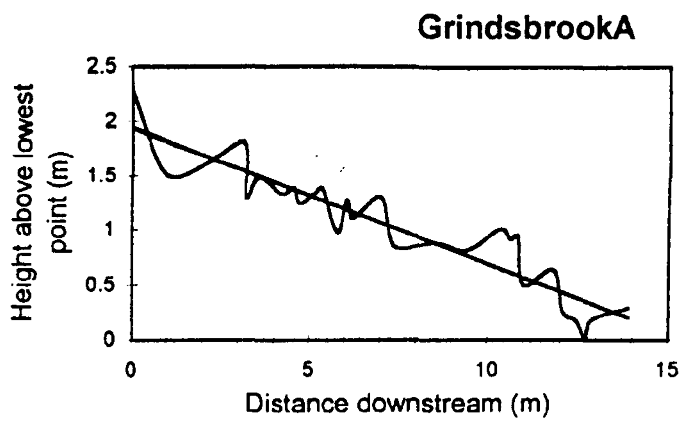

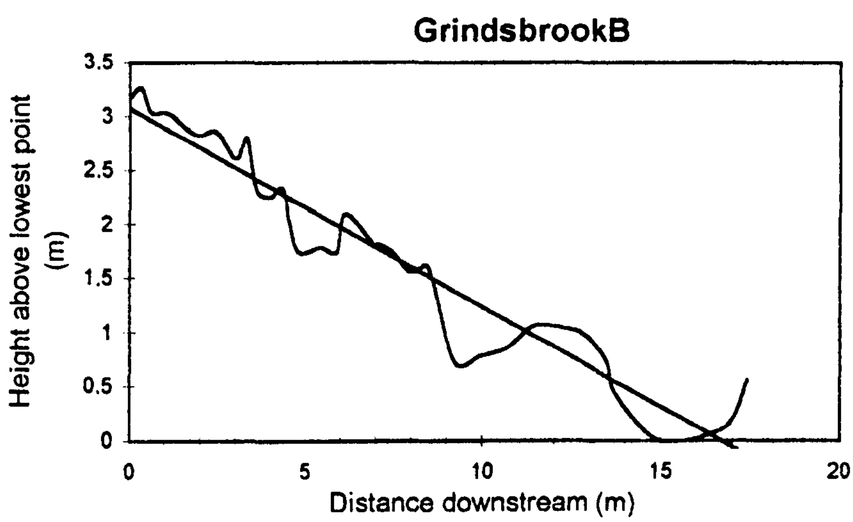

Figure 4.3 continued. Longitudinal profiles for the fieldsites

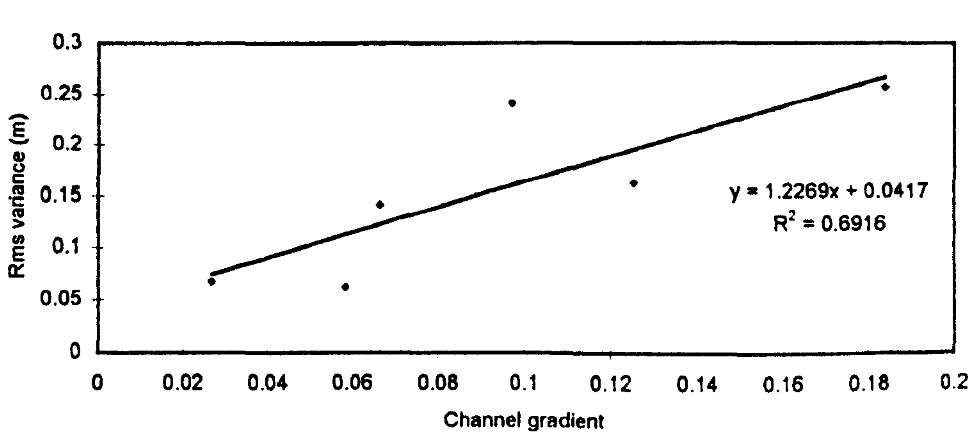

Figure 4.5. Relationship between channel gradient and long profile variance from a straight line

KEY (for Figures 4.4a to 4.4f)

Bank edge

Bedrock step

Water edge (at time of survey)

Flow direction

Large sediment / boulder

(Location of sites shown in Figure 4.4g)

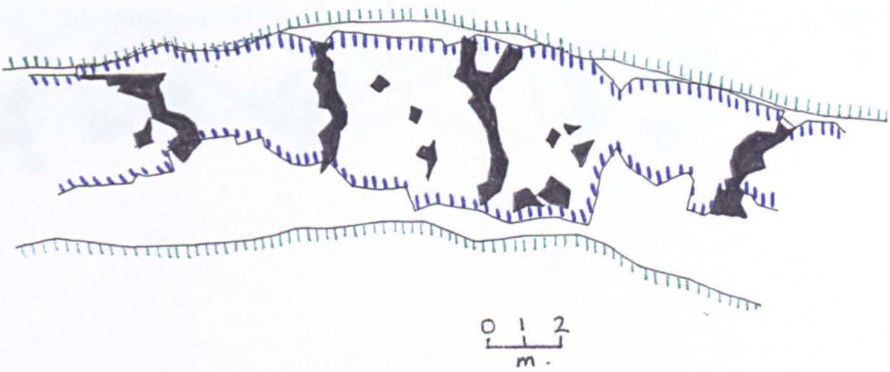

Figure 4.4a River Ashop

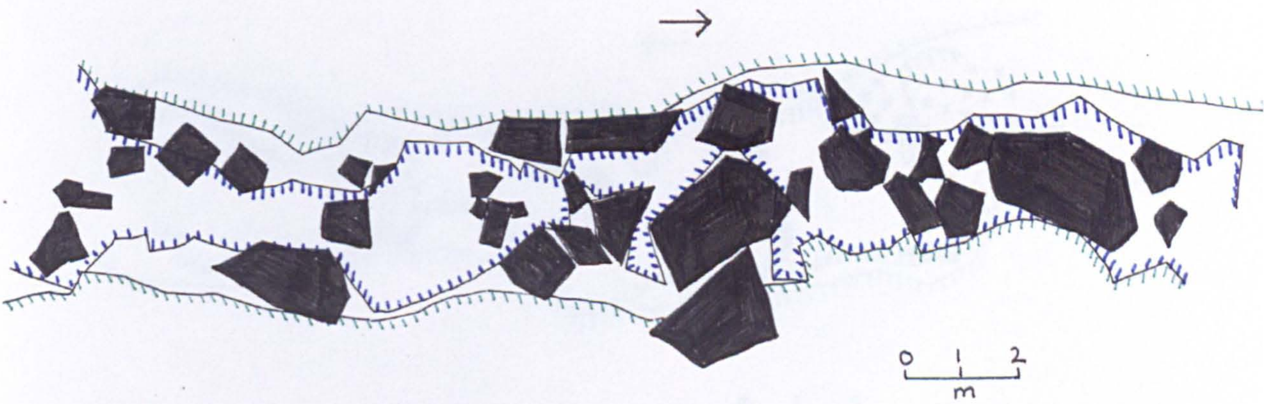

Figure 4.4b Burbage

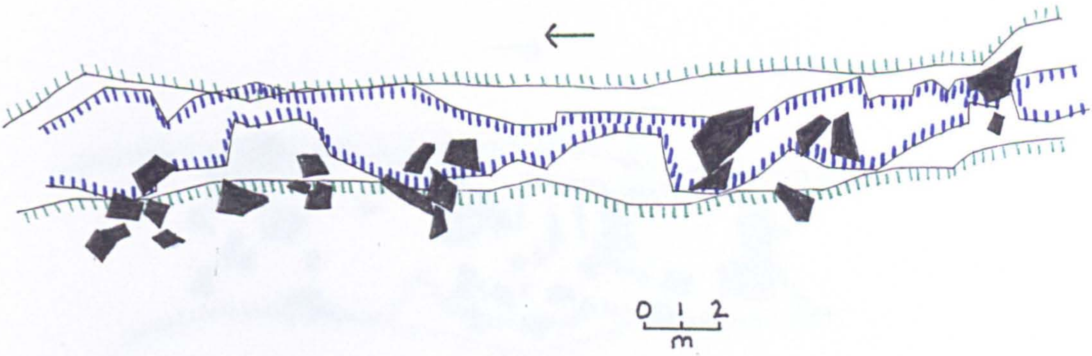

Figure 4.4c Doctors Gate

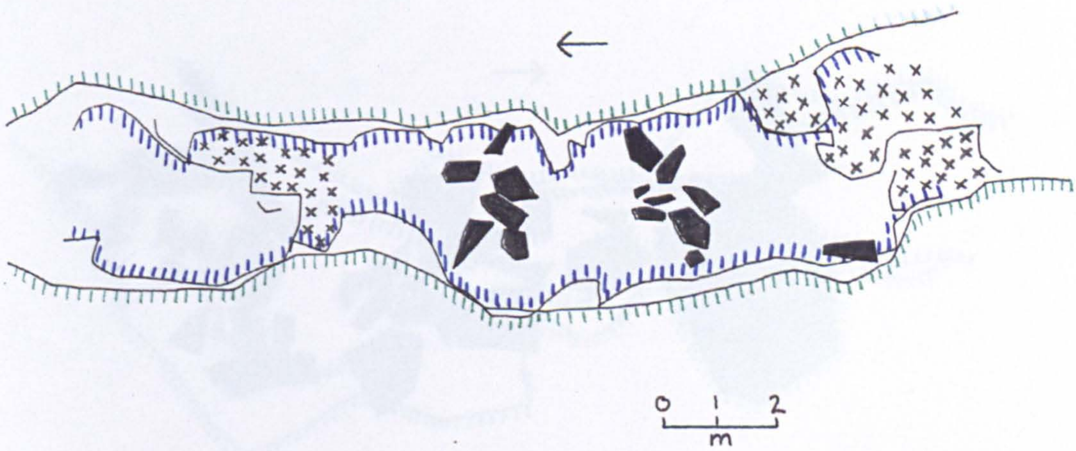

Figure 4.4d Fairbrook

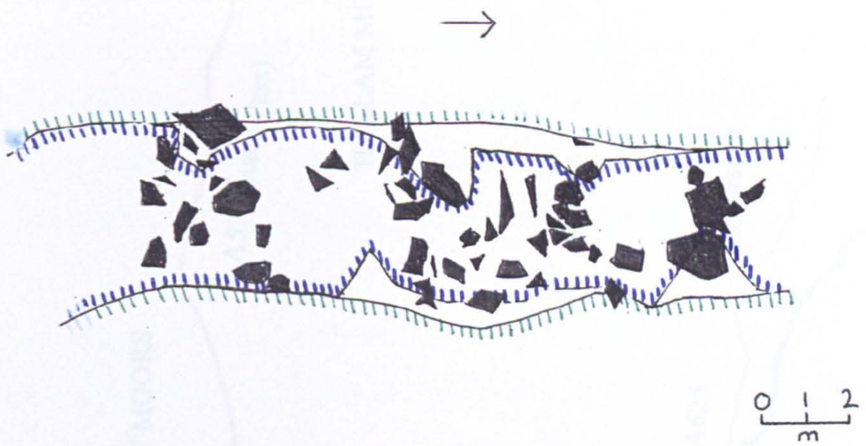

Figure 4.4e Grindsbrook A

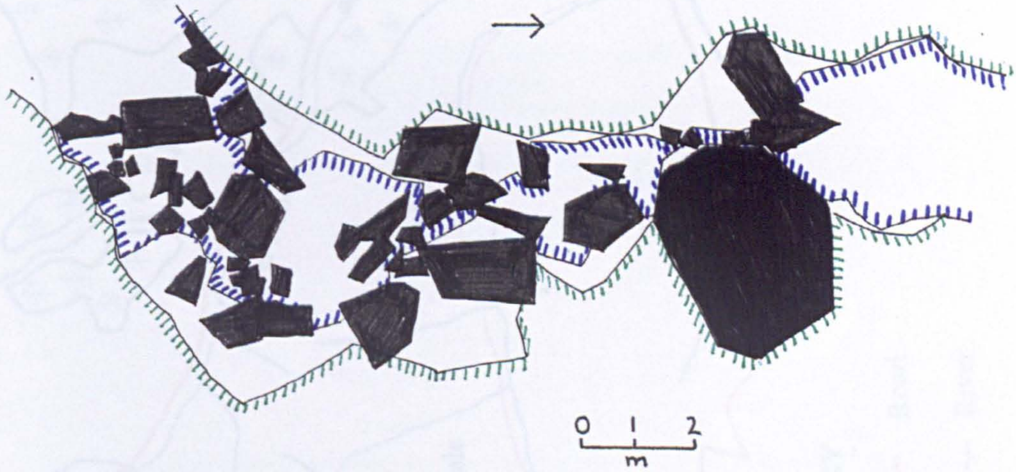

Figure 4.4f Grindsbrook B

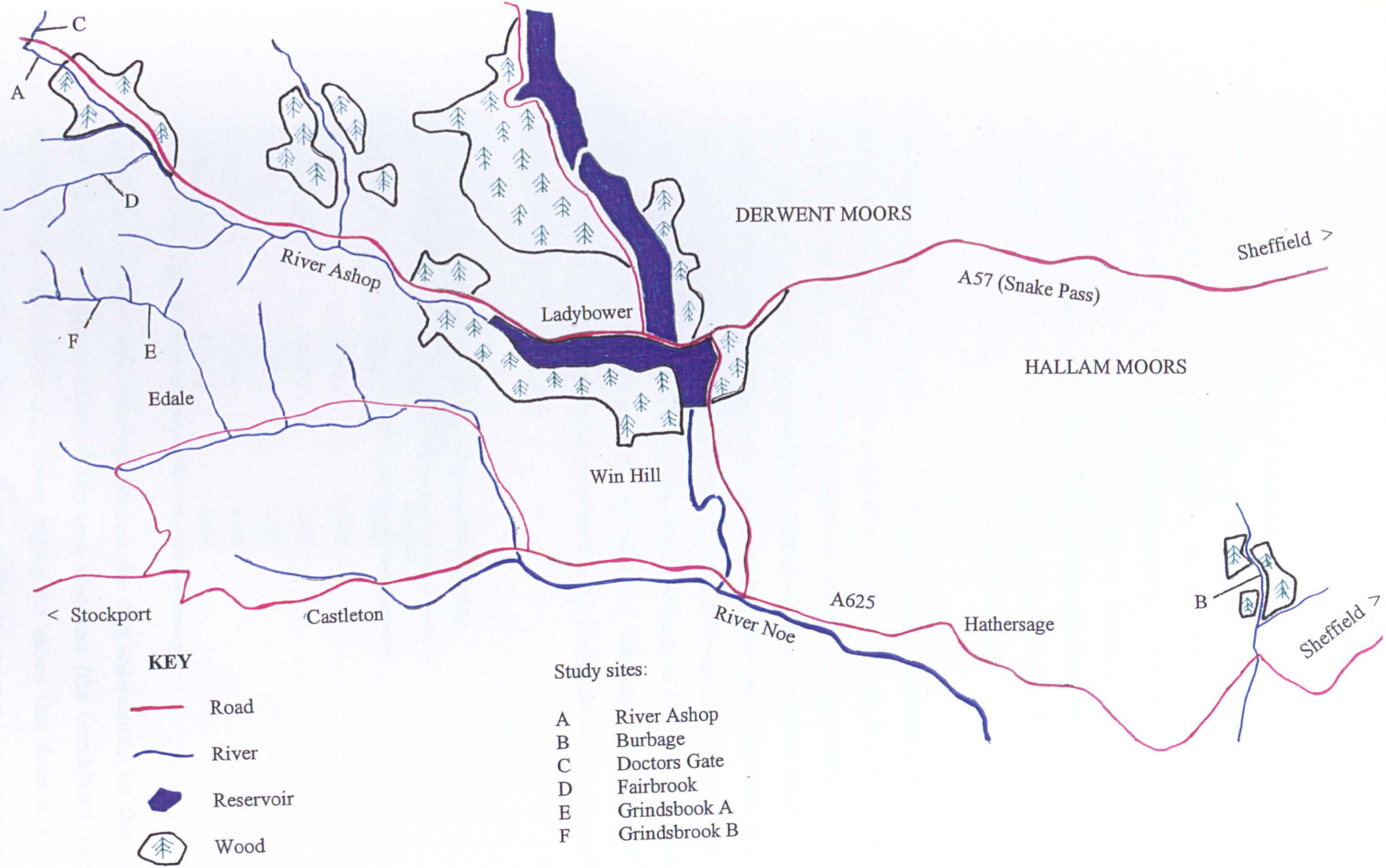
C
A
D
F
E
River Ashop
Edale
Ladybower
DERWENT MOORS
HALLAM MOORS
Sheffield >
A57 (Snake Pass)
Win Hill
< Stockport
Castleton
River Noe
A625
Hathersage
B
Sheffield >
KEY
Road
River
Reservoir
Wood
Study sites:
A River Ashop
B Burbage
C Doctors Gate
D Fairbrook
E Grindsbook A
F Grindsbrook B

4.3.1 Channel slope and long profile variance

A value for channel slope was necessary for calculating the friction factor (used in the analysis of salt dilution gauging considered in the next chapter) and for studying the relationship between step spacing and channel geometry. To determine the slope a long profile was surveyed down the centre of the channel. Survey points were measured on the channel bed and also on the channel surface, although it was decided only to use the channel bed data as this remains constant at varying discharge. Table 4.2 shows the gradient determined from the long profile for each of the sites.

This long profile was also used to study the degree of development of the steps and pools in the reach. If a reach has very well defined steps and pools, the long profile will vary significantly from the straight line approximation of the long profile. To quantify this variance, the sum of the differences (squared) between the actual height and the predicted height from the straight line equation was determined. This sum was then divided by the number of points in the long profile and the square root taken to provide a value representing the root mean square (*rms*) deviation of bed elevation from the linear profile. These values are shown in Table 4.2. The larger the value for this variance (termed χ_{rms}), the more pronounced the steps and pools are, i.e. the profile is further away from a straight line.

Table 4.2. Channel gradient and variance of the longitudinal profile from a straight line approximating the profile.

Site	Gradient	χ_{rms} (m)
Ashop	0.0266	0.068
Burbage	0.0971	0.241
Doctor's Gate	0.0582	0.063
Fairbrook	0.0662	0.142
Grindsbrook A	0.1254	0.163
Grindsbrook B	0.1838	0.257

These values confirm what was expected from the field observations, i.e. that streams with the most visually pronounced step-pool sequences (the Grindsbrook sites and Burbage) have the highest χ_{rms} value. Figure 4.5 shows that there is a positive relationship between the gradient and the degree of variance, i.e. the steeper the channel, the more pronounced the steps and pools were. Calculating this measure was considered less complicated than measuring the step height directly as part of the EDM surveying, which would also be expected to indicate how pronounced the step-pool sequences are in a channel. During the reconnaissance survey an attempt was made to measure the step height, however, it was found that a large amount of judgement was involved in determining where the top of the step was and the bottom of the pool as the sediment was not level. This would also mean it would be necessary to carry out many measurements to be sure of a reasonable estimate of the step height. Therefore, determining an average step height as part of the surveying was considered too time consuming and complicated, so these χ_{rms} variance values were used as a substitute for step height in the data analysis, despite the fact that using this method ignores e.g. sedimentological differences between steps and pools so is not an ideal method.

4.3.2 Step spacing

This measurement was needed for studying the relationships between spacing and channel slope, width and step development (variance of long profile from a straight line). Step spacing is also important as it has been shown by a number of researchers (Wohl and Grodek, 1994, Nowell and Church, 1979 and Davies, 1980) that resistance is affected by roughness spacing (i.e. step spacing). The values for average step spacing were obtained from the plan maps and longitudinal profiles from the EDM survey. It was easy to determine the position of the steps because of the presence of boulders, the change in channel gradient, and the location of the pegs marking the steps. It was considered more accurate to determine spacing this way rather than direct measurement in the field as the method used enabled the overall site to be seen and features such as the differences in the angle of the step with the flow to be taken into consideration. Table 4.3 shows the values determined for step spacing.

Previous workers have found that spacing is between 0.4 to 0.8 times (Grant et al, 1990) and 2.7 times (Whittaker, 1987b) the channel width. This study found a range of 0.85 to 1.4, with an average of 1.15 (see Table 4.3). This is well within the range found by other workers, however, this value is considerably different to the value of 2.7 found from the reconnaissance survey data. This is likely to be a reflection of the differences in how step spacing was determined. For this detailed fieldwork a continuous series of steps and pools were studied, whereas in the reconnaissance survey the steps and pools were not a continuous sequence throughout the entire reach.

Relating step spacing to width and slope indicated that the best relationship was between spacing and width. This linear relationship (shown in Figure 4.6a) has a *r*-value of 0.91 (significant at $p<0.05$ level), whilst the power relationship between spacing and slope (Figure 4.6b) has a *r*-value of 0.525, which is an insignificant value. Multiple regression analysis (of logged data) was performed to study the combined effect of slope, width, χ_{rms} and sediment size (step D_{84} was used) on step spacing. This resulted in a coefficient of determination (R^2) of 0.995. Considering just slope and width gave a result of $R^2 = 0.86$, which is a stronger relationship than that obtained when considering width alone. The correlation between spacing and slope/ χ_{rms} was a very strong one, as seen in Figure 4.6c (logged data) where $r = 0.92$ ($p<0.01$ level). This supports the conclusions of Billi et al (1995), and Judd and Peterson (1969) that the best predictor of step spacing is slope divided by a measure of step or sediment height.

As only six data points were obtained from the detailed fieldwork these points were combined with the data from the reconnaissance survey. Figure 4.7 shows a composite plot of the data with the data from the reconnaissance survey for the relationships between spacing and slope (Figure 4.7a) and between spacing and width (Figure 4.7b). Figure 4.7a also shows the data obtained by Grant et al (1990), Whittaker (1987b), and Billi et al (1995). These graphs show that the reconnaissance survey data and that of these previous workers plot very close to each other, whilst the fieldwork data obtained from this research generally has a closer step spacing, especially at lower gradients. This is likely to be a reflection of the fact that only small reaches were chosen for the fieldwork sites, where there were continuous step-pool sequences. The data obtained by the previous workers were from much longer reaches, over which distance the step-pool sequences were generally not continuous.

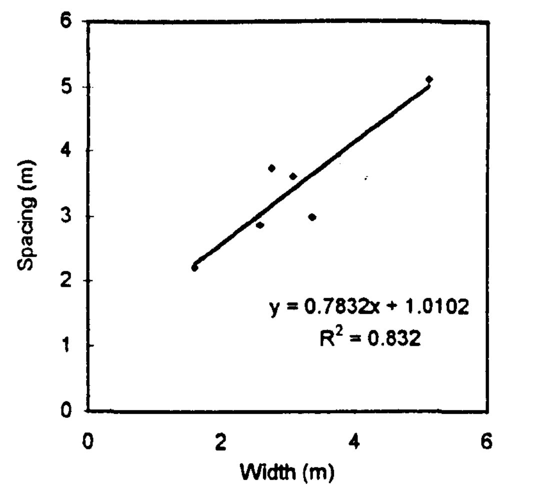

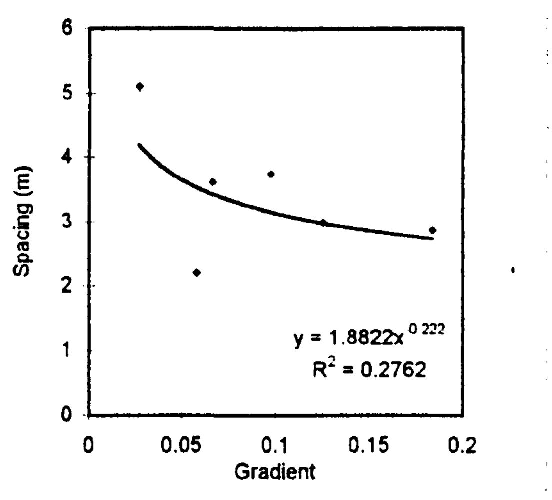

Figure 4.6a

Figure 4.6b

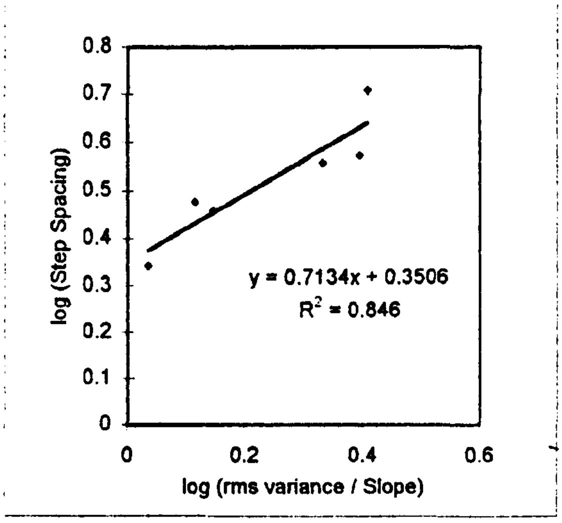

Figure 4.6c.

Figure 4.6. Relationship between step spacing and a)width, b)slope and c) rms variance / slope

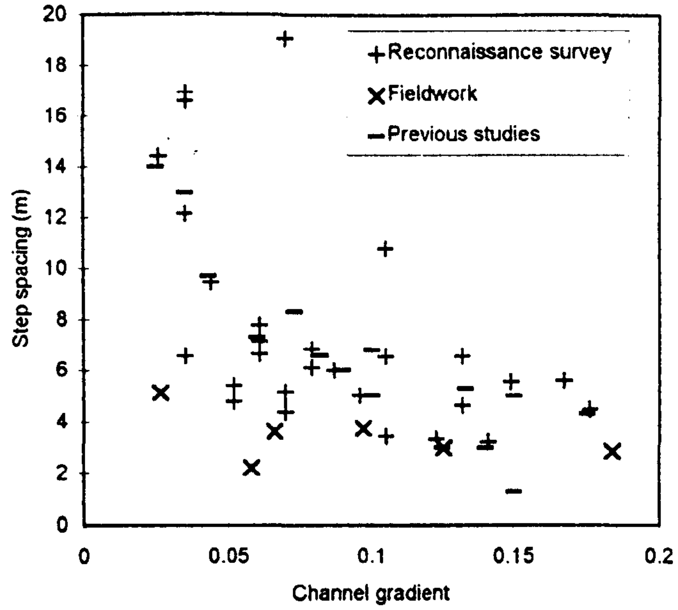

Figure 4.7a.

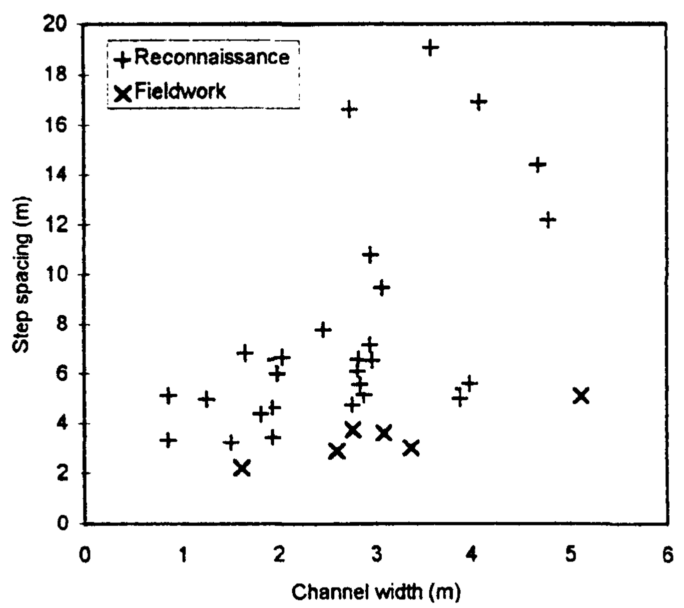

Figure 4.7b.
Figure 4.7. Composite graph showing step spacing and a) slope and b) width

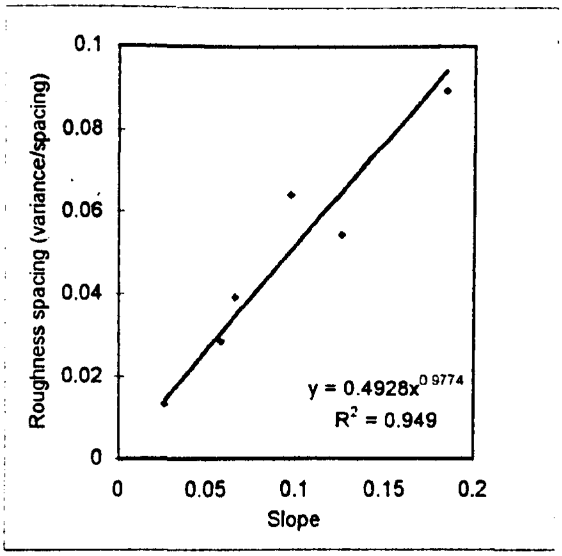

Figure 4.8a.

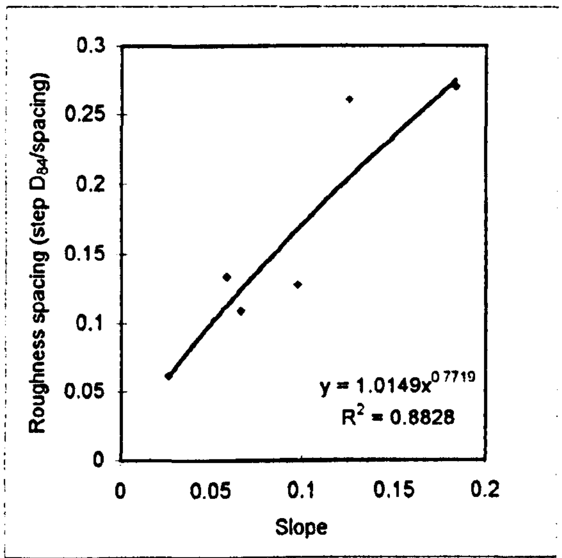

Figure 4.8b.

Figure 4.8. Roughness spacing and slope using a)rms variance and b)D_{84}

Table 4.3 Values used to study the relationship between step spacing and channel characteristics

Site	Average spacing (m)	Bankfull width (m)	Spacing / width	Slope	Step D_{84} (m)
Ashop	5.12	5.12	1.00	0.0266	0.32
Burbage	3.75	2.76	1.36	0.0971	0.479
Doctor's Gate	2.21	1.61	1.37	0.0582	0.296
Fairbrook	3.62	3.08	1.18	0.0662	0.395
Grindsbrook A	3.00	3.37	1.16	0.1254	0.781
Grindsbrook B	2.88	2.59	0.85	0.1838	0.776

4.3.3 Roughness spacing

As mentioned earlier in this chapter, the actual step height was not measured. Therefore, the roughness spacing parameter used by Wohl and Grodek (1994), Davies (1980) and Rouse (1965) could not be calculated for this study, although a value for roughness spacing using χ_{rms} and step D_{84} was determined. They found that at higher slopes the value obtained for roughness spacing (ratio of step height to step spacing) increased, indicating an increased resistance to flow. This was a result of increasing sediment size; step spacing tends to remain near constant on steep slopes as cannot decrease any further. From this research the strongest relationship was found when χ_{rms} was used as a measure of step height (a power law relationship). This is seen in Figure 4.8a, where the r-value obtained was 0.97, significant to $p<0.01$ level. Using step D_{84} as a measure of step height also produced a strong power law relationship (r=0.94, $p<0.01$), as shown in Figure 4.8b. These results support the findings of Davies (1980), i.e. that roughness spacing increases with slope. It is, therefore, probably not step spacing alone that controls resistance, but a combination of step spacing and step height.

This explains, to some extent, why the relationship between slope and step spacing is better for some studies than others. If the difference between the degree of development of the steps is similar between sites then step spacing will correlate strongly with slope as step height will not vary significantly. However, consideration of roughness spacing does not shed any more light on why in this study step spacing correlates better with channel width than slope. Overall, it would appear that the best correlation with spacing is slope in combination with a vertical scale (χ_{rms} was found to be the best such measure), although it is hard to distinguish exactly which are the controlling variables as strong correlations exist between them, e.g. width and D_{84} and slope.

4.4 Detailed transect surveying

4.4.1 Introduction and methodology

This is necessary in order to quantify the form and grain roughness associated with the steps (for example by measuring the vertical height differences between the sediment known as the *K3* value (Ergenzinger, 1992 and de Jong, C., 1992).

Surveying (using EDM) of a number of transects across each reach was carried out. Generally two transects for each step and two for each pool were surveyed, although for some of the steps it was only possible to have one transect, and for some of the longer pools three transects were measured in order to represent them accurately. Hence, for a reach with four step and pool sequences, this generally resulted in16 transects. A 30 m tape measure was stretched out across the transect, and a number of survey measurements were taken across the transect in order to determine the height of the sediment at each point. For each transect approximately 50 measurements were taken. Therefore, for Doctor's Gate (average width of just over 1 m) this meant taking a measurement every 2 cm, whereas at most of the other sites a reading every 5 cm was sufficient. It was important to have a similar number of points per transect to get realistic *K3* values that were comparable between the sites.

The transects were not necessarily perpendicular to the flow; where the steps were not perpendicular to the flow the line of the step was followed instead. In order to determine the base level for comparison of the transects, the water level was also surveyed. The transect surveying was carried out at the same time as the general EDM site surveying. This enabled comparison between the sites based on water level and sediment height relative to this level because of the uniform flow conditions. Before the data from the transects were analysed, the cross-sections were plotted and any points believed to be part of the bank were ignored from further studies.

The measurement errors associated with the analyses carried out are negligible as the data were collected using EDM surveying at short range. However, there were significant assumptions made during the analysis of the data. Most of the analyses are based on the assumption that the water level at the time of the survey can be used as a standard base level for all the transects in all the sites. For comparison with other transects within the same site this is a valid assumption to make as all the transects were surveyed within the same day, and there was no rainfall during this period. For between site comparison it is also considered a valid assumption to make as all the sites were surveyed in a short period of time, within which time there was no rainfall. However, there will be some loss of accuracy associated with this assumption.

From the transect data the following were studied:

- Variability of sediment height (described in 4.4.2);
- *K3* (described in 4.4.3);
- Sediment protrusion (described in Section 4.5).

4.4.2 Variability of sediment height

The standard deviation of the difference in height between adjacent points is shown in Table 4.4. To put the values for standard deviation into context, and enable comparison between the sites, this value was divided by d_{min} (the estimated depth at the minimum discharge observed at each of the sites during the period of the fieldwork). Although the depth of flow in the steps and that in the pools would be slightly different, this value is an acceptable approximation. This measure should, theoretically, produce similar results to the *K3* analysis as both are measures of the variability in sediment height, although *K3* considers maximum differences whereas this standard deviation value looks at the statistical variation between all of the values.

At all the sites the height variability in the steps is greater than in the pools, understandable as larger sediment accumulates in the steps. Burbage is interesting in that it has the highest degree of variability. This suggests that the flow at this site is highly influenced by the sediment.

Table 4.4. The variability in height between adjacent points in the transect survey. *stdev* is the standard deviation of the difference between adjacent points in each transect. The step transects and pool transect averages were determined, and this site average standard deviation then divided by d_{min}.

Site	Step *stdev* (m)	Pool *stdev* (m)	Step $stdev/d_{min}$	Pool $stdev/d_{min}$	Step/pool $stdev/d_{min}$
Ashop	0.048	0.045	0.340	0.322	1.056
Burbage	0.083	0.060	1.088	0.790	1.377
Doctor's Gate	0.032	0.024	0.583	0.435	1.340
Fairbrook	0.053	0.038	0.397	0.288	1.378
Grindsbrook A	0.042	0.039	0.490	0.457	1.072
Grindsbrook B	0.100	0.057	0.323	0.184	1.755

4.4.3 *K3* value

The *K3* value is used to quantify the form and grain roughness associated with the steps (Ergenzinger, 1992). It quantifies the vertical height differences between the rocks making up the step by calculating the maximum difference in height (*K3* value) between any two adjacent of three consecutive points. For each transect the average *K3* value can then be determined. For example, if 3 adjacent points have elevations of 103 mm, 87 mm and 101 mm then the differences in height are 16 mm and 14 mm. The *K3* value for these three points is therefore 16 mm. The values from the transects were then averaged to determine a step average and a pool average *K3* value.

Table 4.5 shows the *K3* values obtained at each of the sites for the steps and the pools. $K3/d_{min}$ values are also shown to quantify the significance of the *K3* values (i.e. show the magnitude of the *K3* variation in relation to the depth). An overall site average *K3* was not determined as the values obtained for the steps and pools are very different, so obtaining an overall average would require an accurate measure of the relative importance of the steps and the pools. This was considered too complicated to implement, so the step and pool values are considered separately.

The results in Table 4.5 are similar to those in Table 4.4 (standard deviation of the difference between the height differences between adjacent points), i.e. the step values are higher than the pool values and the values at Burbage are higher than at any other site.

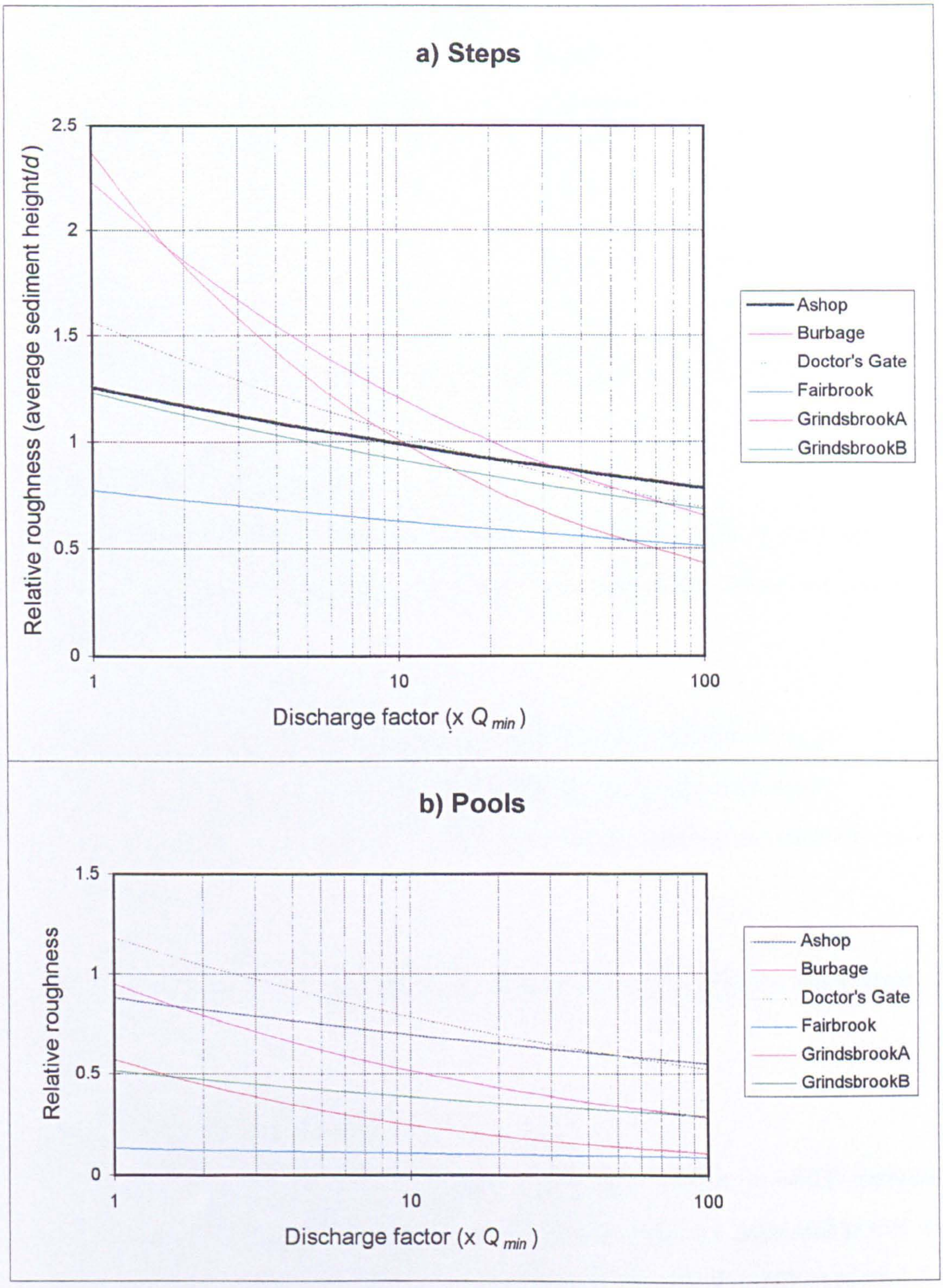

Figure 4.9 Relative roughness (average sediment height/*d*) for a)steps and b)pools

Table 4.5 *K3* values obtained from the transect data.

Site	*K3* Step average (m)	Step *K3* / d_{min}	*K3* Pool average (m)	Pool $K3/d_{min}$
Ashop	0.0717	0.51	0.0632	0.45
Burbage	0.0925	1.22	0.0697	0.92
Doctor's Gate	0.0393	0.71	0.0340	0.62
Fairbrook	0.0597	0.45	0.0431	0.32
Grindsbrook A	0.0656	0.76	0.0525	0.61
Grindsbrook B	0.1259	0.41	0.0768	0.25

4.5 Sediment protrusion

As well as calculating the *K3* values to study the expected effect of the sediment on the flow, the degree of sediment protrusion was quantified. Three parameters were calculated:

1. The average level of the sediment relative to the water surface at d_{min};
2. The percentage of the total sediment protruding at a given water level;
3. The percentage of the channel width that contains protruding sediment at a given water level.

How these values were obtained, as well as the results, will be considered in this section.

4.5.1 Average sediment level

The average level of the sediment relative to the water level is an useful measure, as it can be seen whether there are significant differences between steps and pools, and can also be used as a measure of relative roughness. As discussed in sub-section 4.2.2, it is better to use a range of depths rather than just one value for relative roughness to enable the variation in relative roughness with change in discharge to be observed. Figure 4.9 shows relative roughnesses calculated for a range of depths relative to d_{min} (the same range that was used to produce Figure 4.2). As in Figure 4.2, the Burbage, Doctor's Gate and Grindsbrook A sites show the greatest variation in relative roughness, indicating that the flow is most affected by the sediment at these sites, and again especially at discharges up to 20 times the base discharge. The relative roughness for the steps is greater than for the pools, indicating that the flow is affected by the sediment more in the steps than in the pools. This is the same conclusion as was reached with using D_{84}/d as a measure of relative roughness.

4.5.2 Amount of sediment protrusion

Initial analysis indicated that it would be too complicated to calculate the area of sediment compared with the total channel area at a certain height (arguably the most useful measure for considering the effect of the sediment on the flow) because of the irregular shape of the channel and, therefore, problems in determining the area of the channel. If this is not taken into consideration then the value calculated will not be an accurate estimate. Hence it was decided to use the percentage of the total sediment protruding at a certain height, and the percentage of the channel width containing protruding sediment (both obtainable from the transect data) as measures of the amount of sediment that affects the flow at a certain flow depth. This enables comparison between each of the sites, as well as between the steps and pools.

Although it is not actually the protruding sediment that slows down the flow, but rather the sediment that is at the level of the water and below, the amount of sediment protrusion gives an indication of the range of flows at which the water is significantly affected by the sediment in the channel. If at low flow there is very little sediment protrusion, a slight increase in the flow level will decrease considerably the effect of the sediment. However, if there is a lot of sediment protrusion then even at high flows the sediment may have a considerable effect in slowing down the flow, and, therefore, the friction factor would be expected to be greater.

If a channel is dominated by one very large sediment particle, it might appear that the flow is significantly affected by the sediment. However, it is possible that only a small part of the stream in terms of the total channel width is affected in such a situation. The only sediment actively slowing down the flow is that which is in the channel and with which the flow comes into contact. Therefore, as well as determining the amount of sediment protrusion, the percentage of the channel width that contains protruding sediment was also determined. This is a better measure for comparison of the step and pool characteristics as the percentage of sediment protruding at a certain height is, of course, in proportion to the total amount of sediment in that transect. Thus, at a certain height in the pool there may be the same percentage of this total sediment protruding as in the steps, but this value corresponds to a much greater amount of sediment in the steps.

For determining the percentage of channel width containing protruding sediment, it was assumed that the channel width was constant at all discharges. However, this is not always the case as, especially at very low flows, part of the channel will contain no water and so the sediment in that part of the stream will not affect the flow. Therefore, the results obtained from this analysis should not be used to draw conclusions about the behaviour of the flow at very low water depths and discharges. Despite these assumptions, it is believed that the values obtained for sediment protrusion are a good measure of the degree to which the flow is retarded by the sediment in the channel, as well as for comparing between the sites and between the steps and the pools.

4.5.3 Analysis procedure

The simplest way to carry out the analysis would be to simply consider a horizontal line at a certain height ('slice height'), and determine the amount of sediment protruding at this level. However, at the sides of the channel this value would be misleading as the banks would be treated as protruding sediment. To avoid this, the values at the extremes of the channel were ignored. The cross-section was plotted as a graph so that the banks could be identified for each site, as obviously the amount of the channel width to be ignored was different for each transect.

For calculating the values of sediment protrusion and percentage of the width with protruding sediment, the EDM values were used to determine the lowest point in each transect. The *z* (vertical) values relative to this height were then calculated to ensure that all the values used in subsequent analysis were positive ones. The area of sediment was calculated by multiplying the average height of two adjacent points relative to the 'slice height' and the horizontal distance between them. The total amount of sediment protruding in each transect could then be determined by summing the positive values (negative values meant the sediment was submerged, so these were ignored).

The 'slice height' levels at which the percentage of the total sediment protruding ($\%_{total}$), and the percentage of the channel width containing protruding sediment ($\%_{width}$) were calculated for were d_{min} (assumed to be the water level when the transect was done), and 5 cm (or 10 cm for sites with a lot of large sediment) intervals above and below this level. The values of $\%_{total}$ and $\%_{width}$ when the water level is equal to the 'slice height' in question were then determined. A reach average step value and pool value was then obtained from these values.

4.5.4 Results

The results are shown in Table 4.6a (for $\%_{total}$) and Table 4.6b ($\%_{width}$). Figures 4.10 and 4.11 show these values at a range of 'slice heights'.

Table 4.6a) Percentage of total sediment protruding ($\%_{total}$) b)Percentage of channel width containing protruding sediment ($\%_{width}$).

Column a - The maximum observed value of step value - pool value.

Column b - The height relative to the water level at which the value in Column a was measured.

Columns c + f - the percentage calculated at d_{min} (water level when the transect was done).

Columns d + g - the percentage at the depth equivalent to a discharge 100 times the base discharge (d_{100}) recorded at that site.

Columns e + h - difference between Columns c and d (step data) and Columns f + g (pool data).

Table 4.6a. $\%_{total}$ data

Site	Max. (a)	Height (b)	d_{min} (c)	Step d_{100} (d)	Data (c)-(d)	d_{min} (e)	Pool d_{100} (f)	Data (e)-(f)
Ashop	14	-0.1	21	5	16	16	3	13
Burbage	18	0	44	10	34	25	8	17
Doctor's Gate	25	-0.05	43	10	33	25	7	18
Fairbrook	19	-0.1	9	1	8	4	1	3
Grindsbrook A	39	-0.05	49	2	47	15	0	15
Grindsbrook 'B	51	-0.3	38	8	30	7	0	7

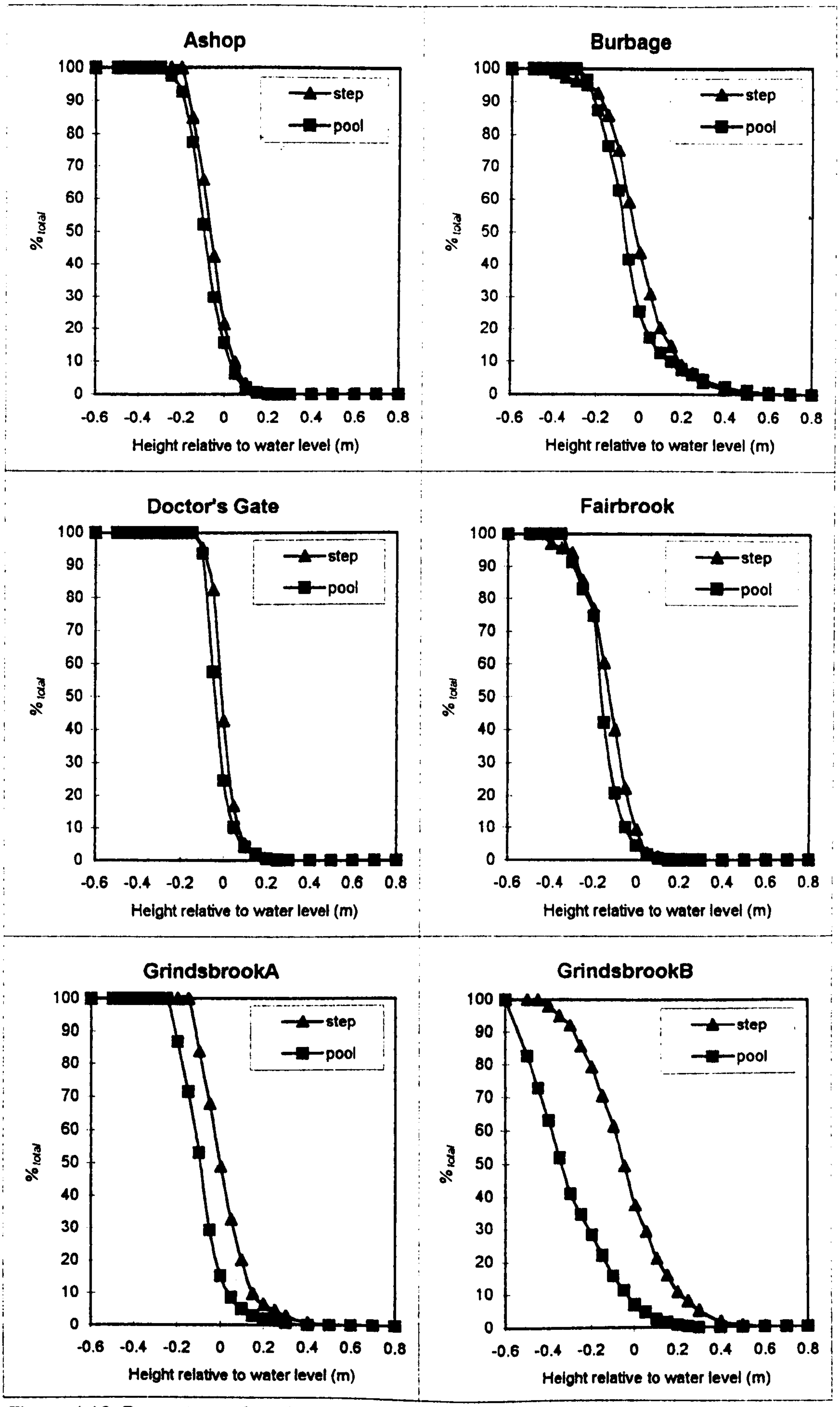

Figure 4.10. Percentage of total sediment protruding ($\%_{total}$) at each of the sites.

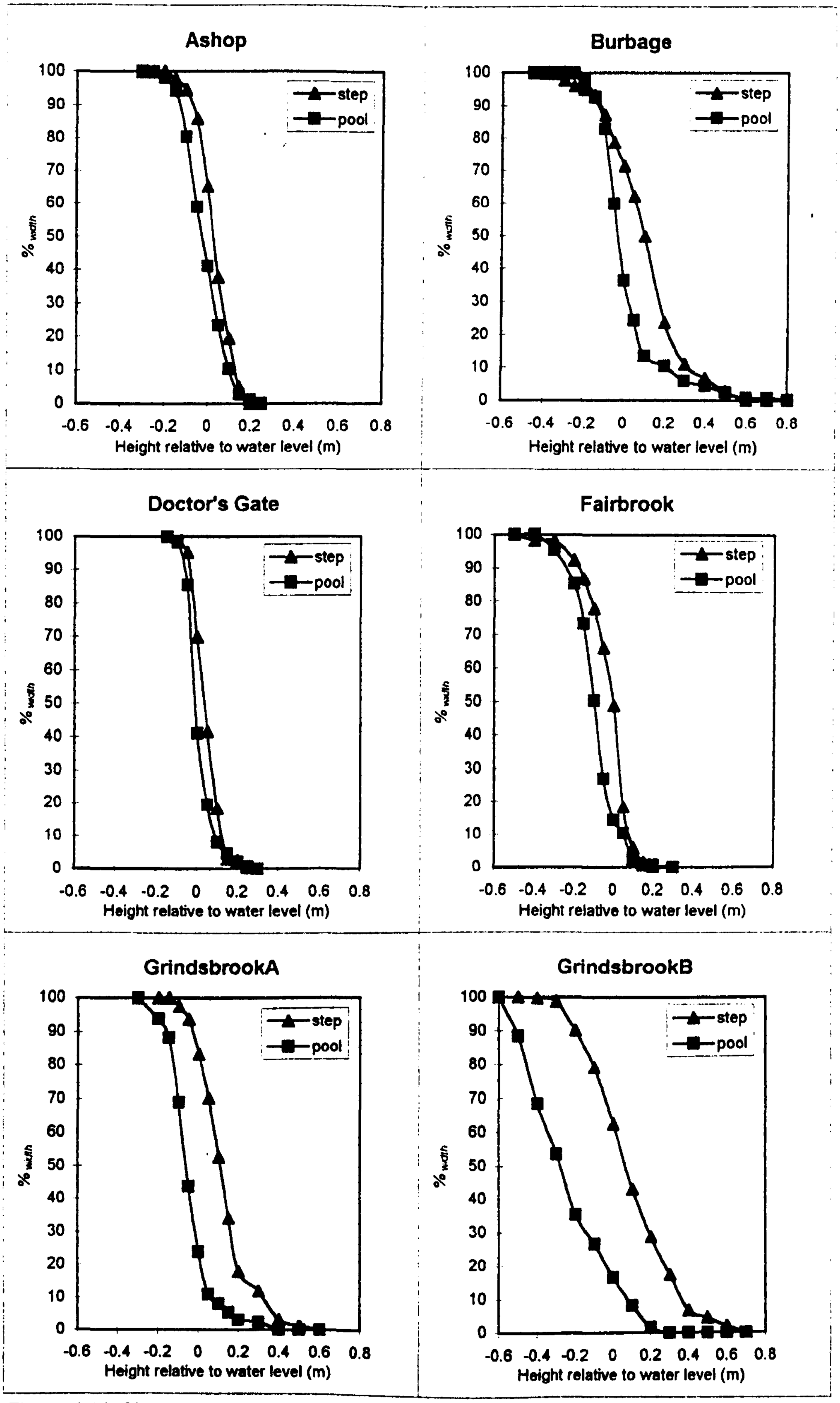

Figure 4.11. $\%_{width}$ at various heights at each of the sites

Table 4.6b $\%_{width}$ data

Site	Max. (a)	Height (b)	d_{min} (c)	Step d_{100} (d)	data (c)-(d)	d_{min} (e)	Pool d_{100} (f)	Data (e) - (f)
Ashop	27	-0.05	65	25	40	41	14	27
Burbage	38	0.05	71	28	43	36	12	24
Doctor's Gate	22	0	70	34	36	41	14	27
Fairbrook	39	-0.05	49	13	36	14	8	6
Grindsbrook A	59	0	83	4	79	24	0	24
Grindsbrook B	54	-0.2	63	23	40	17	0	17

4.5.5 Discussion of results

The values of $\%_{total}$ and $\%_{width}$ were greater in the steps than in the pools for all the sites, as would be expected. The two most interesting sites in terms of the data obtained are Fairbrook and Grindsbrook B. Grindsbrook B is outstanding because of the difference between the steps and the pools. Figures 4.10 and 4.11 show this visually, and Table 4.6 shows the value of the maximum difference between the steps and the pools. For the value of $\%_{total}$ this is 51% - by far the largest difference of any of the sites, and for $\%_{width}$ this value is 54% - the second largest value and considerably larger than the other four sites with a smaller value.

Perhaps more interesting is the height at which this difference occurs. For all the other sites the maximum differences between steps and pools for the two protrusion measures occurs at between 0.1 m below water level and 0.05 m above the water level. However, at Grindsbrook B this maximum difference occurs at 0.3 m below the water surface for $\%_{total}$, and at 0.2 m below the water surface for $\%_{width}$. This is a reflection of the fact that the depth range is largest at Grindsbrook B. The significance of this observation is not known at present, although it would be expected to lead to a large difference in the velocity between the steps and the pools.

Fairbrook is very interesting because of the lack of sediment protruding at the water surface. Only 9% of the total sediment is protruding at the water surface in the steps and only 4% in the pools. The percentage of total width with protruding sediment is also lowest at Fairbrook - 49% at d_{min} for the steps and 14% for the pools - again the lowest values of any of the sites. At d_{100} these values decrease to 1% for both the steps and the pools for $\%_{total}$, and 13% (steps) and 8% (pools) for the $\%_{width}$ values. Fairbrook also had the lowest difference between the $d_{\min}$ and d_{100} values, suggesting that the flow is not significantly affected by the sediment at increasing flow rates. Therefore, the rate of increase of velocity with increasing discharge would be expected to be very high, whilst the depth increase would be low.

The greatest difference between values at $d_{\min}$ and d_{100} is at Grindsbrook A, suggesting that the flow is very significantly influenced by the sediment at this site (more than at the other sites). This would be expected to lead to the opposite effect to that predicted for Fairbrook, i.e. a slow increase in velocity with increasing discharge.

4.6 Conclusions

The significance of the results found in this chapter will not be fully realised until the salt dilution gauging data is also considered (Chapter 7 compares these data with the results of this chapter). However, some initial conclusions can be made from the analyses carried out, and conclusions about the methods used.

4.6.1 Initial findings

The analyses described in this chapter enabled the sediment characteristics of each of the sites to be quantified. In terms of relative roughness, which is believed to have the most significant effect on the flow, the Fairbrook and Grindsbrook A sites are at opposite extremes. Of all the sites, the flow at Fairbrook would be expected to be least affected by the sediment in the channel, with the opposite at Grindsbrook A. Grindsbrook B had the most developed steps and the biggest difference between step and pool sediment, which would have some effect on the flow.

4.6.2 Comparison of the analyses carried out

Sediment characteristics were quantified by looking at sediment size (D_{84}), *K3*, standard deviation of sediment height, and sediment protrusion ($\%_{total}$ and $\%_{width}$). The *K3* value quantifies the unevenness that exists between the adjacent sediment; sediment size looks at the actual size of the sediment in the channel; and the sediment protrusion measures quantify the amount of protruding sediment (perhaps a better measure of how the sediment would affect the flow). The best measure to use should become apparent after analysis of the results from the salt dilution gauging. Table 4.7 shows the values calculated for the three relative roughness measures (i.e. D_{84}, standard deviation of sediment height and *K3*) for the step and pool sediment at each of the fieldsites.

Table 4.7 Comparison of variables describing sediment size / roughness

Site		**Step**			**Pool**	
	St dev (m)	***K3* (m)**	**D_{84} (mm)**	**St dev (m)**	***K3* (m)**	**D_{84} (mm)**
Ashop	0.048	0.0717	320	0.045	0.0632	201
Burbage	0.083	0.0925	479	0.060	0.0697	225
Doctor's Gate	0.032	0.0393	296	0.024	0.0340	152
Fairbrook	0.053	0.0597	395	0.038	0.0431	211
Grindsbrook A	0.042	0.0656	781	0.039	0.0525	207
Grindsbrook B	0.100	0.1259	776	0.057	0.0768	174

For both the step and pool sediment data, whilst Grindsbrook B has much larger values for the standard deviation of sediment height and *K3*, it does not have the largest D_{84} value. Figures 4.12 (steps) and 4.13 (pools) shows the relationships between the different indicators - this clearly shows the similarity between standard deviation and *K3* and the large difference between these two measures and D_{84}. This could be a result of the fact that the D_{84} was determined by using the *b*-axis of the sediment and not vertical height. This suggests that D_{84} is a poor indicator of vertical sediment distribution and that the *K3* value is a better value to use for considering the amount of sediment that is protruding into the flow.

Possibly the best measures for quantifying the amount of sediment that is slowing the flow down are the two sediment protrusion measures (i.e. $\%_{total}$ and $\%_{width}$) as these quantify the actual sediment that is affecting the flow. Therefore, it was expected that these values will be the best for explaining the flow characteristics at the sites.

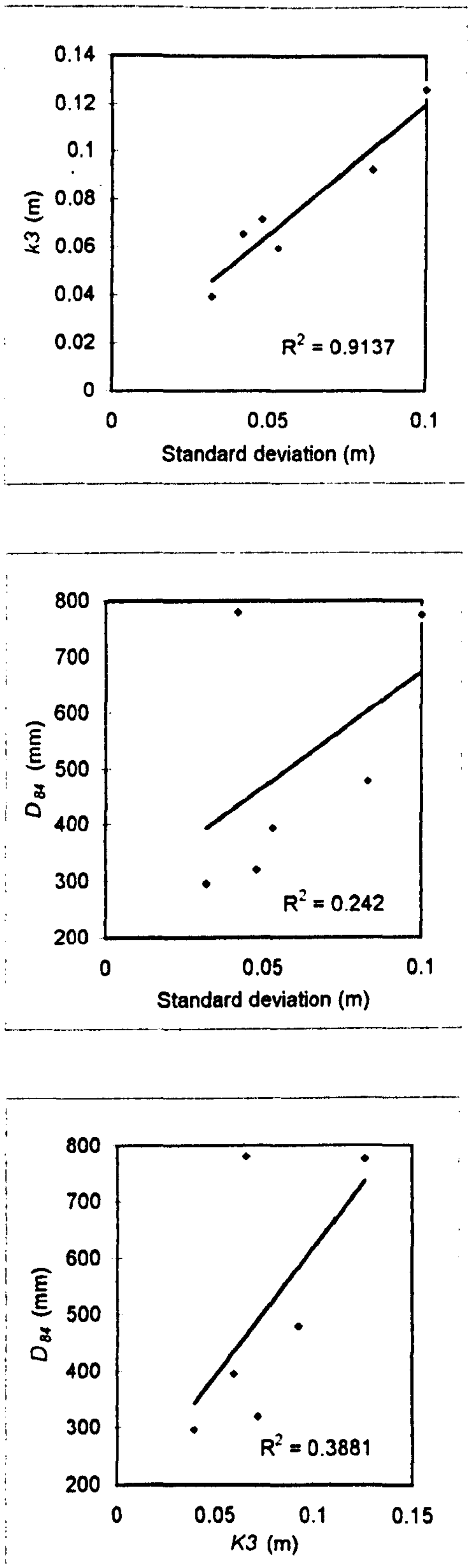

Figure 4.12. Relationships between the three measures for measuring roughness (*K3*, D_{84} and standard deviation) for the step sediment.

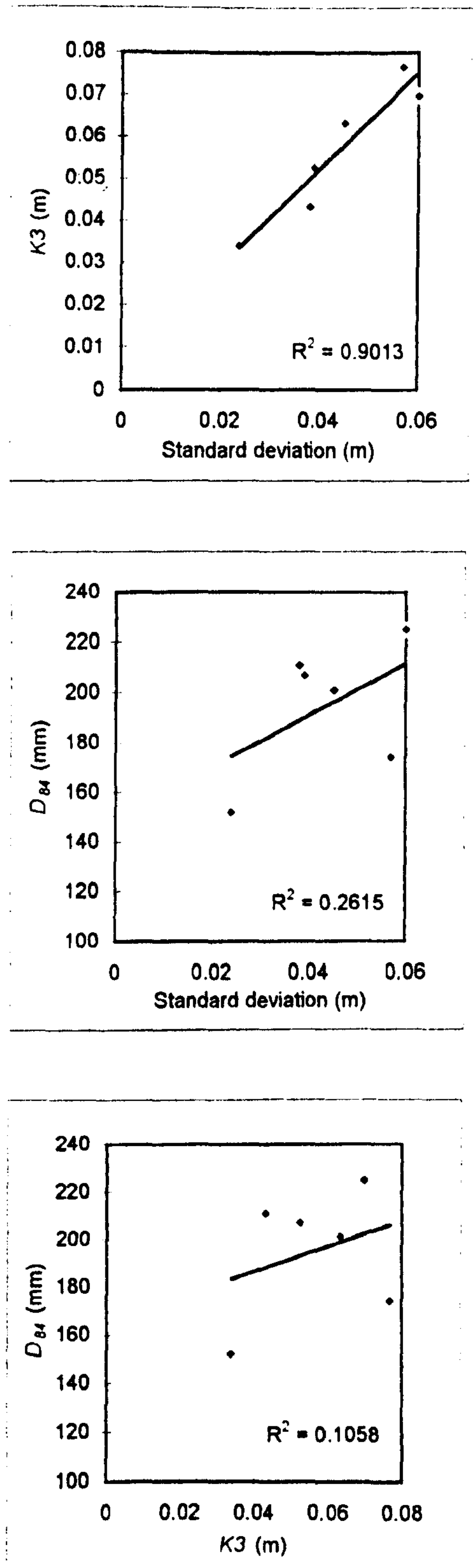

Figure 4.13. Relationships between the three measures for measuring roughness (*K3*, D_{84} and standard deviation) for the pool sediment.

Chapter 5

Field methods II: Salt dilution gauging

5.1 Introduction

As mentioned previously, the aims of the fieldwork part of the research were to:

- Determine the step geometry e.g. step spacing, sediment size and relative roughness of the study sites;
- Investigate the effect that large roughness elements (i.e. steps and large sediment) have on the average velocity of the channel and hence the resistance to flow.

The previous chapter described how the data required to achieve the first aim were collected, i.e. sediment and site characteristics. This chapter will describe the theories and fieldwork methodologies employed to obtain the data necessary to achieve the second aim. The results are presented and discussed in Chapter 7 together with results from Chapter 4. To investigate the effect of large roughness elements, average velocity and resistance to flow needed to be determined at a range of discharges. From these data the variation of velocity and resistance with discharge could be determined. The Darcy-Weisbach equation (described in Chapter 2 and also in Section 5.4 of this chapter) was employed to quantify resistance to flow. It would be expected that the variation of velocity with discharge and other hydraulic geometry relationships would be very different from those in lowland streams, where the effect of steps and large roughness elements is not present. The aim of the fieldwork was to determine the magnitude of this effect and its controlling factors. Thus it was hence necessary to determine the following variables at each of a range of discharges in each reach:

- Discharge through the study reach;
- Average velocity over the reach;
- Average water depth and width in the reach;
- Slope of the reach.

It was decided that salt dilution gauging was the best method to use to obtain discharge and average velocity values because both values can be provided by a single run. Using a current meter would be impractical and probably inaccurate because the flow is too variable, shallow and there is much white water. Salt dilution gauging is an accurate, well established method that has been used successfully by previous workers in similar types of streams to those studied in this research (Beven et al, 1979). The theory behind this method is discussed further in Section 5.2 and 5.3. Determination of the width and depth, and calculation of the friction factor is discussed in Section 5.4. Channel slope was obtained from the site EDM surveys (discussed in Chapter 4).

5.2 Salt dilution gauging theory

Dilution gauging can, in general, be carried out using a number of different chemicals and dyes. However, this discussion will deal only with salt dilution gauging. There are two main types of salt dilution gauging - the single injection method where a quantity of the tracer (dry salt or a salt solution of a certain strength) is added to the stream; and the continuous injection method where there is a steady continuous supply of the tracer solution into the stream (Elder et al, 1990).

5.2.1 Continuous injection method

This method's main advantage is that it is easier than the slug injection method to calculate discharge, but its main drawback is that it is logistically more complicated and time-consuming to implement (Elder et al, 1990). The tracer is added to the stream until an equilibrium concentration is reached at the downstream measuring point. Equation 5.1 can then be used to determine flow discharge, Q in m^3 s^{-1} by knowing the injection rate, R_T in m^3 s^{-1}; background conductivity, C_B; the concentration of the solution, C_S; and the equilibrium concentration of the tracer, C_E (all in μS cm^{-1}):

$$QC_B + R_T C_S = C_E (Q + R_T) \qquad \textbf{[5.1]}$$

5.2.2 Single injection methods

There are two types of single injection methods - using a prepared salt solution of known volume and conductivity (slug injection method), or using a known weight of dry salt (mass balance method). Whichever method is used, the salt solution or dry salt is added into the stream in one injection, although this does not need to be instantaneous (if dry salt is used and it takes a short time to dissolve in the stream, this will not affect the results obtained).

Slug injection method

Using the slug injection method Q can be calculated using Equation 5.2, where V_S is the volume of the salt solution slug, C_C is the measured channel conductivity at a point downstream of the injection point in µS cm^{-1}, t_s is the time when the salt wave started (i.e. when the conductivity rises above the background level), t_e is the time when the salt wave has passed the probe (i.e. background conductivity is resumed) and t is time (all time variables in seconds):

$$Q = C_S \frac{V_S}{\int_{t_s}^{t_e} (C_C - C_B)dt} \qquad [5.2]$$

Mass balance method

For this method a mass M of salt is added to the channel, and its mass concentration M_C in the stream is monitored at the downstream measurement point using a calibrated relationship between M_C and conductivity. Equation 5.3 describes the conservation of the salt:

$$M = Q\int_{t_s}^{t_e} M_C dt \qquad [5.3]$$

This last method was selected as it is the most portable, requiring the least equipment. The following sub-sections will describe how discharge and velocity can be determined using this dry salt mass balance method.

5.2.3 Calculating discharge

To calculate the average discharge, the integral of the salt wave is needed, which can be approximated by the following equation:

$$\int_{t_s}^{t_e} C dt \approx \sum_{t_s}^{t_e} C.\Delta t \qquad [5.4]$$

where C is the excess conductivity in μS cm^{-1} (i.e. above background conductivity) and Δt is the time interval between readings. Using this approximation, Q can be calculated by Equation 5.5:

$$Q = \frac{kM(0.5 + 0.02T)}{\sum_{t_e}^{t_s} C.\Delta t} \qquad [5.5]$$

where k is the calibration constant and T is the temperature of the stream water in °C. The calibration constant of the conductivity meters is defined as the rise in conductivity (in μS cm^{-1}) produced by adding 1 g of salt to 1 m^3 of water (1000 l) at 25°C. To determine this value a range of salt solutions of different strengths (including the range of strengths experienced in the field) were made up using de-ionised water. They were then left to stand until the temperature reached a constant level. As temperature has an effect on the conductivity of a solution it was important to ensure that this was constant and did not vary between the solutions (so was easier to correct to 25°C). The conductivity values were corrected to 25°C by assuming (for temperatures above about 3°C) the temperature dependence is 2% per °C (Church, 1975). The calibration constant is then given by the slope of the graph, i.e. the change in conductivity with salt strength. The following values were determined for k:

- Probe 1 - 1.9552 μS cm^{-1}
- Probe 2 - 1.9454 μS cm^{-1}

As these values are slightly different, it was necessary to know which probe was used at each end of the reach. Therefore, the probes were labelled Probe 1 and Probe 2. Probe 1 was only used at the upstream end of the reach and Probe 2 at the downstream end. This value is significantly less than the theoretical value of 2.14 μS cm^{-1} for pure NaCl. However, the salt used for the probe calibration and the fieldwork was not pure NaCl as it contained anti-caking agents, which would account for this difference. The same brand of salt was used for all the salt dilution gauging, and the value of the calibration constants was checked once during the period of the fieldwork, and also at the end of the fieldwork to ensure the values had remained constant.

5.2.4 Calculating velocity

To calculate the average velocity to each of the probes, firstly the time for the centroid of the salt wave (t_c) to reach the meter has to be found (i.e. the average time it takes the salt to travel from the point of injection to the conductivity meter). Equation 5.6 is used to calculate this time:

$$t_c = \frac{\int_0^\infty yt.dt}{\int_0^\infty y.dt} \equiv \frac{\sum_{t_s}^{t_e} C.\Delta t.t}{\sum_{t_s}^{t_e} C.\Delta t} \equiv \frac{\sum_{t_s}^{t_e} C.t}{\sum_{t_s}^{t_e} C} \qquad [5.6]$$

where t is the time in seconds after the injection of the salt into the stream that the reading was taken. Average velocity ($\overline{U}$) from the position the salt was put into the stream to the probe (distance d) is then calculated from Equation 5.7. The values of average velocity determined from the two probes need not necessarily be similar (as the probe at the upstream end of the reach's average velocity does not include the step-pool sequence, whereas the one at the downstream end does), so these values cannot be used as an accuracy check.

$$\overline{U} = \frac{d}{t_c} \qquad [5.7]$$

To determine the average reach velocity (i.e. between the two probes), Equation 5.8 is used, where t_{c1} refers to Probe 1 and t_{c2} to Probe 2. The distance d in Equation 5.7 is replaced by $x_2 - x_1$ in Equation 5.8, where x_1 is the distance from the injection point to Probe 1, and x_2 is the distance from the injection point to Probe 2.

$$\overline{U} = \frac{x_2 - x_1}{t_{c2} - t_{c1}} \qquad [5.8]$$

5.2.5 Mixing length

The term mixing length corresponds to the distance it takes for the salt to completely mix with the water in the stream through vertical and lateral turbulent dispersion. Beyond this distance the tracer salt concentration is uniform throughout a cross-section. Before this is achieved the concentration is not uniform, meaning that different conductivity readings will be obtained depending on the probe's location in the cross-section. This results in the conductivity recorded by the meter being too high or too low, and so the average velocity and discharge measured in the channel will not be accurate as the conductivity recorded is not representative. Therefore, this mixing length is the minimum distance that the conductivity meters must be from the location where the salt is added to the stream.

This mixing length is estimated as being about 15 times the channel width (Elder et al, 1990); 25 times the channel width (Day, 1976); or can be expressed by various relationships involving factors such as average velocity and width (Kite, 1993; Church, 1975). The data obtained by Day (1976) was studied in detail as this study specifically looked at the mixing length in four steep streams (gradients 0.0176 to 0.0273) at a range of discharges. Approximately twelve conductivity meters were used in Day's study to determine the salt concentration at various positions downstream of the point of salt injection. The point where the conductivity readings obtained became constant was assumed to be the position where total mixing had occurred. From the data obtained during this study it was apparent that the mixing length is not a fixed distance, but varies depending on discharge, velocity and other undetermined effects.

It was, however, necessary to obtain a relationship with width for use in this study, as velocity and discharge would not be known before the run had taken place. Also, as it was considered too complicated to vary the point of salt injection each time it was necessary to establish a mixing length valid for all discharges. From Day's study the data in Table 5.1 were obtained, which are the minimum and maximum discharges at each stream, and the mixing length found at this flow level during the study. The maximum distance necessary for total mixing was 20.6 channel widths, but most were well below 20. Therefore, it was decided for this research that 20 channel widths (taken as the channel width obtained when the study sites were originally identified; this was the average of approximately 6 readings) would be considered the distance downstream of the salt injection point necessary for complete mixing.

Table 5.1. Mixing length data from Day (1976)

Site	Mixing length (m)	Width (m)	Mixing length / width	Discharge ($m^3 s^{-1}$)
Stream 1	100	5.6	17.9	0.57
Stream 1	150	9.1	16.5	6.11
Stream 2	30	4.9	6.1	0.2
Stream 2	210	10.2	20.6	4.35
Stream 3	100	4.3	17.4	0.35
Stream 3	100	11.4	8.8	8.45
Stream 4	25	2.7	9.3	0.13
Stream 4	62.5	5	12.5	1.32

5.2.6 Other sources of error

It was important not to have the distances x_1 and x_2 longer than necessary to achieve total mixing because of the following potential problems:

- increased longitudinal dispersion of the tracer meaning lower excess conductivity (there is a more attenuated salt wave), leading to greater error;
- greater risk of running out of data logger memory as it takes longer to return to background conductivity;
- salt loss (e.g. dead zones).

It has been estimated that 0.1% - 0.3% of the tracer is lost per minute it is in the stream (Kellerhals, 1970) because of dead zones and other physical and chemical effects. This can, therefore, lead to an overestimation of discharge, although it is not usually considered a sufficiently serious problem to warrant applying a correction to the values obtained (Beven et al, 1979; Elder et al, 1990; Day, 1976). However, bearing in mind the nature of the streams to be studied in this research (i.e. the increased likelihood of dead zones), salt loss was considered a potential problem worthy of further investigation.

Provided that the mixing length has been reached, any difference between the estimated discharges at the two probe locations must be due to experimental error, salt loss, or some difference between the probes. To establish whether salt loss was a problem, the following study was carried out. At Grindsbrook A at a constant low flow, three salt dilution runs were carried out. The first used Probe 1 at the upstream end and Probe 2 in the downstream position. The second run had the probes in reversed positions, with the third run carried out with the probes returned to their initial positions. If, for all three runs, the upstream probe's integral is greater than the downstream's then it can be assumed that there is some degree of salt loss. It was found that for all three runs that there was salt loss of 1% a minute, considerably larger than the estimate made by Kellerhals (1970). This would lead to considerable underestimation of discharge at low flows, where the salt can be in the stream for as long as 20 minutes before the centroid reaches the probes.

This study therefore suggests that the effect of salt loss is potentially important, and so should be limited as far as possible. Therefore, the actual distance from the salt emplacement point to the upstream conductivity meter was as close to the estimated mixing length as possible. At low flow (when this study at Grindsbrook A was carried out) there is more potential for error as there are more dead zones, and the flow is moving slower, giving rise to greater potential salt loss. Therefore, the gaugings carried out at low flow will be less accurate than those carried out at high flow, and it is prudent to make additional low flow gaugings to average out any inaccuracies. During the selection of the study reaches, it was relatively easy to find study reaches without significant dead zones. However, it proved impossible to avoid the presence of any dead zones over the mixing distance from the salt injection point to the upstream probe (Probe 1).

As well as errors from incomplete mixing and salt loss, there are other potential errors associated with salt dilution gauging. Gilman (1977) warns of problems associated with the discharge varying during the period the readings are taken. This is not a problem with this research, as any changes in discharge during the time that the gauging was carried out would also be matched by a change in velocity. Generally, the discharge did not change over the time the gauging was carried out. The position of the probes is important; if they are put into a dead zone then the readings obtained will not be representative of the average reach flow. If the temperature changes considerably over the time the readings are taken then this will also lead to an inaccuracy. It was necessary to consider these two factors when designing the fieldwork methodology to be employed.

5.3 Fieldwork methodology and data analysis

As the reaches were shorter than the distance necessary for complete mixing to take place, it was not possible to determine velocity by adding salt at the upstream end of the reach and having a conductivity meter at the downstream end. Therefore, two conductivity meters were necessary - one at the upstream end of the reach (Probe 1) and the other at the downstream end (Probe 2), with the salt added to the stream further upstream. Both probes were attached to the same data logger. Figure 5.1 shows the experimental set-up.

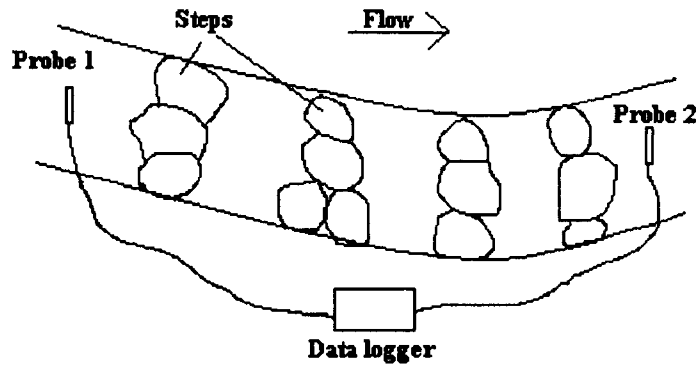

Figure 5.1. Experimental set up for the salt dilution gauging.

Gaugings at as wide a range of discharges as possible were required in order to build up accurate relationships between the measured variables which are valid for different flow levels. Extra runs were carried out at similar low discharges to limit errors from salt loss. The following things needed to be considered for the salt dilution gauging runs carried out:

- position of the conductivity meters,
- salt quantity and location of injection,
- operation of the data logger,
- data analysis and extrapolation,
- errors.

5.3.1 Position of the conductivity meters

The exact position of the probes was matched as closely as possible to a sketch drawing of that part of the reach, in an attempt to maximise consistency. Some variation was observed in the flow in different parts of the stream, so to avoid any problems associated with this ,the probes were put in the stream at a similar position for each run. This position was in free-flowing water, away from dead zones (which may occur just downstream of a small rock) and any air bubbles. A stone was placed on top the probes to weight them down so that they did not move downstream with the flow.

The background conductivity was recorded before the run was started - this was important as it was necessary to know when background levels were resumed and hence the run completed. The distance between the probes was needed for calculating the average velocity in the stream; this distance was obtained from the EDM surveys. In order to calculate discharge it was also necessary to know the temperature of the stream, as this is needed to correct the conductivity readings (Equation 5.5). Therefore, a temperature probe was used to determine temperature at the positions of the two probes before and after each run, although the values were almost always identical.

5.3.2 Salt injection position and quantity

The dry salt was added to the stream approximately 20 channel widths upstream from the upstream probe in order to ensure complete mixing (as explained in Section 5.2.5). The amount of salt injected into the stream depended on the discharge and the site. Doctor's Gate at low flow needed only 100 g of salt, whereas the larger streams at high discharge needed at least 600 g. The salt was kept in labelled, pre-weighed bags of 100 g, 200 g and 500 g, and when each stream was visited the required quantity of salt was estimated from the level of the water, and knowledge from previous runs. When the salt was added to the stream, the stopwatch was started, and any salt that sank to the bed was stirred (by hand) to encourage rapid dissolution.

After several runs had been carried out at each of the sites it was possible to estimate the amount of salt required in order to obtain a peak conductivity 20-30 $\mu S\ cm^{-1}$ above the background level. This was considered desirable for the following reasons. Firstly, it was important to be as consistent as possible in order to minimise errors and variations from salt loss etc. Maintaining the peak conductivity at a constant value was not always possible as the decision concerning the amount of salt to be used was subjective, based on an estimate of the flow level. Secondly, this level of conductivity above the background level was sufficient to produce a well-defined salt wave, and it was considered best to avoid using unnecessarily large quantities of salt.

5.3.3 Operation of the data logger

A Grant Squirrel data logger was used to store the simultaneous conductivity readings from both the probes. After the salt had been added the data logger was set to start recording. The time between injection of the salt and starting of the data logger was recorded using a stopwatch. At very high flow it was necessary to start the data logger before adding the salt into the stream, as the time it took to return to the data logger from the salt injection position was longer than the travel time of the salt wave.

In general, recordings were made every second. However, if the discharge was very low there was a danger of the data logger's memory being filled before the stream returned to background conductivity. If this was considered a possibility recordings were made every 2 seconds. This was only necessary at Doctor's Gate at low flow. The data logger used was an 'averaging Squirrel', so the value recorded is the average value over the one second period preceding the recording time. This means that there is a one second delay between the data logger being set to record and the first recording. When the conductivity returned to the background level the recording was stopped, and the data from the Squirrel downloaded to a PC.

5.3.4 Analysis of the salt dilution gauging data

The data recorded by the data logger consisted of a series of times and the conductivity values at each time for both probes. After the data had been imported into Microsoft Excel, analysis was carried out. During all the runs, the background conductivity fluctuated between two values with a difference of 2 $\mu S\ cm^{-1}$. This is a reflection of the fact that the resolution of the Squirrel data logger used is 2 $\mu S\ cm^{-1}$. Both of these values were treated as the background conductivity, with excess conductivity being calculated by subtracting the recorded value from the higher of the two background readings. When an attempt was made to calculate an 'average' conductivity from these two values there was a larger discrepancy between the two discharge values.

If the memory of the data logger was filled before the conductivity returned to its background level, as happened once at the Doctor's Gate reach, the conductivity values were extrapolated using a negative exponent to determine the time at which the background conductivity level was returned to. This method was found to provide an accurate estimate when used on runs where the full run was recorded.

5.3.5 Error analysis

The following error sources will be considered in this sub-section:

- salt loss,
- data logger resolution,
- failure to achieve total mixing.

As there were two conductivity meters, there are two possible accuracy checks. These are:

1. Comparison of the salt-wave integrals ($\sum_{t_e}^{t_s} C.\Delta t$) obtained from the two probes. If complete mixing has not been achieved then the upstream integral will be different to the downstream integral. This is likely to be a positive difference (i.e. the upstream probe having a greater value) as the probes were placed in the main part of the flow. However, there is the possibility that any difference is because of salt loss or is because of the data logger's resolution; it is impossible to establish the cause of any difference. Therefore this method is useful as a general accuracy check but cannot be used to detect a specific source of error.

2. Comparison of the discharge and velocity estimates. The velocity value is not affected by whether total mixing has been achieved or not, whereas the discharge value is. Thus, if the values obtained for a particular run plot a significant distance away from the general discharge and velocity relationship, then it is probable that total mixing had not occurred for that run.

The estimated accuracy of the salt dilution method in determining discharge is ±5% (Beven et al 1979). Therefore, if the integral values obtained from the two probes were more than 5% different it was assumed that complete mixing had not been achieved, or there had been considerable salt loss. If this occurred, the data from that run was ignored. This only happened once, at the Grindsbrook A site, under very low flow conditions. However, the salt-wave integral obtained from the upstream probe was almost always greater than the one from the downstream probe, suggesting that there was measurable salt loss over the study reach. This strongly suggests that there would also have been salt loss between the position the salt is put into the stream and the probes, which would lead to a systematic under-estimation of discharge.

From analysis of all the runs at all the sites, the data in Table 5.2 were obtained for average percentage salt loss per minute (assuming that this is the main source of error). The variation between the sites is a reflection of differences in the number of dead zones, and splits in the flow within the channel. The standard deviation is very large, and for some of the runs the downstream probe integral was greater than that of the upstream probe. Therefore, it was decided not to apply a correction factor based on the average salt loss at each of the sites as the variability was too great, and there was not conclusive proof that the discrepancy between the sites was because of salt loss. For this study absolute accuracy was not necessary - the aim was to establish relationships between the flow variables. This is still possible with slightly inaccurate results. Also, there have been very few other studies with which to compare absolute values. A difference between the integrals of 5% translates into a difference in discharge of about the same percentage. Considering that the average maximum discharge was 30 times greater than minimum discharge, a 0.05 difference in discharge is insignificant.

Table 5.2 Average estimated salt loss at each site

Site	Minimum discharge ($m^3 s^{-1}$)	Maximum discharge ($m^3 s^{-1}$)	max/min	Average salt loss per minute (%)	Standard deviation (%)
Ashop	0.028	0.528	19	0.19	0.79
Burbage	0.0048	0.1897	40	0.56	0.43
Doctor's Gate	0.0014	0.0793	57	0.22	0.84
Fairbrook	0.0379	0.2810	7	0.47	0.92
Grindsbrook A	0.0142	0.3487	25	0.66	0.53
Grindsbrook B	0.0132	0.3032	23	0.26	0.33

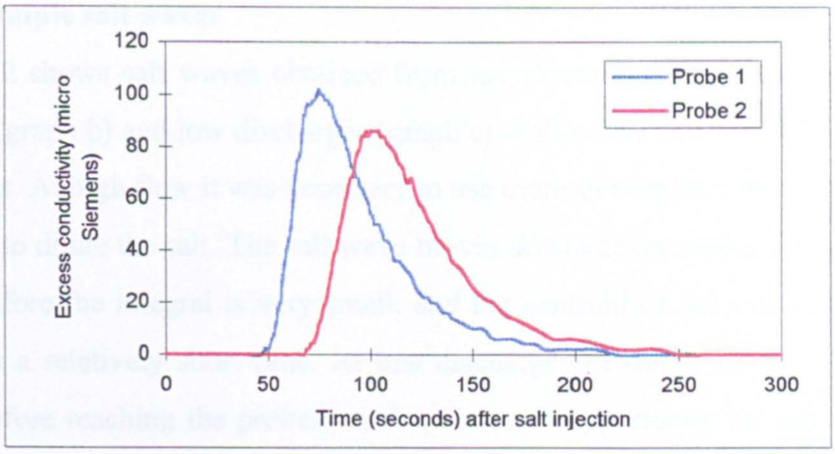

Figure 5.2a. High discharge.

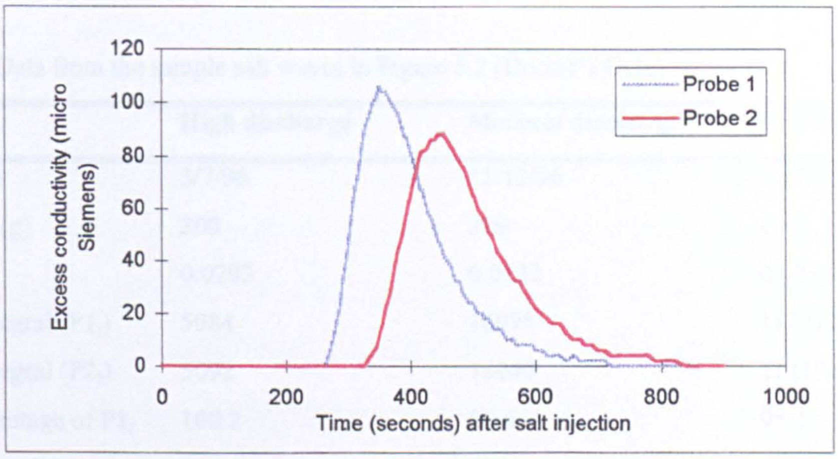

Figure 5.2b. Medium discharge.

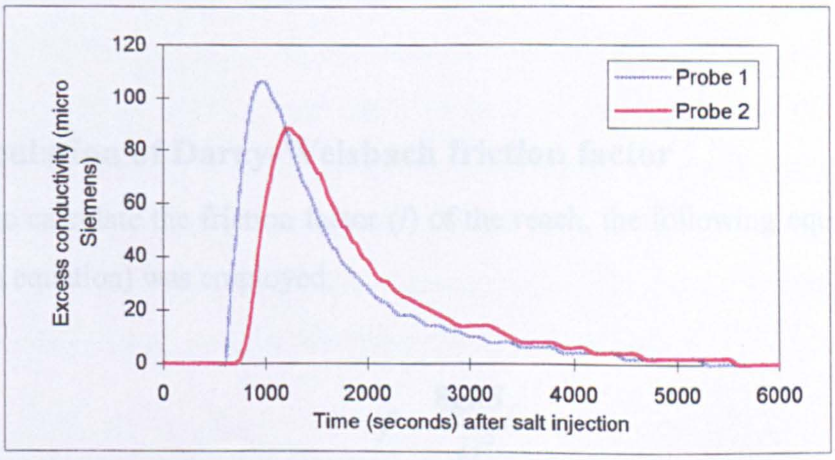

Figure 5.2c. Low discharge.

Figure 5.2. Example salt dilution graphs for Doctor's Gate. Time is the time in seconds after the salt was put into the stream. The conductivity value is the value above background conductivity. Note different x-axis scales.

5.3.6 Example salt waves

Figure 5.2 shows salt waves obtained from the Doctor's Gate site at high (graph a), medium (graph b) and low discharges (graph c). Table 5.3 shows information about the salt waves. At high flow it was necessary to use more salt because there was more water in which to dilute the salt. The salt wave moves downstream very quickly at high flow, and therefore the integral is very small, and the centroid of the salt wave reaches the probes in a relatively short time. At low discharge the salt is in the water for much longer before reaching the probes, so there is more opportunity for salt loss, which is dependent on time in the stream (Kellerhals, 1970). This is reflected in the fact that the difference between the integrals is greatest for the low flow run data.

Table 5.3. Data from the sample salt waves in Figure 5.2 (Doctor's Gate)

	High discharge	**Medium discharge**	**Low discharge**
Date of run	3/7/96	11/12/96	26/7/96
Salt added (g)	300	200	100
Q ($m^3 s^{-1}$)	0.0793	0.0132	0.0014
Probe 1 integral ($P1_I$)	5084	16098	117772
Probe 2 integral ($P2_I$)	5092	16040	112198
$P2_I$ as percentage of $P1_I$	100.2	99.6	95.3
Probe 1 centroid (sec)	94	296	1608
Probe 2 centroid (sec)	121	489	1913

5.4 Calculation of Darcy-Weisbach friction factor

In order to calculate the friction factor (*f*) of the reach, the following equation (Darcy-Weisbach equation) was employed:

$$f = \frac{8gRS_f}{\overline{U}^2} \qquad [5.9]$$

S_f is the energy gradient of the reach, g is the gravitational constant, $\overline{U}$ is the reach average velocity determined in Equation 5.8, and R is the hydraulic radius. Slope was calculated from EDM measurements of the reach in question. Often the water surface slope is used for friction slope, but it was decided for this study to use the bed slope. To obtain an accurate estimate of water surface slope would require surveying the water surface every time a salt dilution reading was taken, as the water surface slope would be expected to vary slightly with discharge. This was considered impractical because of the time involved, and the fact that it would mean that two people would be required every time salt dilution was done. It was also considered that the average bed slope over the length of reach studied was unlikely to differ significantly from the water surface slope averaged over the same distance

The hydraulic radius of the reach is calculated from $R = \frac{wd}{w + 2d}$. Therefore, it was necessary to obtain values for average channel depth and width. Use of the continuity equation meant that only the width or the depth needed to be known, as the other could be determined from this equation. In order to establish which parameter would be best to measure in the field and which to determine from the continuity equation (or whether it was necessary to determine both directly), an initial study was carried out at Grindsbrook A to look at the errors associated with measuring width and depth. This study is described in the following sub-section.

5.4.1 Width and depth error analysis

Thirty-four width readings (at 50 cm intervals over the length of the reach) were taken, and for every width reading three depth readings were taken across the stream (i.e. a total of 102). These amounts represented approximately the same measurement effort. Then statistical analysis was carried out in order to study the variability and the errors associated with these width and depth measurements. The results obtained were used in the continuity equation to determine the error associated with:

- using width measurements obtained from the field and calculating depth from the continuity equation;
- using depth measurements obtained from the field and calculating width from the continuity equation.

Table 5.4 Width and depth error analysis. Interval (m) is the± error associated with the average value and error (%) is the interval (i.e. +/- one standard error) as a percentage of the average.

Variable	Average (m)	Interval (m)	Error (%)
Width - measured	2.48	0.23	9.3
Width - calculated	3.47	0.63	18.3
Depth - measured	0.0830	0.014	16.9
Depth - calculated	0.116	0.014	11.7

The results obtained from this study are shown in Table 5.4. It was found that because of the larger variation in depth than width in the field (leading to very high errors for depth), it was statistically more accurate to determine width directly from field data and calculate depth indirectly from the continuity equation.

5.4.2 Measuring width in the field

The discussion in the previous sub-section highlighted the importance of determining as accurate an estimate of width as logistically possible, as the error in width is passed into the depth error. The channel width is highly variable in steep streams because of the steps and pools and the presence of boulders in the channel. It was, therefore, considered vital to minimise this error, bearing in mind practical time constraints. The following errors were found from a study using many width measurements, where the error shown is the interval (i.e. one standard error) as a percentage of the average value:

- 68 readings - 6.5% error,
- 34 readings - 9.3% error,
- 17 readings - 13.2% error.

It was decided that 34 width measurements was the absolute minimum number required to keep the error associated with width to below 10%. For most sites about 50 width measurements were taken at equal intervals along the reach. However, Doctor's Gate has a very variable width in relation to its size, so at least 60 measurements were needed there. This was done by measuring width every 30 cm in order to equally sample the entire reach. It was only necessary to measure width between the probes as the study was looking at friction factor in the study reach only (i.e. it was not necessary to measure width from the position the salt was put into the stream to the upstream probe as well). The width measured is the water surface width i.e. the distance between the water's edges minus the distance occupied by any sediment protruding above the water surface.

5.4.3 Calculating width

As the sites were visited and values for discharge and width obtained it was possible to build up a graph relating width and discharge. At all the sites there was a clear relationship between the two parameters, which meant that estimating width from the discharge calculated was feasible. However, this was only done once there were enough data points to ensure that the error associated with the regression prediction was smaller than the error associated with direct field measurement (i.e. an error of under 10% was possible). Error analysis of the relationships obtained showed that once about 8 data points for each site had been obtained it was as accurate to estimate width as it was to measure it directly. However, this was not true for Doctor's Gate, where width was always measured in the field.

However, whilst the relationships obtained could be used to estimate width accurately for values of discharge within the range already observed (interpolation), it cannot reliably be used for higher or lower values of discharge (extrapolation) because the width-discharge relationship could vary. Therefore, if when a site was visited the water level was lower than that seen before at that site, it was decided that width measurements would be taken (in practise this situation did not arise as by the time 8 data points had been collected summer and low flow conditions had passed). If the discharge was higher than that observed before at that site it was not always possible to measure width because of the flow depths and speeds associated with high flow conditions. Fortunately the graphs of discharge and width indicated that there is an upper limit for width i.e. when bankfull width is reached and no sediment protruding, so it was possible to use this value for the width at higher discharges as the banks were very steep.

5.4.4 Friction factor errors

As described earlier in this chapter, an error of 5% was assumed with the discharge and velocity readings. A value of 5% was also assumed with the slope readings as whilst the slope readings were determined from very accurate EDM readings, the long profile transect was chosen subjectively, and so may not have been exactly a straight line down the channel.

The following maximum errors were associated with the parameters used in the Darcy-Weisbach equation (again the error shown is the interval as a percentage of the actual value for that variable):

- width - 10%
- depth - 12%
- velocity - 5%
- discharge - 5%
- slope - 5%

The following equations for calculating errors were then used to determine the overall error associated with friction factor and hydraulic geometry:

$$(A \pm E_A) + (B \pm E_B) = A + B \pm \sqrt{E_A^2 + E_B^2} \qquad [5.10]$$

$$(A \pm E_A)(B \pm E_B) = AB \pm AB\sqrt{\left(\frac{E_A}{A}\right)^2 + \left(\frac{E_B}{B}\right)^2} \qquad [5.11]$$

$$\left(\frac{A \pm E_A}{B \pm E_B}\right) = \frac{A}{B} \pm \frac{A}{B}\sqrt{\left(\frac{E_A}{A}\right)^2 + \left(\frac{E_B}{B}\right)^2} \qquad [5.12]$$

$$C(A \pm E_A) = CA \pm CE_A \qquad [5.13]$$

$$(A \pm E_A)^n = A^n \pm nA^{n-1}E_A \qquad [5.14]$$

Here A and B are the values of the variable on which the operation is to be performed, and E_A and E_B are the numerical values of the errors associated with A and B respectively. This leads to an overall 19% error in the calculated value of friction factor. This value is acceptable as many readings were taken over wide range of discharges. However, this error depends mainly on the width error and this will vary slightly between runs depending on the site and the discharge. At higher discharges there will probably be less variability in width, and, therefore, a lower error will be present than for the low flow readings. So, as was concluded after considering the salt loss errors, it was important to carry out extra readings at similar low flows.

Chapter 6

Flume methodology

6.1 Introduction and flumework aims

This chapter will only describe the methodologies and techniques employed for the flumework; the actual results, observations and conclusions are considered in Chapters 9 and 10. The reasons for carrying out the flumework were three-fold. Firstly, the fact that it would be highly unlikely to witness step-pool formation in the field meant that flume studies were considered the best way to investigate step formation, and the effects of step formation on the flow. Secondly, more control is possible in flumework in terms of discharge and slope, meaning that relationships between factors such as discharge and friction factor could be studied under a range of conditions, enabling detailed study of the effect of roughness elements on the flow. In the field this range is limited to available fieldsites, and the flow conditions when the runs were carried out. Thirdly, using a miniature current meter meant that it was possible to obtain velocity profiles from the flume (for example, over a step-pool sequence), something that was not possible to do in the field.

The following aims for the flumework were identified following consideration of the data that the flumework could provide, the aims identified in Chapter 2, and study of previous work carried out in flumes.

1. Establish whether it is possible to create steps in the flume being used, and if so, study the range of flow conditions under which they form, how they compare with the features observed in the field, and how the flow conditions compare with previous work that has created step and pool sequences in the flume.
2. Study the formation of steps and pools (by visual observation and investigation of the flow conditions), test existing theories of step formation, and develop a new theory if the existing theories are found to be inadequate.
3. Compare the hydraulic geometry relationships to those at the fieldsites.

4. Investigate the hydraulic effects of the steps and pools on the flow, in particular the effect on flow resistance.
5. Study in detail the velocity profiles over a step pool sequence, compare these profiles with an existing model (Wiberg and Smith, 1991) that estimates the vertical velocity distribution, and adapt this model if necessary.

Therefore, the research design needed to collect the data necessary to investigate these aims. This chapter will consider the flume setup and procedures that were carried out to obtain these.

6.2 Flume and sediment characteristics

Flume studies attempting to create steps and pools have been carried out by Whittaker and Jaeggi (1982), Ashida et al (1984), and Grant (1994). The flume characteristics used for the studies carried out by Whittaker and Jaeggi (1982), and Grant (1994), who used two flume set-ups, are shown in Table 6.1.

Table 6.1 Sediment and flume characteristics used in previous flume studies forming steps and pools. n/i = no data available for that variable

Variable	Whittaker and Jaeggi (1982)	Grant	(1994)	This research
Flume length (m)	10	11	11	8
Flume width (m)	0.132	0.5	0.25	0.3
Typical slope	0.0977 - 0.2410	0.04	0.04	0.0625
Discharge ($m^3 s^{-1}$)	0.0008-0.0062	0.004	0.004	0.01
D_{84}/D_{16}	3	17	15	4
D_{max} (mm)	50	64	30	64
D_{50} (mm)	16	5	3	16
w/D_{max}	2.64	7.81	8.33	4.76
Sediment range (mm)	2-50	0.1-64	0.1 - 30	4-64
Sediment depth (cm)	n/i	10	10	10

6.2.1 Flume set-up

The flume used was an Armfield tilting flume that was 8 m long, 0.3 m wide, with a maximum achievable slope of 0.0667. The discharge was controlled by entering a value (corresponding to discharge) into a computer, where this value represents how wide to open a pneumatic valve in the re-circulation pipe. The corresponding discharge could be read approximately from the standard Armfield flowmeter and determined accurately from a rating curve compiled previously using a miniature current meter. The first consideration was what values to use for slope, sediment size and discharge for the runs. As an initial guideline, the conditions observed in the fieldsites were scaled down to the size of the flume in terms of the sediment size in proportion to the width, and the values used by other workers were also studied (i.e. the values in Table 6.1).

The sediment mix used was similar to that used by Whittaker and Jaeggi (1982) and Grant (1994) for their flume experiments (which generated steps), scaled to the dimensions of the flume used, and was also similar to the ratio of sediment to channel size observed in the field. Table 6.2 shows the sediment mix used for this flume study (displayed graphically in Figure 6.1), and that used by the above referenced studies. Grant (1994) used very fine sediment, whereas Whittaker and Jaeggi (1982) and this study used a coarser sediment mix - hence the differences between the values, especially the value of D_{84}/D_{16} (seen in Table 6.1). This work produces a value of 4, which is closer to the estimated field situation, where an average D_{84}/D_{16} sorting of 5 was found (where, again, fine sediment was not included in the sediment survey; 8 mm was the finest considered).

Table 6.2 Sediment distribution used for selected flume studies. The values used obtained for this research were obtained by considering sediment weight

Particle size (mm)	**Cumulative This study**	**Percentage Grant (1994)**	**Finer Whittaker and Jaeggi (1982)**
4	0	42	0
5.6	5	51	5
8	16	60	16
11.2	30	76	30
16	50	82	50
22.4	70	87	70
31.5	84	90	84
45	95	94	95
63	100	100	100

The largest particles used (i.e. the 45 mm to 64 mm size fraction) were painted for easy recognition. From the field study it was clear that the largest particles make up the steps, therefore, it was expected that most of the sediment in the flume steps would be made up of this particle size range. These painted particles were not labelled individually as the aim of having the tracers was just to see how many of them moved and whether they became concentrated in the steps.

6.2.2 Initial flume runs

Initially it was not known exactly what discharge and slope values were necessary to produce sediment movement and initiate step formation, or even if steps would form at all. Therefore, eleven initial flume runs were carried out to establish what range of slope and discharge values was likely to produce steps and pools. The positions of the tracers before and after the run were plotted, and the level of the sediment after the run was marked on the sides of the flume enabling long profiles to be drawn after the run was completed. This enabled identification of the steps and pools that formed (if any). The observations and results from these initial runs are described in Chapter 9. These runs, therefore, established the range of discharge and slope values to be used for the main set of flume experiments, described in the next section.

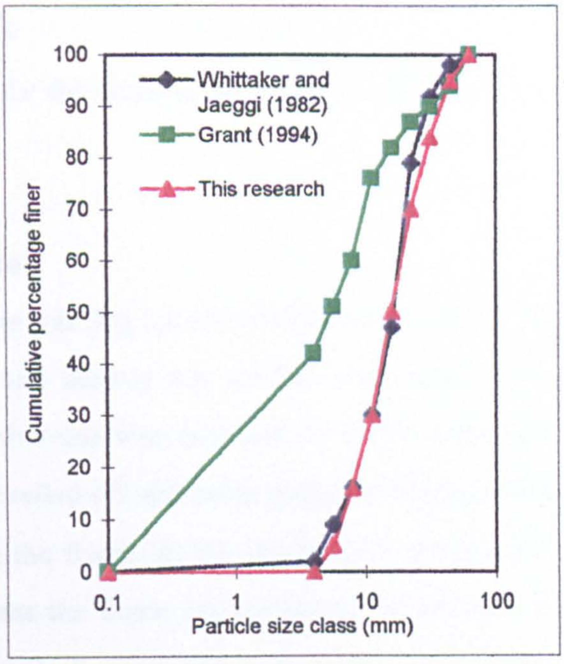

Figure 6.1a

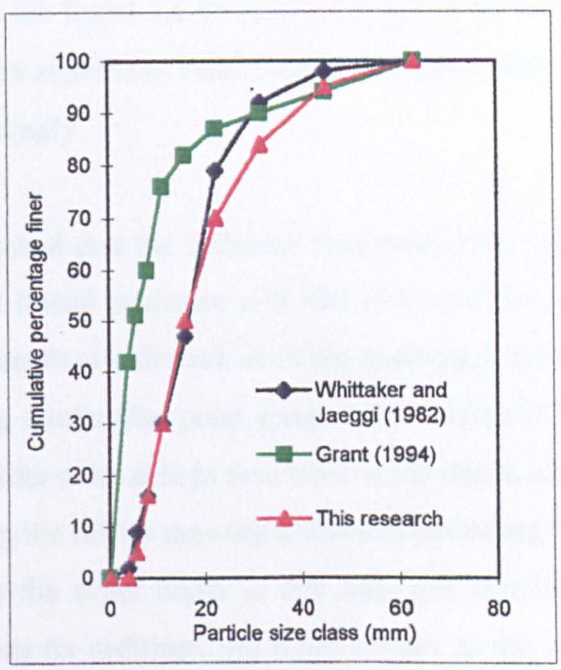

Figure 6.1b

Figure 6.1 Sediment distribution curves for selected flume studies using a) log scale and b) arithmetic scale

6.3 Main flume work

The procedure followed for the detailed set of runs carried out after these initial runs is described below:

6.3.1 Pre-run procedure

The sediment in the flume was dug up and mixed up in order to break up any features from the previous run, and destroy any surface armouring. Observations from the initial studies indicated that this was necessary to allow entrainment. The surface of the sediment was then levelled off and point gauge readings of sediment height taken at 10 cm intervals along the flume (in the streamwise direction) and at 5 cm, 15 cm and 25 cm intervals across the flume (in the lateral direction). The point gauge was attached to a trolley that ran along the top of the flume. These data were then used to determine statistically whether there was any significant trend in sediment height thickness down or across the flume, i.e. to establish whether the sediment was indeed level or not. If there was a significant trend found in any direction then the sediment level was adjusted accordingly.

Once it had been established that the sediment was level, long profiles of sediment height were obtained at lateral positions y=0 and y=30 cm (i.e. either side of the flume). Readings of the depth of sediment, at 10 cm intervals, were measured through the glass side-wall using a ruler (the point gauge only worked in the range $5<y<25$ cm). This was done in order to be able to determine water depth, as the water surface was recorded later during the run by drawing a line corresponding to it on the side of the flume. Working out the water depth in this way was considered preferable to using regression equations for sediment and water surface as this method used direct measurements of water depth at the same location as sediment height. Having the initial level of the sediment marked also meant that an estimate of the depth of scouring or sediment accumulation could be made.

The following procedures were also carried out prior to each flume run:

- Sediment heights for six transects were measured so that *K3* values (as determined for each of the fieldsites) could be calculated. The point gauge was used to take readings every 4 mm at three transects across the flume (starting from 5 cm in from each side) and at every 4 cm down the flume for a distance of 2 m.
- *x-y* locations of all visible tracers were measured using the point gauge, and it was noted whether they were on the surface or buried.

6.3.2 Flume run procedure

The initial runs carried out gave an indication that the range of slope and discharge likely to produce steps and pools was limited. However, to compare the flume results with the hydraulic geometry relationships and friction factor relationships observed in the field, and also to compare flow conditions in the flume prior to and after step formation, a wider range of discharge was desirable. Therefore, the flume was run at a series of discharges. Generally, the flume was run at one low discharge and one or two medium discharges before being run at the step-forming discharge. After a period of time at this high discharge the flume was again run at the medium discharge(s) and then finally the low discharge. This procedure is described in detail below:

The flume was run for 15 minutes at each of the lower and medium discharges, during which it was checked that there was no significant sediment movement (determined by whether any of the tracers moved). At the end of each 15 minute run the water level was marked on both sides of the flume using a colour-coded pen. The discharge was then increased to the higher step-forming discharge to initiate sediment movement and step and pool formation. The initial water level at this discharge was recorded, although this was only very approximate because of the fact that the time it took to mark the water level on the side of the flume was longer than the time it took for sediment movement to start.

If there was no tracer movement at the expected step-forming discharge then this flow level was treated as another medium flow run and the discharge was increased slightly to a higher flow for step formation. Therefore, the number of medium discharge runs was either one or two. Generally the flume was run at the step forming flow for about 20 minutes (based on the time that Grant (1994) used; also, it was observed during the initial run series that step break-up became likely if the flume was run at the high discharge for too long).

At the end of the time that the flume was run at this maximum discharge the water level was marked on the side of the flume. The flow was then decreased to the same discharges as the flume was run at before the step-forming flow. Again, the flume was run at each of these discharges for about 15 minutes and the water surface was marked on the other side of the flume. During some of the runs, point gauge profiles of sediment height and water height were also taken as well as velocity profiles. After the lowest discharge the flume was switched off and sediment and water height long profiles for $y=0$ and y=30 cm were measured every 10 cm from the colour-coded wax pencil marks on the sides of the flume. The detailed sediment transect measurements were repeated (in the same positions as previously), and the final position of the tracers was plotted.

6.3.3 Calculation of flow variables

Depth

An interval of 10 cm was used for measuring sediment and water height was, following statistical analysis of the errors involved with various intervals. For measurements taken every 10 cm the error associated with the average height values was 6% (standard error of 1.81 mm); when measurements were taken every 20 cm the error increased to 9% (standard error of 2.47 mm). Each flow was characterised as being either before or after step formation, and depth was calculated as either water level minus pre-step sediment height at that position, or water level minus post-step sediment height. Water depth for each point along the long profile was therefore determined, and an average flow depth calculated. The error associated with this depth value is, therefore, 8.5% (a combination of the errors from water height and sediment height). For some of the runs depth was measured directly using the point gauge whilst the flume was running.

Slope

To remain consistent with the fieldwork methodology, the sediment slope was used for the calculation of friction factor. It became clear early on in the flume work that one of the effects of running the flume at a high enough discharge to produce steps and pools was to move sediment down the flume. As no new sediment was added into the flume, this resulted in a decrease in sediment gradient as sediment accumulated at the bottom of the flume. Therefore, the slope of the sediment after the run was determined from the long profiles. It was found that there was a reduction in the effective slope, so different slope values were used to calculate the pre-step and post-step friction factor.

Velocity

Two methods were used to determine velocity - indirect calculation using the continuity equation and direct measurement using a miniature current meter and taking a number of velocity profiles in order to calculate the average velocity. For runs where velocity profiles were taken the sediment and water heights at the different discharges were also measured, meaning that a comparison of the two velocity values could be performed. Study of the velocity profiles revealed that there was a large amount of variation in velocity because of the sediment affecting the flow. Therefore, calculating a flume average velocity from the velocity profiles would have required taking many velocity profiles at various locations in the flume. For this reason it was decided to determine average flume velocity indirectly using the continuity equation and use the current meter only to determine detailed information regarding the flow conditions over a step-pool sequence.

For measuring velocity directly, a miniature Nixon current meter was used. For each profile, velocity readings were measured every 0.5 cm up the profile, meaning that typically at least 10 points were taken. Measurements were not possible in the bottom 7 mm of the flow because of the geometry of the propeller. Generally profiles were measured at 5 cm intervals streamwise along a step-pool sequence and at either one or three lateral positions across the flume. This is described further in Chapter 10. The current meter was attached to a trolley that could move along the flume and lowered into the flow. A depth gauge indicated the depth of the current meter at the time of the measurement. To obtain the measurement, the current meter was held in the flow until a steady frequency reading was observed. This was typically between five and ten seconds. There was an established relationship between the frequency value (in Hertz) and velocity.

Width

A width value is needed for the calculation of hydraulic radius, and also for determining velocity from the continuity equation. A constant value of 0.3 m was used, even though this introduces a slight error as at lower discharges there would be more sediment protrusion and so a narrower active width than at high discharges. This was considered acceptable as there was much less protrusion in the flume than in the field because of the relatively deeper flow depths caused by the inability of width to increase beyond the flume walls.

6.3.4 Limitations and problems

One possible drawback with running the flume at a series of lower discharges first is that there will be some sediment armouring, meaning there will not be as much sediment movement at the step-forming discharge as if the flume had just been run at the step forming discharge. It is, therefore, possible that any differences between results from this research and other workers' are a result of this procedure as no lower discharge runs were made by them. However, the methodology used in this study enables more detailed comparison of before and after flows, as a wider range of discharges are studied, and is more like the field situation.

Flow conditions at the time steps and pools are formed are of great interest to this research. However, these are very hard to determine because as soon as steps are initiated and the sediment starts to move the flow conditions are slightly altered in response to this. Depth is the main variable used to determine the flow conditions, but, as was found with the fieldwork, the error associated with depth is considerable because it varies significantly. Therefore, the results that were collected from the flumework are not ideal, but should be sufficiently accurate to provide some insight into the flow conditions before and after step formation.

Chapter 7

Hydraulic geometry

7.1 Introduction

This chapter will discuss the flow results obtained from the field salt dilution gauging and the flume runs in relation to the field sediment results in Chapter 4 in order to investigate the magnitude of the effect from the roughness elements and identify its controlling factors. Hydraulic geometry is important, as a general description of the hydraulic behaviour of a stream can be obtained from the relationships of velocity, width and depth with discharge. The relationship of friction factor with discharge will also be described. These relationships can be used to compare the different sites to investigate what controls this hydraulic geometry based on the site characteristics, and to compare these values with those typical of lowland streams. Appendix 3 shows the data that was analysed in this chapter.

7.1.1 Hydraulic geometry theory

As considered in Chapter 2, hydraulic geometry can be defined by the following equations:

$$w=aQ^b \tag{7.1}$$

$$d=cQ^j \tag{7.2}$$

$$\overline{U}=kQ^m \tag{7.3}$$

Once two of these equations are known the third can be determined because the sum of the exponents and the product of the intercepts equal unity. The relationship between discharge and friction factor (f) can be described by Equation 7.4:

$$f=pQ^r \tag{7.4}$$

Assuming a constant slope and approximating R by d in the Darcy-Weisbach equation, it follows that $r=j-2m$ (i.e. velocity has the most influence on the relationship between discharge and friction factor). As well as these relationships with discharge, there are also relationships between width and depth, and velocity and depth, as considered by Ferguson (1986). The cross-sectional shape dictates the width increase accompanying any depth increase; if the banks are very steep there is little width increase possible, whereas if the banks are gently sloping a greater increase in width is possible. The Darcy-Weisbach resistance equation defines the dependence of mean velocity $\overline{U}$ on mean depth d (which, for wide channels, is very close to the value of R, hydraulic radius, used in the equation). Therefore, as these three variables (velocity, depth and width) are related to discharge by the continuity equation, this implies that the hydraulic geometry relationships equations depend on the $w(d)$ and $v(d)$ relationships and that the hydraulic geometry relationships are only power laws if the $w(d)$ and $v(d)$ relationships are.

7.1.2 Data collection and analysis

To establish accurate relationships valid for a wide range of flows it was necessary to collect data at a variety of flow levels in the field and in the flume. Data collection at different flow levels was continued until significant relationships were found between all the variables. However, it was not possible to study the flow in the flume at very low discharges because of problems associated with measuring depth when there were many protruding particles. Also, for the flume only those data obtained after steps were formed were considered in order to be able to compare with the field sites. Despite the fact that the flume is not able to adjust its width the flume data is relevant as gives an indication of the hydraulic geometry relationships in a very small channel with steps and pools.

The values for the exponents obtained are in Table 7.1 and the intercepts in Table 7.2, which were estimated using ordinary least squares regression in Microsoft Excel by regressing, for example, velocity on discharge (the data first needed to be logged as power relationships existed between the variables). Despite the fact that Excel does not allow for error in the x variable (i.e. discharge) this was not considered problematic as the correlations between the variables were very strong (all significant to $p<0.01$ level). The average values for the exponents are comparable to those obtained by Lisle (1986) for steep streams with steps and pools (Table 2.2). There is, however, considerable variation between the values from the different sites. This is, undoubtedly, a reflection of the channel and sediment characteristics at each site. The following section will consider each of the relationships with discharge studied and discuss the controlling factors for each.

Table 7.1. Exponents obtained for the hydraulic geometry relationships.
Values in parentheses are the standard error values associated with the exponents

Site	**Velocity exponent *m***	**Width exponent *b***	**Depth exponent *j***	**Friction exponent *r***
Ashop	0.70 (0.05)	0.21 (0.02)	0.10 (0.06)	-1.29 (0.16)
Burbage	0.54 (0.03)	0.20(0.02)	0.27 (0.03)	-0.81 (0.08)
Doctor's Gate	0.63 (0.03)	0.20 (0.01)	0.18 (0.04)	-1.07 (0.09)
Fairbrook	0.81 (0.08)	0.10 (0.01)	0.09 (0.07)	-1.52 (0.22)
Grindsbrook A	0.46 (0.02)	0.16 (0.02)	0.38 (0.02)	-0.57 (0.06)
Grindsbrook B	0.70 (0.05)	0.17 (0.02)	0.13 (0.05)	-1.26 (0.13)
Fieldsite average	0.64	0.17	0.19	-1.09
Flume (after steps)	0.58 (0.02)	n/a	0.41 (0.02)	-0.91 (0.04)

7.2 Description of the hydraulic geometry

7.2.1 Discharge and velocity relationship

This relationship describes the rate of increase of velocity with increasing discharge. It would be expected in any stream that as the flow rate increases and the flow becomes deeper, the velocity becomes greater as the bed resistance decreases. In steep streams with steps and pools this resistance decrease is more significant because of the size of the roughness elements involved. This means that the rate of velocity increase is larger in steep streams than in lowland streams. Also, as described by Bathurst (1993) there is the added effect of 'ponding' which is drowned out at higher flows, thus increasing velocity further.

Table 7.2 Intercepts obtained for the relationships with discharge. The values in parenthesis are the range of uncertainty (95% interval) of the intercept value (calculated as the antilog of standard error).

Site	Velocity intercept	Width intercept	Depth intercept	Friction factor intercept
Ashop	0.83	6.11	0.20	0.57
	(+15% to -13%)	(+4% to -4%)	(+16% to -14%)	(+51% to -34%)
Burbage	0.81	3.93	0.32	3.17
	(+13% to -12%)	(+8% to -8%)	(+16% to -14%)	(+45% to -31%)
Doctor's Gate	2.13	2.68	0.18	0.16
	(+15% to -13%)	(+6% to -6%)	(+20% to -17%)	(+55% to -35%)
Fairbrook	1.58	3.55	0.18	0.34
	(+23% to -19%)	(+3% to -3%)	(+21% to -17%)	(+79% to -44%)
Grindsbrook A	0.56	4.29	0.42	11.17
	(+8% to -7%)	(+7% to -6%)	(+8% to -7%)	(+22% to - 18%)
Grindsbrook B	0.55	3.43	0.54	19.71
	(+17% to -15%)	(+6% to -5%)	(+18% to -16%)	(+54% to -35%)
Fieldsite average	1.08	4.00	0.31	5.85
Flume	9.12	n/a	0.35	0.0069
	(+13% to -12%)		(+11% to -10%)	(+22% to -18%)

The graphs showing the relationships between discharge and velocity for each of the sites are shown in Figure 7.1, with a composite graph showing all the sites together in Figure 7.2. Table 7.3 considers the errors associated with velocity when it is predicted from discharge alone. The uncertainty range for the flume, Burbage and Grindsbrook A are relatively low (<±10%), whereas the range at Grindsbrook B is very high (-18% to +22%). Figure 7.2 shows that the flume data plots on a different line to the field data as has a much larger intercept value, as seen in Table 7.2. This will be considered in Section 7.2.6. The exponents from the graphs are in Table 7.1, and show a wide range in the values. The extremes are Grindsbrook A (0.46) and Fairbrook (0.81), with a fieldsite average of 0.64. This average value is comparable to that found by previous studies of channels with steps and pools, where values of between 0.57 (Beven et al, 1979) and 0.70 (Newson and Harrison, 1978) have been found, and is greater than the value in Table 2.2 for typical sand and gravel channels (0.34 and 0.49 respectively). The flume value (0.58) is between the value for Doctor's Gate and Burbage.

Fairbrook had the greatest exponent value, indicating that as discharge increases the roughness elements are washed out rapidly, meaning that velocity is able to increase rapidly at this site. The lowest exponents are from Grindsbrook A and Burbage, which both have a lot of large, protruding sediment, meaning that even at deeper flows the sediment still affects the flow in the channel so velocity cannot increase to the same extent as it can at sites with a lower relative roughness. This is quantified in Table 7.4 which shows that Fairbrook has the lowest value for average step sediment height (determined from the detailed transect measurements described in Chapter 4) divided by d_{min} (i.e. the estimated depth, using hydraulic geometry, at the minimum discharge observed at that site during the course of the fieldwork). Fairbrook also has the lowest percentage of channel width containing protruding sediment at d_{min}. Values for these measures could not be determined for the flume as it was not possible to estimate a d_{min} value.

Conversely, Grindsbrook A and Burbage have the highest and second highest values for these two parameters. Therefore, it seems logical to assume that these measures of sediment protrusion control the value of the exponent. Figure 7.3 shows the relationships between the exponent value and these two parameters for all the fieldsites, confirming the significance of sediment protrusion in controlling the increase of velocity with increasing discharge. Considering the wide range of channel and sediment characteristics studied during the fieldwork it was considered likely that the amount of step protrusion for any channel with steps and pools would be within the range in Figure 7.3, i.e. the best-fit lines would not need to be extrapolated (hence the impossible intercept values). The best relationship with the exponent value was obtained when using the average step sediment height divided by d_{min}. As seen in

Table 7.5, using this relationship allowed the exponent value to be predicted with an uncertainty range of ±0.039 (equivalent to 11% of the observed range in the exponent value). Using the percentage of the channel width with protruding sediment at d_{min} produces a larger uncertainty range (±0.078; 22% of the observed range).

It is, perhaps, interesting that these measures are better predictors of the exponent than consideration of the amount of sediment available (i.e. the difference in the amount of sediment protruding at d_{min} and at the estimated maximum depth observed at that site during the research). This suggests that the sediment protruding at the surface at d_{min} still affects the flow when submerged at higher flow. It was found that it is the step sediment measures that have the most control over the value of the exponent, indicating that even though the pools take up more of the channel length, it is the step sediment that has the most control on the reach average resistance and, therefore, velocity.

Table 7.3 Percentage uncertainty range in the predicted values from using hydraulic geometry equations

	Velocity (%)	Width (%)	Depth (%)	Friction factor (%)
Ashop	-16 to +20	-5 to +5	-17 to +20	-41 to +69
Burbage	-9 to +10	-10 to +12	-10 to +11	-24 to +31
Doctor's Gate	-13 to +15	-6 to +6	-17 to +20	-35 to +54
Fairbrook	-16 to +19	-2 to +2	-15 to +17	-39 to +65
Grindsbrook A	-9 to +10	-8 to +9	-9 to +10	-22 to +29
Grindsbrook B	-18 to +22	-7 to +7	-19 to +23	-42 to +71
Flume	-5 to +5	n/a	-4 to +4	-8 to +8

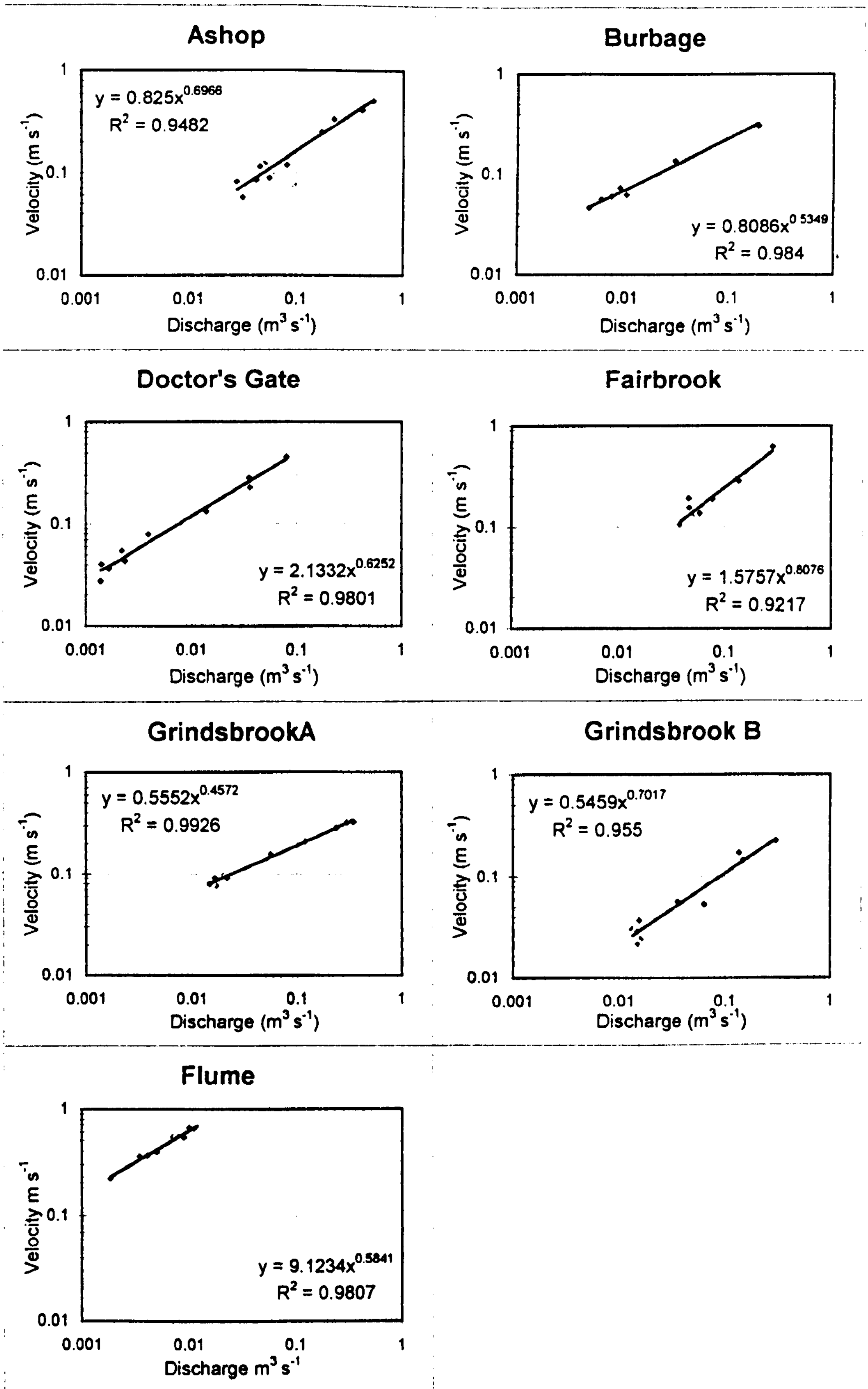

Figure 7.1. Relationship between discharge and velocity

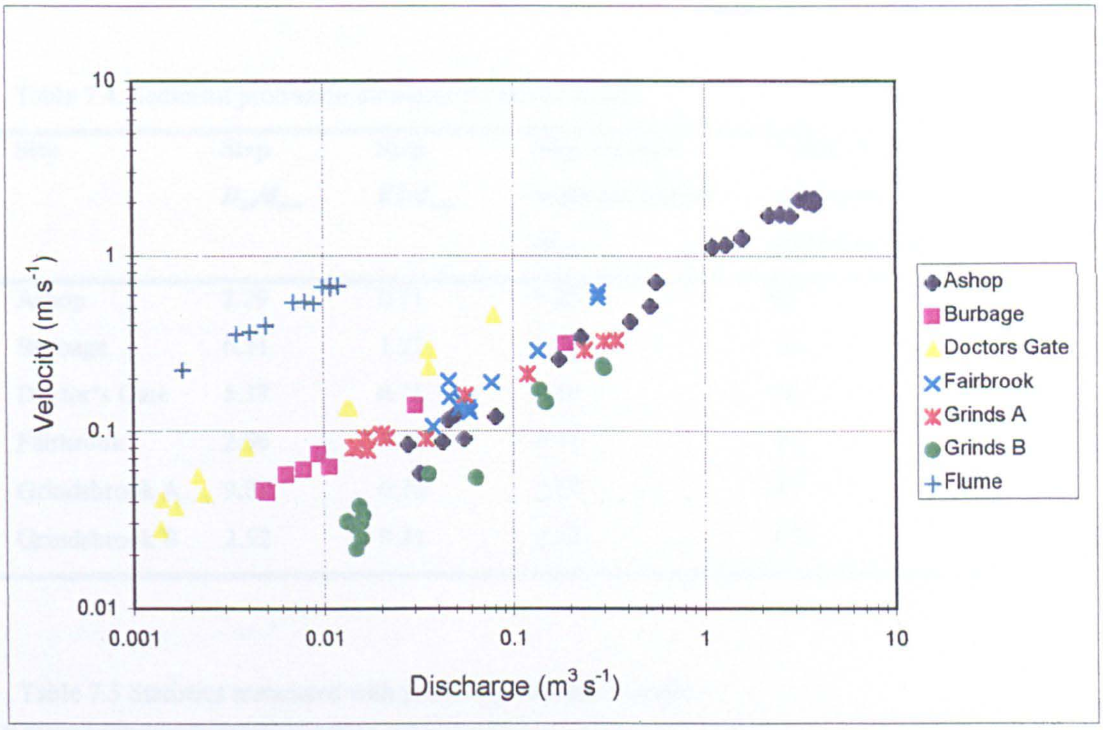

Figure 7.2. Composite graph of discharge and velocity relationship

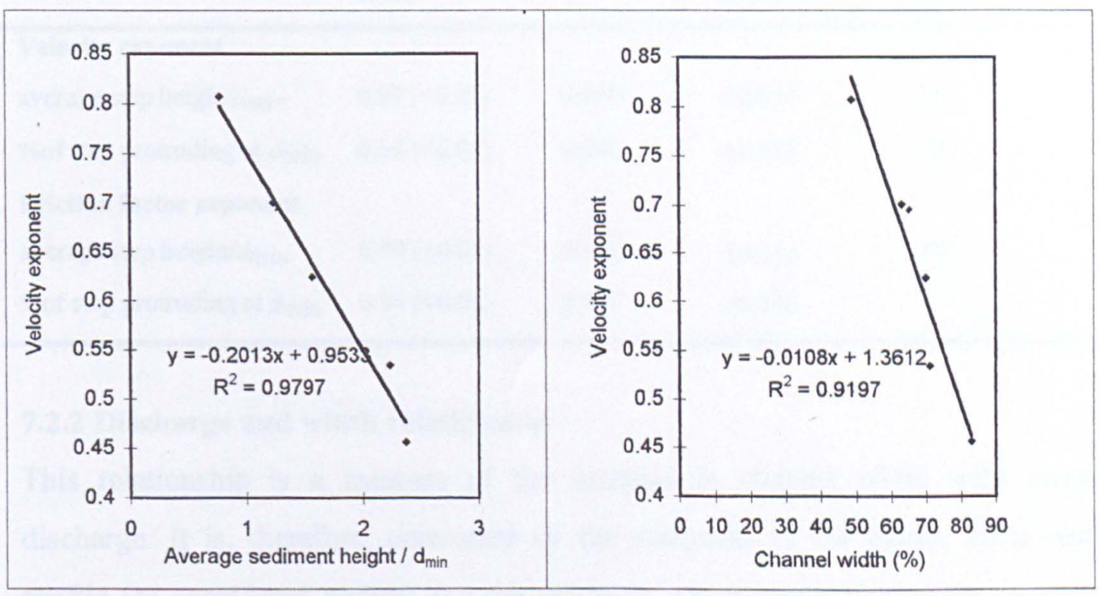

Figure 7.3a

Figure 7.3b

Figure 7.3. Relationship between sediment protrusion and discharge/velocity exponent using a) average sedment height / d_{min}; b) percentage of width with protruding sediment.

Table 7.4. Sediment protrusion measures for the fieldsites

Site	Step D_8/d_{min}	Step $K3/d_{min}$	Step average sediment height $/d_{min}$	%Step width with protruding sediment at d_{min}
Ashop	2.29	0.51	1.25	65
Burbage	6.31	1.22	2.23	71
Doctor's Gate	5.37	0.71	1.56	70
Fairbrook	2.96	0.45	0.77	49
Grindsbrook A	9.07	0.76	2.37	83
Grindsbrook B	2.52	0.41	1.23	63

Table 7.5 Statistics associated with predicting exponent values

Relationship	*r*-value (significance level)	standard error	Uncertainty range (interval)	Interval as % of observed exponent range
Velocity exponent				
average step height/d_{min}	0.99 (<0.01)	0.020	±0.039	11
%of step protruding at d_{min}	0.96 (<0.01)	0.040	±0.078	22
Friction factor exponent				
average step height/d_{min}	0.99 (<0.01)	0.062	±0.122	18
%of step protruding at d_{min}	0.94 (<0.01)	0.127	±0.249	37

7.2.2 Discharge and width relationship

This relationship is a measure of the increase in channel width with increasing discharge. It is, therefore, controlled by the steepness of the banks, cross-sectional profile (as considered earlier) and the extent to which protruding clasts are drowned out, as the channel width measured was water width, not bed width. The values obtained from the fieldsites range from 0.10 at Fairbrook to 0.21 at Ashop, with an average value of 0.17 (the flume could not be included in this analysis). Figure 7.4 shows graphs of the relationship for each of the fieldsites, with the composite graphs of all the sites in Figure 7.5.

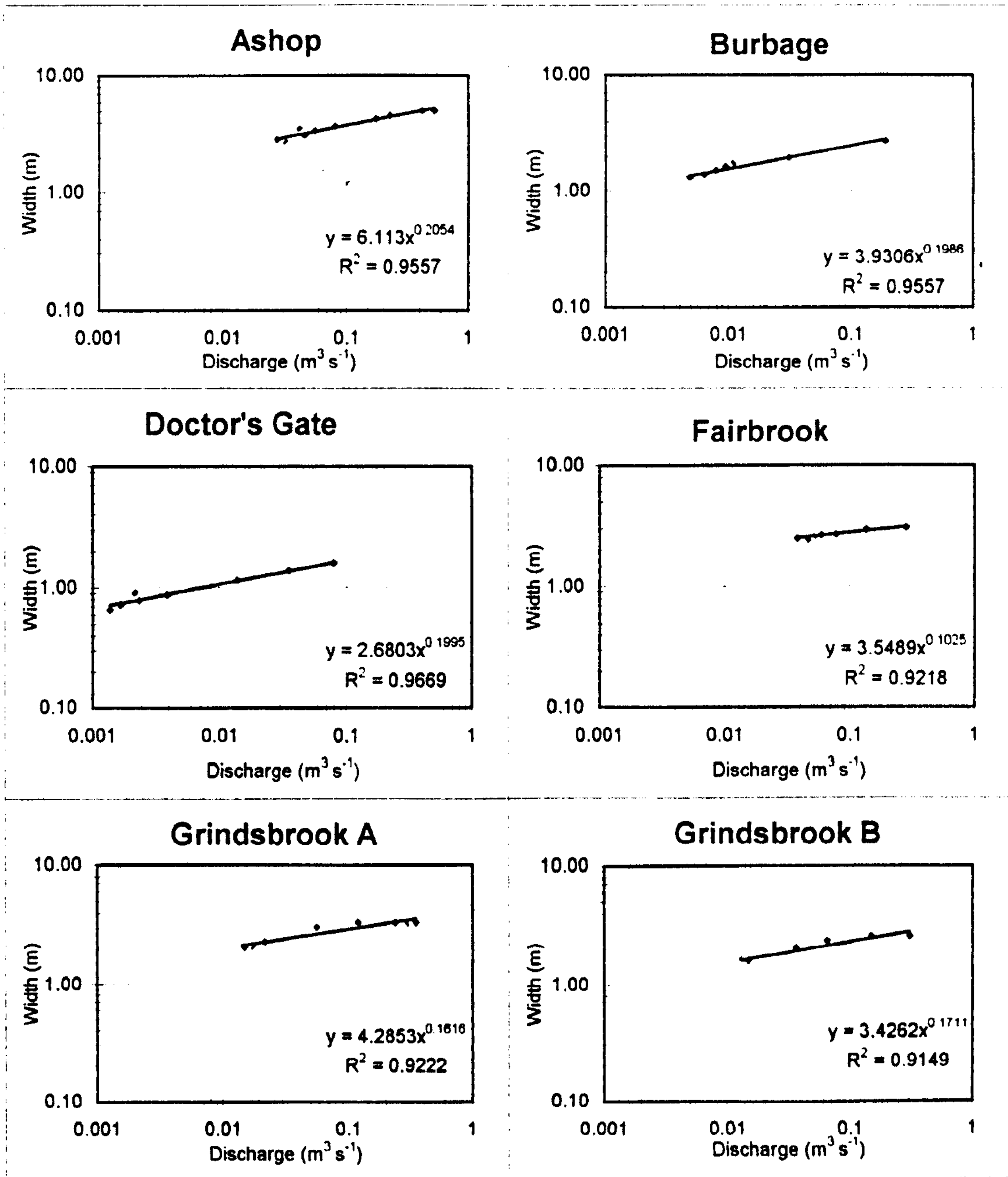

Figure 7.4. Relationship between discharge and width for all the fieldsites

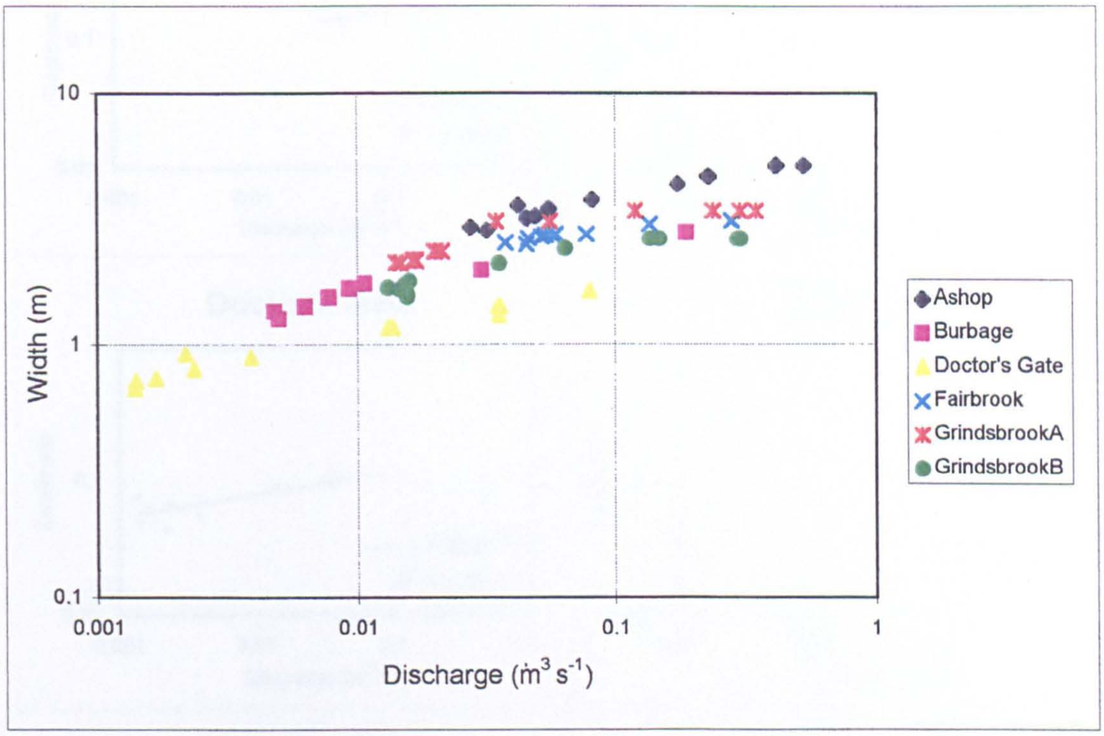

Figure 7.5. Composite graph of the relationship between discharge and width

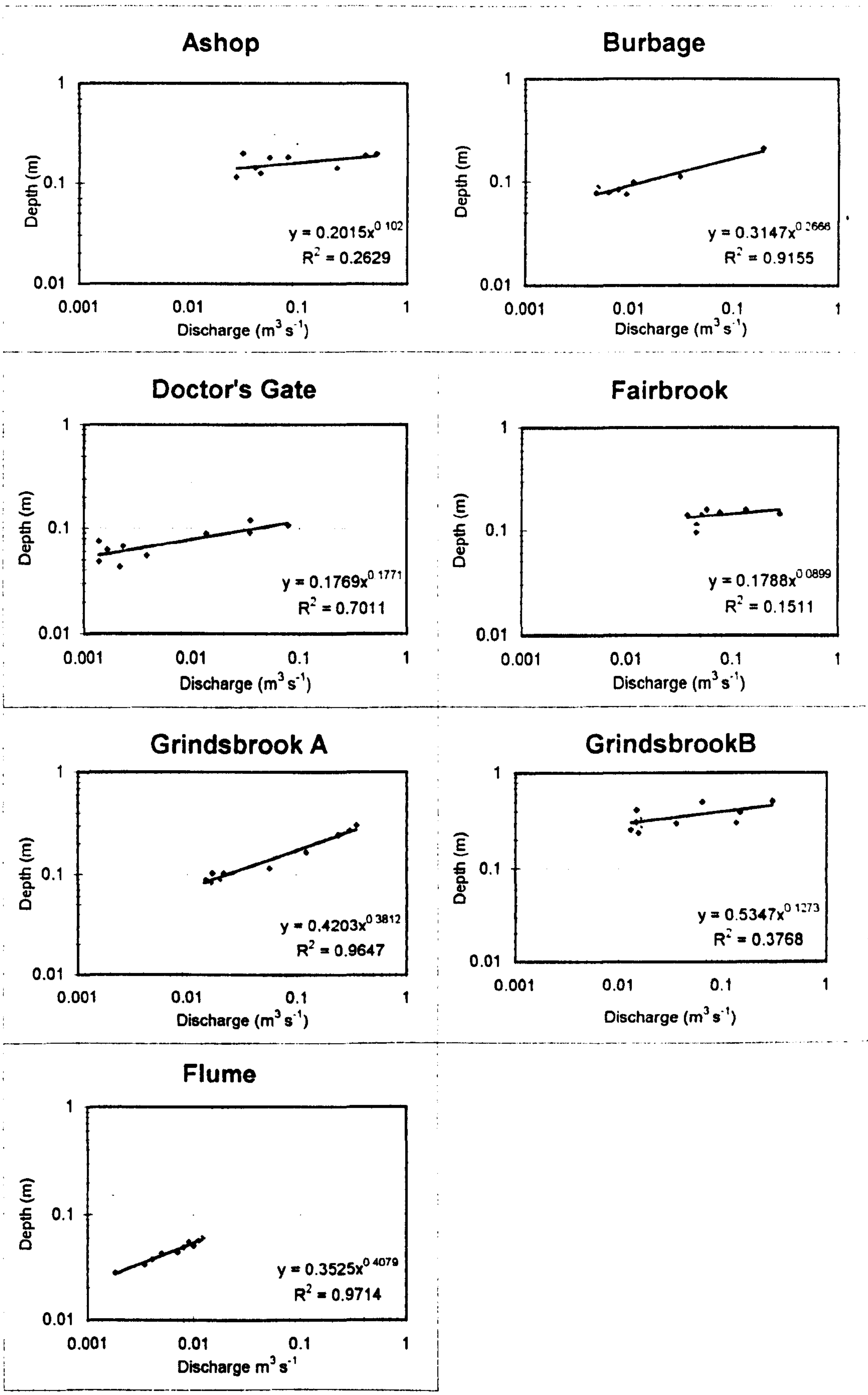

Figure 7.6. Relationship between discharge and depth for all the sites

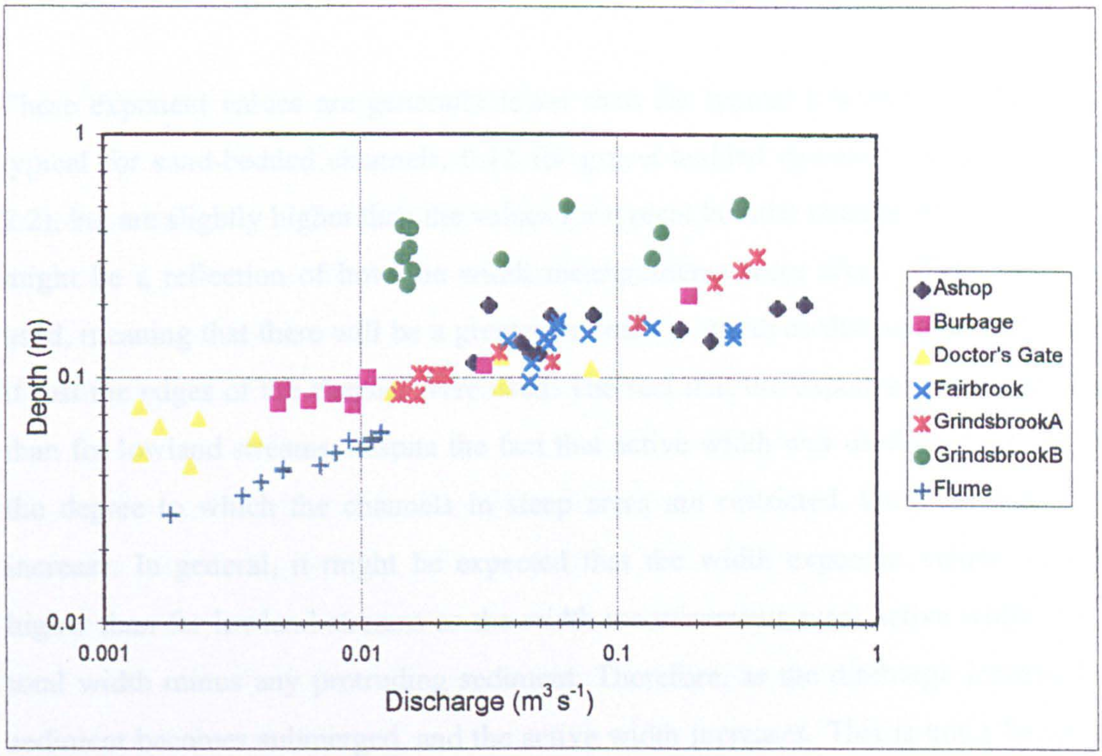

Figure 7.7. Composite graph of the relationship between discharge and depth

These exponent values are generally lower than for typical lowland streams (0.26 is typical for sand-bedded channels, 0.12 for gravel-bedded channels, as seen in Table 2.2), but are slightly higher than the values for typical boulder streams (0.1 - 0.13). This might be a reflection of how the width measurements were taken. Water width was used, meaning that there will be a greater increase in width as discharge increases than if just the edges of the channel were used. The fact that the exponent values are lower than for lowland streams, despite the fact that active width was used, is a reflection of the degree to which the channels in steep areas are restricted, thus inhibiting width increase. In general, it might be expected that the width exponent values would be higher than for lowland streams as the width measurements were active width, i.e. the total width minus any protruding sediment. Therefore, as the discharge increases, the sediment becomes submerged, and the active width increases. This is not a factor with lowland streams, where width increases are usually just at the sides of the channel (from e.g. low-angle point bars).

This is confirmed by the fact that Ashop has the highest exponent, and is the most like a lowland stream in terms of channel shape as it has gently inclined banks, whilst at Fairbrook most of the sediment is already submerged and the channel sides are very steep and restrictive, meaning that the width exponent for this site is lower than the other sites. The other sites have characteristics between those of Fairbrook and Ashop. It is also important to note that width only increases until bankfull width is reached, i.e. the steep banks cause width to level off. When this point is reached all the increase in discharge must be accommodated by increases in depth and velocity only (until the banks are topped and then width can increase very rapidly).

7.2.3 Discharge and depth relationship

Figure 7.6 shows the relationship between these two parameters for each of the sites, and Figure 7.7 the composite graph for all the sites. The exponent values obtained from the field data vary considerably, from 0.09 (Fairbrook) and 0.10 (Ashop) to 0.27 (Burbage) and 0.38 (GrindsbrookA). The average, 0.19, is the same as that found by

Lisle (1986) for streams with steps and pools. All the sites have values lower than the typical value of 0.4 for lowland streams. This is a reflection of the very high velocity exponents observed. Table 7.3 shows that the error associated with calculating depth from the hydraulic geometry relationships is generally greater than 10%, with the error greatest for Grindsbrook B and least for the flume, Grindsbrook A and Burbage, reflecting the variation in the range in depth observed.

The exceptional feature about Grindsbrook A that might have led to its very high exponent value is the fact that it has the highest sediment protrusion of all the sites (as can be seen in Table 7.4) and, therefore, the lowest velocity exponent value. As this hinders the rate of velocity increase, this leads to higher depth and width exponents to compensate for this. Width can increase to some extent but is limited by the banks. By contrast, depth can increase freely. At Fairbrook and Ashop the velocity exponents are very high; also at Ashop there is the added factor of a very high width exponent. The exponent associated with the flume relationship is 0.41, which is considerably larger than the field exponents. This is understandable considering that the width of the channel cannot increase and so an increase in depth compensates for this.

7.2.4 Velocity and depth relationship

This relationship provides information about how the flow in the stream is affected by the sediment, and to what extent. If there is a large increase in velocity with increasing depth this indicates a rapid lowering of friction factor, and so less of an effect from the sediment as the sediment is drowned out rapidly. Conversely, a sluggish increase in velocity with depth indicates a larger resistance effect. The discharge and velocity relationship shows this effect to some extent, but can be seen better when studying the relationship between velocity and depth.

Consideration of the actual velocity and depth field data produced poor correlations because of the large depth error. All the streams apart from Grindsbrook A and the flume have very small exponents for the relationship between discharge and depth compared to that which would be expected in lowland streams, meaning that a small error in depth is quite significant compared to the range in depth. Therefore, theoretical values for depth and velocity were calculated using hydraulic geometry based on values determined for a range of discharges from $Q_{\min}$ to 100 times $Q_{\min}$ (where $Q_{\min}$ is the estimated minimum discharge at each of the sites during the period of the fieldwork, as described in Chapter 4). As seen in Table 7.3 there are considerable errors associated with using the hydraulic geometry equations, however, using these equations will eliminate the scatter in the field data. For the flume, the actual data was used.

The site relationships are shown in Figure 7.8, with the exponent values in Table 7.6. As the values are determined using the power hydraulic geometry relationships, the *d(v)* relationship is also a power one. From the equations in Section 7.1.1, $d = cQ^{j}$ and $v = kQ^{m}$, it follows that $d = ck^{m/j}v^{j/m}$. This reflects the general trend that at deeper depths the effect of the sediment is greatly reduced, except for Grindsbrook A and the flume. As Grindsbrook A had such a large range in depth, the effect of the error in depth is not so pronounced as at the other sites, so the actual field data could be studied as well (also shown in Figure 7.8). This produced an exponent of 0.768, very close to the theoretical value of 0.810. The only logical explanation is that for some reason a velocity increase was not possible, i.e. it was still being resisted by the sediment (supported by the fact that this site also had the lowest discharge and velocity relationship exponent).

The sediment at Grindsbrook A was very large, but still slightly smaller than at Grindsbrook B, which produced a velocity profile similar to the other sites. The difference between the sites is that the relative roughness at Grindsbrook A was higher. Also, the pool sediment was a lot larger at Grindsbrook A than at Grindsbrook B meaning that the relative roughness in the pools is larger as well. For the flume, with a value nearly as high as for Grindsbrook A (0.668), the explanation is unlikely to be associated with the sediment characteristics, but rather a reflection of the restriction in width leading to a greater depth increase. At the other extreme is Fairbrook with an exponent value of 0.111, again reflecting the sediment characteristics that led to the low exponent for the discharge and velocity relationship (described in 7.2.1), i.e. the fact that the sediment is able to become submerged with only a slight increase in discharge.

Table 7.6 Value of the exponent for the relationship between velocity and depth

Site	Exponent value
Ashop	0.146
Burbage	0.498
Doctor's Gate	0.283
Fairbrook	0.111
Grindsbrook A	0.810
Grindsbrook A (actual data)	0.768
Grindsbrook B	0.181
Flume	0.668

7.2.5 Discharge and friction factor relationship

Table 7.1 shows the values obtained for the friction factor exponent from this research, and Figure 7.9 shows graphs of the relationship for each of the sites. Figure 7.10 illustrates the composite graph. The larger the negative value of the exponent, the greater the decrease in friction factor with increasing discharge, i.e. the more rapid the rate of velocity increase. If a site has a large negative value it indicates that the sediment in the stream does not have as much an effect on the flow as a site with a lower exponent. Table 7.3 gives the errors associated with predicting friction factor from the hydraulic geometry relationships, which are very considerable. This is especially true at the sites where there is only a slight change in depth with discharge (Grindsbrook B, Ashop and Fairbrook).

As the velocity component of the relationship is squared in the Darcy - Weisbach equation used to calculate friction factor, it is velocity that has the biggest control on the friction factor value (i.e. $r=j-2m$) if slope remains constant. This is reflected in the fact that the sites with the extremes of friction factor exponent are Fairbrook and Grindsbrook A - the same two sites which exhibit extremes of velocity exponent. Fairbrook has a value of -1.52, Grindsbrook A has a value of -0.57, the average of all the fieldsites is -1.09, while the value for the flume is -0.91. This average value and the flume value are similar to the value of -0.99 obtained by Beven et al (1979) in their study of upland streams.

It would be expected that the same factors controlling the velocity exponent would control the friction factor exponent, i.e. percentage of the channel with protruding sediment at d_{min} and step average sediment height divided by d_{min}. As can be seen in Figure 7.11, this is found to be the case. This indicates that at Fairbrook there is a greater contrast in the sediment conditions at low and high flow than there is at Grindsbrook A, leading to these differences in value. Table 7.5 shows the errors associated with using these relationships - the best relationship is produced by using the step average sediment height divided by d_{min}.

As seen in Table 7.1, the values obtained from this research for the friction factor exponent are very different from those for typical lowland streams. This is obviously a reflection of the fact that lowland streams do not have the same decrease in relative roughness as discharge increases. Also, in lowland streams, as depth increases in response to discharge increase, there may be a change in the bedforms present (e.g. plane bed to ripples) which increases the resistance and thus reduces the contrast in resistance to flow between low and high flows. However, for some cases the converse is true e.g. dune to upper-stage plane bed transition. In steep streams this effect does not exist, and there is also an added effect increasing the difference between low and high flow identified by Bathurst (1993). He stated that "if relative submergence becomes relatively large ($R/D_{84} > 4$), the rapidity of change [of decreasing resistance] may also be encouraged by a change in the dominant resistance process from boulder form drag to bed material relative roughness".

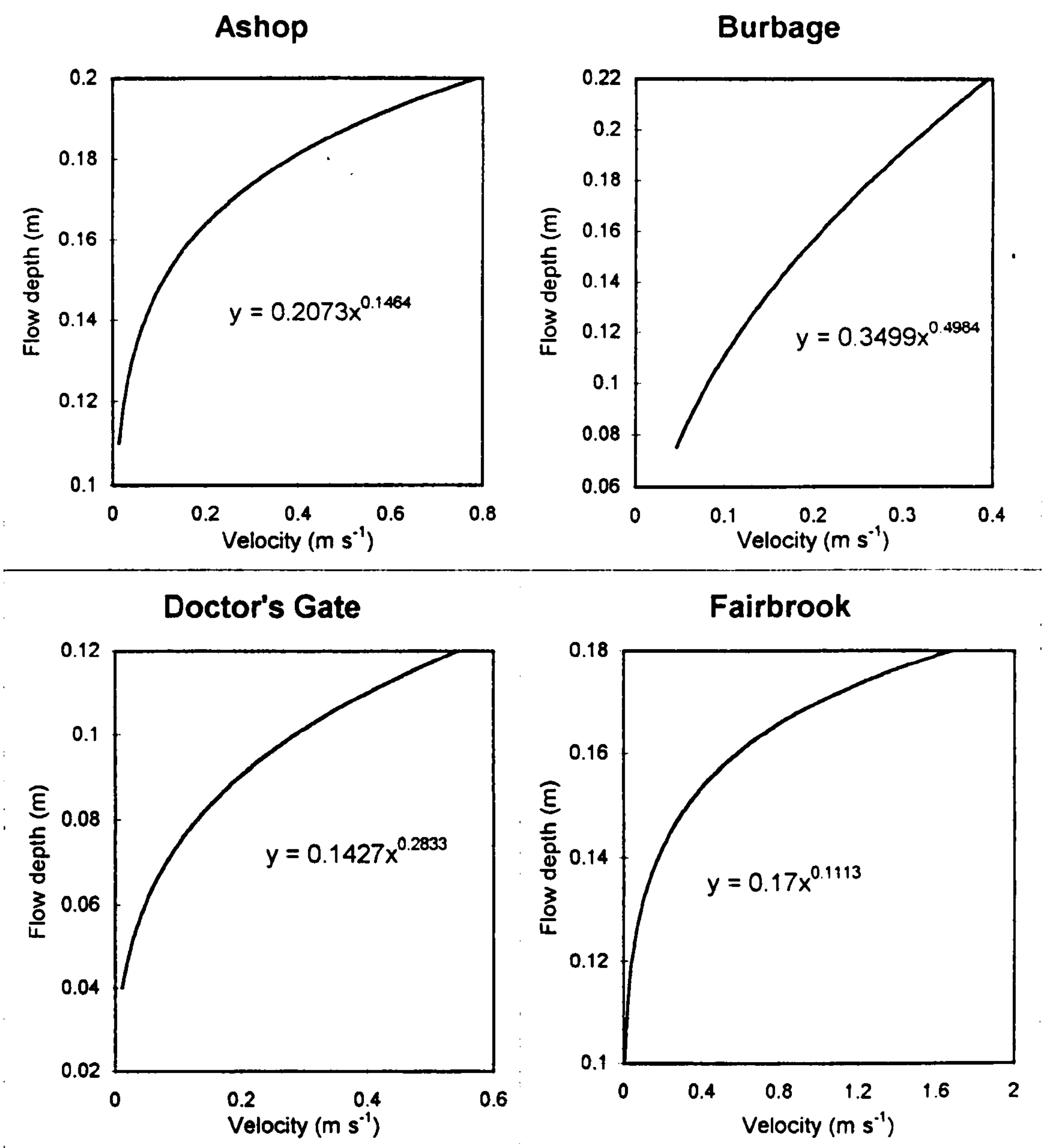

Figure 7.8. Relationship between reach average velocity and flow depth.
(note the use of different scales for the graphs)

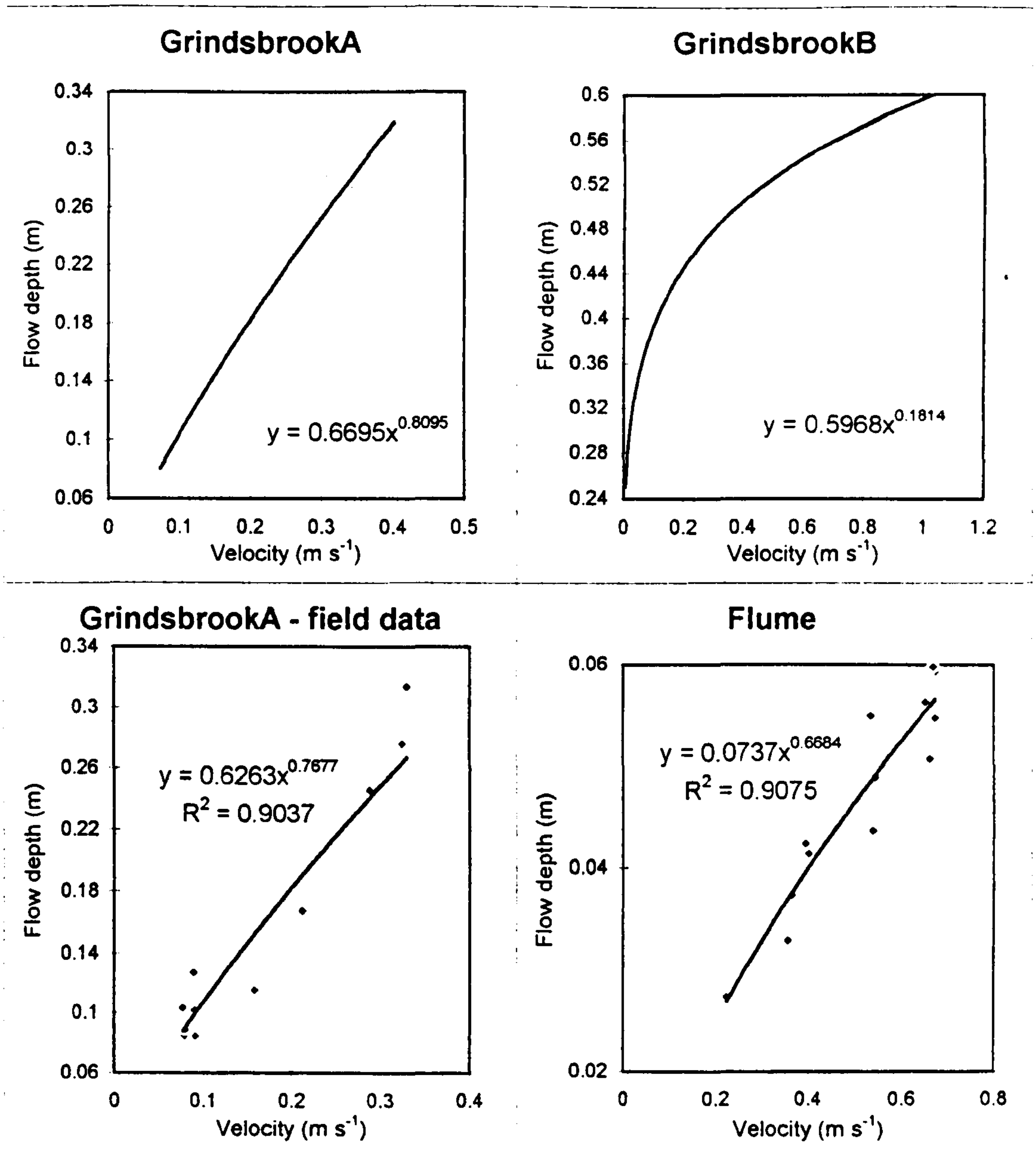

Figure 7.8. (continued). Relationship between reach average velocity and flow depth. (note the use of different scales for the graphs)

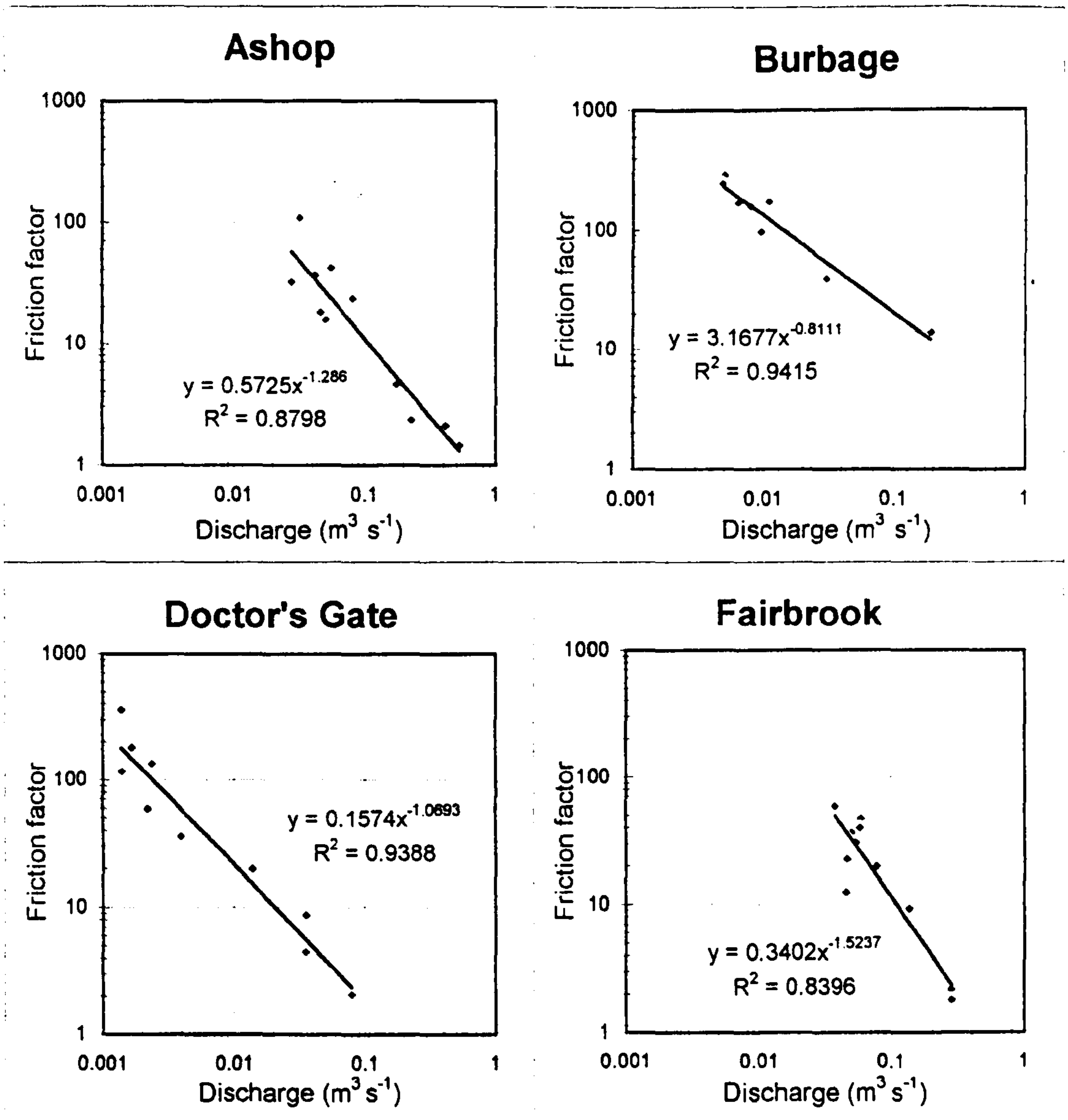

Figure 7.9. Relationship between discharge and friction factor.

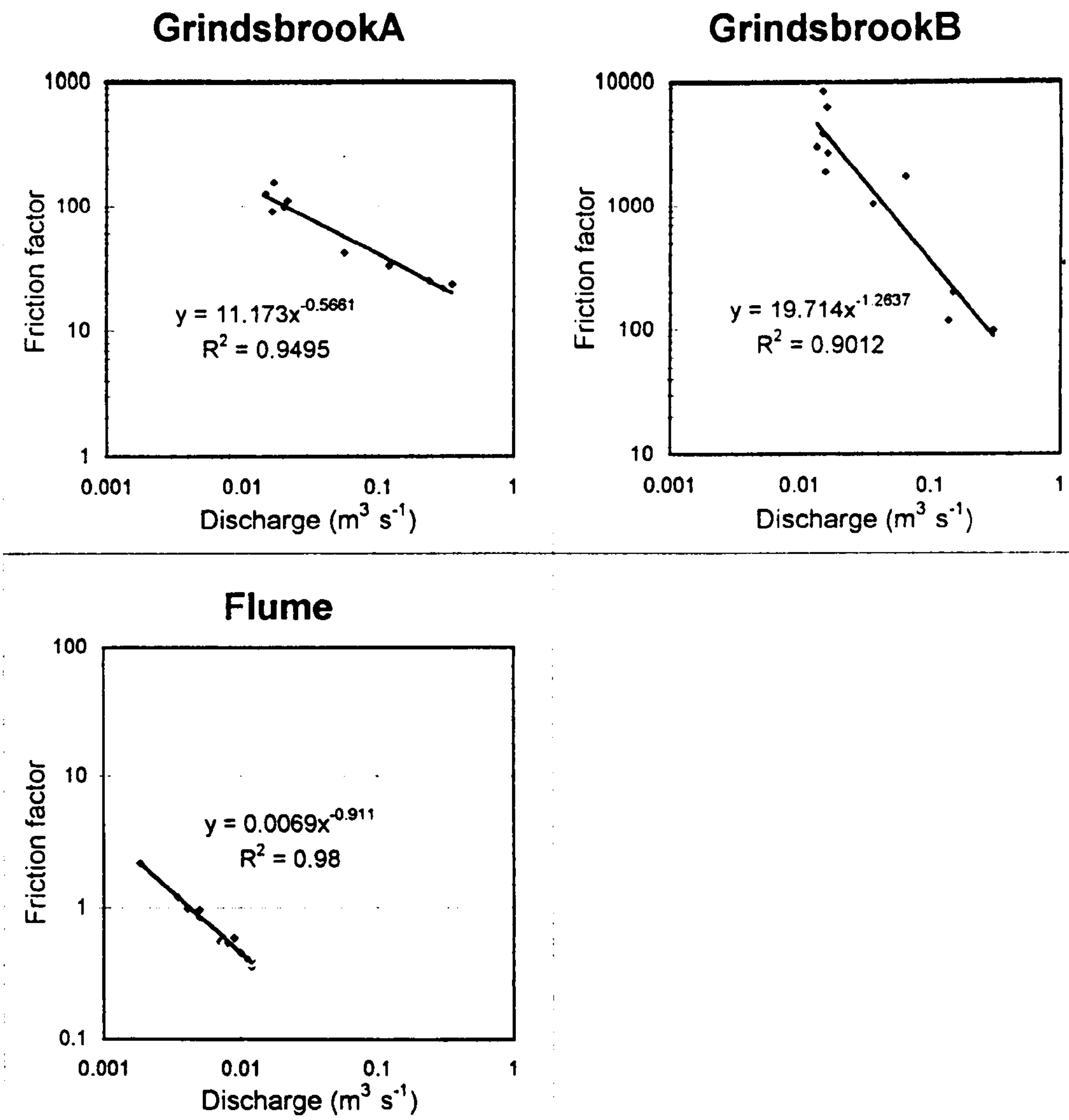

Figure 7.9. continued. Relationship between discharge and friction factor.
(Note the use of different y-axis scale ranges for Grindsbrook B and the flume).

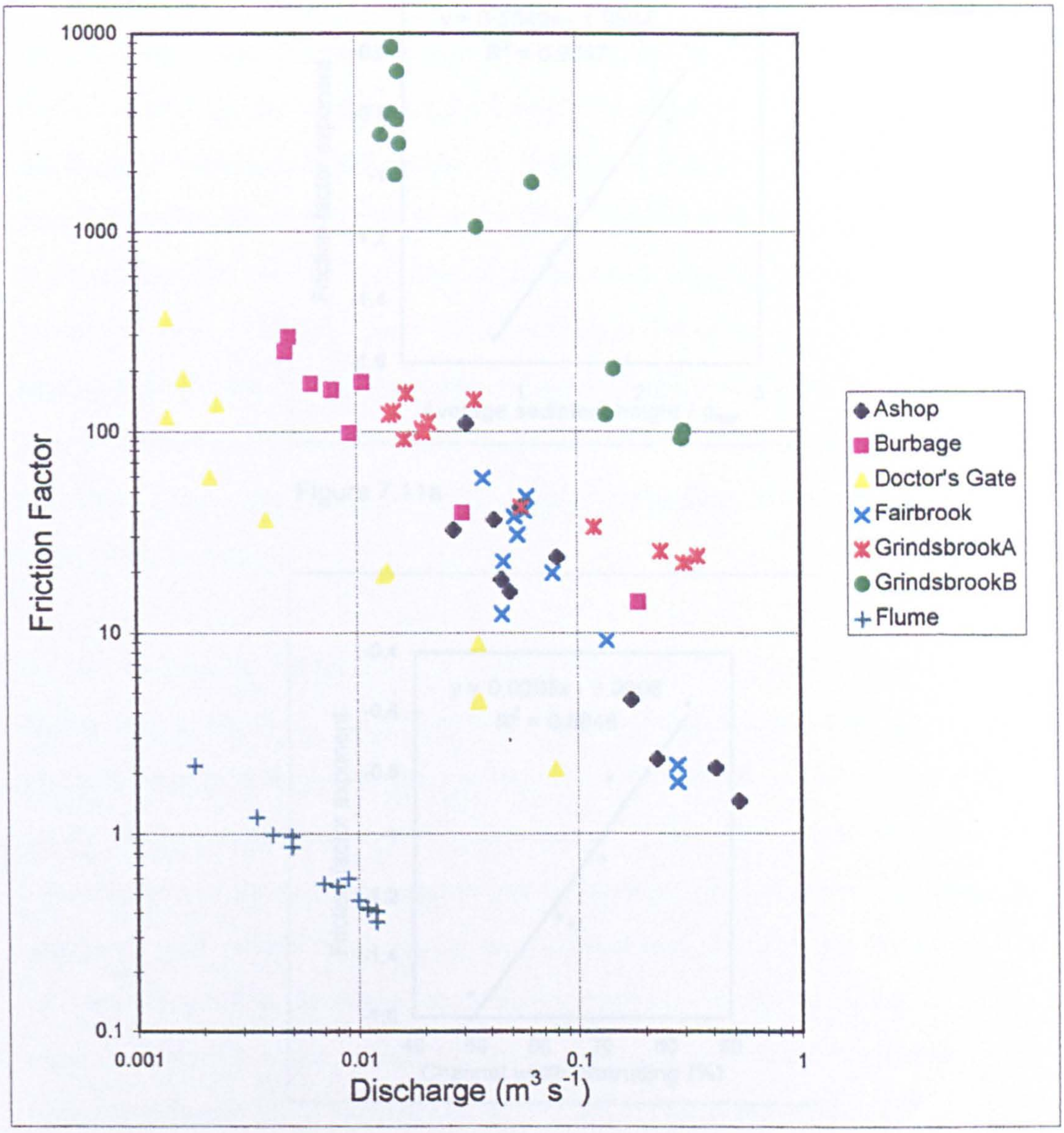

Figure 7.10. Composite graph of the relationship between discharge and friction factor

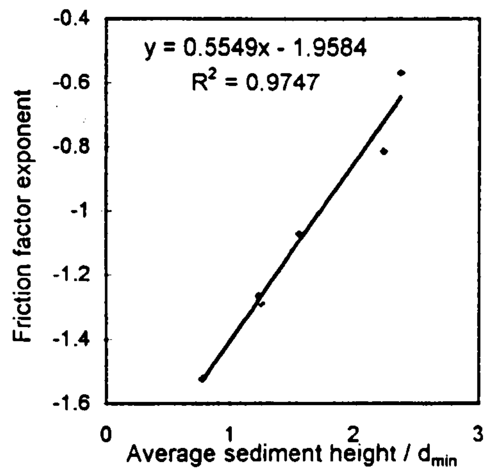

Figure 7.11a

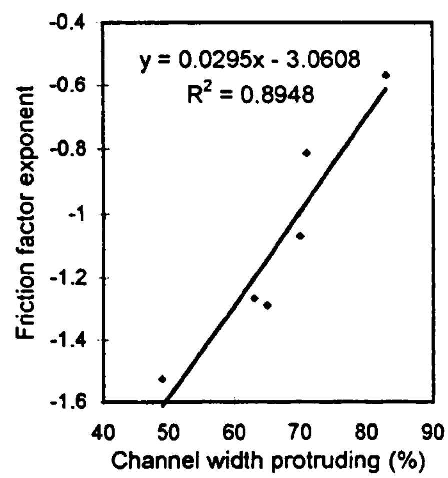

Figure 7.11b

Figure 7.11. Relationship between friction factor exponent and a) average sediment height/d_{min} and b) percentage of width with protruding sediment at d_{min}

7.2.6 Intercept value

As noted previously, there is considerable difference between the sites in the values of the intercepts for the relationships of velocity, width, depth and friction factor with discharge. These values are shown in Table 7.2, and can be seen graphically in the graphs showing the composite plots for these relationships by differences in the heights at which the lines plot at. The value of the intercept represents the predicted value of the y variable (e.g. velocity) when the discharge is equal to 1 m^3 s^{-1}, a value which is unobtainable in the flume. The range of intercept values is largest for the friction factor intercept because of the very large range in friction factor values observed during the research. Thus, the intercepts from this relationship were studied to determine controlling factors.

As can be seen in Figure 7.2, for a given discharge the flume values of velocity are higher than in the field. This is because of the fact that at a given discharge the friction factor is significantly lower than at the fieldsites, which would be expected to be a result of the restriction in width meaning a higher depth and therefore increased submergence of the sediment and reduced resistance. Visual extrapolation of the flume discharge and width relationship and comparison data points from the fieldsites indicates that at low discharges the width imposed on the flume is slightly wider than a natural channel's width would be, given the associated flow conditions, whereas at higher discharges (above about 0.06 m^3 s^{-1}) the width is narrower and hence the flow is deeper, and velocity faster. This is amplified as discharge increases, leading to the very large intercept value.

Study of Table 7.2 and the composite graphs show that the most striking fieldsite is Grindsbrook B, which plots on a considerably different line for all the relationships. For the friction factor relationship, the values plot at higher friction factor values than would be expected. At the other extreme is Doctor's Gate, although it is not as different from the other sites as Grindsbrook B. These variations are independent of rate of change of friction factor with discharge, suggesting that it is a constant factor controlling the intercept value, i.e. something inherent about the site. Slope is of some importance as a parameter in the Darcy-Weisbach equation, so this is a factor leading to the very large friction factor values at Grindsbrook B. However, it does not explain why Doctor's Gate is at the other extreme, as this site was not the one with the lowest slope. The main differences between the Grindsbrook B site and Doctor's Gate were:

- the difference between the size of the step and pool sediment;
- variance of the long profile from a straight line.

It was found that Step D_{84} /Pool D_{84} and Step D_{84} /Pool D_{16} were the best predictors of the intercept values, as seen in Figure 7.12, with the statistics describing the relationships in Table 7.7. Both these factors are a measure of how well defined step-pool sequences are in a reach, and suggests that the difference between the step and pool sediment has an important effect on all the relationships studied. This theory is backed up by the fact that the Grindsbrook A and Grindsbrook B sites have the two highest values, and being part of the same stream are likely to have similar sediment characteristics. The best relationships were with predicting friction factor relationship, a reflection of the fact that there is much more variation in the intercept values for friction factor. Multiple regression also using χ_{rms}, roughness spacing and *K3* did not improve the relationships significantly.

Table 7.7 Statistics associated with predicting intercept values

Relationship	*r*-value (significance level)	Standard error	Uncertainty range (interval)	Interval as % of observed intercept range
Velocity intercept				
Step D_{84}/Pool D_{16}	0.57 (not sign.)	0.59	±1.16	73
Step D_{84}/Step D_{84}	0.60 (not sign.)	0.57	±1.12	71
Friction factor intercept				
Step D_{84}/Pool D_{16}	0.99 (<0.01)	1.42	±2.78	14
Step D_{84}/Step D_{84}	0.98 (<0.01)	1.81	±3.55	18

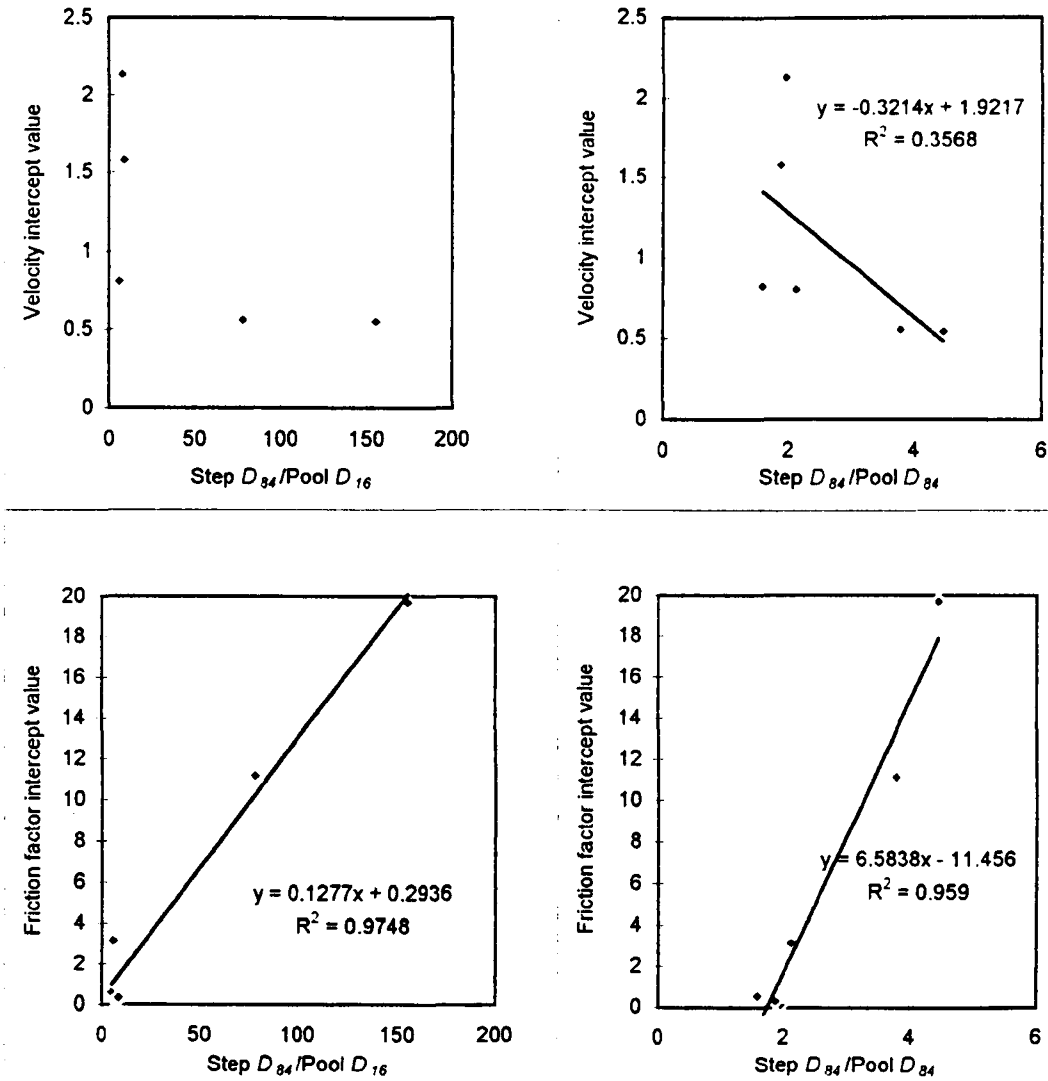

Figure 7.12. Relationship between intercept values and sediment sorting measures

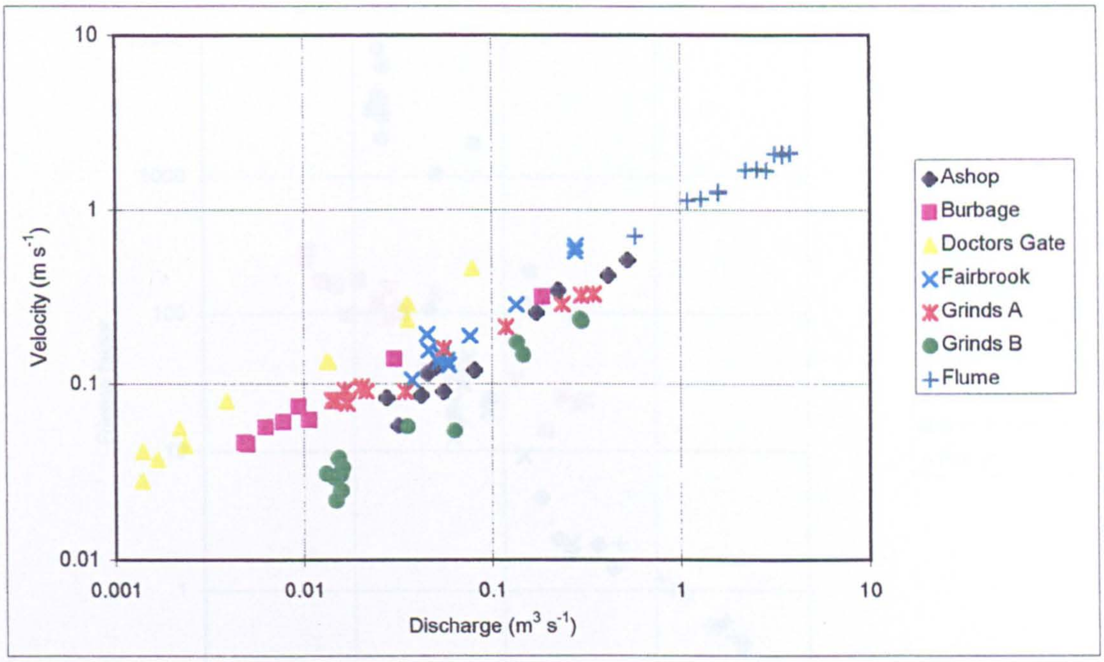

Figure 7.13a. Discharge and velocity relationship

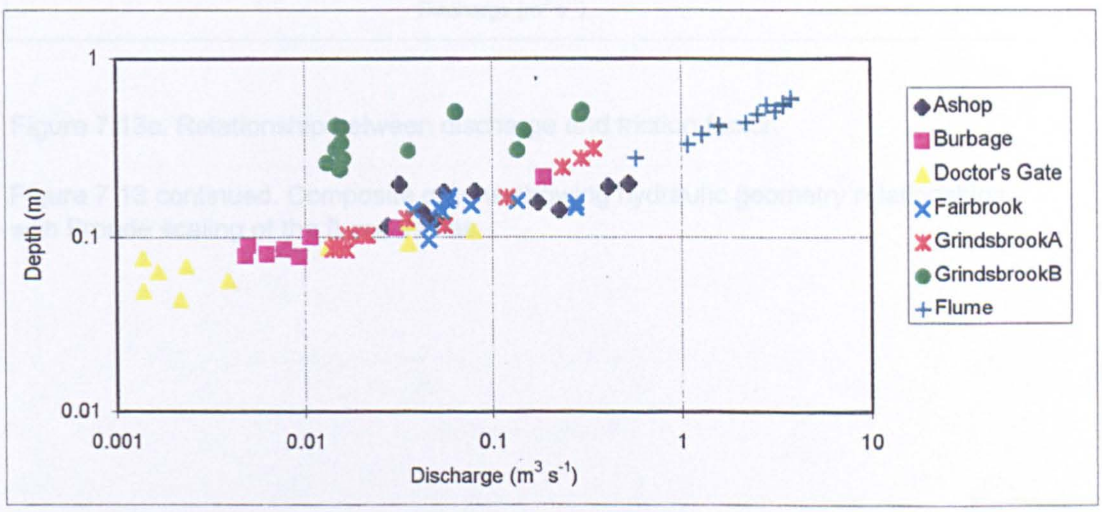

Figure 7.13b. Discharge and depth relationship.

Figure 7.13. Composite graphs showing hydraulic geometry relationships with Froude scaling of the flume values.

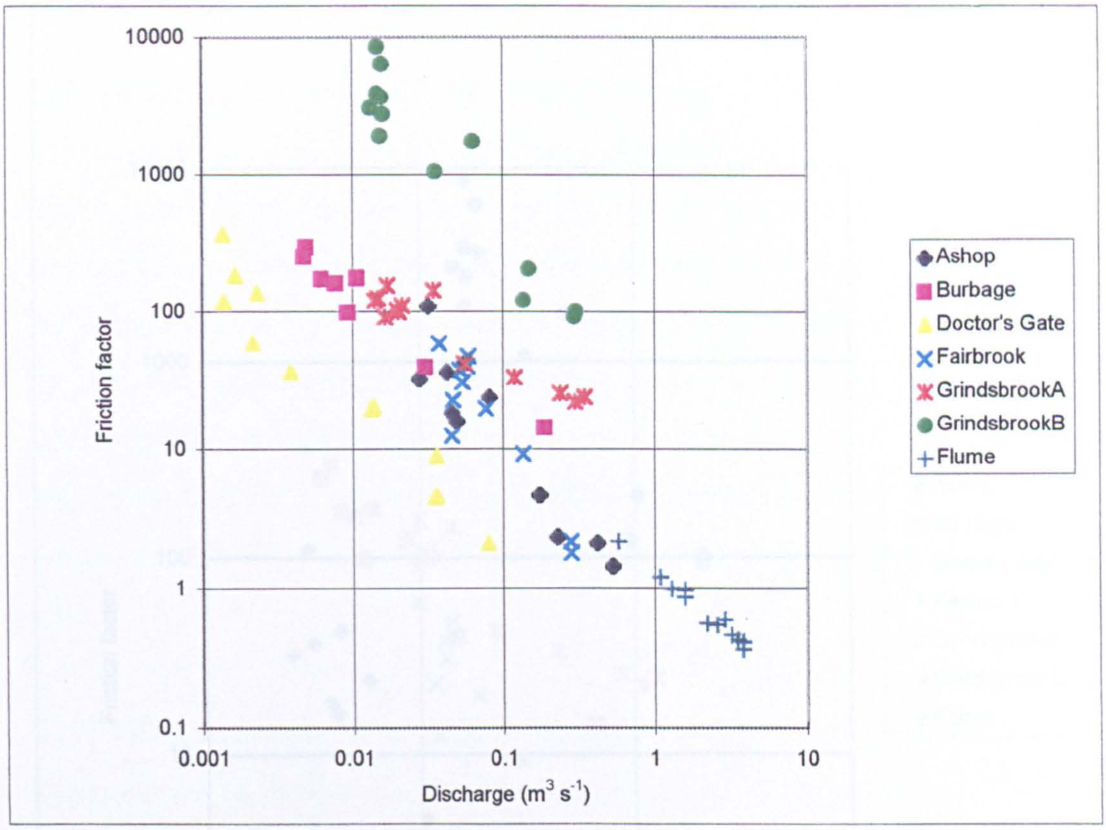

Figure 7.13c. Relationship between discharge and friction factor.

Figure 7.13 continued. Composite graphs showing hydraulic geometry relationships with Froude scaling of the flume values.

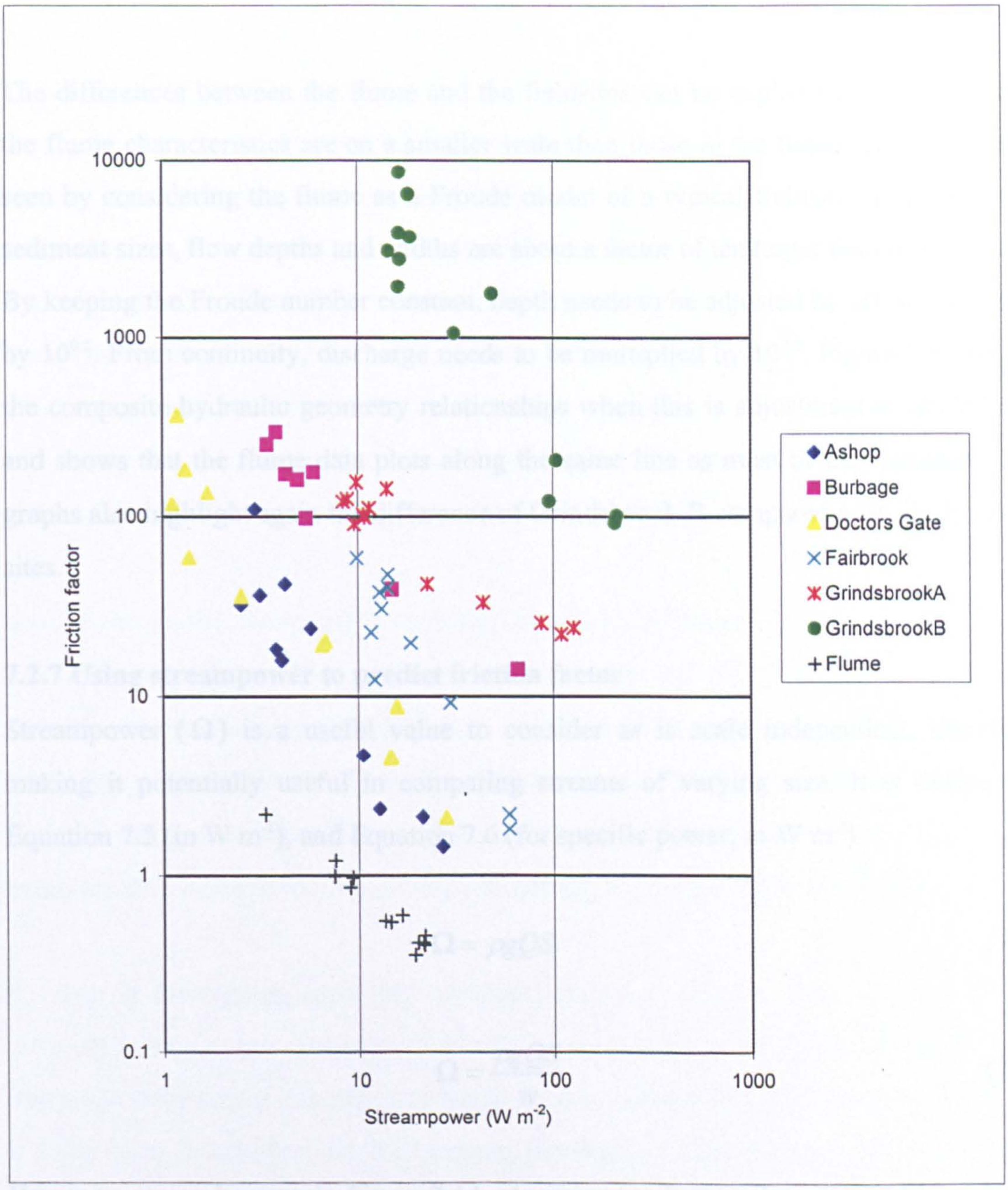

Figure 7.14. Composite graph showing the relationship between streampower and friction factor for the field sites and the flume.

The differences between the flume and the fieldsites can be explained by the fact that the flume characteristics are on a smaller scale than those in the fieldsites. This can be seen by considering the flume as a Froude model of a typical fieldsite. The fieldsites' sediment sizes, flow depths and widths are about a factor of ten larger than in the flume. By keeping the Froude number constant, depth needs to be adjusted by 10^1 and velocity by $10^{0.5}$. From continuity, discharge needs to be multiplied by $10^{2.5}$. Figure 7.13 shows the composite hydraulic geometry relationships when this is adjustment is carried out, and shows that the flume data plots along the same line as most of the fieldsites. The graphs also highlight again the difference of Grindsbrook B compared with all the other sites.

7.2.7 Using streampower to predict friction factor

Streampower (Ω) is a useful value to consider as is scale independent, therefore, making it potentially useful in comparing streams of varying size. It is defined in Equation 7.5 (in W m^{-1}), and Equation 7.6 (for specific power; in W m^{-2}).

$$\Omega = \rho g Q S \tag{7.5}$$

$$\Omega = \frac{\rho g Q S}{w} \tag{7.6}$$

However, as can be seen in Figure 7.14, streampower is actually a very poor predictor of friction factor. Despite the fact that it is scale independent, the different sites still plot on different lines reasonably parallel to each other. This indicates that the differences between the sites is a result of something unrelated to scale (most likely the degree of development of the steps or some other sediment measure), as the flume and Grindsbrook B sites plot at opposite sides of the graph.

7.2.8 Conclusions

Generally, the values obtained from the flume were within the range observed in the field (except for the relationship between discharge and depth). For the fieldsites a wide range of exponent and intercept values were observed, with Fairbrook and Grindsbrook A at the extremes. The effect of the sediment at Fairbrook decreases very rapidly as discharge increases, whereas it still affects the flow at high discharges at Grindsbrook A. The degree of sediment protrusion was found to be the most important characteristic controlling the exponent value, whereas the difference in sediment between the steps and pools had the strongest effect on controlled the intercept value.

It is interesting that the roughness spacing (described in Chapter 4) and *K3* did not seem to have any significant effect on the exponent and intercept values for the friction factor and velocity relationships with discharge, despite the fact that they are considered to be a measure of resistance to flow. Therefore, it is postulated that it is the size of the sediment in relation to the flow depth and the sediment range, and not the actual step bedforms that are most important for determining the hydraulic geometry of the sites.

As seen in the figures, generally the data points for different sites plot on slightly different lines, i.e. the relationships cannot be completely generalised. As the same is true when considering streampower which is scale-independent, this suggests that there is some other factor involved, for example, the degree of development of the step-pool sequences and the associated energy dissipation over these steps. This in turn would affect the velocity of the channel and, therefore, the hydraulic geometry relationships. Energy dissipation is considered further in Chapter 8.

Chapter 8

Effects of steps on flow conditions

8.1 Introduction

This chapter will consider the following:

- Prediction of reach average resistance to flow and velocity, calculated from channel and sediment characteristics and hydraulic geometry relationships based on the field and flume results (a total of 81 sample points). Relationships found by previous workers (Thompson and Campbell, 1979; Bathurst, 1985; Grant,1997) were tested for validity (Section 8.2).
- The effects of steps on flow resistance and hydraulic geometry. Flow conditions in the flume before and after step formation were compared in order to study this (Section 8.3).

8.2 Predicting friction factor and velocity

It would be useful to be able to determine velocity and friction factor for any steep stream with steps and pools, not just ones where established empirical relationships can be exploited. Several approaches were considered, based on using the hydraulic geometry relationships, relative roughness measures, and equations proposed by previous workers (Thompson and Campbell, 1979; Bathurst, 1985; Grant, 1997). Any valid relationship would ideally be able to predict both the field and flume results found.

8.2.1 Hydraulic geometry equations

The fact that strong hydraulic geometry relationships were found means it is possible to estimate velocity and friction factor at a study reach in a situation where, for example, the site had a gauging station so discharge can be easily determined. It would then be possible to determine reach average velocity and friction factor by exploiting the relationships found between the exponents and the intercepts and sediment characteristics. As described in Chapter 7, for predicting the value of the exponent, the best relationship found was between the exponent and average sediment height divided by $d_{\min}$ (i.e. the relative roughness when the stream is at minimum discharge observed during the course of the fieldwork). However, determining this value is very involved, as detailed transect surveying to determine the average sediment height would be necessary, as well as an estimate of minimum depth.

It is easier to measure the percentage of channel width with protruding sediment at $d_{\min}$, which was almost as good a predictor of the value of the exponent, and involves just one value which can be used for each discharge level (although a value for $d_{\min}$ would need to be estimated). This percentage of channel width containing protruding sediment could be determined easily by a number of transects across the steps in the study reach, preferably two transects per step. Use of a tape measure would be adequate to determine the width of the channel with protruding sediment and the total width of the channel. As the sites studied during this research had a very wide range of characteristics in terms of slope, width and sediment characteristics, the relationships found would be expected to hold for all other streams with steps and pools.

Sediment distribution for the steps and pools would need to be known to use the hydraulic geometry equations, as using Step D_{84} /Pool D_{16} produced the best estimate of the friction factor intercept value (these measures did not produce significant relationships with the velocity intercept value). As with estimating the percentage of the channel width with protruding sediment, only one value is needed rather than a separate value for each discharge level. Figure 8.1 shows, for the Doctor's Gate site, the predicted friction factor values and the actual values. The value of $\left(\frac{8}{f}\right)^{\frac{1}{2}}$ is, on average, underestimated by a factor of 2.5. As considered in Chapter 7, there is a large uncertainty involved in estimating both the exponent and the intercept, hence this difference. The lack of any theoretical basis for this factor leads to the conclusion that this approach is not recommended for predicting the friction factor value.

8.2.2 Using Froude number to predict friction factor

As seen in Figure 8.2, there is a very strong relationship between friction factor and Froude number for the field and the flume data, as both these values are calculated using velocity and depth. Therefore, if Froude number can be predicted accurately, so can friction factor. Grant (1997) used Equation 8.1 for predicting Froude number, based on work carried out by Bayazit (1983) using a Keulegan-type relationship.

$$Fr = 2.18\left[\ln\left(\frac{d}{D_{84}}\right) + 1.35\right]S^{0.5} \qquad \textbf{[8.1]}$$

Figure 8.3a shows the predicted values of Froude number using Equation 8.1, and the actual values of Froude number using both field and flume data. There is a considerable amount of scatter from the field data as a result of inability to determine depth accurately, and the uncertainty range of the predicted value is ± 0.48 (95% confidence interval). Considering that the highest value of Froude number was less than unity this is a very large uncertainty. Plotting the flume data alone shows a stronger relationship, as there was a wider range of depth than observed in the field. Therefore, a wider range of Froude values were observed. This is shown in Figure 8.3b. It is concluded that this approach is not a useful one for use with field sites, and that equations directly relating friction factor and relative roughness are probably a better approach (as well as being the standard approach taken by previous workers), as considered in the following sub-sections.

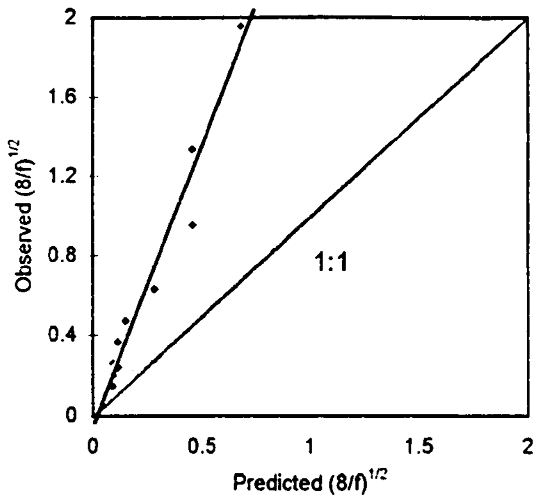

Figure 8.1. Predicted and observed values using hydraulic geometry equations (Doctor's Gate).

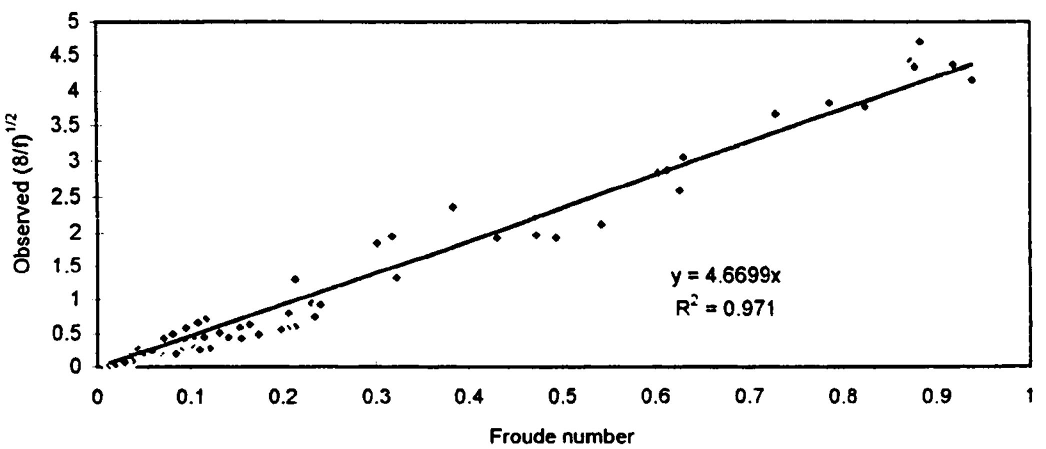

Figure 8.2. Relationship between Froude number and friction factor

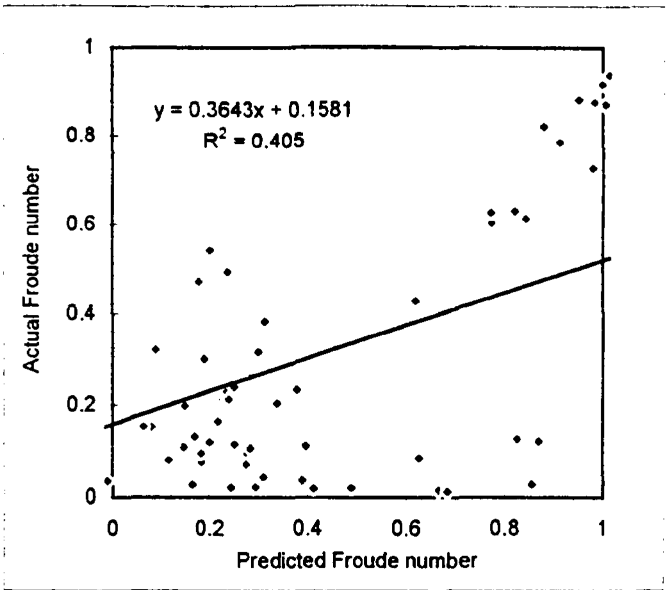

Figure 8.3a. All field and flume data

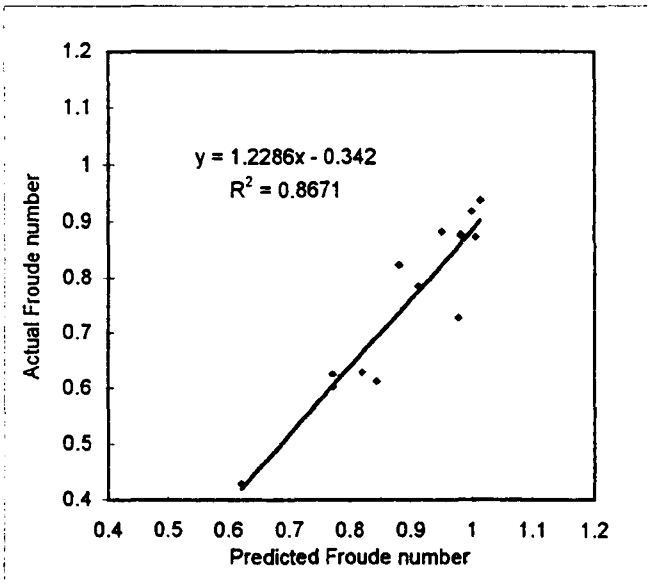

Figure 8.3b. Flume data only.

Figure 8.3. Predicted Froude number using Grant (1997) relationship

8.2.3 Using measures of relative roughness to predict friction factor

Friction factor is controlled by sediment protrusion, so it would be logical to assume that a strong relationship would exist between the values calculated for friction factor and a measure of relative roughness. There are three measures for roughness for which values were available for the field and the flume. These are:

- D_{84},
- $K3$,
- χ_{rms} (i.e. square-root of mean squared variance of the sediment long profile from a straight line).

Average sediment height values were determined from the field transects carried out, however, these values were relative to water level, which cannot be related to the flume. The values for D_{84} and $K3$ from the flume studies are for the entire sediment distribution, whereas the field values are from the step sediment distribution only. However, this was not considered a problem bearing in mind the large difference between the field and flume sediment, and carrying out a sediment survey in the flume after each flume run was considered too time consuming. For calculating relative roughnesses the depth value used was the reach average depth (as determined by using the continuity equation and the salt-dilution gauging results in the field, and using the sediment and water height data in the flume) and not the average depth in the steps or in the pools. Determining separate average depth values for the steps and the pools was logistically impossible because of the work and errors involved in measuring depth directly. For the equations that use hydraulic geometry (e.g. Thompson-Campbell equation) this was used as opposed to average depth.

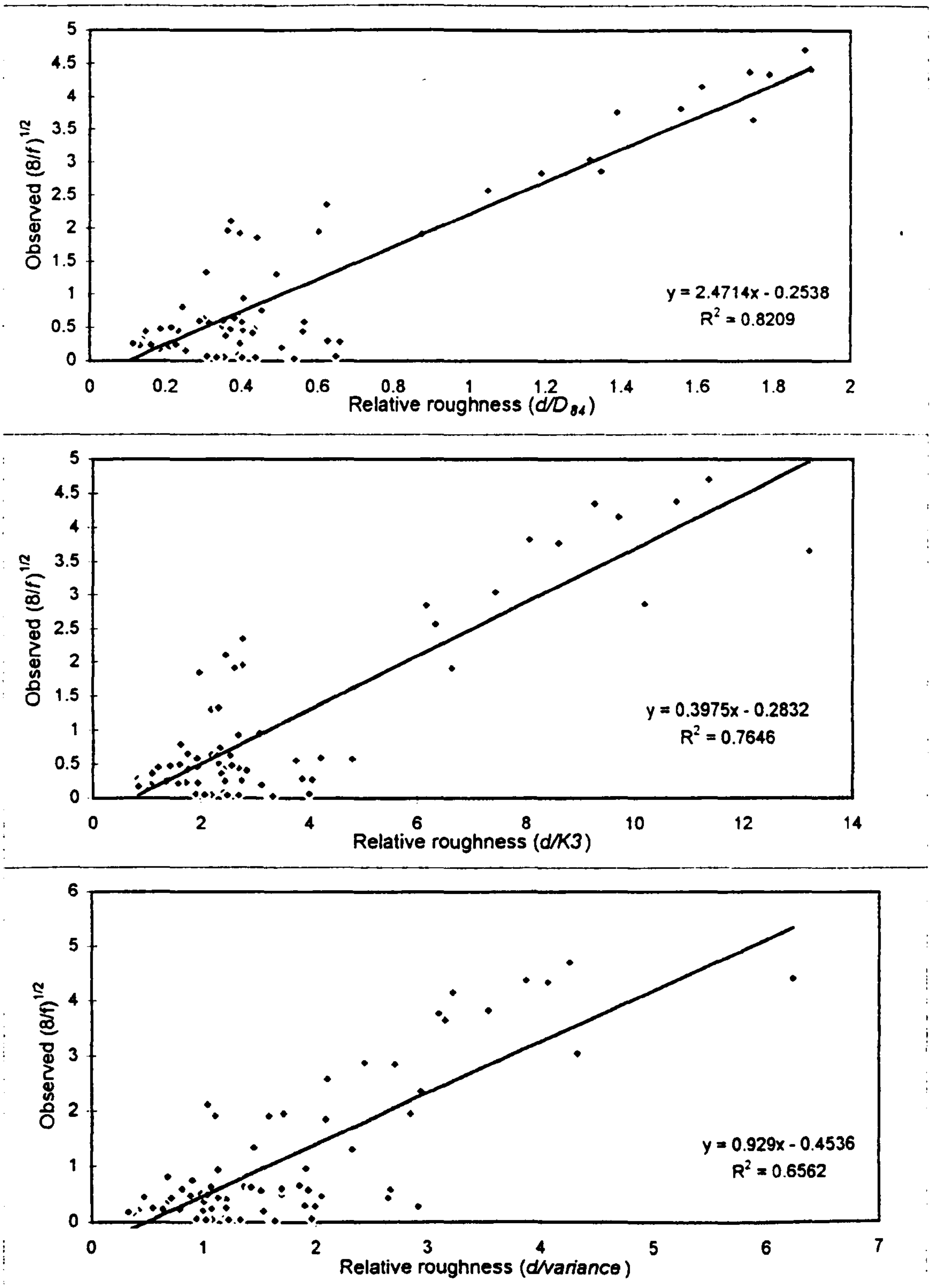

Figure 8.4 Relationship between friction factor and relative roughness using D_{84}, $K3$ and variance.

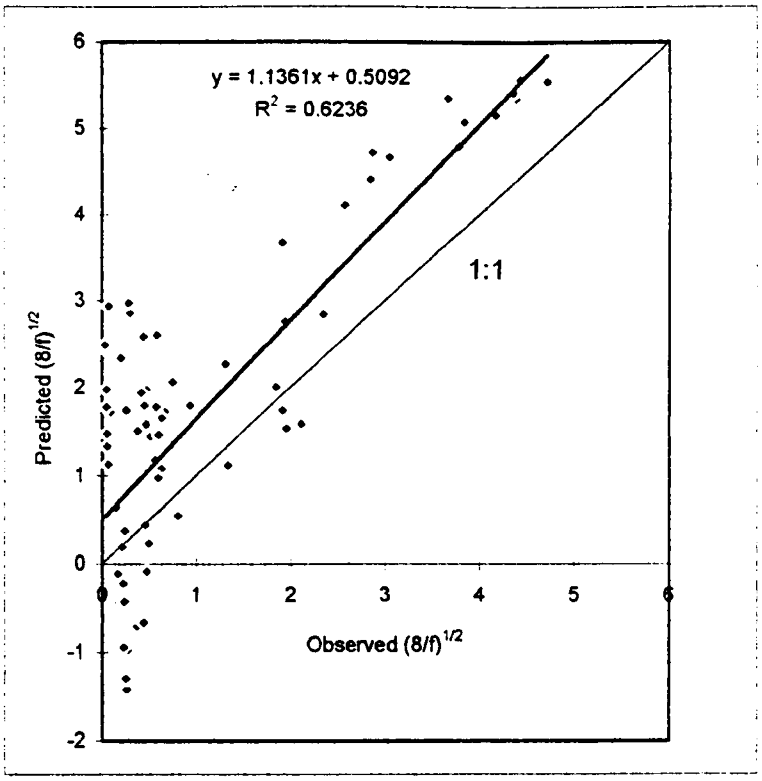

Figure 8.5. Predicted and observed $(8/f)^{1/2}$ using Equation 8.5 (Bathurst, 1985)

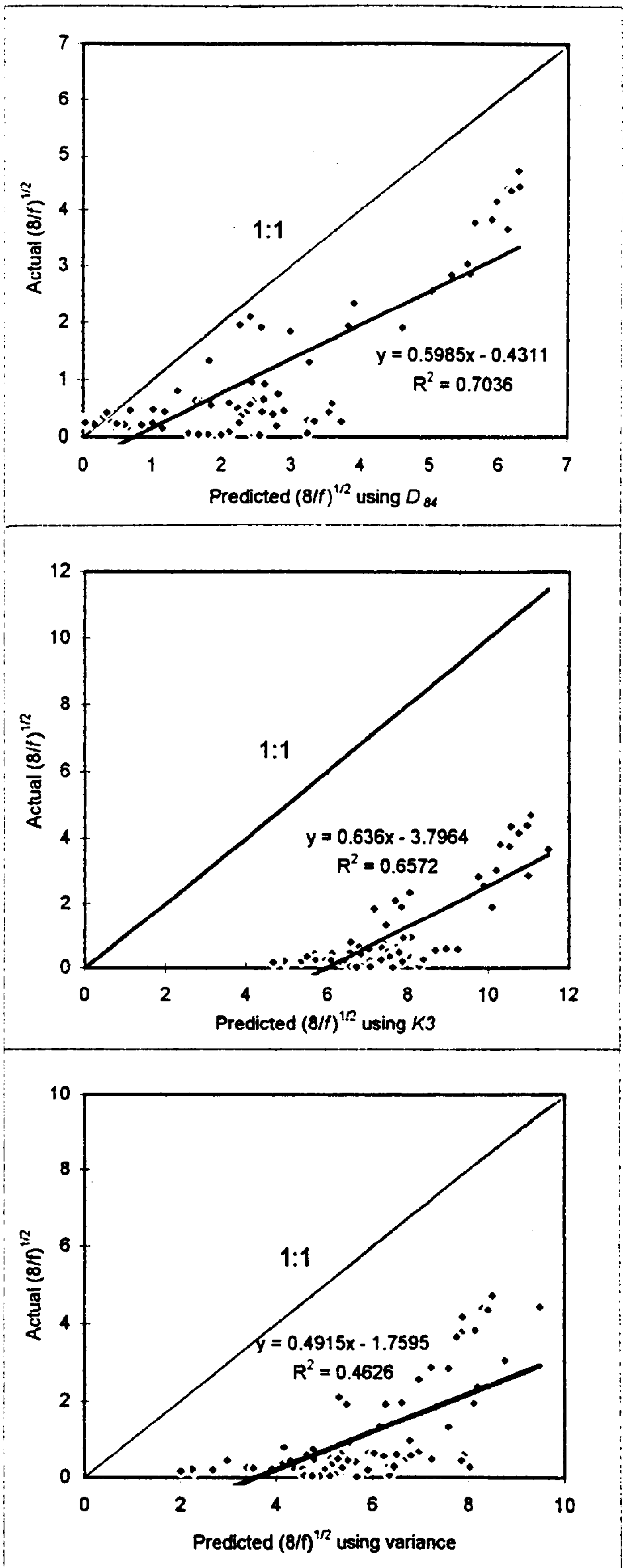

Figure 8.6 Predicted friction factor with Thompson-Campbell equation using D_{84}, $K3$ and variance compared with actual values.

Figure 8.4 shows the relationships between $\left(\frac{8}{f}\right)^{1/2}$ and relative roughness calculated using a) D_{84}, b) *K3* and c) χ_{rms} (variance). The empirical relationships found are shown in Equations 8.2, 8.3 and 8.4:

$$\left(\frac{8}{f}\right)^{1/2} = 2.4714\left(\frac{d}{D_{84}}\right) - 0.2538 \qquad \textbf{[8.2]}$$

$$\left(\frac{8}{f}\right)^{1/2} = 0.3975\left(\frac{d}{K3}\right) - 0.2832 \qquad \textbf{[8.3]}$$

$$\left(\frac{8}{f}\right)^{1/2} = 0.929\left(\frac{d}{\chi_{rms}}\right) - 0.4536 \qquad \textbf{[8.4]}$$

All the relationships are significant at $p<0.01$ level, and the statistics associated with each of the correlations are shown in Table 8.1. The standard error associated with the value of $\left(\frac{8}{f}\right)^{1/2}$ was calculated using Excel's STEYX worksheet function, and the root mean square (*rms*) predicted error was calculated using the SUMXMY2 Excel worksheet function. It proved difficult to ascertain which of the relative roughness measures was the best predictor of $\left(\frac{8}{f}\right)^{1/2}$ as although d/D_{84} has the highest *r*-value (0.91) and the lowest standard error value (0.54), d/χ_{rms} has the lowest rms value (0.94 compared to 1.00 for d/D_{84}). Judging the correlations visually suggests that d/D_{84} is the best predictor, particularly at higher relative roughness values.

The main problem found with these relationships is the fact that there is a large error associated with depth. It is believed that relative roughness is the main control on friction factor, however, the field data are not accurate enough to reduce the depth scatter sufficiently to identify the relationship precisely. Therefore, there is a considerable amount of scatter in the graphs in Figure 8.4. Thus, it is postulated that the values for friction factor obtained from the equations are more accurate than the field measurements. However, the relationship is purely empirical. It is also interesting to note that despite the conclusion reached in Section 4.6.2 following consideration of the sediment data collected, i.e. that D_{84} was a poor indicator of vertical sediment distribution, it was found to be the best predictor of friction factor.

8.2.4 Using previous equations to predict friction factor

Chapter 2 described equations based on boundary layer theory used to predict the value of friction factor. Equations suggested by Bathurst (1985) and Thompson and Campbell (1979), which have been previously used with success in steep streams, were tested using the data obtained from the field and flume. Equation 8.5 is the adjusted Keulegan equation proposed by Bathurst (1985),

$$\left(\frac{8}{f}\right)^{1/2} = 5.62\log\left(\frac{d}{D_{84}}\right) + 4 \qquad \textbf{[8.5]}$$

Figure 8.5 shows the relationship found using this equation. This slightly over-predicted the value of $\left(\frac{8}{f}\right)^{1/2}$, but produced reasonable estimates for the flume and for fieldsites with very low d/D_{84} values. Table 8.1 considers the strength of this relationship, and the errors associated with using it to predict the value of $\left(\frac{8}{f}\right)^{1/2}$. The 95% confidence interval is ±1.54, and the *rms* value is 1.30, suggesting that this equation is not as good a predictor as Equation 8.2.

As described in Chapter 2, Thompson and Campbell (1979) modified Nikuradse's resistance equation to produce Equation 8.6. This equation has been shown to work well for a range of relative roughnesses (Church et al, 1990).

$$\left(\frac{8}{f}\right)^{1/2} = 5.62\left(1 - \frac{0.1k_s}{R}\right)\log\left(\frac{12R}{k_s}\right) \qquad \textbf{[8.6]}$$

There are some variations of this equation in the literature (i.e. slightly different values for the coefficients). Equation 8.6 is the same as that used by Bathurst (1982a) amongst others. Equivalent sand roughness height, k_S, was taken to be $4.5\,D_{50}$ by Thompson and Campbell (1979) and Bathurst (1982). For this research Step D_{84} was used.

All three of the roughness measures used in 8.2.3 were also used with this equation in place of k_S. Figures 8.6a - c show the predicted values using Equation 8.6 compared with the actual values, with the *r*-values and errors shown in Table 8.1. The relationship using D_{84} has the highest *r*-value, the lowest uncertainty range (±1.37), and by far the lowest *rms* value (1.73). However, it is not as good a predictor of $\left(\frac{8}{f}\right)^{1/2}$ as the empirical relationship using Equation 8.2, especially for the flume data.

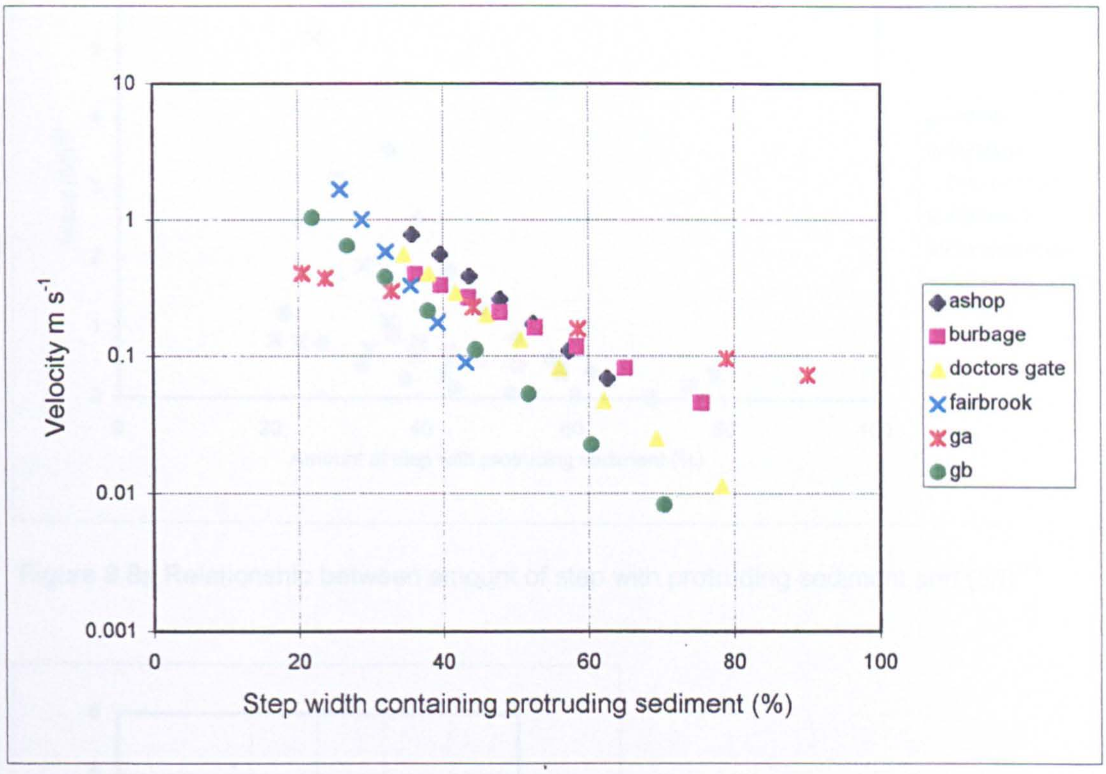

Figure 8.7 Relationship between step protruding sediment and velocity

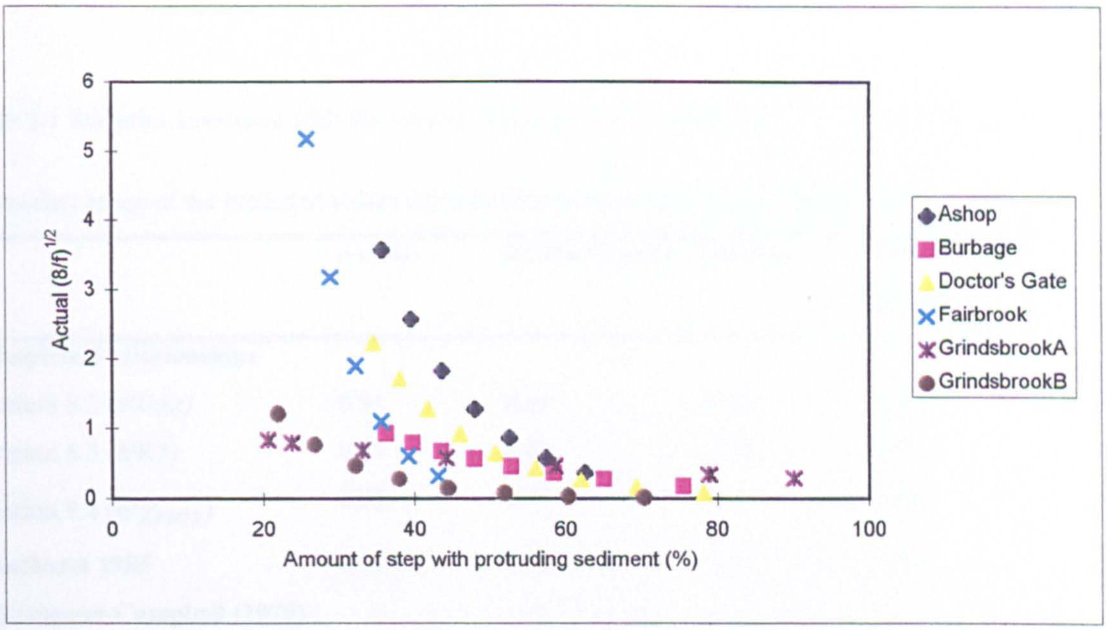

Figure 8.8a Relationship between amount of step with protruding sediment and $(8/f)^{1/2}$

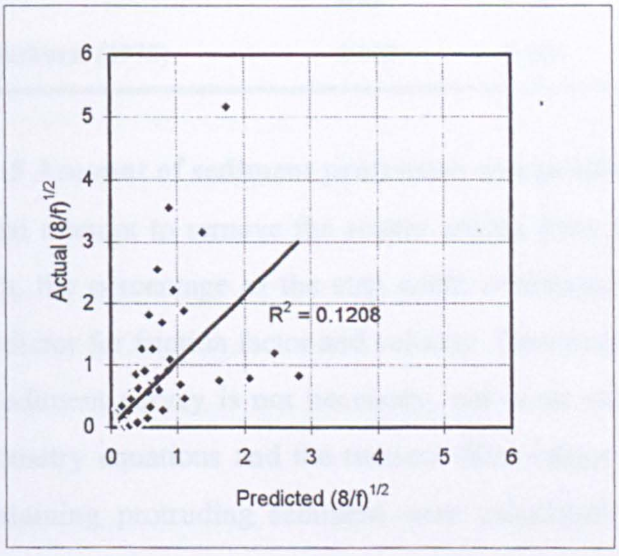

Figure 8.8b Predicted versus actual values of $(8/f)^{1/2}$ using equation in Figure 8.8a

Table 8.1 Statistics associated with the various equations used to predict $\left(\frac{8}{f}\right)^{1/2}$. The interval value is the uncertainty range of the predicted values (95% confidence interval, i.e. 1.96*standard error).

	r-value	standard error	interval	Rms of sum |pred-obs|
1. Empirical relationships				
Equation 8.2 (d/D_{84})	0.91	0.54	1.06	1.00
Equation 8.3 (d/K3)	0.87	0.62	1.22	2.90
Equation 8.4 (d/χ_{rms})	0.81	0.75	1.47	0.94
2. Bathurst 1985	0.79	0.78	1.54	1.30
3.Thompson-Campbell (1979)				
D_{84}	0.84	0.70	1.37	1.73
K3	0.81	0.75	1.47	6.63
χ_{rms}	0.68	0.94	1.84	4.83
4. Bathurst (1978)	0.623	0.806	1.58	28.51

8.2.5 Amount of sediment protrusion as a predictor of friction factor

In an attempt to remove the scatter arising from the error in water depth for the field data, the percentage of the step width containing protruding sediment was used as a predictor for friction factor and velocity. This would be easy to determine in the field as a sediment survey is not necessary, nor is an estimate of depth. Using the hydraulic geometry equations and the transect data, values for the percentage of channel width containing protruding sediment were calculated for a range of discharges, and the corresponding velocity and friction factor values were determined.

As seen in Figure 8.7, the relationship between the percentage of the step width containing protruding sediment and velocity produced a reasonable relationship, (although there is scatter, especially at higher flows), with the different reaches plotting on different lines. Grindsbrook A is significantly flatter than the other sites, reflecting the differences in hydraulic geometry between this site and the other field sites. This suggests that it is impossible to produce a true generalisation using this approach as there are some reach dependent factors that cannot be accounted for. However, this approach does have potential as it is relatively easy to estimate in the field, but the standard error of the predicted value of velocity is 0.255 m s^{-1}, meaning that the uncertainty range is ±0.50 m s^{-1}. Considering the observed velocity range was only approximately 1.7 m s^{-1} this relationship is not a useful one to use, although as with the previous relationships found it is probable that the predicted velocity values are actually more accurate that the measured ones because of the large depth error. Figure 8.8a shows the relationship between $\left(\frac{8}{f}\right)^{1/2}$ and the percentage of step with protruding sediment, and Figure 8.8b shows the predicted values obtained using this relationship and the actual values. Whilst the relationship is significant to $p<0.01$, the uncertainty range associated with using this relationship is ±1.89, meaning that this approach does not enable friction factor to be predicted accurately.

Also, this approach could not be used for the flume as the sediment was submerged at most flows, and extrapolating the relationship to consider a situation where all the step sediment was submerged indicated a flow velocity approaching 10 m s^{-1} which would be unobtainable in the flume. This suggests that either this relationship only holds for a range of percentages, or for the unnatural flume situation, where the channel width is imposed, the relationship cannot be used.

It would be necessary to test this relationship with actual field data estimating the percentage of step containing protruding sediment, as opposed to calculating values using hydraulic geometry. Two assumptions were made for using this approach; firstly, that the hydraulic geometry equations are accurate for the range of flows studied in this analysis. Secondly, the depth increases used are for average channel depth for calculating velocity and average step flow depth for calculating protrusion. Therefore, this analysis is only really valid if the increase in step depth is equivalent to the overall channel depth increase, which is unlikely to be true. However, this analysis demonstrates the potential of using the relationship between protrusion and velocity.

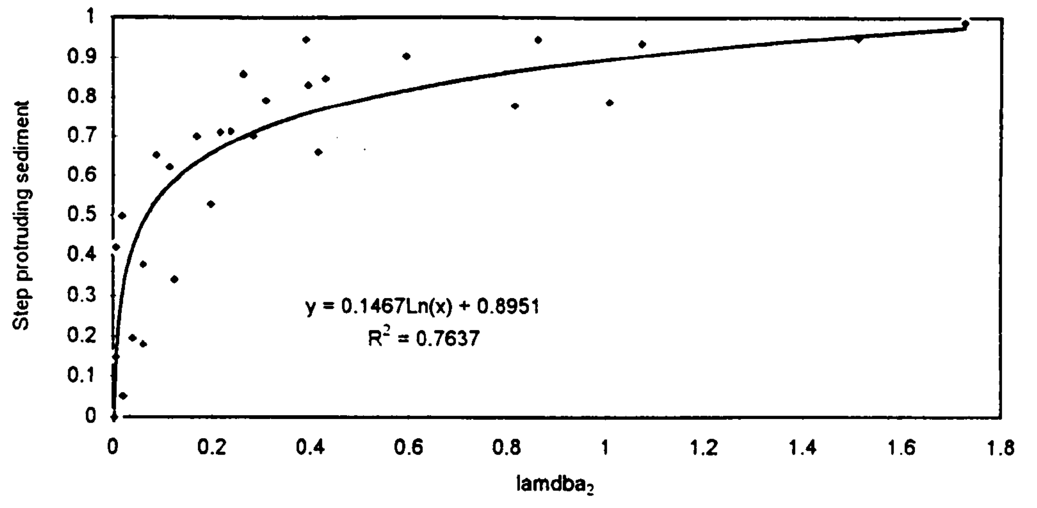

Figure 8.9 Relationship between Bathurst's (1978) lambda$_2$ and the proportion of protruding sediment (Equation 8.7)

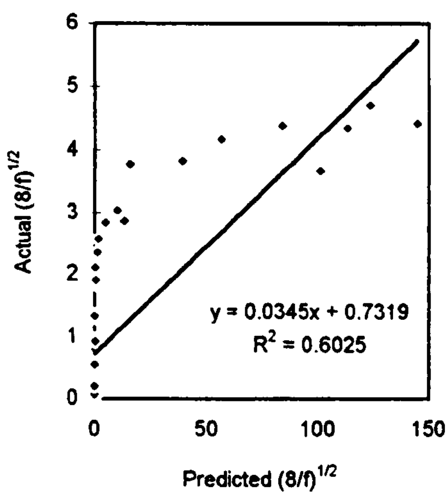

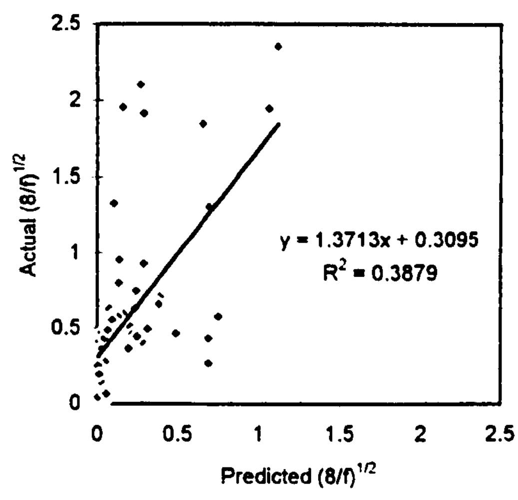

Figure 8.10a. All flume and field data. (note use of different scales for x and y)

Figure 8.10b. Field data only.

Figure 8.10. Predicted and actual values for $(8/f)^{1/2}$ using Equation 8.8 (Bathurst, 1978)

This measure of protrusion is similar to that used by Bathurst (1978), based on the work of Judd and Peterson (1969). He proposed a value, λ_2, equal to the ratio of the basal plan area of an obstacle to the area of the boundary per element. This value can be estimated using Equation 8.7, and is related to friction factor as in Equation 8.8.

$$\lambda_2 = 0.360 \log\left(\frac{1.52 D_{84}}{R}\right) \qquad [8.7]$$

$$\left(\frac{8}{f}\right)^{1/2} = \left(\frac{R}{0.748 D_{84}}\right)^{5.83} \left(\frac{w}{d}\right)^{7(\lambda_2 - 0.08)} \qquad [8.8]$$

The relationship between the percentage of channel width containing protruding sediment and λ_2, calculated using Equation 8.7, is shown in Figure 8.9, where only data points predicting positive values were considered. Figure 8.10 shows Equation 8.8 for all the data points (Figure 8.10a) and for the field data only (Figure 8.10b). The statistics associated with these relationships are given in Table 8.1. As can be seen, the error in these predicted values is large, especially for the flume data, meaning that this approach cannot be recommended as a useful predictor.

8.2.6 Conclusions

Determining generalisations that can be applied to all the sites to estimate flow conditions proved very difficult because of the large error associated with the depth values, and the fact that the sites displayed a wide range of sediment and channel characteristics. Of the previous equations tested, the best predictor of $\left(\frac{8}{f}\right)^{1/2}$ was found to be the Thompson-Campbell equation with D_{84}. However, considering all the approaches the best predictor for the field and flume data values was demonstrated to be the empirical linear relationship in Equation 8.2 using D_{84} for relative roughness. Both these results suggest that D_{84} is the best indicator of sediment protrusion and, therefore, friction factor. However, for high values of R/D_{84} (i.e. lower values of relative roughness) it is likely that $\left(\frac{8}{f}\right)^{1/2}$ and, therefore, velocity would be overestimated.

However, using these equations requires an estimate of depth, which is very hard to determine accurately, questioning the practicality of using these relationships. Other approaches that do not require a depth value (the percentage of step with protruding sediment and hydraulic geometry), were found to have some success. Predicting the exponent value and intercept value carried large errors, so the best approach might be to carry out a limited number of gaugings to establish the intercept and exponent values. Equations considering drag forces acting on the sediment in the channel and calculation of an average velocity profile are discussed in Chapter 10.

The main parameters controlling friction factor and hence resistance and velocity, are those that are a measure of relative protrusion, for example average sediment height divided by flow depth, and the percentage of the step width containing protruding sediment, as opposed to e.g. *K3* measuring roughness or roughness spacing. Therefore, it appears that it is overall sediment size that is most important. This suggests that step-pool bedforms do not actually affect the resistance to flow to any significant degree, except, perhaps, at a discharge higher than those observed during the course of the fieldwork. However, the steps are very important as it is here that most of the large sediment accumulates. Therefore, it appears to be the step sediment characteristics that are most important in affecting the flow in the channel.

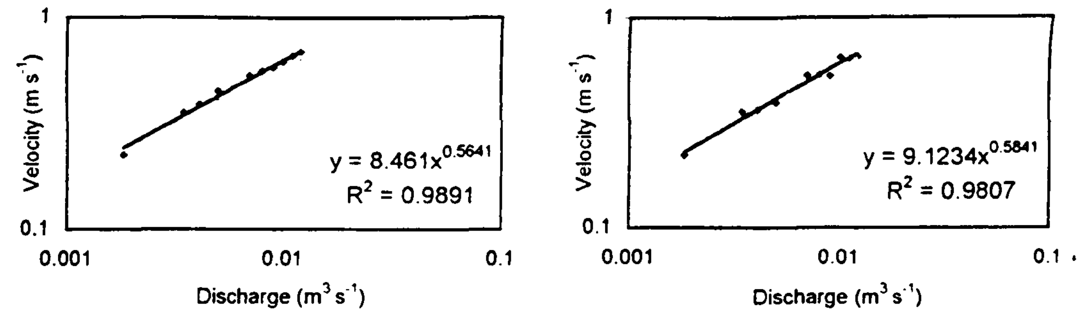

Before step formation After step formation

Figure 8.11a. Discharge and velocity hydraulic geometry relationships for the flume

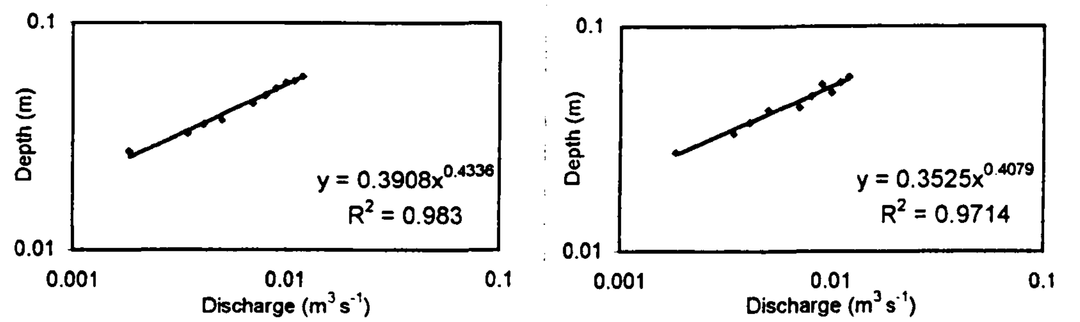

Before step formation After step formation

Figure 8.11b. Discharge and depth hydraulic geometry relationships for the flume

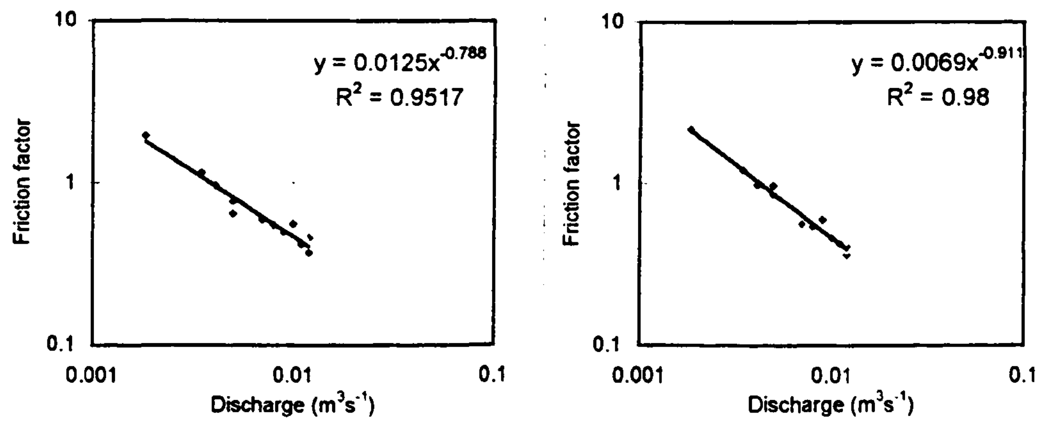

Before step formation After step formation

Figure 8.11c. Discharge and friction factor relationships for the flume

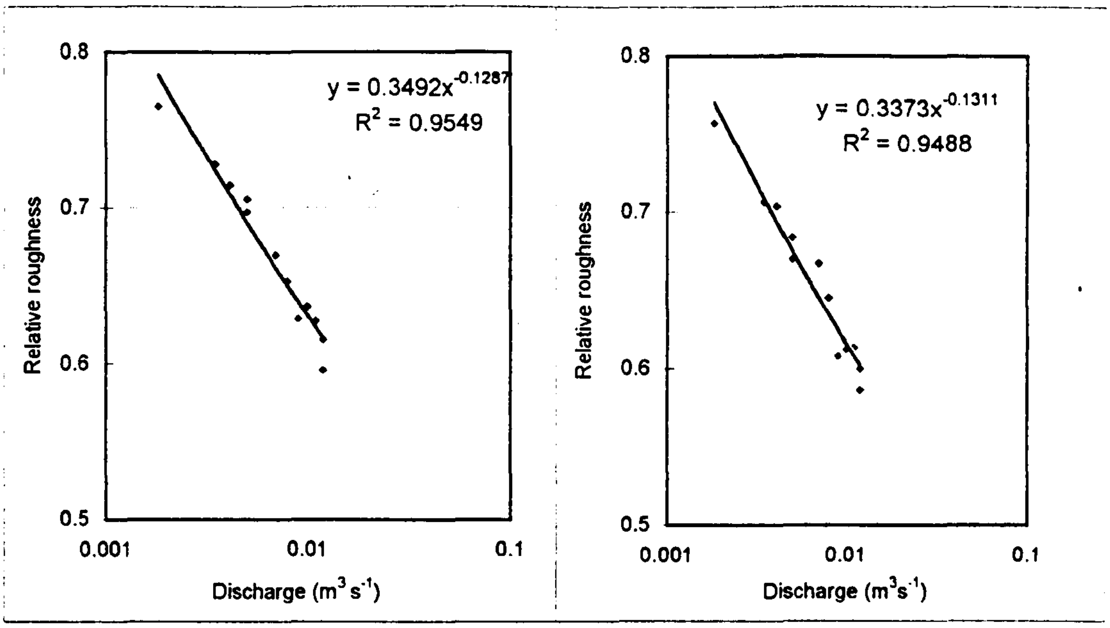

Before step formation After step formation

Figure 8.11d. Discharge and relative roughness relationships for the flume

8.3 Effects of step formation

For each flume run, the flume was run at a range of discharges before the step-forming discharge was initiated (i.e. at discharges considerably less than that needed for sediment movement and step formation), and then again at these discharges after the step-pool sequences had formed. Sediment height was measured before and after the step-forming discharge using the point gauge; water height was measured (from flume side markings) during the low and medium discharge flows, at the start of the step forming discharge, at the end of the step forming discharge and during the low and medium discharge flows following the step formation. Water depth, and therefore velocity and other flow measures could be determined for each of these conditions. Appendix 4 shows the flow data for before and after step formation.

This procedure is only useful if there is no net erosion or deposition at any of the flows except step-forming discharge. It was found that this was true for the low and medium flows before step formation (there was some sediment movement of a few very small particles but nothing significant). However, for the low and medium flows after the steps had been formed there was some continued scouring in the pools. Therefore, sediment height profiles were also measured for the flows after step formation. This means that flume average water depth and, therefore, velocity can be estimated for each of these conditions. From these values hydraulic geometry relationships, friction factor and Froude number can be determined for flows before formation of the steps, and following their formation. Detailed transects of the sediment were also measured before and after the steps had formed - these were done across the flume and down the flume, enabling study of the effect of the flow on the sediment.

8.3.1 Hydraulic geometry

Graphs showing the hydraulic geometry relationships for flow before and after step formation are shown in Figure 8.11. Table 8.2 shows the values of the exponents, intercepts and the errors associated with these. It can be seen that the value of the velocity exponent increases from 0.564 before formation of the steps to 0.584 after formation of the steps. This is a reflection of the fact that one of the effects of step formation is to increase the difference in velocity between low and high flow conditions. The depth exponent decreases from 0.434 to 0.408, i.e. the difference in flow depth between low and high flow is reduced as a result of the steps. This could be a reflection of the fact that at low flow the steps resist the flow more, meaning that velocity is decreased and hence depth increases. However, it is possible that these differences are just a result of errors associated with these relationships, as the differences are within the uncertainty range, meaning that the differences are not statistically significant.

Table 8.2 Differences in hydraulic geometry relationships as a result of step formation. *Rr* is the value for relative roughness (using average sediment height); *Fr* is the Froude number. The lower and upper values, and the uncertainty range show the extremes of the 95% confidence interval.

	Q / v **relationship**		***Q / d*** **Relationship**		***Q / f*** **relationship**		***Q / Rr*** **relationship**		***Q / Fr*** **relationship**	
	Before	**After**	**Before**	**After**	**Before**	**After**	**Before**	**After**	**Before**	**After**
r-value	0.99	0.99	0.99	0.99	-0.98	-0.99	-0.98	-0.97	0.97	0.96
Exponent										
Value	0.564	0.584	0.434	0.408	-0.788	-0.911	-0.129	-0.131	0.347	0.380
standard error	0.018	0.025	0.017	0.021	0.054	0.039	0.008	0.009	0.026	0.035
Lower	0.529	0.536	0.340	0.367	-0.893	-0.988	-0.145	-0.149	0.296	0.311
Upper	0.599	0.633	0.467	0.449	-0.683	-0.834	-0.112	-0.113	0.399	0.449
Intercept										
Value	8.46	9.12	0.39	0.35	0.01	0.01	0.35	0.34	4.32	4.91
Uncertainty range (percentage)	-8.6 to +9.4	-11.7 to +13.3	-8.3 to +9.0	-10.1 to +11.2	-23.6 to +30.9	-17.9 to +21.8	-4.2 to +4.3	-4.5 to +4.7	-12.4 to +14.2	-16.3 to +19.4
Uncertainty Range (values)	7.73 to 9.26	8.06 to 10.33	0.36 to 0.43	0.32 to 0.39	0.01 to 0.02	0.01 to 0.01	0.335 to 0.364	0.322 to 0.353	3.79 to 4.93	4.11 to 5.86

By calculating the value for discharge that is equal for the pre- and post- step equations, the crossover discharges for the relationships can be determined. For the discharge and velocity relationship, this crossover discharge occurs at 0.023 $m^3 s^{-1}$, i.e. after the steps have been formed the velocity is lower at a given discharge than before the steps were formed up to this discharge value. For the discharge and depth relationship, this crossover occurs at 18 $m^3 s^{-1}$, where the depth is greater at a given discharge after steps have been formed up to this flow level (however, this discharge is unobtainable in the flume used). Friction factor is higher for a given discharge after steps have been formed up to 0.009 $m^3 s^{-1}$. As discussed in Chapter 9, the discharge range within which steps formed was approximately 0.009 to 0.012 $m^3 s^{-1}$.

8.3.2 Flow resistance

Previous studies have suggested that one of the results of step formation is to increase resistance to flow and hence velocity decreases. Whittaker and Jaeggi (1982) determined the friction factor before and after the steps were formed to study the effect of the steps on resistance to flow. They found that the effect of the steps was to increase friction factor by as much as a factor of 10. The current research also found that the overall effect of the steps was to increase friction factor, but by less than found by Whittaker and Jaeggi (1982). This is despite the fact that relative roughness decreased due to the increase of depth, indicating that the increase in resistance is caused by the change in the shape of the bed.

Figure 8.11c shows the relationship between discharge and friction factor before and after step formation, and Table 8.3 shows values determined from the equations describing the relationships at various discharges within the range studied during the flume runs. This illustrates that whilst the steps generally increase friction, this effect is most pronounced at low flows. As discharge increases, the difference between the two friction values decreases, and at very high (step forming) flows the friction factor is slightly lower for flows after step formation (this crossover occurs at 0.009 $m^3 s^{-1}$). The reason for this decrease at high flows may be the ability of the flow at high discharges to 'skim' over the steps, and the fact that the pools are hydraulically smoother after step formation. When calculating the friction factor after the steps had been formed, it was important to use the effective bed slope as opposed to the flume slope (as described in 6.3.3). Failure to do this would lead to higher values of post-step friction factor. This is one explanation offered for the reason why the differences found by Whittaker and Jaeggi (1982) between pre- and post- step friction were a lot greater than the differences found in this research.

It is unclear why the value of the intercept for the relationship between discharge and friction factor changes from 0.0123 to 0.007 as a result of the step formation. As described in Section 8.2, it would be expected that since the steps increase the variance of the long profile from a straight line, the intercept value would increase. However, the change is insignificant when compared with the intercept values from the field sites, and also as the value of the intercept gives the friction factor at 1 $m^3 s^{-1}$, a value which could not be obtained in the flume anyway. Therefore, it was considered unwise to draw any conclusions from the intercept values. As with the exponent values the uncertainty ranges do not overlap, indicating the differences in the equations are significant. Table 8.3 also shows the uncertainty ranges of these predicted values; at most discharges there is little or no overlap of the uncertainty ranges, indicating that the differences are significant.

8.3.3 Sediment transects

During the flumework, point gauge measurements of sediment height for a number of transects across and down the flume were taken in order to study the effect of the step formation on the sediment variation in these transects. From these, *K3*, standard deviation of bed elevation and χ_{rms} could be determined for pre- and post- step formation. The only significant difference in these sediment characteristics occurred when the transect was across the flume in a location containing steps. This is despite the fact that the step-pool sequences appeared to be significant visually. This suggests that the effect of the steps is to change the pattern of the variance (i.e. by organising the sediment into steps and pools), rather than to change the actual average variance.

Overall, it appeared that the effect of running the flume was to slightly smooth the sediment, with steps at some positions interrupting this. The long profile transects usually had higher variance from a straight line after the step-forming runs as usually the transects included one or two step and pool sequences, although not significantly.

Table 8.3 Differences in friction factor and velocity as a result of flume step formation. The 95% interval uncertainty ranges (for friction factor and velocity) are shown in parentheses.

Discharge		**Friction factor**			**Velocity**	
m^3s^{-1}	**Before steps**	**After steps**	**Change %**	**Before steps**	**After steps**	**Change %**
0.002	1.67	1.98	19	0.254	0.242	-4.8
	(1.50-1.86)	(1.83-2.14)		(0.245-0.263)	(0.230-0.254)	
0.003	1.22	1.37	13	0.319	0.307	-4.0
	(1.10-1.36)	(1.27-1.48)		(0.308-0.331)	(0.292-0.322)	
0.004	0.97	1.06	9	0.376	0.363	-3.4
	(0.87-1.08)	(0.98-1.15)		(0.362-0.389)	(0.345-0.381)	
0.005	0.81	0.86	6	0.426	0.413	-3.0
	(0.73-0.90)	(0.80-0.93)		(0.411-0.441)	(0.393-0.434)	
0.006	0.70	0.73	4	0.472	0.460	-2.7
	(0.63-0.78)	(0.68-0.79)		(0.456-0.489)	(0.437-0.483)	
0.007	0.62	0.63	2	0.515	0.503	-2.4
	(0.56-0.69)	(0.58-0.68)		(0.497-0.534)	(0.479-0.528)	
0.008	0.56	0.56	0	0.555	0.544	-2.1
	(0.50-0.62)	(0.52-0.61)		(0.536-0.575)	(0.518-0.571)	
0.009	0.51	0.50	-1	0.593	0.582	-1.9
	(0.46-0.57)	(0.46-0.54)		(0.573-0.615)	(0.554-0.611)	
0.010	0.47	0.46	-3	0.630	0.619	-1.7
	(0.42-0.52)	(0.43-0.50)		(0.608-0.653)	(0.590-0.651)	
0.011	0.44	0.42	-4	0.665	0.655	-1.5
	(0.40-0.49)	(0.39-0.45)		(0.641-0.689)	(0.623-0.688)	
0.012	0.41	0.39	-5	0.698	0.689	-1.3
	(0.37-0.46)	(0.36-0.42)		(0.674-0.723)	(0.656-0.724)	

8.3.4 Energy dissipation over the steps

It is possible to estimate the energy dissipation over the steps using Equation 8.9, which using the equation for Froude number (defined in Equation 2.4), can be simplified to produce Equation 8.10 (Chadwick and Morfett, 1993). Subscript 1 refers to the energy (E), flow depth (d), and velocity (V) just before the hydraulic jump; subscript 2 to those just after the jump.

$$\Delta E = E_1 - E_2 = \left(d_1 + \frac{V_1^2}{2g}\right) - \left(d_2 + \frac{V_2^2}{2g}\right) \quad [8.9]$$

$$\Delta E = \frac{(d_2 - d_1)^3}{4d_1 d_2} \quad [8.10]$$

Equation 8.10 indicates that, theoretically, it is possible to estimate the energy lost as a direct result of the hydraulic jump, provided that the flow depths just before and after the hydraulic jump are known. Estimates for these flow depths were obtained for the flume using the long profiles in Figure 10.1 and 10.2. Table 8.4 shows the estimated values for energy loss, as well as the estimated Froude Number just before the jump. It was not possible to estimate these values for the field as the necessary flow depths were not measured.

Table 8.4. Estimated energy dissipation over two flume step-pool sequences

Figure	Q ($m^3 s^{-1}$)	w (m)	y_1 (m)	V_1 ($m s^{-1}$)	E_1	Fr_1	y_2 (m)	V_2 ($m s^{-1}$)	E_2	ΔE	% loss
10.1	0.0041	0.3	0.003	4.92	1.229	28.6	0.058	0.23	0.061	1.168	95
	0.008	0.3	0.021	1.28	0.104	2.81	0.063	0.43	0.072	0.032	30
	0.011	0.3	0.026	1.39	0.124	2.74	0.081	0.46	0.092	0.032	26
10.2	0.0041	0.3	0.018	0.76	0.047	1.80	0.056	0.25	0.059	-0.012	-25
	0.006	0.3	0.026	0.78	0.057	1.54	0.049	0.41	0.058	-0.001	-1
	0.008	0.3	0.032	0.83	0.067	1.48	0.053	0.51	0.066	0.001	1
	0.01	0.3	0.029	1.14	0.095	2.13	0.051	0.65	0.072	0.022	24

Generally, the energy losses are greater for higher Froude numbers. This is shown in Figures 8.12a and 8.12b (where 8.12b excludes the value for 0.0041 $m^3 s^{-1}$ from Figure 10.1). Only Figure 8.12a produces a relationship significant to the p=0.01 level.

There are several limitations of the data that should be considered. Firstly, as the data were measured indirectly from the long profiles, there are few data points. It is very unlikely, therefore, that the values represent an accurate average, especially considering the difficulty of measuring water depth accurately in the presence of white water. It is also likely that energy dissipation is over-estimated somewhat, as the minimum depth before the jump and the maximum depth after the jump was used. The value used for width may not be accurate, meaning that the calculated velocity value is also inaccurate as a value of 0.3 m (i.e. the width of the flume) was used, whereas in reality it was probably less than this as a result of protruding step sediment. Protruding sediment is probably the reason why the values for 0.0041 $m^3 s^{-1}$ for Table 8.4 are so different from the others, which would explain why the estimated depth is so much shallower than for the others. Also, data was only available for the flume, and previously described results have shown that the field and flume results do not plot on the same line (for example the hydraulic geometry relationships described in Chapter 7).

However, despite these limitations, it is likely that the data provides an indication of the amount of energy dissipation likely over steps with hydraulic jumps. From Henderson's (1966) classification hydraulic jumps (see Figure 8.13), the values obtained for Froude number upstream of the jump indicate that weak jumps, or just oscillating jumps, were present in the flume, as the values for upstream Froude number are generally between 1.48 and 2.81. This is also backed up by the estimated energy losses – a weak jump corresponds to energy losses of 10 to 30% over a single step, which generally corresponds to the values in Table 8.4. This suggests that over a series of steps and pools there is a considerable amount of energy loss. There will be some extra energy loss from the channel boundary, however, the energy losses over the steps is most significant.

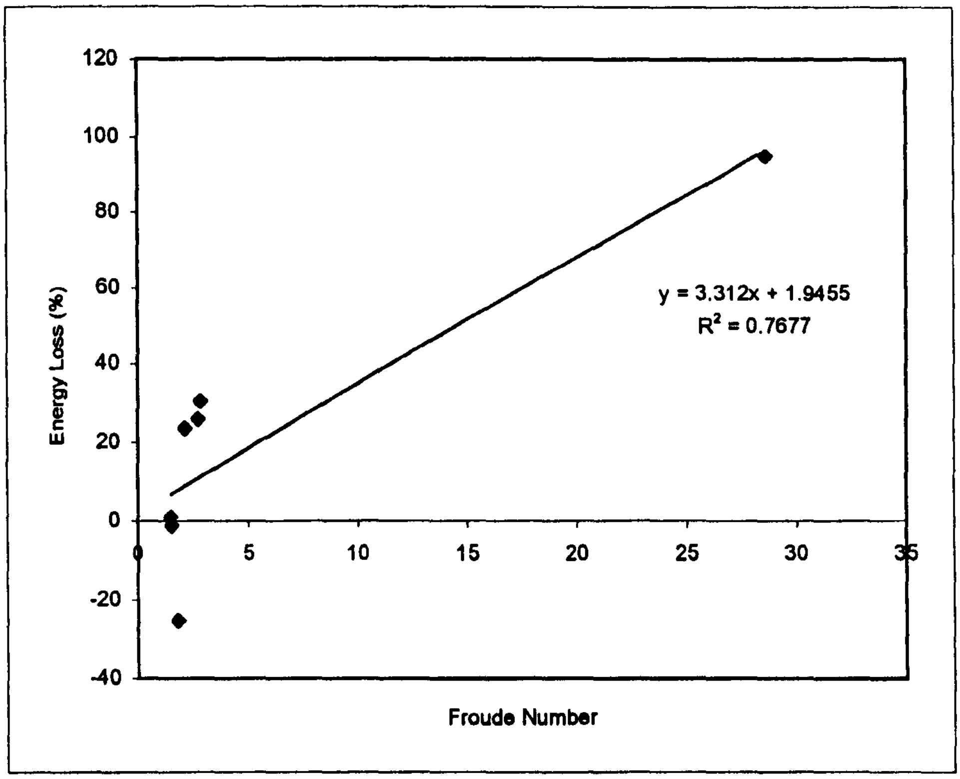

Figure 8.12a

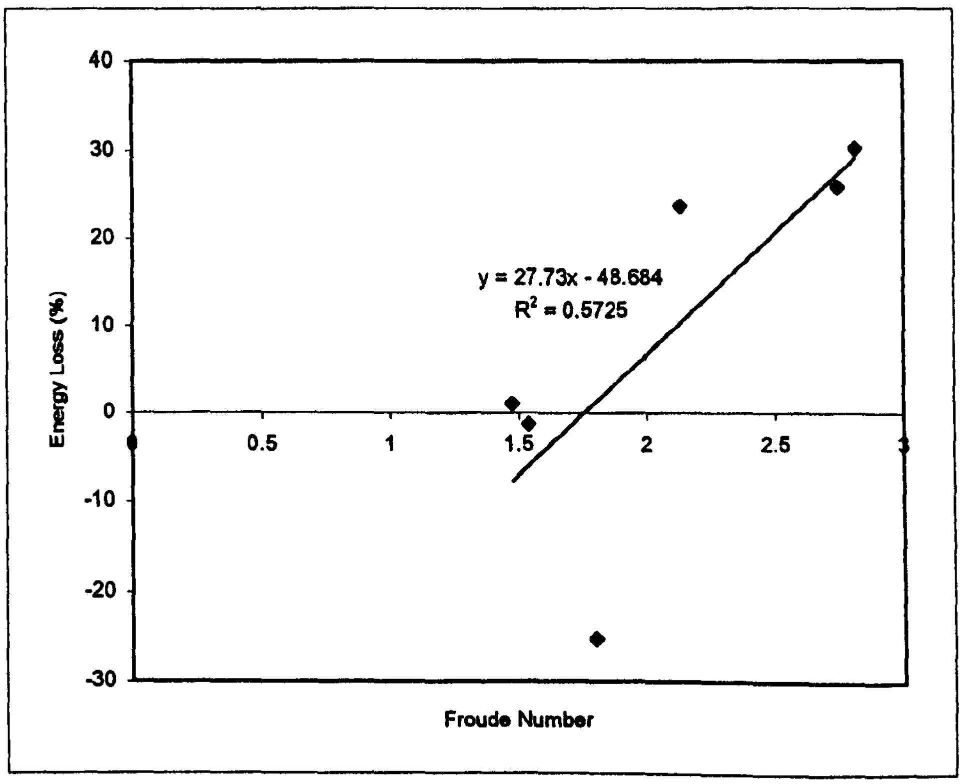

Figure 8.13b

Figure 8.12 Relationship between Froude Number and estimated percentage energy loss for the flume. Figure 8.12b excludes the value for 0.0041 m3 s-1 from Figure 10.1

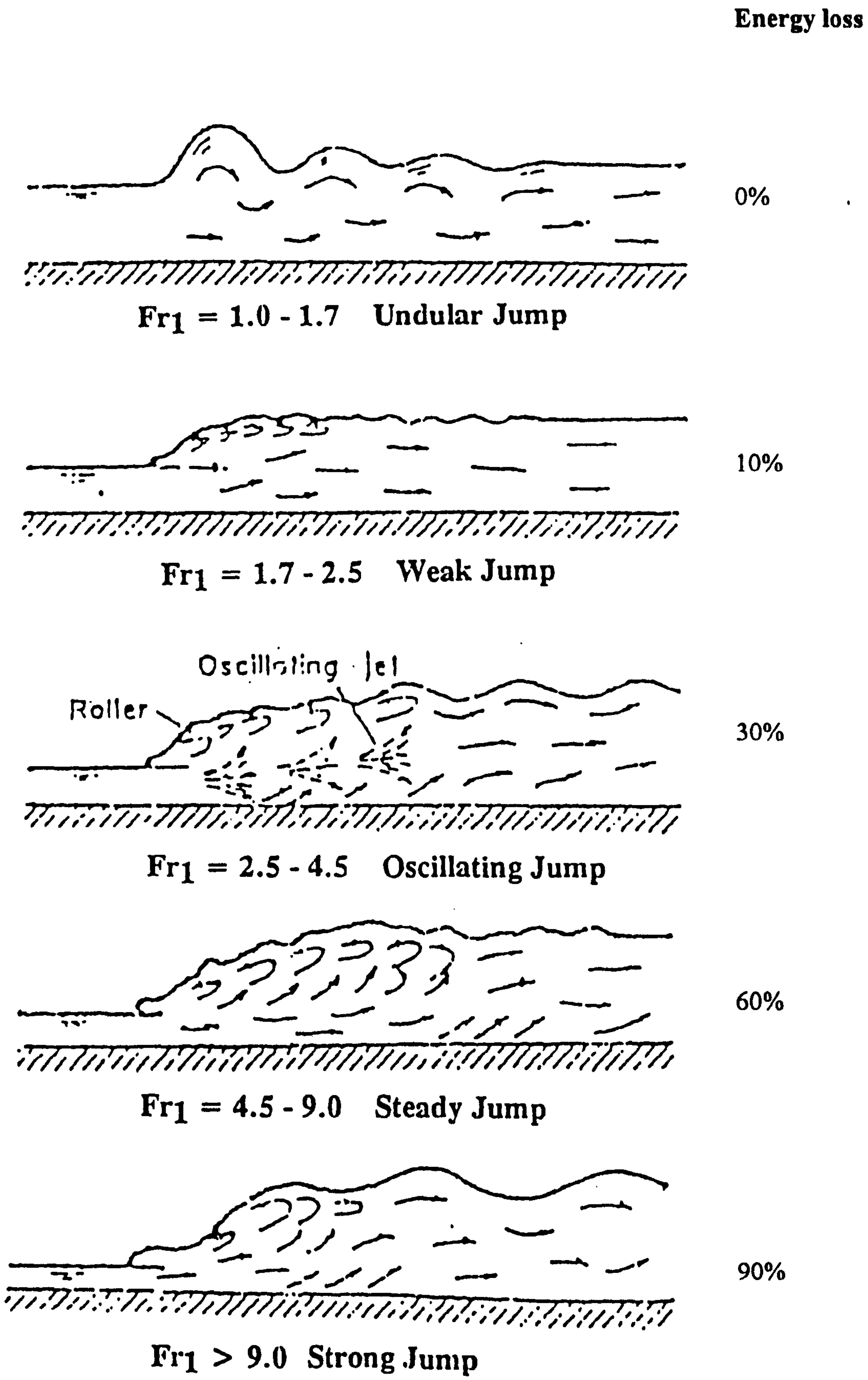

Figure 8.13 Classification of hydraulic jumps and expected energy loss (based on Henderson, 1966)

8.3.5 Conclusions

The values for friction factor before and after step formation were significantly different, demonstrating the importance of steps and pools. Also, the equations relating discharge and friction factor for before and after step formation were significantly different. At flows up to about 0.009 $m^3\ s^{-1}$ (flows slightly lower than step forming flows) the resistance to flow is increased as a result of step formation, whereas at flows higher than this value (step-forming and, therefore, low frequency flows) the resistance is reduced.

From Henderson's (1966) classification of hydraulic jumps, it would appear that the steps in the flume produced weak hydraulic jumps, with an energy loss of between 10 and 30%. As the amount of energy dissipated is related to the development of the step, it follows that sites with better developed steps will experience greater energy loss than those with not so well developed sites. This may explain why it was not possible to find equations that could be accurately applied to all the sites, and why the results in Chapter 7 show the different field sites and the flume plotting on different, parallel lines.

Chapter 9

Step formation

9.1 Introduction

The hydraulic conditions necessary for step formation, as observed during the flumework, and field relationships between step spacing and channel characteristics will be considered in this chapter. Theories of step formation based on these findings will be reviewed and modified. Section 9.2 will consider observations from the flume experiments in which steps were produced. Section 9.3 will describe the flow conditions that produced these steps, and proposed field conditions for step formation, and Section 9.4 will consider theories of step formation.

9.2 Flume observations of step formation

The best observations of the complete process of step-pool formation were made during the initial runs carried out to identify the probable range of discharge and slope required to produce steps and pools (this range is shown in Figure 9.1). A summary of these runs is given in Table 9.1. During these initial runs no detailed data were collected, so full attention could be given to the sequence of events leading to step-pool formation.

9.2.1 Step formation

The location of the steps formed were recorded in order to determine whether these initial sites were at the same location as the steps at the end of the run. Locations of significant scouring were also recorded, as were the positions of any hydraulic jumps. The degree of development of any steps was also noted, i.e. whether they were well or poorly defined. The vertical extent of sediment accumulation and scouring sites was also estimated based on the initial sediment level that was marked on the side of the flume. Figure 9.2a and b show examples of steps that were created during the flume runs.

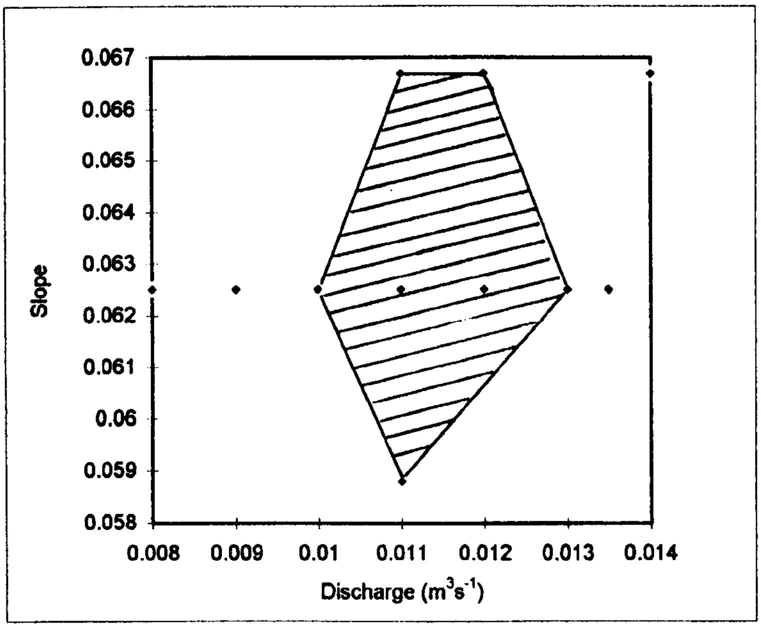

Figure 9.1. Discharge and slope range within which steps formed (shaded area).

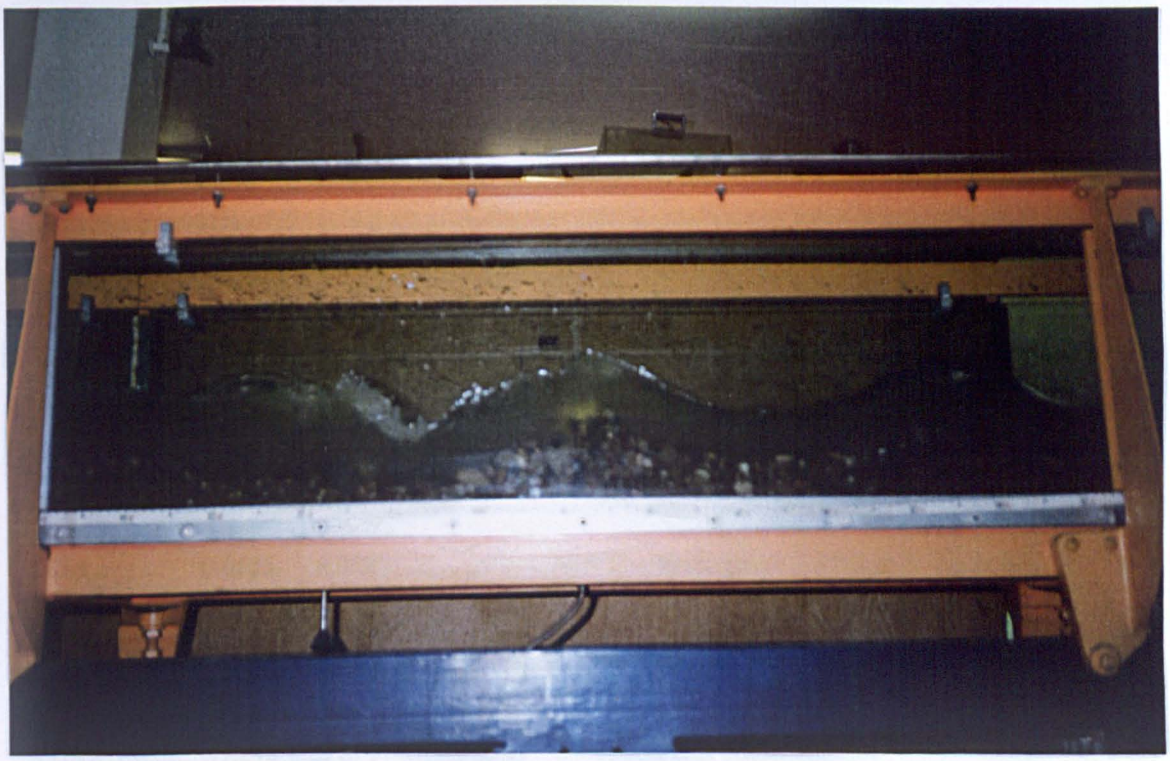

Figure 9.2a

Figure 9.2b

Figure 9.2 Examples of step-pool sequences formed in the flume

Table 9.1 Summary of the initial set of flume runs carried out to study step formation

Run ID (Q // slope)	**Slope**	**Discharge ($m^3 s^{-1}$)**	**Step spacing (m)**	**Observations**	**Notes**
11//17	0.0588	0.011		No steps	Large sediment did not move
8//16	0.0625	0.008		No steps	Large sediment did not move
9//16	0.0625	0.009		No steps	Some clustering of sediment
10//16	0.0625	0.010	0.75	Clear steps	
11//16	0.0625	0.011	0.87	Clear steps	
12//16	0.0625	0.012	0.39	Clear steps	
13//16	0.0625	0.013	0.89	Indistinct steps	
13.6//16	0.0625	0.0136		No steps	Armouring - sediment not dug up before run.
11//15	0.0667	0.011	0.88	Clear steps	
12//15	0.0667	0.012	0.77	Indistinct steps	
14//15	0.0667	0.014		No steps	Sediment transport rate too high - any steps that formed were broken up.

Standing waves appeared in the flow as soon as the flume run was started, i.e. before any steps had formed. The wavelength of these standing waves was relatively constant, and approximately equal to the flume width. They were in phase with low-amplitude bedforms in the sediment of the same wavelength (i.e. approximately 0.3 m). The first sediment to move was the smaller, loose sediment, and those tracers that were protruding into the flow. The tracers tended to move down the flume until they were stopped by other tracers or large particles. This would then initiate a cluster as more sediment would then become trapped. The standing wave at this position would increase its height, and the standing wave pattern was adjusted so that the water surface mirrored this sediment pattern. Scouring was initiated in the trough of the new standing wave. Usually a hydraulic jump was present in the trough. Scouring of the sediment in the trough would occur at high and medium discharges.

It was clear that the spacing of the initial standing waves and bed steps formed during the run was considerably different. The standing waves were spaced every 30 cm or so (approximately one channel width) whereas the steps were spaced much further apart - between two and three times the width. The standing wave pattern after the steps had formed was considerably different from the pattern at the start of the run, and non-uniform wavelengths and amplitudes were observed. The locations of the peaks and troughs of the standing waves observed before and after step formation also changed. This could be determined as the water surface before and after steps were formed was marked on the side of the flume. Where there were distinct steps, the height of the standing wave was higher than prior to the step formation. Sometimes steps were destroyed and new ones formed at other locations, suggesting that step formation is an iterative process. It was not found that the grains congregated beneath an existing hydraulic jump or standing wave; rather it was the embryonic step that controlled the position and size of the hydraulic jumps and standing waves that followed the creation of the step. Step destruction appeared to occur where a step was very large and protruded considerably into the flow, and so was easier to entrain. All the sediment was submerged at step-forming flows.

9.2.2 Factors affecting step formation

From Table 9.1 it can be seen that there were a few cases where the slope and discharge were within the range expected to produce steps and pools, although none were formed. In these cases, there must have been something preventing the formation of steps and pools. Possible explanations for this are considered in this section.

One explanation is associated with sediment transport. It appears that for steps and pools to form, a wide range of sediment is necessary to enable the larger sediment to capture other larger sediment, with relatively fine sediment in the pools to be scoured. Also, the flow conditions need to be such that entrainment of the large, protruding, sediment is initiated, whilst most of the other sediment remains stationary, unless it is scoured from the pools. Runs 11//17, 8//16 and 9//16 failed to produce steps and pools as the sediment transport rate was not high enough to enable entrainment of the large sediment. Conversely, Run 14//15 failed to produce steps and pools because the sediment transport rate was too high, meaning that all sediment sizes could be entrained, thus preventing step formation.

Before Run 13.6//16 the sediment in the flume was not dug up, meaning that armouring from the previous low discharge run was still intact. Therefore, sediment transport initiation was prevented and steps did not form. However, if sediment supply is too high steps will be destroyed, as observed during run 12//16. At the end of this run, sediment that had accumulated at the bottom of the flume was added to the top of the flume. The result of this was the break-up of the steps that had formed, a process also found by Grant (1994).

It is also postulated that there is an element of chance involved. For steps to form, it was seen that when the tracers move downstream, they need to rest against other tracers to form clusters, which in turn trap more sediment. Since the way in which sediment moves downstream is of a random nature (i.e. it cannot be predicted what path a particular particle will take), it follows that there is a random nature to step formation. During one run lots of tracers may rest against each other (probably leading to well defined steps), whilst during another run they may largely miss other tracers, leading to poorly defined steps. This can be seen in the field where some reaches of a channel have very well defined steps, whilst a nearby reach of similar dimensions and slope may not have steps at all. This is the explanation offered for why Run 12//15 did not produce steps, where the slope and discharge values were within the range at which steps were found to form, and there was no initial bed armouring preventing entrainment. This may help to explain why width was found to be a controlling factor of step characteristics, as considered in Section 9.4.3.

9.2.3 Step characteristics

Most of the steps that formed consisted of at least three tracers, and were at least one clast high. Generally, the *b*-axis was transverse to the flow, and the *c*-axis was equal to the vertical height of the sediment particle. Although sediment sampling of the steps and pools was not carried out, it was clear from the location of the tracers that all the steps contained tracers, whilst none of the pools did (unless they were buried under the sediment surface). The steps sometimes extended across the whole channel, but sometimes only extended across half or two-thirds of the channel width. At nearly all of the steps a hydraulic jump existed as the flow plunged into the pool.

In order to test relationships between variables such as step spacing and the flow conditions, an estimation of average step spacing was required. Zero crossing analysis, as used by Whittaker and Jaeggi (1982), was inappropriate as the individual steps were the same height as the grain roughness (i.e. individual particles), and so step spacing was measured visually. The position of the steps was noted whilst the flume was running, and then the average spacing of the steps within the sequence determined. This was considered preferable to averaging a number of longitudinal bed surface profiles (meaning an individual clast's effect would be averaged out and any undulations present would be the result of any steps and pools). Step spacing was found to be between 2.5 and 3 channel widths. It was not possible to test the relationship between spacing and slope as the range of slope was too limited, but it was possible to compare the average values from the flume with those obtained in the field; Figure 9.3a shows the field and flume step spacing and slope relationship. Figure 9.3b shows the spacing and width relationship with average flume value added. These graphs strongly suggest that it is width that controls the spacing of the steps, rather than slope. As width is not a significant hydraulic control, this suggests that perhaps the fact that width affects the chances of a cluster forming (i.e. more chance of two large clasts missing each other in a wide channel) is an important one for step formation.

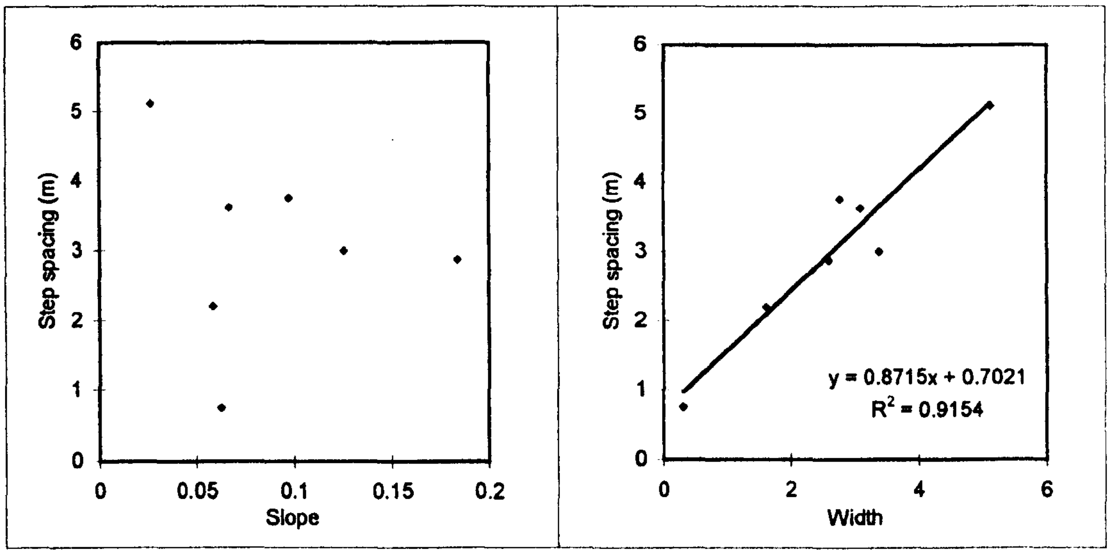

Figure 9.3 Relationship between step spacing and a)slope and b)width.

9.2.4 Comparison with field steps and pools

In terms of the actual step characteristics, those created in the flume matched those observed in the field. As in the field, the steps comprised the largest sediment, with the finer sediment accumulated in the pools. There were hydraulic jumps between the steps and pools, as observed in the field. Also similar was the fact that a limited sequence of steps and pools formed with regular spacing, but before and after the sequence there was an absence of these features. In both the flume and the field, the steps were usually perpendicular to the flow, and were best observed at low discharges when the step sediment protrudes into the flow slightly. However, in the flume there were more incomplete steps, i.e. ones that did not extend fully across the flume, possibly as a result of the unnaturally smooth walls or the lack of a sufficient quantity of step forming particles. Another factor could be the limited time the flume was run at a step forming discharge for; in the field it is likely that the steps are formed gradually over a number of high flow events. Overall, the features were very similar, therefore, it was concluded that the features produced in the flume were the same features as the steps and pools observed in the field.

9.3 Flow conditions at step-pool formation

As described in Chapter 6, during the detailed flume runs sediment height and water height were measured, meaning that water depth could be calculated. From this value, and discharge and initial slope, it was possible to calculate a number of flow values that characterised the flow conditions for creation of steps and pools. These conditions are summarised in Table 9.2. Whilst it was not possible to observe step formation or movement of step sized sediment in the field, it was possible to estimate the probable flow conditions necessary to move the step sized sediment by using approaches based on estimated Froude number, critical shear stress, and critical discharge. These estimated and calculated flow conditions are described in this section.

Table 9.2 Flow conditions at the time of step formation for detailed flume runs

Run ID (date)	**Slope**	**Discharge ($m^3 s^{-1}$)**	**Velocity ($m s^{-1}$)**	**Flow depth (m)**	**Froude number**	**Shear stress ($N m^{-2}$)**	**Step spacing (m)**
3/12/96	0.0588	0.012	0.659	0.059	0.85	34.9	0.81
16/1/97	0.0555	0.012	0.697	0.060	0.93	31.2	0.76
28/1/97	0.0625	0.011	0.666	0.055	0.91	33.7	0.63
6/2/97	0.0588	0.011	0.666	0.056	0.91	31.7	0.75
25/2/97	0.0667	0.009	0.621	0.051	0.85	35.4	0.66
6/3/97	0.0564	0.01	0.584	0.055	0.85	28.3	0.87

9.3.1 Slope

Whittaker and Jaeggi (1982) found that a slope of 0.075 formed the division between antidunes and steps and pools during their flume experiments. Below 0.075 antidunes were predominant; above 0.075 steps and pools predominated. However, Grant (1994) found steps and pools developed on a slope of 0.04. During the flume research, slopes of between 0.054 and 0.067 produced step-pool sequences. In the field, steps were observed on a wide range of slopes; from 0.026 to 0.176. It is, therefore, postulated that the actual value of slope is not important; rather it is the flow conditions (e.g. Froude number) and sediment size and sorting characteristic of steeper slopes that are most important.

9.3.2 Froude Number

Froude number, which provides a dimensionless measure of the flow conditions by relating the inertial and gravitational forces at work, can be calculated by using the following formula:

$$Fr = \frac{\overline{U}}{\sqrt{gd}} \qquad [9.1]$$

where $\overline{U}$ is the average velocity, g is the acceleration due to gravity, and d is the average flow depth. For flows producing steps and pools in the flume a range of $0.82<Fr<0.93$ was found, with an average of 0.88. This is similar to the range found by

Grant (1994), which was $0.7<Fr<1.0$. Grant (1997) suggests that a Froude number close to unity is necessary for sediment entrainment in steep streams.

From the assumption of step-forming Froude number being approximately equal to 0.88, it was possible to estimate the depth of flow by exploiting the relationships between discharge and Froude number, and the hydraulic geometry relationships considered in Chapter 7. However, this does require extrapolation of the relationships found. The estimated flow depths required for a Froude number of 0.88 are in Table 9.3. Also shown are the step D_{84} *c*-axis values of the sites. As a generalisation, it can be stated that the sediment particle's *b*-axis is twice that of its *c*-axis, and that when lying on a stream bed it is the *c*-axis that is aligned with the vertical (Wiberg and Smith, 1991, and also flume observations from this research).

Table 9.3 Estimated conditions for step formation using different approaches

Site		**Froude**	**Number**	**Critical**	**unit Q**	
	Step D_{84} c-axis (m)	*Critical Depth (m)*	*Depth minus Step D_{84} c-axis (m)*	*Critical depth (m)*	*Depth minus Step D_{84} c-axis (m)*	*Maximum observed depth (m)*
Ashop	0.16	0.21	0.05	0.23	0.07	0.20
Burbage	0.24	0.31	0.07	0.31	0.07	0.22
Doctor's Gate	0.15	0.13	-0.02	0.17	0.02	0.12
Fairbrook	0.20	0.17	-0.03	0.18	-0.02	0.17
Grindsbrook A	0.39	0.55	0.16	0.38	-0.01	0.31
Grindsbrook B	0.39	0.59	0.20	0.49	0.1	0.51

The data in Table 9.3 suggests that at the critical depth for step formation the step D_{84} sized sediment was submerged at all but the Doctor's Gate and Fairbrook sites. However, consideration of the sediment in these two sites indicates that it is likely the sediment *was* submerged, as at Doctor's Gate the sediment is very flat and platy, whilst at Fairbrook most of the steps are bedrock (also reflected in the fact that these two sites have the lowest values for *K3*). At this flow depth the largest sediment in the steps would not be submerged.

The lack of a gauging record for the area where the study reaches were located meant that is was not possible to compare these estimated step-forming flow depths with recorded maximum discharges. However, Table 9.3 also shows the maximum observed depths at each of the fieldsites. These occurred at high flow, but lower than step-forming flows. Comparing these values with the predicted critical depths suggests that the Froude number approach over-estimates critical depth for Grindsbrook A as a depth of 0.55 m is considered to be unreasonably high considering that the maximum observed depth was only 0.31 m. For the other sites, generally, the predicted critical depths seem reasonable.

9.3.3 Shear stress

The values obtained for run average shear stress, τ_r, calculated using Equation 9.2 below are given in Table 9.2.

$$\tau_r = \rho g d \sin\theta \qquad \textbf{[9.2]}$$

Here ρ is water density (1000 kg m^{-3}), d is the water depth, and θ is the local bed slope. Grant (1994) also used the ratio of average shear stress for the run (τ_r) to the shear stress needed to move the largest grain size in the sediment mix (τ_{cr}),

$$\tau^* = \frac{\tau_r}{\tau_{cr}} \qquad \textbf{[9.3]}$$

He found $0.5 < \tau^* \leq 1.0$, which supports the finding from this research that steps form in a relatively narrow range of flow conditions where there is a limited amount of sediment transport. Generally, he found that D_{90} and coarser sediment did not move, whereas it was found during this research that the steps were made up of D_{95} sized sediment (i.e. the tracers), indicating the movement of sediment of this size. This may be a result of the sediment range used in the flume, as the fieldwork results have suggested that the largest sediment is not involved in the step forming process.

As outlined in Chapter 2, the theory of critical shear stress considers that the value of τ_{cr*} in Equation 9.4 is constant at a value of 0.06 (Shields, 1936). Use of Equation 9.4 in conjunction with Equation 9.2 theoretically means that the flow depth for entrainment of particle size D can be determined.

$$\tau_{cr*} = \frac{\tau_{cr}}{(\rho_s - \rho)gD} \qquad [9.4]$$

However, this theory is complicated by the fact that the critical Shields value (0.06) is not appropriate for use in steep streams with a large sediment size range (Bathurst, 1987a and b; Wiberg and Smith, 1987). Wiberg and Smith (1987) suggest that a much lower value of non-dimensional critical shear stress than the Shields value is necessary because of protrusion effects, however, Bathurst (1987a and b) suggests that a higher value is necessary, indicating that the hiding and protrusion effects in steep streams with large sediment are uncertain. Table 9.4 also shows the estimated values for non-dimensional shear stress using Equations 9.2 and 9.4, assuming that the step D_{84} sediment is just submerged when it is entrained (which was indicated from the Froude number analysis). All the calculated values are considerably less than the Shield value of 0.06, indicating that protrusion effects are considerable.

Table 9.4 Predicted values of τ_{cr*}

Site	Shields (1936)	Grant (1997)
Ashop	0.0076	0.012
Burbage	0.025	0.038
Doctor's Gate	0.015	0.020
Fairbrook	0.018	0.018
Grindsbrook A	0.029	0.037
Grindsbrook B	0.045	0.070

9.3.4 Critical unit discharge

As there are considerable problems associated with determining a value for non-dimensional critical shear stress, use of a critical unit discharge (q_{cr}) has been suggested (Bathurst, 1987a and 1987b; Bathurst et al, 1987 and Ferguson, 1994), and originally developed by Schoklitsch (1962). The equation below (Bathurst, 1987b) was used to estimate the critical flow depth for sediment entrainment (by using the hydraulic geometry relationship between discharge and depth).

$$q_{cr*} = \frac{q_{cr}}{g^{0.5} D_{16}^{1.5}} = 0.21S^{-1.12} \qquad [9.5]$$

Whilst it is acknowledged that there are also problems applying this approach to steep streams (Ferguson, 1994) it is interesting that, as shown in Table 9.3, the results are similar to those obtained from the critical Froude number analysis. It is again estimated that the step D_{84} sediment is submerged at entrainment conditions for all but the Fairbrook and Grindsbrook A sites. As explained earlier, the Fairbrook site is bedrock; however, no explanation is offered for the discrepancy at Grindsbrook A. It is, therefore, considered likely that at step forming conditions the step D_{84} sized sediment is submerged at all the sites, although as with the critical Froude number analysis, the largest sediment is not. This is supported by Grant et al (1990) and Bowman (1977) who reached the same conclusions.

9.3.5 Antidunes and step spacing

Equation 9.6 (Kennedy, 1963) has been used extensively by workers studying steps and pools (for example, Shaw and Kellerhals, 1977; Grant et al, 1990; Billi et al, 1995) to explain step spacing and predict whether the flow conditions are those necessary for antidune development. L_{min} is the minimum antidune spacing (in m) expected with the given flow conditions, $\overline{U}$ is the reach average velocity.

$$L_{min} = \frac{2\pi\overline{U}^2}{g} \qquad [9.6]$$

$$L = 0.8L_{min} + 0.14 \qquad [9.7]$$

Grant (1994) found a strong positive relationship between step spacing (L) and L_{min}, strengthening the argument that steps and pools are related to antidunes; this is Equation 9.7, with values in m. However, this research does not support this. The values of L_{min} calculated from the flumework and fieldwork using Equation 9.7, and the associated flow conditions (using Equation 9.6 and the hydraulic geometry relationships) are shown in Table 9.5. In this table, the values for step spacing are those actually measured during the course of the field and flumework. The values for L_{min} were calculated using Equation 9.7, with the velocity value calculated using Equation 9.6. Using the hydraulic geometry relationships determined for each of the fieldsites and the flume, the values for discharge and depth were then estimated.

Overall, the estimated flow values are not reasonable, especially for the flume, where the values do not match the measured values at step forming flows shown in Table 9.2. Even if the actual step spacing is taken as being the value of L_{min}, the values are still unreasonable; for example, for the flume the predicted velocity is still 1.09 m s^{-1}.

Therefore, it is proposed from this research that $L_{\min}$ is not related to step spacing, indicating that it is unlikely steps are formed by the same process as antidunes, as the equations relating antidune spacing and flow conditions do not produce acceptable results.

Interestingly, predicting $L_{\min}$ for the flume using the estimated flow conditions at step formation (Table 9.2) and Equation 9.6 gives an average value of 0.27 m (Table 9.6 shows these calculated values for $L_{\min}$, compared to the measured step spacing). This value of 0.27 m is very close to the observed standing wave spacing in the flume (which was approximately 0.3 m), suggesting that Equation 9.6 does accurately predict standing wave and antidune spacing. However, considering that in the flume the calculated $L_{\min}$ spacing and step spacing were very different, Equation 9.6 cannot be used for estimating step spacing, and, therefore, the flow conditions necessary for antidune and step formation are different. It can hence be concluded that antidunes and steps-pool sequences are unrelated in terms of conditions necessary for their formation, and so are separate, unrelated features.

Table 9.5 Predicted flow values based on $L_{\min}$ and hydraulic geometry relationships

Site	Actual Spacing (m)	*Predicted* L_{min} (m)	Predicted Velocity (m s^{-1})	Predicted Discharge (m^3 s^{-1})	Predicted Depth (m)
Ashop	5.12	6.23	3.12	6.75	0.24
Burbage	3.75	4.51	2.65	9.23	0.57
Doctor's Gate	2.21	2.59	2.01	0.91	0.17
Fairbrook	3.62	4.35	2.61	1.87	0.44
Grindsbrook A	3.00	3.58	2.36	23.76	1.41
Grindsbrook B	2.88	3.42	2.31	7.82	0.69
Flume average	0.75	0.76	1.09	2.68	0.61

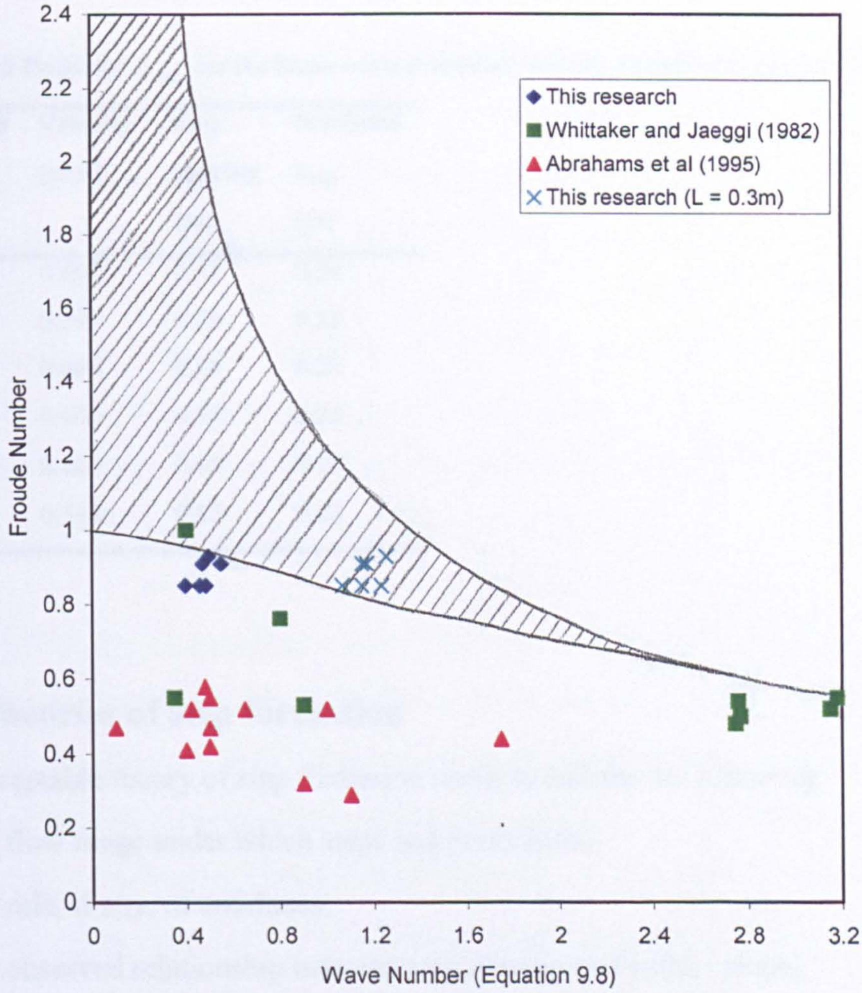

Figure 9.4. Phase diagram indicating domain of antidunes and data points from step-pool studies (adapted from Allen, 1984 and Abrahams et al, 1995)

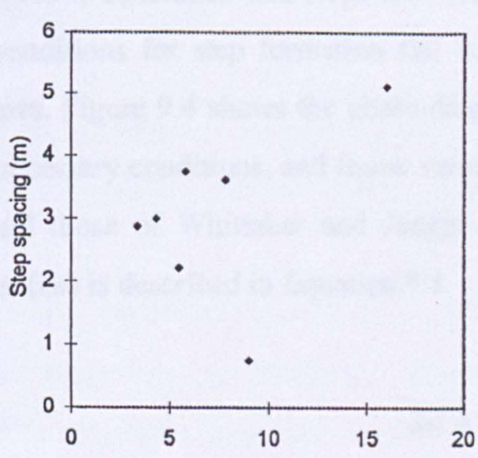

Figure 9.5 Relationship between width/D_{84} and step spacing.

Table 9.6 Predicted L_{min} for the flume using calculated velocity at step formation and Equation 9.6

Run ID (date)	Velocity ($m\ s^{-1}$)	Step spacing (m)	Predicted L_{min} (m)
3/12/96	0.659	0.81	0.28
16/1/97	0.697	0.76	0.31
28/1/97	0.666	0.63	0.28
6/2/97	0.666	0.75	0.28
25/2/97	0.621	0.66	0.25
6/3/97	0.584	0.87	0.22

9.4 Theories of step formation

An acceptable theory of step formation needs to address the following:

- the flow range under which steps and pools form,
- the role, if any, of antidunes,
- the observed relationship between step spacing and width / slope,
- the existence of bedrock steps.

9.4.1 Connection between antidunes and steps

Grant (1994) concluded that steps are related to standing waves, and showed that the flow conditions for step formation fall within the range of conditions necessary for antidunes. Figure 9.4 shows the phase diagram (wave number and Froude number) for these necessary conditions, and flume values from this research (using the data in Table 9.3) and those of Whittaker and Jaeggi (1982) and Abrahams et al (1995). Wave number (kd) is described in Equation 9.8.

$$kd = \frac{2\pi d}{L} \qquad [9.8]$$

As can be seen in Figure 9.4, the step forming flow conditions, when using the step spacing for the value of L, do not fall within the antidune zone. However, replacing step spacing with the observed standing wave spacing (taken as 0.3 m, i.e. the same as the flume width) generally results in flow conditions that do fall within the antidune zone. Also, the data points relating to the flume studies carried out by Whittaker and Jaeggi (1982) and Abrahams et al (1995) do not fall within the flow range necessary for antidune formation either. This adds to the conclusion from the previous section that steps are not related to antidunes and standing waves (although the standing waves *are* related to antidune features).

Also during the flumework, it was observed that the location of the steps was not related to the location of the standing waves, as the standing wave pattern changed as a result of the step formation. Grant (1994) and Whittaker and Jaeggi (1982) concluded that the standing waves control the formation and location of the steps. However, the flume runs carried out for this research found that, in fact, the opposite was true, i.e. the standing waves were controlled by the steps as the initial standing wave pattern was modified to match that of the steps and pools. There were some low amplitude bed undulations present in the flume which were in phase with the standing waves, but these features were not steps. They were of much lower amplitude than the steps that subsequently formed, and had a smaller wavelength. These are likely, therefore, to be antidune-type features.

Therefore, this research does not support the theory that step-pool formation is linked to antidune formation for the following reasons:

- There is no relationship between L_{min} and actual step spacing (as seen in Table 9.6),
- The Froude number needed for antidunes is defined as 0.844 to 1.77 (Kennedy, 1963), although a narrower range of 0.9 to 1.6 was found by Shaw and Kellerhals (1977) and Whittaker and Jaeggi (1982). However, although this puts the Froude Number at step formation from the flume studies just within the range necessary for

antidune formation, when also considering the non-dimensionless wavelength (as defined in Equation 9.8), the flow conditions do not fall within the range defined for antidunes shown in Figure 9.4.

- Using the equation developed for antidunes relating antidune spacing and velocity (Equation 9.6) results in highly unlikely flow conditions. Therefore, it was concluded that the flow conditions for step formation cannot be predicted using the equation developed for antidune formation and so, therefore, steps and antidunes are not the same feature.
- Flume observations showed that prior to step formation, there were low amplitude bedforms present with a wavelength approximately equal to the flume width (0.3 m), mirrored by standing waves. As Figure 9.4 shows, these features fall within the flow conditions necessary for antidunes, and using Equation 9.6 accurately predicts their wavelength. These features became less obvious as the steps were formed, and the standing waves could be seen to move into phase with the steps instead as they developed. It is concluded, therefore, that these initial features were antidunes, and that the steps were separate, distinct features.
- The field studies suggest that steps and pools are more complicated than simply being antidune type features with a regular spacing dependent on flow conditions at time of formation. Width and a random element appear to be important for step-pool development.

However, the confusion between antidunes and steps is understandable, as it appears that flows similar to antidune forming flows are necessary for step formation in order to have the flow balanced so that the larger sediment moves.

9.4.2 The process of step formation

It has generally been accepted that the process of step-pool formation takes place at very high (near peak) discharge (Judd and Peterson, 1969; Whittaker and Jaeggi, 1982; Wohl and Grodek, 1994). This was also suggested by the current fieldwork results, where predicted step-formation flow conditions meant the step D_{84} sediment was just submerged. This would be the case for near bankfull flow. It would appear that some large sediment is entrained by the flow, which moves until it becomes trapped by other large sediment. This embryonic step then grows as more sediment is trapped. A sequence of steps is formed as this process is repeated in other locations of the channel. There was no evidence from the flume research that the formation of one step triggers the formation of others downstream, so it is possible that they are isolated features. The step-pool profile becomes more attenuated as larger sediment is trapped at higher flows, and pools are scoured at lower flows (as was observed in the flume).

9.4.3 Controls on step spacing

In the field, it was observed that the spacing is strongly related to channel width. This is despite the fact that width is not an important hydraulic variable. It is possible that the relationship found with width is a result of some other relationship, for example slope and sediment size were found to be related to width, and they are also important in terms of hydraulics. However, the relationship of step spacing with width was most significant, especially when also considering the flume spacing, indicating that this *is* the controlling factor for determining step spacing. It would have been useful if, in the flume, there had been the possibility to study the step spacing and slope relationship in more detail, as width was fixed. However, the range of slope under which steps formed was too narrow to establish any such relationships.

One possible solution for this, based on flume observations, is associated with probabilities. It was observed in the flume that there was a degree of randomness involved in the step formation. The tracers needed to become stuck between or behind other tracers for steps to form. If the channel is very wide in comparison to the step sediment size (taken as step D_{84}), then the chances of this sediment coming into contact with similar sized sediment are a lot lower than in a channel with sediment of a comparable size to channel width. Sediment size is correlated with slope meaning that larger sediment is found on steeper slopes, so this theory would explain the relationship between spacing and slope to some extent. However, as seen in Figure 9.5 the relationship between the number of step D_{84} sized particles that would fit across the channel (using average width) and actual spacing is not a good one, with the flume point plotting away from the general trend. This could be a reflection of the unnatural conditions of the flume. It also follows that the number of steps, and, therefore, the spacing, is restricted by the amount of mobile large sediment in the stream. If there are a large number of particles big enough to make up the steps, the chances of step formation are increased. This indicates that sediment supply is also important.

9.4.4 Bedrock steps

The flume studies also suggest that the step forming process is iterative, and in the field it is probable that a number of flood events are required. This is based on the fact that in the flume sometimes only half a step formed, because during the time that the flume was running not enough large enough particles were captured by the embryonic step. Also, as found by Whittaker and Jaeggi (1982), and supported by this research, steps can break up and new ones form elsewhere.

This raises problems with including bedrock steps in a theory of step formation, as the process forming bedrock steps cannot be iterative. If it was, then partially formed steps in the field that had been abandoned as sites for steps would have been observed, which were not. The explanation offered for the correlation between step spacing and width does not explain why bedrock steps also correlated with width. It is, therefore, proposed that alluvial sediment is involved in the formation of bedrock steps, for example, if there were some large alluvial particles that initially formed the steps which then scoured the bedrock downstream of the step as a result of the hydraulic jump produced. However, conducting research to test this proposal would be very difficult. One way could be to carry out flume experiment using large sediment and also a soft, quickly erodible bed material.

9.5 Conclusions

It has been concluded from the flume and field studies that step formation is not related to antidunes. Rather, steps are formed as a result of the large range of sediment in the channel and the fact that the larger sediment can accumulate together to form steps, resulting in an absence of large sediment in the pools. It is also suggested that steps are individual features, and that sections of the channel can be viewed as being almost isolated, with the large sediment in this section forming a step. The step spacing is postulated, therefore, to be determined by the amount of large sediment present and the width of the channel, and not the flow conditions or slope (except indirectly). The presence of bedrock steps is slightly problematic as it cannot be explained by this theory, so it is suggested that alluvial sediment was originally involved in their formation.

Future study that could confirm this theory would involve introduction of more large sediment into the flume, and the study of the effect this has on step spacing and the extent of step development. Use of video recordings would also be useful to determine the order of step formation - if they are individual features there would be no consistent order to the step formation i.e. it would not matter if downstream or upstream steps are formed first. If, however, the formation of one step triggers the development of a whole sequence of steps, then it would be expected that the step sequence would be consistently initiated by one upstream (or downstream) step first. From the flume runs it appeared that the former situation was true, however, there was not time to study this in detail because of the speed of step development.

Chapter 10

Velocity distribution in steep streams

10.1 Introduction

It would be very useful to be able to model the velocity distribution in steep streams, as this would enable study of the velocity profile and how it is affected by the sediment in the channel, and average velocity and friction factor could also be estimated. As described in Chapter 2, the log-law of velocity distribution does not apply to high-gradient streams with large sediment. One of the possible approaches that can be used to estimate velocity is to consider the total drag force as a result of the presence of individual clasts. This chapter will describe an attempt to model velocity distribution using such an approach, based on the method used by Wiberg and Smith (1987 and 1991). Firstly, characteristics of the velocity profiles over steps and pools identified from the detailed flume runs will be described. The model will then be described, and results of its application to step-pool fieldsites and flume described.

10.2 Velocity distribution over the step-pool sequences

To provide further insight into the flow behaviour within a step-pool sequence, velocity profiles at a range of discharges were measured over step-pool sequences during some of the detailed flume runs. Detailed sediment and water height profiles were also taken, meaning that the effect of the sediment at different parts of the step-pool sequence could be studied. It was also considered useful to investigate how submergence of the elements reduces the associated flow resistance, as this may help explain the hydraulic geometry characteristics found at the fieldsites.

10.2.1 Methodology for obtaining velocity profiles

For three of the flume runs (6/2/97, 18/2/97 and 6/3/97), detailed velocity profiles were taken over an entire step-pool sequence. After steps had been formed, a typical sequence was selected and the following carried out:

- sediment and water level transects (at each of the discharges) were measured at 1 cm intervals,
- velocity profiles were taken at 5 cm intervals along the step-pool profile using a miniature Nixon current meter.

For runs 6/2/97 and 18/2/97 the profiles were taken at 5 cm intervals along the sequence (i.e. streamwise) at just one lateral position across the flume. For the 6/3/97 run, profiles were taken at three lateral positions across the flume, again at 5 cm intervals along the sequence. For each profile, velocity readings were measured every 0.5 cm up the profile, meaning that typically at least 10 points were taken. As described in Section 6.3.3, the current meter was attached to a trolley that could move along the flume and lowered into the flow, and the current meter was kept in the flow until a steady frequency reading was recorded. This was typically between about five and ten seconds. Because of the time involved in taking the velocity profiles, it was not possible to measure velocity profiles at the step-forming discharge.

As noted in Chapter 9, if the flume was run at this high discharge for too long the steps broke up. Therefore, velocity profiles were only measured at low and medium discharges. The nature of the flow over a step and pool sequence meant that there were some problems associated with obtaining the readings. At some positions it was not possible to obtain a value for velocity because of the presence of features such as hydraulic jumps. The presence of white water also made it very difficult to determine the overall depth of the velocity profile, which is needed in order to obtain an average velocity value.

The results obtained are shown in Figure 10.1 (6/2/97 run), Figure 10.2 (18/2/97 run), and Figures 10.3a-c (6/3/97 run for the three positions across the flume). Each figure contains a graph showing the sediment and water levels at each discharge, and separate graphs for each discharge showing the structure of the velocity profiles and the value of the average velocity for each profile.

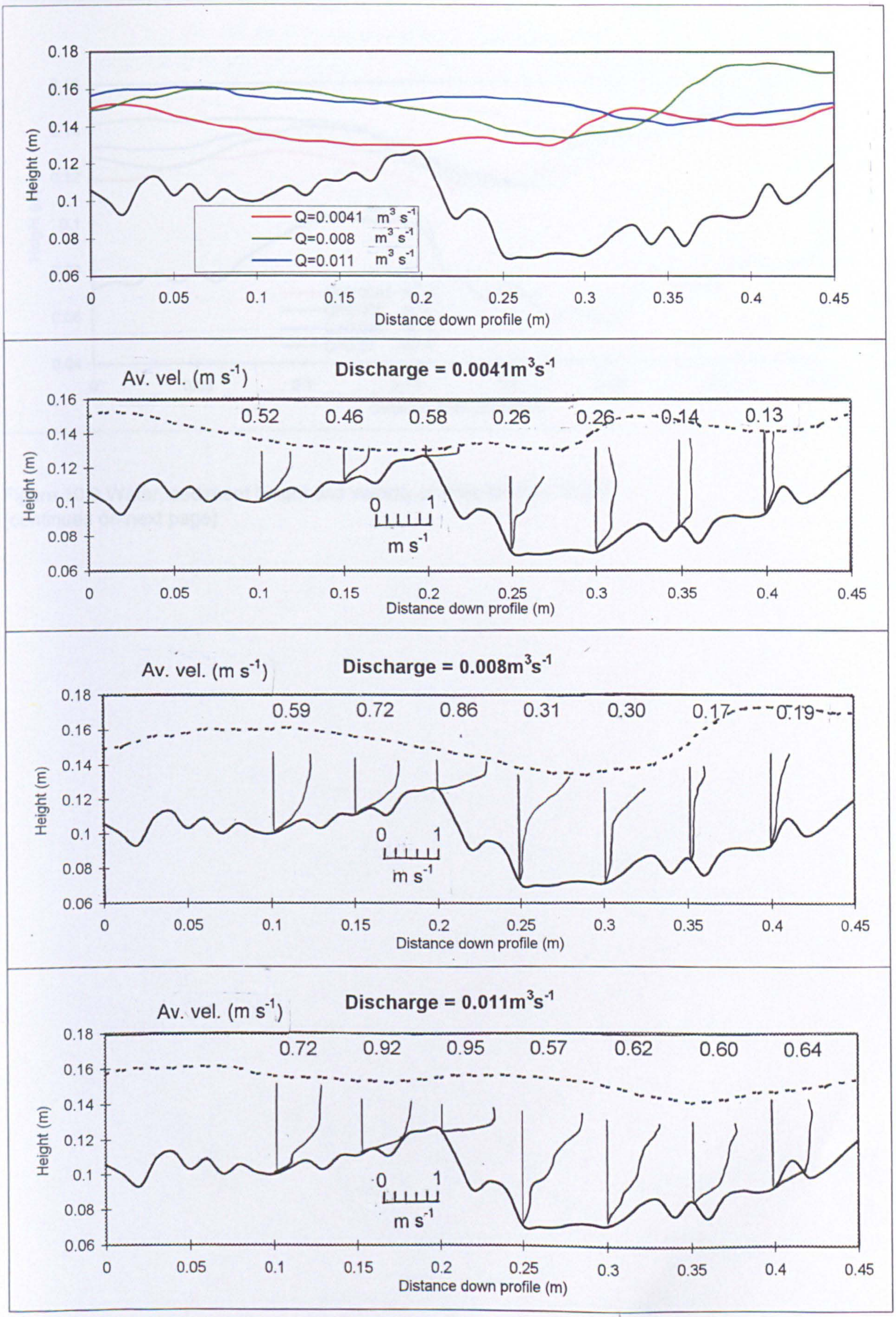

Figure 10.1 Water, sediment height and velocity profiles for Run 6/2/97

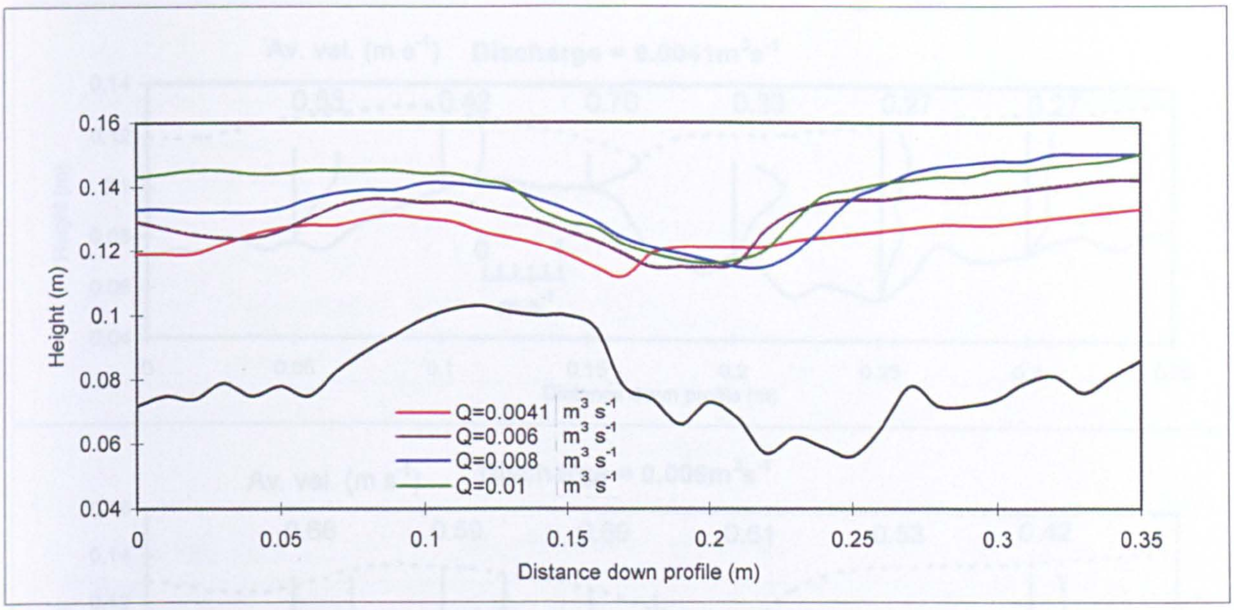

Figure 10.2 Water, sediment height and velocity profiles for Run 18/2/97
(continued on next page)

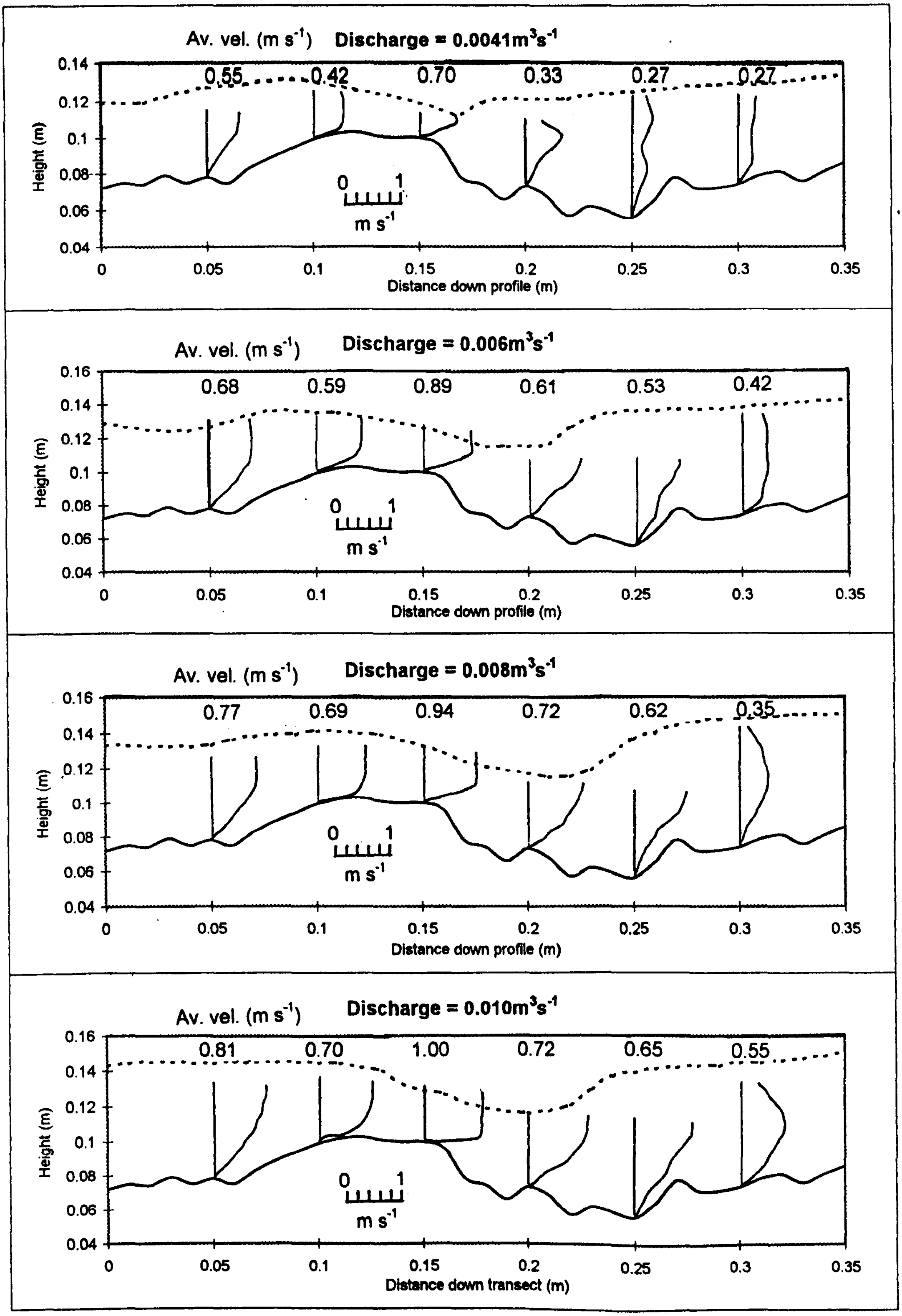

Figure 10.2. Water, sediment height and velocity profiles for Run 18/2/97

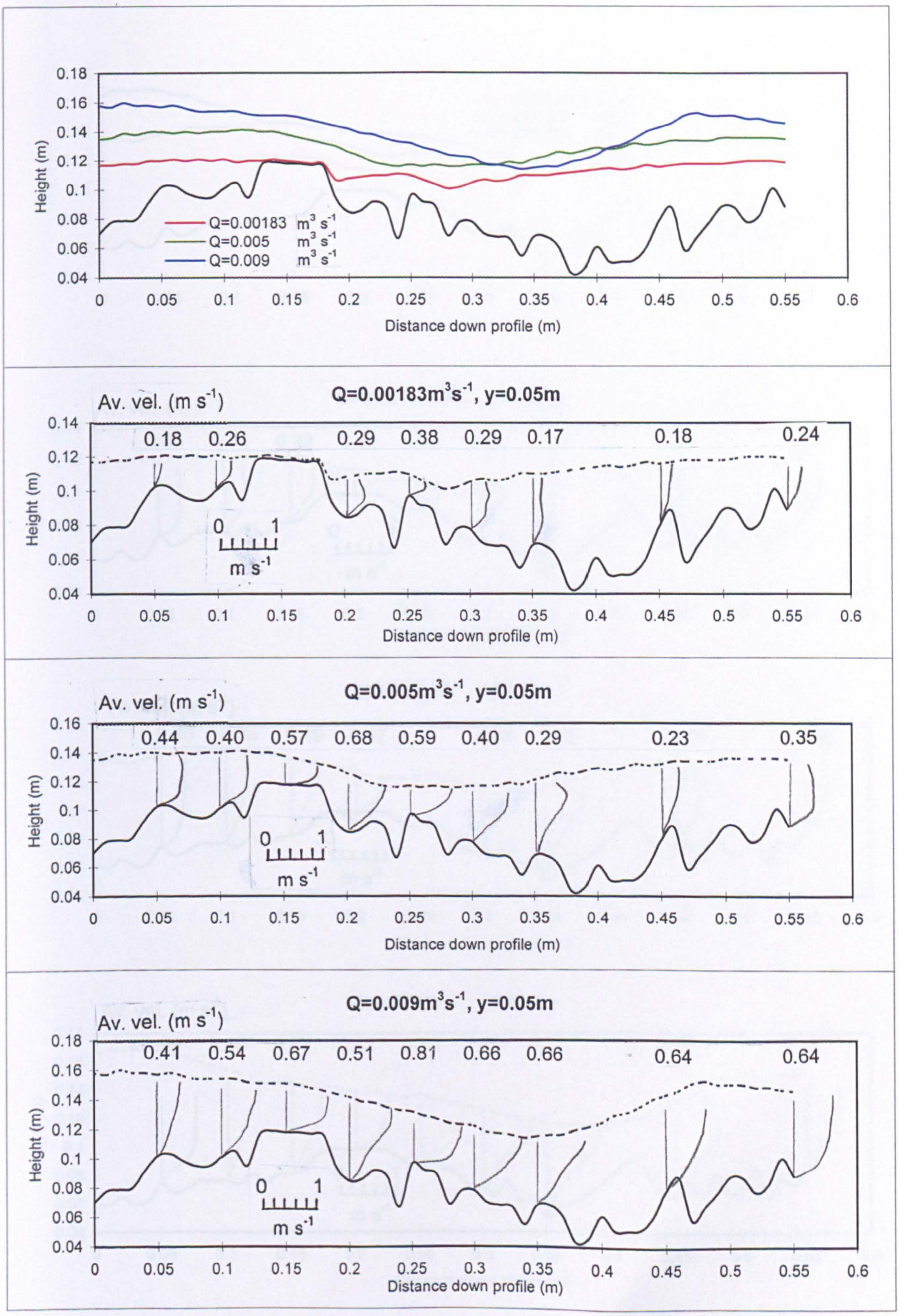

Figure 10.3a Water height, sediment height and velocity profiles for Run 6/3/97, y=0.05m

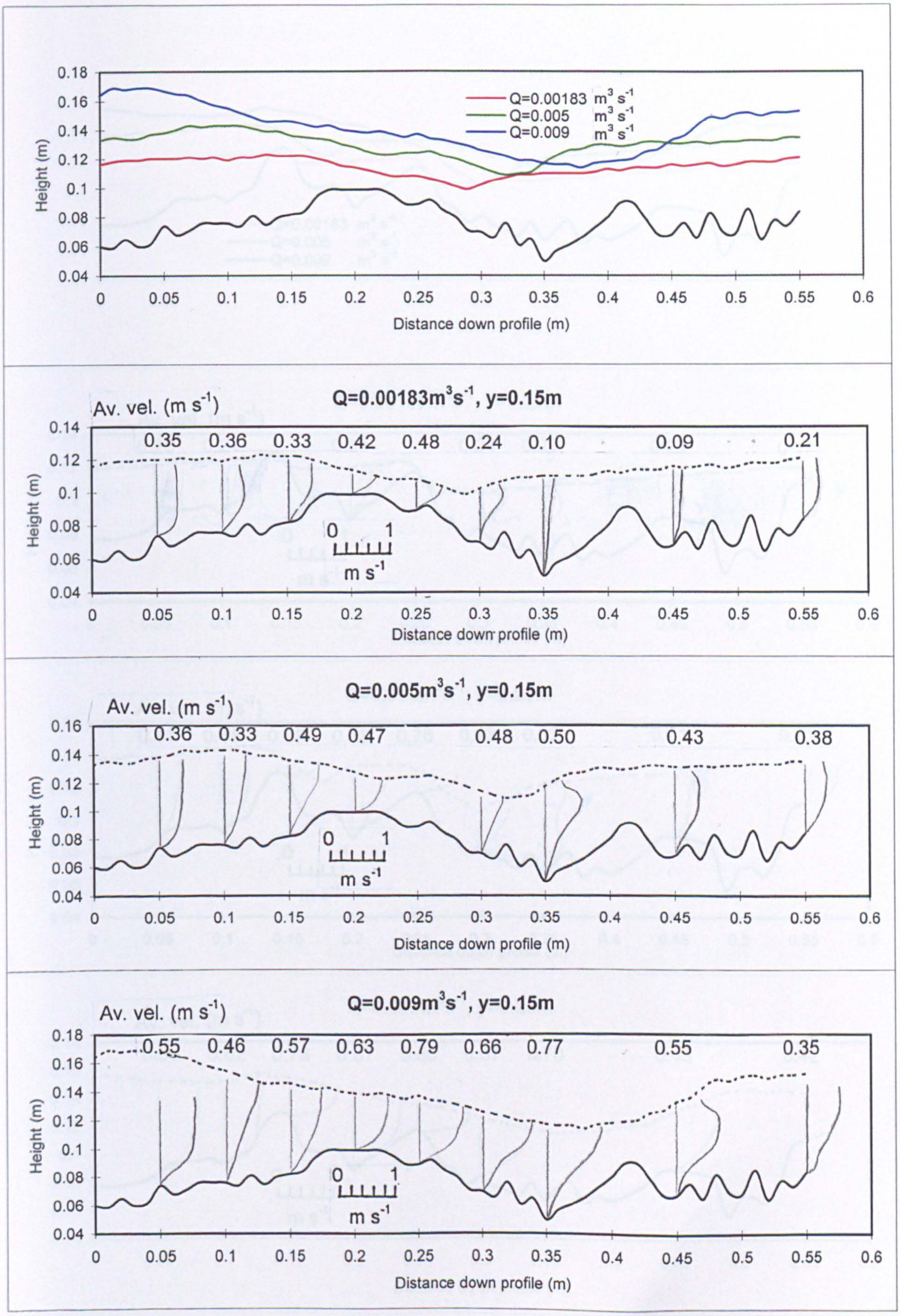

Figure 10.3b Water height, sediment height and velocity profiles for Run 6/3/97, y=0.15m

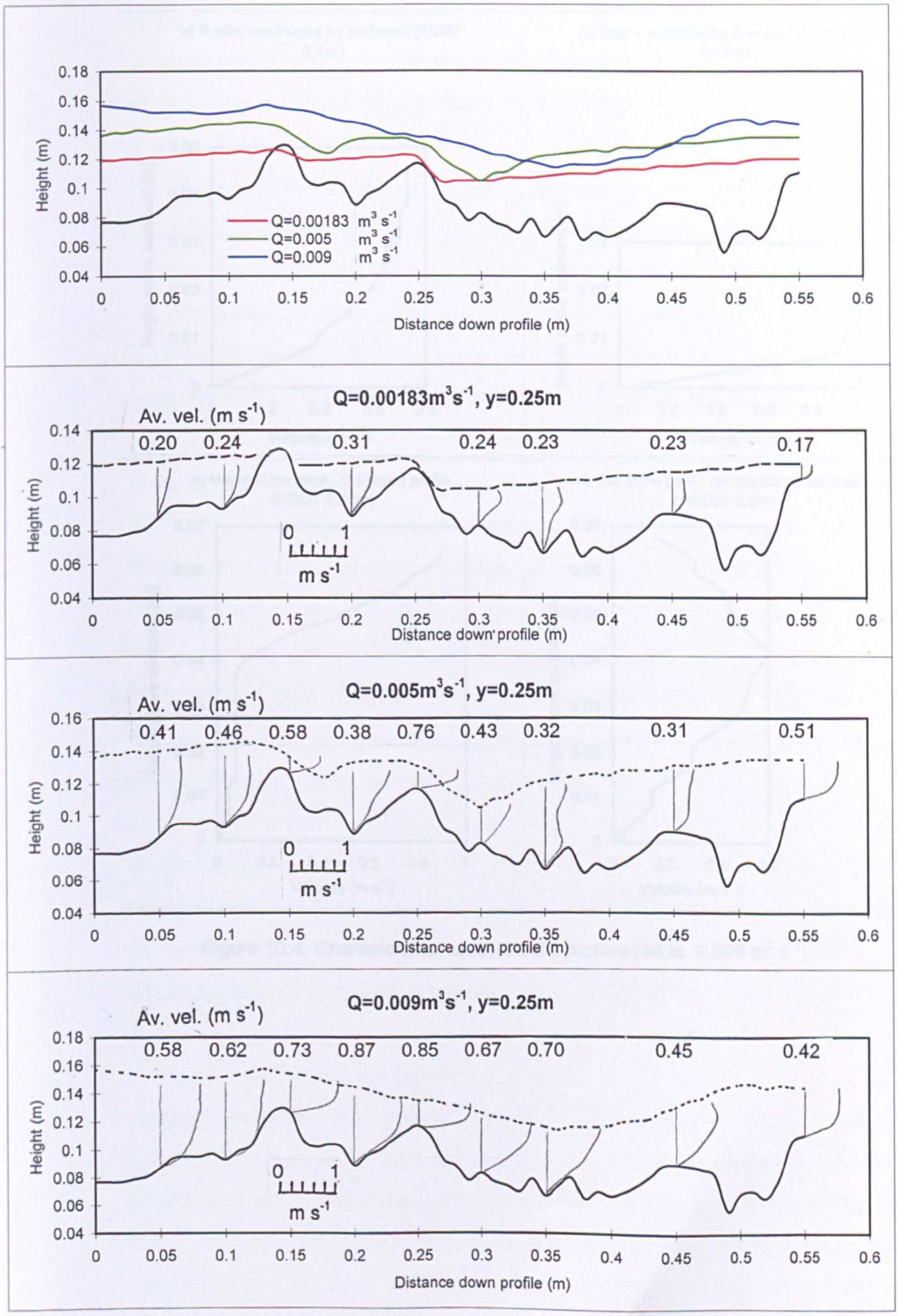

Figure 10.3c Water height, sediment height and velocity profiles for Run 6/3/97, y=0.25m

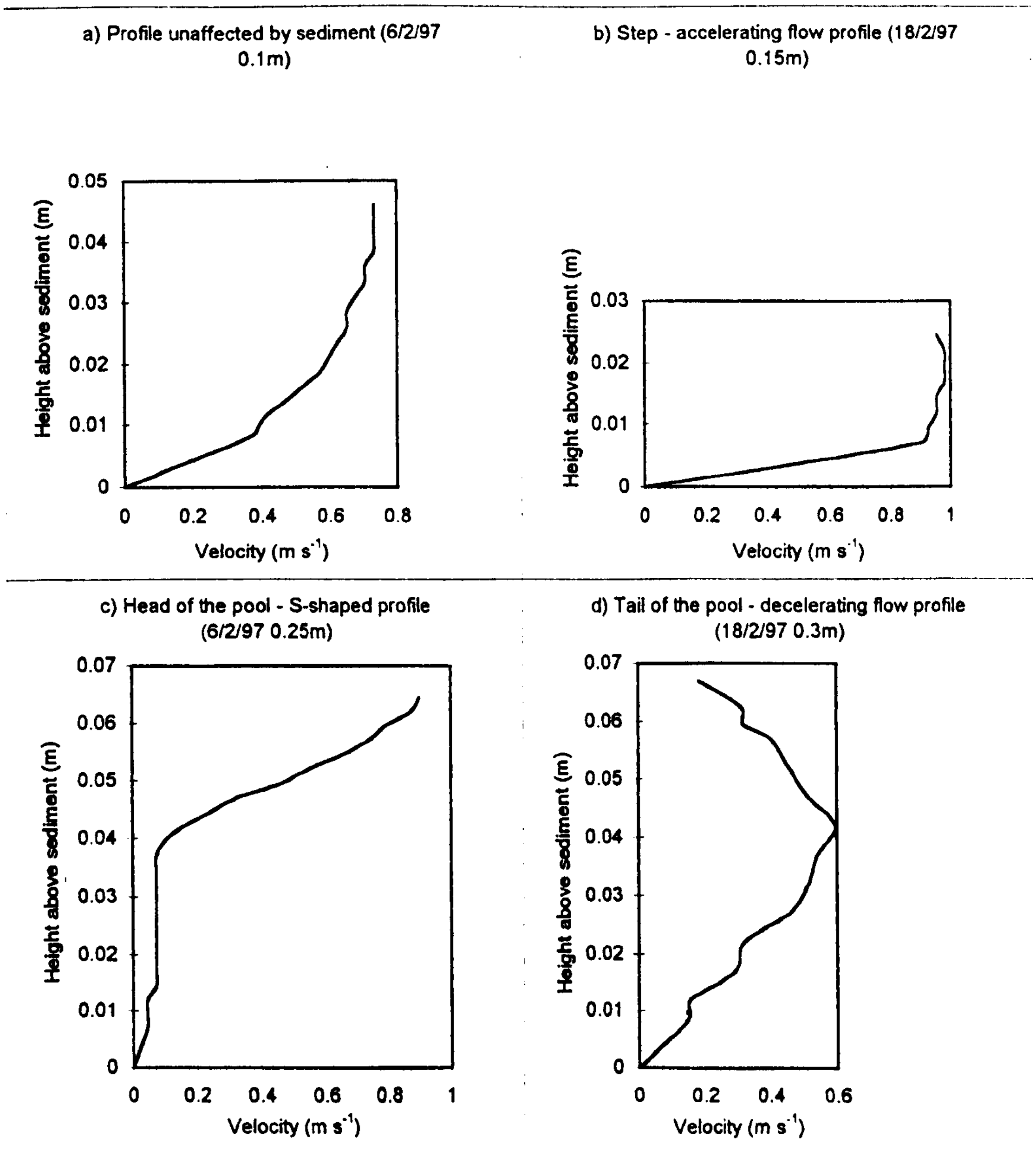

Figure 10.4. Characteristic flume velocity profiles (all at $0.008\ m^3\ s^{-1}$).

10.2.2 Water and sediment profiles

Over the step-pool sequence itself the step profile can be clearly seen in all the figures, which also show the sediment profile mirrored by the water surface. At the higher flows at which velocity profiles were taken (e.g. 0.011 m^3 s^{-1}), the water surface does not mirror the shape of the step-pool sequence to the same extent as at the lower flows. This may explain the decrease in friction factor observed at high flows following formation of steps - the slope is slightly lower than before the steps were formed, and the flow is not affected by the sediment to such an extent. The location of hydraulic jumps is a major factor, as they alter the water profile. At higher discharges very pronounced hydraulic jumps were observed which disrupted the profile considerably.

10.2.3 Average velocity

The values for average velocity for each of the velocity profiles are shown in Figures 10.1 to 10.3. The value of average velocity is determined by the location in the step-pool sequence as this controls the depth of the flow. As expected, the highest velocity values were found over the step part of the sequence, where the sediment slope is often steep, and the flow is shallow. In the area immediately downstream of the step there is a zone of very low velocity corresponding to the location of a hydraulic jump and the sudden deepening of the flow and decrease in gradient.

10.2.4 Velocity distribution

Obviously, there was much variation between the profiles obtained. However, they can be classified into four main groups based on the characteristics of the velocity profile and location in the step-pool sequence:

a) Profile unaffected by sediment

Figure 10.4a shows the characteristics of this type of profile. Basically, it is a log distribution profile as would be expected in lowland streams with no large sediment. This type of profile was typical of the part of the sequence before the step. The fact that this type of profile was present indicates that although there are large clasts present in the flow that disrupt the velocity profile, these effects are localised, meaning that although the velocity profile is affected by the overall presence of sediment in the channel, some parts of the channel have velocity profiles that remain unaffected by the detailed arrangement of the sediment.

b) Step - accelerating flow profile

The fastest flow was found over the step part of the sequence where the sediment slope is steep, and the water surface profile mirrors this. The flow is also shallow, which results in a very fast flow. This can be seen particularly well in Figure 10.4b, and also in Figure 10.3c where there are two parts to the step, and the flow is very fast over both. This profile is also characterised by the presence of accelerating flow. For most of the profile the velocity gradient is very high, however, the velocity is near constant in the top half of the profile. This is believed to be a result of the white water present as the flow goes over the step. The result of this effect is a 'dogleg' shaped profile as the rapidly increasing velocity suddenly becomes constant.

c) Head of the pool - S-shaped profile

The velocity is generally very slow in the pool as the flow is deep. Immediately downstream of the step there is a 'shadow zone' of very sluggish flow with a small velocity gradient (shown in Figure 10.4c). It can be seen from this profile that the velocity shadow zone does not extend to the top of the step - velocity starts to increase once the flow is above approximately halfway up the step. Near the surface the flow is fast and there is a relatively steep water surface slope. These two flow zones lead to a S-shaped profile as a result of the considerable increase in velocity above the level of the step. However, the S-shaped profile was not that well developed as generally the flow was not deep enough for a logarithmic shaped profile to develop in the top part of the profile.

d) Tail of the pool - decelerating flow profile

At the end of the pool there is an upward slope in the water surface, leading to a decrease in velocity near the top of the profile representing this zone of decelerating flow. Figure 10.4d and 10.2 show examples of this type of profile. The graph in Figure 10.4d shows that the upper and lower parts of the profile are near mirror images of each other, as the magnitude of velocity increase in the bottom part of the profile and the velocity decrease in the top part are very similar. This switch occurs at about 60% of the total depth. In this part of the step-pool sequence there is also usually a hydraulic jump, which also acts to slow down the flow.

10.2.5 Conclusions

The velocity profiles observed in the flume show that there are characteristic velocity profiles present at different parts of the step-pool sequence. The presence of the steps and large sediment, therefore, has a considerable effect on the velocity profiles, with the size of the sediment making up the steps and the degree of step development, expected to determine the profile characteristics to some extent. This suggests that it might be possible to model the velocity profile based on the step and sediment characteristics present in the channel. This possibility is considered in the rest of the chapter.

10.3 Drag forces from sediment and steps

This section and 10.4 follow the approach used by Wiberg and Smith (1987 and 1991) to develop a model that demonstrated potential in its ability to predict average velocity and velocity profiles based on the sediment characteristics in the channel. This section considers how the modelling of the sediment was carried out; Section 10.4 considers the flow modelling. Section 10.5 describes how the mathematical equations from Sections 10.3 and 10.4 were implemented using Visual Basic, and Section 10.6 describes the results obtained using the model and the refinements made to it.

10.3.1 Drag force

As flow is forced around the boulders, a drag force is exerted on the clast which produces resistance to the flow because of a decrease in momentum (Wiberg and Smith, 1991). This drag force, F_D, on an object (e.g. a boulder) in a flow of uniform velocity $\overline{U}$ is given in Equation 10.1 below (Bathurst, 1993; Wiberg and Smith, 1991):

$$F_D = \frac{\rho}{2} A_F \overline{U}^2 C_D \qquad \textbf{[10.1]}$$

where A_F is the frontal cross-sectional area of the object, and C_D is the drag coefficient (factors affecting it were considered in Section 2.6). This equation can be modified to produce Equation 10.2, which considers the drag force produced by each component (size fraction) m of the sediment distribution.

$$(F_D)_m = \frac{\rho}{2}(A_F)_m \rangle \overline{U}^2 \langle_m (C_D)_m \qquad [10.2]$$

Therefore, τ_D, the stress associated with the resistive drag of the sediment on the flow at a height z can be determined by considering the value of F_D for all size fractions, and the area A_{TA} (the bed-parallel, planar area affected by one object), i.e.:

$$\tau_D(z) = \sum_{m=i}^{M}\left(\frac{F_D}{A_{TA}}\right)_m \qquad [10.3]$$

where i is the smallest size sediment present at height z, and M is the largest.

In order to model the drag force from the sediment in the channel it is necessary to estimate the values for A_{TA} and A_D. Wiberg and Smith (1991) derived the following equation for $\tau_D(z)$ following consideration of the volume of the sediment, the volume of the channel affected by each particle, and the concentration of the sediment at a certain height:

$$\tau_D(z) = \frac{3}{4}\rho\sum_{m=i}^{M}\frac{(C_D)_m c_m}{D_{mx}}\int_{z_0}^{z_m}\overline{U}^2 dz \qquad [10.4]$$

where c_m is the proportion of that sediment fraction m (with x axis equal to D_{mx}) in the sediment distribution. It is assumed that the sediment is elliptical, and that $D_{mx} = D_{my} = 2D_{mz}$, i.e. the sediment axes in the downstream and cross-stream directions are equal, and are twice the size of the vertical sediment axis. If there is sediment in the channel large enough to protrude through the surface of the flow an extra drag force $(\tau_D)_S$, exists which needs to be considered, described as:

$$(\tau_D)_S = \frac{3}{4}\rho\sum_{m=i_S}^{M}\frac{(C_D)_m c_m}{D_{mx}}\int_{z_0}^{z_S}\overline{U}^2\,dz \qquad [10.5]$$

10.3.2 Sediment distribution

A reasonable approximation of the sediment in a channel can be obtained by considering the distribution as being lognormal. A sediment size can be converted to phi units by using Equation 10.6, where D is the sediment size in mm.

$$\phi_m = -\log_2 D_m \qquad [10.6]$$

Therefore, the proportion of the total sediment distribution represented by a certain grain size fraction ϕ_m can be calculated by using the normal distribution law and knowing the value of ϕ_{50} (i.e. the phi value of the D_{50} sized sediment) and the standard deviation σ of the sediment distribution in ϕ units, calculated using Equation 10.7:

$$\sigma = \frac{\phi_{84} - \phi_{16}}{2} \qquad [10.7]$$

However, the standard equation used for normal distribution assumes that the total of the proportions is 1. Since the maximum concentration of sediment on the bed, c_b, is taken to be 0.6 (Wiberg and Smith, 1991), the standard equation for normal distribution is modified and the value of c_b is used instead of unity. This modified equation is Equation 10.8:

$$c_m = \frac{c_b}{\sigma(2\pi)^{0.5}}\exp\left[-0.5\left(\frac{\phi_m - \phi_{50}}{\sigma}\right)^2\right] \qquad [10.8]$$

10.3.3 Drag coefficient

Equations to determine the value of the drag coefficient C_D have been widely reported in the literature (for example, Coleman, 1967; El Khashab, 1986, and Noori, 1984), however, most of the work has been carried out on artificial elements. As described in Chapter 2, drag coefficient is dependent on Reynolds number, Froude number, roughness and channel geometry. Equation 10.9 has been proposed by El Khashab (1986) and Noori (1984) to calculate a reasonable estimate of C_D, where R is the hydraulic radius of the channel, defined as being equal to $\frac{wd}{2d+w}$ (w is the channel width). θ is the angle in degrees between the channel bed and horizontal (i.e. channel gradient).

$$C_D = \frac{2gR}{\overline{U}^2 \cos\theta} \qquad \textbf{[10.9]}$$

It has also been found that the value of C_D does not depend on the velocity at a height in the profile (Ranga Raju and Garde, 1970; Noori, 1984), therefore, an average velocity value can be used. Bathurst (1996) suggested a constant value of 0.37 can be used. Wiberg and Smith (1991) used the classical relationship (between Reynolds number and C_D) for a sphere (Flammer et al 1970; Coleman 1967). However, the work carried out by El Khashab (1986) and Noori (1984) shows that there is no unique direct relationship between the two.

10.4 Fluid forces

10.4.1 Forces acting in the flow

Shear stress can be considered as the sum of fluid stress (stress of fluid parcels on other fluid parcels) τ_f , and a drag stress associated with the form drag produced by flow around the roughness elements τ_D and any sediment protruding through the flow $(\tau_D)_S$, i.e.:

$$\tau_T(z) = \tau_f(z) + [\tau_D(z) - (\tau_D)_s] \qquad \textbf{[10.10]}$$

The fluid stress τ_f is related to the vertical velocity gradient by considering the fluid stress as the product of a vertical, turbulent eddy coefficient and the vertical velocity gradient. This relationship is shown in Equation 10.11. By using this equation, it is assumed that the flow is steady and uniform; this will not be true over the steps where there is flow acceleration and deceleration, but for most of the flow this is probably a valid assumption. Combining Equations 10.10 and 10.11 produces Equations 10.12 and 10.13. *K(z)* is eddy viscosity, which is the product of a velocity scale and an eddy length scale. In Equation 10.11 the velocity scale used is a local shear velocity v_{*f}, with L_e the eddy mixing length (the value for which is considered further later in the chapter).

$$\tau_f(z) = \rho K(z)\frac{\partial u}{\partial z} = \rho v_{*f} L_e \frac{\partial u}{\partial z} \quad [10.11]$$

$$v_{*f} = \left\{\frac{\tau_f}{\rho}\right\}^{1/2} = \left\{\frac{\tau_T - [\tau_D - (\tau_D)_s]}{\rho}\right\}^{1/2} \quad [10.12]$$

$$\frac{\partial u}{\partial z} = \frac{1}{L_e}\left\{\frac{\tau_T - [\tau_D - (\tau_D)_s]}{\rho}\right\}^{1/2} \quad [10.13]$$

Taking advantage of $\tau_T(z) = \rho g h S\left(1 - \frac{z}{d}\right) = \rho u_{*T}^2\left(1 - \frac{z}{d}\right)$, where u_{*T} is the bed shear velocity, and $\tau_b = \rho g d S = \rho u_{*T}^2$ for channels with uniform flow, Equation 10.13 can be rewritten as Equation 10.14. Substituting in Equations 10.4 and 10.5, and using $u^* = \frac{u}{u_{*T}}$ as a measure of dimensionless shear velocity (Wiberg and Smith, 1991) results in Equation 10.15, which is the equation that needs to be solved by the model.

$$\frac{\partial u}{\partial z} = \frac{u_{*T}}{L_e}\left\{\left(1 - \frac{z}{d}\right) - \frac{[\tau_D - (\tau_D)_s]}{\tau_b}\right\}^{1/2} \quad [10.14]$$

$$\frac{\partial u^{*}(z)}{dz}=\frac{1}{L_e}\left\{\left(1-\frac{z}{d}\right)-\frac{3}{4}\left[\left(\int_{z_0}^{z}\left(u^{*}\right)^2 dz\right)\left(\sum_{m=i}^{M}\frac{c_m\left(C_D\right)_m}{D_{mx}}\right)+\sum_{m=i}^{M}\left(\frac{c_m\left(C_D\right)_m}{D_{mx}}\int_{z}^{z_m}(u^{*})^2 dz\right)\right]\right.$$

$$\left.+\frac{3}{4}\sum_{m=i_s}^{M}\left(\frac{c_m\left(C_D\right)_m}{D_{mx}}\int_{z_0}^{z_s}\left(u^{*}\right)^2 dz\right)\right\}^{1/2} \qquad [10.15]$$

10.4.2 Eddy mixing length

This is a measure of the size of the eddies present that act to redistribute the fluid momentum and, therefore, the velocity i.e. make the velocity profile more uniform. The value used for mixing length is very important - if it is large then the profile will be more uniform and the effect of the sediment is not so pronounced. Wiberg and Smith (1989 and 1991) use a weighted average of two different equations; one is designed for use in flows with low bed relief (where the mixing length is proportional to the distance from the bed), the other considers the effect of sediment in the flow. In streams with a significant amount of sediment the length of the eddies is controlled by the size of the wakes from the sediment so the eddies are proportional to the size of the sediment and the concentration. The weighted average, L_3, of these two extremes (termed L_1 and L_2 respectively) is calculated by considering the concentration of sediment at that height in the flow. Equation 10.16 is used to calculate L_1 for the bottom 20% of the flow, whilst Equation 10.17 can be used for the rest of the flow (Rattray and Mitsuda, 1974). However, it is debatable how applicable this equation is to the current situation, as it was developed for the interface in estuaries between water masses of different densities.

$$L_1=\frac{\kappa z(1-z/d)}{(1-z/d)^{1/2}} \qquad [10.16]$$

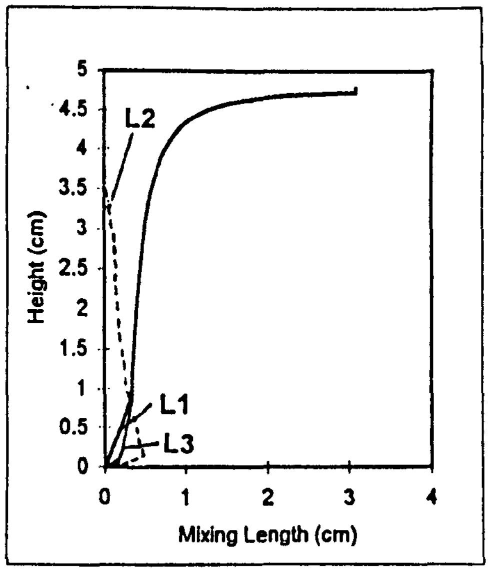

Figure 10.5. Model predicted mixing lengths (using Equations 10.16 to 10.19)

$$L_1 = \frac{0.064d}{(1 - z/d)^{1/2}} \quad [10.17]$$

$$L_2 \propto \sum_{m=i}^{M} D_{mz} c_m \quad [10.18]$$

$$L_3 = (1 - \sum_{m=i}^{M} c_m) L_1 + \kappa L_2 \quad [10.19]$$

where κ is von Karman's constant, taken as 0.41. However, as seen in Figure 2 of Wiberg and Smith's (1991) paper and Figure 10.5 (which shows the mixing lengths calculated for the Q=0.008 m^3 s^{-1} flume run), this weighted average is nearly identical to L_1. This suggests that their choice of mixing length is essentially the same as that devised for channels with low relative roughness.

10.4.3 Zero depth level

It was necessary to consider the value of z_0, i.e. the theoretical bottom of the flow. This is difficult to define in channels with very poorly sorted sediment. Nikuradse (1933) suggested that $z_0 = \frac{k_s}{30}$, where k_s is the bed roughness length. Schlitchling (1979) suggested using the level obtained from levelling the sediment, which basically means using an average sediment size for k_s; Wiberg and Smith (1991) use a constant value of medium sand (0.05cm). They also state that the model was insensitive to the value of z_0 chosen as the flow is very sluggish in the bottom part of the flow near the bed.

10.5 Computer modelling

10.5.1 Initial velocity estimate

The equations relating the velocity gradient to the forces in the flow were derived in the previous section, with the equation to be solved shown as Equation 10.15. However, this equation needed to be modified in order to model it using a programming language. One of the terms is the integral of the velocity gradient from z_0 to z_m, where *m* is the sediment component in question, which is a value between i (the smallest sediment size present at that level) and M (the largest). The velocity profile is calculated in an iterative manner, i.e. an initial approximate estimate is calculated and then refined. This is because the integral of the entire velocity profile needs to be solved, but calculated values are only known up to the height in question (z_{iq}) in the profile.

This initial estimate is determined by splitting the part of Equation 10.15 defined by Equation 10.4 (i.e. the expression for τ_D) into two terms - one that is the integral of the velocity profile up to z_{iq}, and one that is the integral of the velocity profile above z_{iq}. Equation 10.20 shows the initial estimate, i.e. up to z_{iq}. Calculating the value of drag coefficient needs a value for average velocity, which is not known initially. Therefore, for the initial estimate of the velocity gradient the value suggested by Bathurst (1996) for C_D, 0.37, was used. Using this, Equation 10.15 can be simplified by Equation 10.20 for the purpose of calculating the initial estimate.

$$\tau_D(z) = \frac{3}{4}\rho\left(\sum_{m=i}^{M}\left\{\frac{(C_D)_m c_m}{D_{mx}}\int_{z_0}^{z} u^2 dz\right\} + \sum_{m=i}^{M}\left\{\frac{(C_D)_m c_m}{D_{mx}}\int_{z}^{z_m} u^2 dz\right\}\right) \qquad \textbf{[10.20]}$$

$$\frac{\partial u^*(z)}{\partial z} = \frac{1}{L_e}\left\{\left(1-\frac{z}{d}\right) - \frac{3}{4}\left[\sum_{m=i}^{M}\frac{c_m}{D_{mx}} 0.37\int_{z_0}^{z}(u^*)^2 dz\right]\right\}^{1/2} \qquad \textbf{[10.21]}$$

A finite difference method is appropriate for modelling the velocity profile, i.e. to consider the velocity difference (determined by the velocity gradient) between two heights in the profile a small (finite) distance apart. Therefore, the profile needs to be split into small segments. It was decided for simplicity that the profile would be split into 100 flow levels. Any sediment above the water level is then added on top of this. From Equation 10.21, the actual value at each point in the profile can then be calculated using Equation 10.22.

$$u(i) = u(i-1) + \frac{\Delta z}{L_e}\left\{\left(1-\frac{z}{d}\right) - \frac{3}{4}\left[\sum_{m=i}^{M}\frac{c_m}{D_{mx}} 0.37\int_{z_0}^{z}(u^*)^2 dz\right]\right\}^{1/2} \qquad [10.22]$$

10.5.2 Refining the profile

After this initial estimate has been derived, the entire equation in Equation 10.15 can be used if the values obtained for the initial estimate are then used for the velocity above z_{iq}. The entire profile can then be refined until the value obtained for average velocity does not change significantly between successive profile calculations. Equation 10.23, which is the finite differentiation representation of Equation 10.15, was solved to determine the final solution.

$$u(i) = u(i-1) + \frac{\Delta z}{L_e}\left\{\left(1-\frac{z_{iq}}{d}\right) - \frac{3}{4}\left[\left(\sum_{i=z_0}^{z}u(i)^2\Delta z\right)\left(\sum_{m=i}^{M}\frac{0.37c_m}{D_{mx}}\right) + \sum_{m=i}^{M}\left(\frac{0.37c_m}{D_{mx}}\sum_{i=z}^{z_s}u(i)^2\Delta z\right)\right]\right\}^{1/2}$$
$$+\frac{3}{4}\sum_{m=i_s}^{M}\left(\frac{0.37c_m}{D_{mx}}\sum_{i=z_0}^{z_s}u(i)^2\Delta z\right) \qquad [10.23]$$

10.5.3 Implementation of the model

Visual Basic (version 3.0) was used to write the computer model. Values for the sediment characteristics, step characteristics, flow depth and slope are required from the user, or default values used. The profile is then calculated and the values at each height exported to a file, which can then be read into Excel and analysed.

Originally it was decided to use the sediment D_{10} value in order to obtain a value dependent on the sediment distribution in question. However, it was found that the calculated value of z_0 was so small that the bottom of the sediment was used instead. The main aim of the model was to determine an average value for velocity and friction factor, and to study the effect that the sediment had on the flow. Therefore, consideration of the bottom few millimetres of the flow was not considered important.

10.5.4 Assumptions

To model the flow, several assumptions were made associated with the various equations that were used. Firstly, the flow and sediment properties were estimated by using the equations described in Sections 10.3 and 10.4. The main sediment assumption was that sediment distribution can be described by a lognormal distribution. From the sediment surveys carried out as part of the fieldwork, this was found to be a reasonable approximation as the maximum sediment sizes predicted using Equation 10.8 were close to the actual values measured for the fieldsites. The main flow assumption is associated with the use of Equation 10.4 that assumes uniform steady flow. It is unlikely that uniform steady flow is always the case in steep streams, but use of the equation provides an approximation of the flow conditions.

10.6 Results

10.6.1 Initial Testing using average velocity values

Initially the model was tested using the same methods used by Wiberg and Smith (1991) to calculate C_D (i.e. using relationship with Reynolds number) and mixing length. The data in Wiberg and Smith (1991) Table 1, which are field data collected by Marchant et al (1984) and the predicted average velocity from their (Wiberg and Smith, 1991) model were compared with the average velocity values predicted using this model. The predicted values from their model and this model were within 2% of each other (shown in Figure 10.6), reflecting the slight differences between the two in terms of the grid set-up, position of z_0, etc. The model was then altered to calculate C_D using Equation 10.9 (which uses profile averaged velocity). These results are shown in Table 10.1, which shows the field data and predicted average velocity values from this model, and also in Figure 10.7 (where the measured velocity value used is the midpoint of the range given in Table 10.2).

When compared to the measured velocity range, it is clear that there are limitations to the model's ability to predict average velocity, whichever method is used to calculate C_D. In general, it would appear that the effect of the sediment is underestimated - when the relative sediment size in relation to the flow depth is small (i.e. the sediment is completely submerged) the predicted velocity is too slow, and when the relative sediment size is high the velocity is overestimated.

Table 10.1. Measured and predicted average velocity values for the Marchant et al (1984) data.

Slope	D_{50} (cm)	D_{84} (cm)	Depth (cm)	D_{84} / depth	Measured U range (cm s^{-1})	Predicted U using Re/C_D relationship (cm s^{-1})	Predicted U using Equation 10.9 (cm s^{-1})
0.022	6	18.36	79	0.23	137-236	277	274
			58	0.32	72-171	218	202
			61	0.30	94-135	227	213
0.005	10.4	23.8	101	0.24	162-252	154	109
			129	0.18	187-284	184	145
			66	0.36	114-176	109	59
0.006	9.1	20.12	131	0.15	286-314	221	185
			112	0.18	193-250	200	158
			72	0.28	123-150	138	94
0.002	10.4	18.3	86	0.22	93-167	99	57
			110	0.17	199-245	118	75
			64	0.29	76-121	77	41
0.029	23.9	32.25	88	0.37	140-285	287	269
			97	0.33	175-378	311	296
			56	0.58	86-217	189	149
0.008	6	16.7	58	0.29	131-138	146	99
			53	0.32	101-109	135	86
0.022	15.8	26.85	62	0.43	95-104	203	179
			85	0.32	188-233	263	251
0.013	11.1	20.9	63	0.3	161-213	195	148
			88	0.24	201-245	254	210
			45	0.46	68-124	145	91
0.009	11.9	21.84	76	0.29	115-229	165	133
			96	0.23	201-258	202	173
			58	0.38	41-79	131	93

Using Equation 10.7 to calculate C_D (which uses a profile averaged velocity) resulted in the estimated average velocity values being 93.5% of the measured velocity values (a mid-point of the measured velocity range in Table 10.1 was used). The approach followed by Wiberg and Smith (1991) using the Re/C_D relationship resulted in an average predicted value that was 117.5% of the measured values. Therefore, it is considered that reasonable values for predicting average velocity were obtained using the model. It is unclear, however, exactly what the characteristics of these streams were in terms of steps and pools - it was assumed that there were not significant step pool sequences, only large sediment. The following section compares the model predicted values with the measured reach average velocity values obtained during the fieldwork part of this research, in which reaches did contain step-pool sequences.

10.6.2 Comparison with fieldwork results

The reach average velocity values obtained from the salt dilution gauging carried out as part of this research were also compared with predicted values from the model. These measured and predicted values are shown in Table 10.2 and Figure 10.8. C_D was calculated using the same method as used by Wiberg and Smith (1991) and the third mixing length equation was used (i.e. the same as for Section 10.6.1). Sediment values (i.e. D_{50} and D_{84}) were calculated as described in Section 4.2 (Figure 4.1 shows the grain size distribution curves). As seen in Table 10.2 and Figure 10.8, the model considerably overestimates velocity for all the fieldsites, and underestimates velocity for the flume.

Table 10.2. Measured and predicted average velocity values for the field and flume data.

Site	Slope	D_{50} (cm)	D_{84} (cm)	Depth (cm)	D_{84}/Depth	Measured U (cm s^{-1})	Predicted U (cm s^{-1})	Predicted / measured
Ashop	0.0266	12.7	26.35	11.5	2.3	8.3	15	1.8
				19.8	1.3	5.7	20	3.5
				13.9	1.9	8.6	16	1.9
Burbage	0.0971	15.8	35.2	7.8	4.5	4.6	63	13.7
				11.2	3.1	14.0	64	4.6
				21.7	1.6	31.7	106	3.3
Doctor's Gate	0.0582	11.7	22.4	7.5	3.0	2.8	29	10.4
				4.3	5.2	5.5	39	7.1
				9.1	2.5	28.6	29	1.0
				12.0	1.9	23.0	32	1.4
Fairbrook	0.0662	13.2	30.3	14.2	2.1	10.6	48	4.5
				9.6	3.2	19.3	41	2.1
				17.0	1.8	12.9	56	4.3
Grindsbrook A	0.1254	21.2	49.4	8.5	5.8	8.0	96	12.0
				12.7	3.9	9.0	95	10.6
				20.3	2.4	34.3	117	3.4
				31.4	1.6	33.0	184	5.6
Grindsbrook B	0.1838	20.95	47.5	26.1	1.8	3.1	204	65.8
				41.8	1.1	2.2	319	145.0
				50.3	0.9	5.4	383	70.9
Flume	0.066	0.8	3.15	3.3	0.95	35.7	6	0.17
	0.055	0.8	3.15	4.9	0.64	54.5	25	0.46
	0.055	0.8	3.15	6.0	0.53	67.4	39	0.58

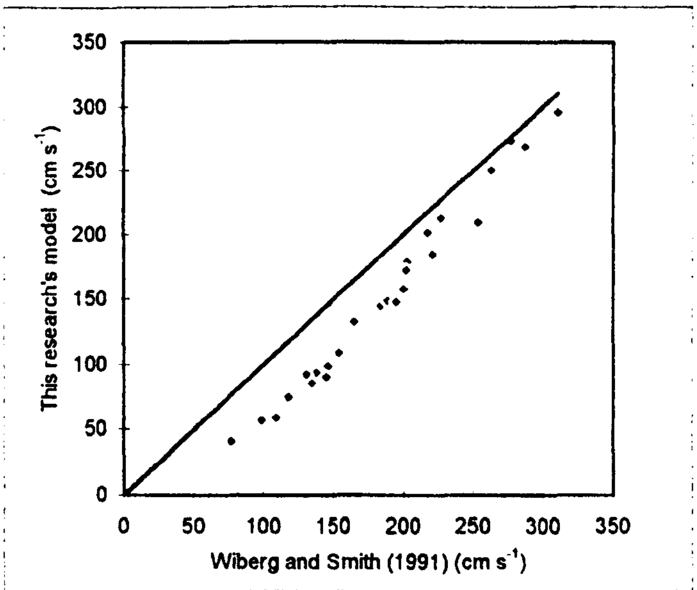

Figure 10.6. Model predicted velocity compared with Wiberg and Smith (1991).

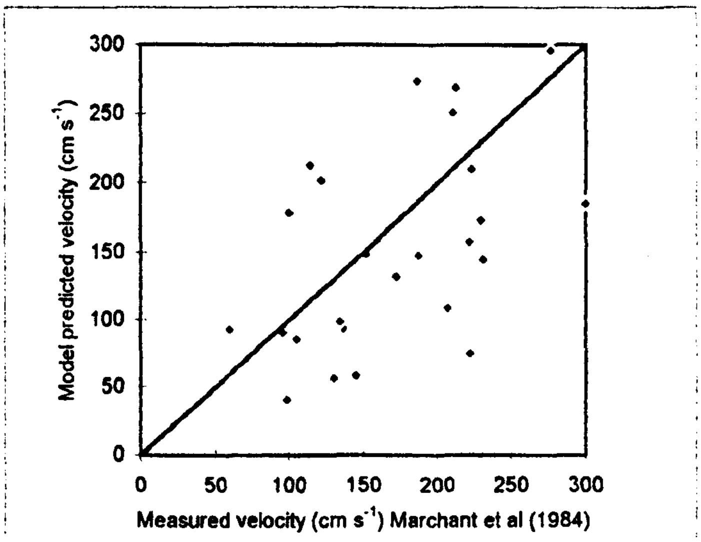

Figure 10.7. Model predicted velocity compared with fielddata in Marchant et al (1984).

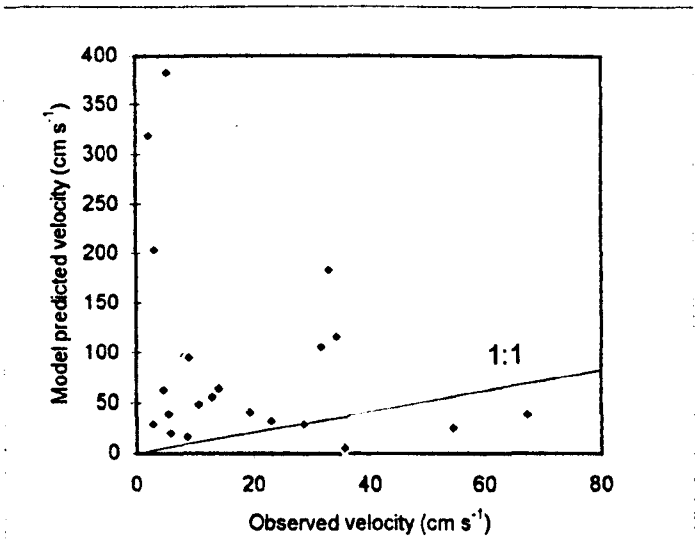

Figure 10.8. Model predicted velocity compared with fieldwork results.

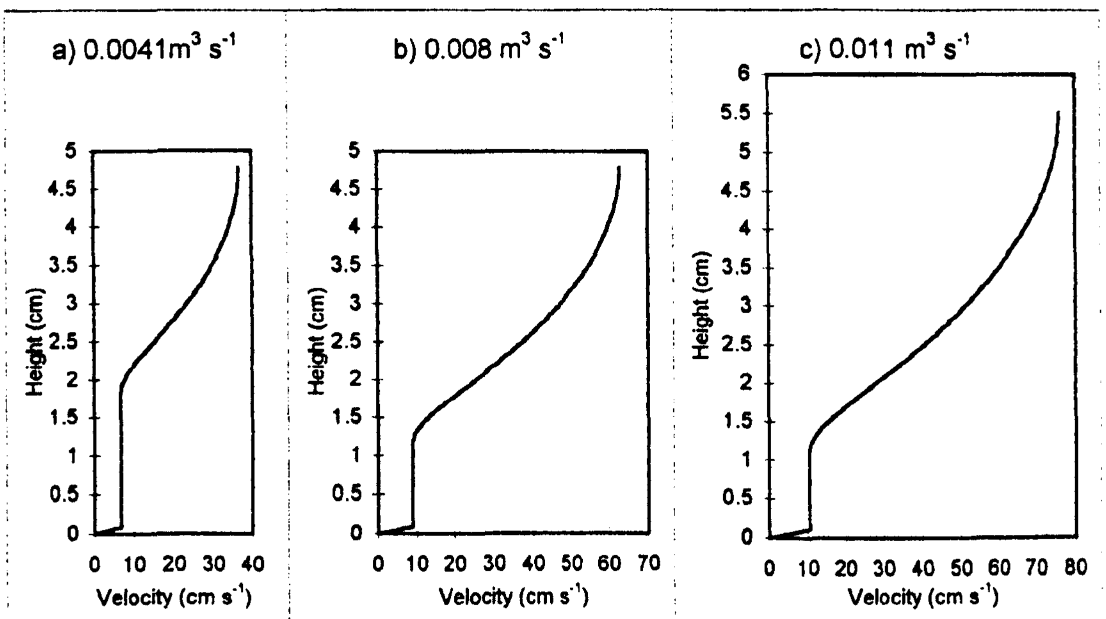

Figure 10.9 Predicted velocity profiles: slope = 0.058824, D_{50} = 0.8 cm, D_{84} = 3.15 cm, Step D_{max} = 6.4 cm, step spacing = 0.75 m, flow depth = a) 4.783 cm, b) 4.783 cm, c) 5.5508 cm

The predicted and measured average velocity values are further apart in Table 10.2 than in Table 10.1, which suggests that either the measured velocity values from the fieldwork were inaccurate (which is unlikely considering salt dilution gauging is a well established method that has been used in streams with step-pool sequences and a number of readings were taken at each site) or it indicates that step-pool sequences have an effect on the flow as a result of their form, rather than just a result of the particle sizes, and that this effect is not captured in the model. This is, perhaps, not surprising as the model only considers sediment size and not bedforms. As discussed in Section 8.3.4, energy dissipation over a step (from the hydraulic jump) is likely to lead to an energy loss of up to about 30%.

This fact goes some way to explaining why the predicted velocity is so much greater than the actual velocity, but cannot explain the difference entirely (especially considering that the velocity component of Equation 8.9 is squared, meaning that a 30% decrease in energy would translate into, at most, a velocity decrease equal to the square root of this percentage). However, only energy dissipation in the flume was considered, and no satisfactory relationship between e.g. Froude number and energy number was found. Also, the combined effect of a sequence of steps and pools would lead to further energy losses. This means that the effect of energy dissipation may have been underestimated, especially for very well developed steps such as those at the Burbage, Grindsbrook A and Grindsbrook B sites. Also, there will be some energy losses from the channel boundary.

Another explanation could be that the clustering together of large clasts into steps causes more flow resistance than the model predicts with its assumption that each clast protrudes from the same base level. Also, the predicted values are, on average, 2.4 times greater than the measured values for the Ashop fieldsite, which has the least developed step-pool sequences; they are 93.9 times greater for the Grindsbrook B site which has the most developed step-pool sequences. The predicted values for the flume, where the relative roughness was considerably lower than for the fieldsites, and the steps were less developed, were less than the measured values. This supports the conclusion reached in Section 10.6.1, i.e. that velocity is underestimated in reaches where the relative roughness is small. It was, therefore, considered appropriate to attempt to model the effect of the steps, with the average step spacing in a reach in terms of channel width, and the step sediment size compared with the pool sediment size representing the degree of step development in the reach. This might provide more information concerning how significant the effect of steps and pools is. This is considered further in the next section.

10.6.3 Refinements to the model

Three main refinements were considered:

- Consideration of different mixing length equations
- Calculation of C_D
- Modelling of the step-pool sequences

Study of the first two refinements, i.e. equations for mixing length and C_D highlighted the fact that the model is very sensitive to these two values. Therefore, it is very important to be able to calculate these values accurately. When the mixing length equation for flow with considerable sediment (L_2 in Section 10.4.2) was used, the predicted average velocity values were closer to the measured velocity values, but still up to ten times greater. Calculating C_D using Equation 10.11, and also the relationship between C_D and Froude number (El Khashab, 1986) produced a slight improvement in the predicted values compared to the measured values, but not a significant one. It is considered likely that C_D and mixing length cannot be calculated accurately for streams with step-pool sequences, meaning that the model cannot usefully be used in such streams.

The third refinement considered was the inclusion of step characteristics in the model. It has been shown from the fieldwork that the step sediment has a considerable control over the flow conditions. There is a concentration of large sediment in the steps, meaning that the sediment distribution would not be expected to have a lognormal distribution in the steps, which was also found from the fieldwork. Therefore, it was decided to consider the step sediment separately, i.e. to approximate the step dimensions. This also solves the problem of attempting to carry out a sediment survey involving sediment from the steps and the pools. As found during the fieldwork, this is logistically very difficult.

The step sediment distributions found from the fieldwork were studied in order to define a relationship between D_{50}, D_{84}, D_{max} and the overall sediment distribution, without making the necessary sediment survey too complicated. The fact that the steps behave like a solid wedge of sediment rather than isolated elements on the channel bed also needed to be taken into consideration. It was found that the proportion of the step containing sediment at a certain height, and, therefore, the area affected by sediment, can be approximated by considering the value of D_{max} and assuming a linear relationship between height and this proportion. This assumes that 100% of the step width contains sediment at the base of the step, whilst at the top of the step this percentage is D_{max} (b-axis) divided by the step width with a linear relationship in between these extremes. This was considered a reasonable approximation considering that it was important to make the sediment survey as easy as possible to implement, and better than no consideration of step sediment.

One of the assumptions made for calculating the sediment distribution was that the sediment is aligned with its x-axis perpendicular to the flow (b-axis) and the z-axis is half that of the x-axis. This assumption does not extend to step sediment, where the sediment is jammed together and the particle cannot achieve this theoretical alignment. Based on observations from the field, it was approximated that the x-axis is equal to the z-axis, which is not necessarily equivalent to the b-axis. Therefore, when obtaining the step D_{max} values it is important to measure the x-axis and not the b-axis. D_{max} values from a number of the steps in the study channel should be taken and averaged, along with the step width. The relative proportions of the channel with steps and pools can be estimated from field observations, and the model weighted to account for this.
For this research a modification to the above equations was made to account for the wake effects from the step sediment. Values for L_2 and L_3 were also calculated for the

step sediment, i.e. the concentration of sediment in the steps and the size of the sediment were considered. Equation 10.24 was then used to produce a weighted average based on the proportion of steps in the channel to determine a value for the mixing length based on all the sediment and steps in the channel.

$$L_{3AV} = (1-\psi)L_{3SED} + \psi L_{3STEP} \qquad [10.24]$$

Where ψ is the proportion of the channel reach in question containing steps.

The effects of this refinement were tested by using the data from the 6/2/97 run (step spacing 0.75m, slope 0.0588) where a number of velocity profiles were taken (shown in Figure 10.1). Accounting for the steps slightly increased the predicted average velocity, as seen in Table 10.3 which shows the results of the testing. At the bottom of the profile the predicted velocity was slightly lower than without the step refinement, whilst in the upper part of the profile the predicted velocity was greater.

Table 10.3. Results of testing the model with and without accounting for steps

Discharge ($m^3 s^{-1}$)	Flow depth (m)	Average velocity ($m s^{-1}$)	Predicted velocity (no steps) ($m s^{-1}$)	Predicted velocity (steps) ($m s^{-1}$)
0.0041	0.036	0.37	0.13	0.17
0.008	0.048	0.55	0.28	0.33
0.011	0.055	0.65	0.38	0.42

Whilst using this refinement did bring the predicted average velocity closer to the actual values, they were not close enough for the model to be a useful tool in predicting average velocity and, therefore, friction factor. It was necessary to decrease the step spacing to 0.20m for the predicted velocity to equal the actual velocity. The predicted velocity profiles are described in the next section.

10.6.4 Modelling the flume velocity profiles

The flume velocity profiles from the runs in Table 10.3 were compared with the model predicted velocity profiles. There are problems with doing this, however, as the model profiles were an overall average profile for the entire reach, whereas the flume profiles were for a particular location over the step-pool sequence. However, it was hoped that similar features to those described in Section 10.2 would also be identifiable in the modelled profiles. Figure 10.9 shows the model predicted profiles. It can be seen that velocity remains near constant in the lower part of the profile - this is a result of the very large drag coefficient because of the sediment present. In the upper parts of the profile a logarithmic shaped profile is able to develop.

The flume profile closest to the predicted profile in terms of average velocity and shape is the one immediately after the steps (at 0.25m down the profile in Figure 10.1). However, the predicted velocity starts to increase at a lower depth in the profile than the actual velocity profiles did. This suggests that the mixing length predicted by the model is not a realistic one. The use of the model is, therefore, very limited. However, the fact that the sediment conditions in the flume (and steep streams in general) are complicated by the presence of step-pool sequences would make it very hard to predict one overall 'average' velocity profile. It is possible that further refinements could improve the accuracy of the model, however, this was beyond the scope of this research. It is proposed that any accurate model would need to calculate drag coefficient and mixing length more accurately, meaning that a better understanding of how to calculate these measures, and what other flow characteristics affect them would be necessary.

10.6.5 Conclusions

As discussed, the predicted and measured velocities were considerably different. For the field sites the model over-predicts velocity (by up to 145 times for the Grindsbrook B site) and under-predicts velocity (by about half) for the flume. Reasons for this are likely to be a combination of energy losses over the hydraulic jump, inability to accurately calculate the mixing length, and not being able to model accurately the effect of the step as a bedform as a result of its form (as opposed to just the effect of having large sediment in the flow). Further research could be directed towards investigating the energy losses in more detail, especially in the field, as it is deemed likely by this writer that, especially for streams with well developed steps and pools, the combined result of a number of step-pool sequences is to reduce the available energy by significantly more than 30%.

Also, a limitation of the model is that the equations on which it is based are generally defined for uniform flow, i.e. where there is no acceleration / deceleration and the value for mean velocity is constant. The channels considered in this research contain abrupt changes in both geometry (as a result of the presence of steps and large clasts) and flow regime (as there is an alternation between super-critical and sub-critical flow over the steps, marked by hydraulic jumps), meaning that the flow is non-uniform. However, at present there are no appropriate equations for non-uniform flow that could be used instead.

Assuming that the velocity profile could be accurately estimated, the model has two main applications; study of the velocity profile (and the effect of the step-pool sequence on it) and determination of average velocity and friction factor. Empirically determining the mixing length necessary to predict the values measured could help estimate how pollutants etc. would be dispersed in steep streams with step-pool sequences. There are practical considerations, however, associated with using the model, as to use the model it is necessary to know the following:

- average flow depth,
- maximum step sediment size,
- step spacing,
- pool sediment D_{50} and standard deviation.

As established during the fieldwork, obtaining these values can be complicated and inaccurate (especially flow depth). Also, it is considered improbable that accurate estimates of C_D and mixing length can be obtained for streams with step-pool sequences. Therefore, it is likely that the model can only be used for streams with large sediment if they lack well-developed step-pool sequences.

Chapter 11

Conclusions

This chapter will summarise the results found from the research and relate them to the research aims described in Chapter 2.

11.1 Overall conclusions

11.1.1 Conditions necessary for step-pool formation

- In the flume, the discharge range that produced steps and pools was 0.01 m^3 s^{-1} to 0.013 m^3 s^{-1}, and the slope range was 0.0625 to 0.0667. The flow was near critical, with a range of $0.82<Fr<0.93$ (0.88 average). The maximum sediment size was 64mm, with a D_{50} of 16mm.

- It is not the absolute flow values that determine whether steps and pools form, but a combination of the sediment sorting and near critical Froude values.

- The characteristics of the flume steps were similar to those found in the field in terms of sediment characteristics in relation to channel geometry, indicating that the features formed in the flume were the same as those observed in the field.

11.1.2 Hydraulic conditions leading to step formation

- Step and pool formation is an iterative process, requiring more than one flow event, as just one run of the flume produced more incomplete steps than were observed in the field. There was no evidence that the formation of one step triggered the formation of a sequence of steps and pools; each step appeared to be formed individually.

- The formation of steps and pools is not related to antidune processes. The frequency of the initial standing waves did not match the final step spacing, but the steps, once formed, controlled the frequency and amplitude of the standing waves.

- The strongest relationship between step spacing and channel geometry was that between step spacing and channel width. It was postulated that this was because a narrower channel needs fewer particles to form a step, so as channel width decreases, step spacing decreases.

11.1.3 The effect of steps and large elements on flow resistance

- The hydraulic geometry of the steep streams studied was significantly different to that of lowland streams. There was considerable difference between the fieldsites, reflecting the different sediment characteristics of the sites, and possibly differences in the amount of energy dissipation over the steps. The exponents of the hydraulic geometry equations were found to be controlled by the amount of sediment protrusion at each of the sites, and the intercepts of the equations were controlled to some extent by the difference in sediment size between the steps and pools (Step D_{84} / Pool D_{84}) at each site.

- In the flume, the hydraulic geometry relationships were affected by the presence of steps. For the discharge and friction factor relationship, there was an increase in resistance to flow after step formation up to flows of about 0.009 $m^3 s^{-1}$ (flows slightly lower than step forming flows). At flows above this, the resistance to flow was found be reduced as a result of the steps.

- The Thompson-Campbell equation (using D_{84}) predicted friction factor most accurately. Overall, the best relationship between predicted and actual values was the empirical relationship using D_{84} as a relative roughness measure. The percentage of the step width containing protruding sediment was also found to be an important control on friction factor. The fieldsites studied had a wide range of channel characteristics, suggesting that this empirical equation would have success if used on any steep stream.

11.1.4 Velocity profiles in steep streams with large roughness elements

- Flume experiments identified characteristic profiles at different locations in the step-pool sequence, illustrating the importance of these features on the flow. The 'S-shaped' profile considered characteristic of steep streams was found to be most developed immediately downstream of the step. Near the bed there was a velocity shadow where the flow was very slow, but the velocity gradient started to increase approximately half way up the height of the step, leading to a 'S-shaped' profile.

- The Wiberg and Smith (1991) model was found to be a poor predictor of velocity for the fieldwork sites, indicating that it is limited to streams with a higher relative submergence than these sites. The model was modified to attempt to account for streams with steps and pools. However, this did not improve the results enough for it to be considered a useful tool for such flows. This may be a result of the energy losses as a result of the hydraulic jumps, estimated to be up to 30% over a single step and the inability to accurately predict the mixing length.

11.2 Future work

- The problem of how bedrock steps are related to alluvial steps and whether they are formed by same process is considered worthy of future study.

- In this research only reach average flow and resistance was studied. Salt dilution gauging using a greater number of conductivity probes could show the variation in flow conditions between steps and pools, and identify any relationships between resistance and step characteristics.

- Field data testing of the relationship between the percentage of step width containing protruding sediment and velocity is recommended for future study.

- Fieldwork methodology to improve the accuracy depth measurements in steep streams is recommended to be studied prior to future research in this field. Detailed EDM surveying is one approach, which would enable distinct depth values for the steps and pools.

- Study of mixing length and drag coefficient in steep streams could identify relationships that can be used to improve the accuracy of computer modelling to predict velocity.

- It was not possible to estimate energy losses in the field as the required, detailed depth measurements were not carried out. Investigation into this may well help explain the failure of the Wiberg-Smith model in streams with steps and pools, as well as explaining why the field data plotted on distinct lines for the various relationships considered, despite using scale independent measures such as stream power.

References

Abrahams, A.D., Li, G, and Atkinson, J.F. (1995). Step-pool streams: adjustments to maximum flow resistance. *Wat. Resour. Res.*, 31: 2593-2602.

Allen, J.R.L.(1984). Sedimentary Structures: their character and physical basis. Elsevier, Amsterdam.

Andrews, E.D. (1983). Entrainment of gravel from naturally sorted riverbed material. *Geol. Soc. Am. Bull.*, 94: 1225-1231.

Andrews, E.D. and Parker, G. (1987). Formation of a coarse surface layer as the response to gravel mobility. In: Thorne, C.R. et al (Ed.), Sediment Transport in Gravel-Bed Rivers, Wiley, Chichester: 269-300.

Ashida, K., Egashira, S. and Ando, N. (1984). Generation and geometric features of step-pool bed forms (in Japanese). *Bull. Disaster Prev. Res. Inst. Kyoto Univ.*, 27: 341-353.

Bathurst, J.C. (1978). Flow resistance of large scale roughness. *J. Am. Soc. Civ. Eng. Hydraul. Div.*, 104: 1587-1603.

Bathurst, J.C. (1982a). Flow resistance in boulder-bed streams. In: Hey, R.D., Bathurst, J.C. and Thorne, C.R. (Ed.). Gravel-bed rivers, Wiley, Chichester: 443-462.

Bathurst, J.C. (1982b). Theoretical aspects of flow resistance. In: Hey, R.D., Bathurst, J.C. and Thorne, C.R. (Ed.). Gravel-bed rivers. Wiley, Chichester: 83-105.

Bathurst, J.C. (1985). Flow resistance estimation in mountain rivers. *J. Am. Soc. Civ. Eng. Hydraul. Div.*, 111: 625-643.

Bathurst, J.C. (1987a). Critical conditions for bed material movement in steep, boulder-bed streams. In: Beschta, R.L. et al (Ed.), Erosion and sedimentation in the Pacific Rim. *IAHS Publ.*, 165: 309-318.

Bathurst, J.C. (1987b). Measuring and modelling bedload transport in channels with coarse bed materials. in Richards, K.S. (Ed.), River Channels: Environment and Process. Blackwell, Oxford: 272-294.

Bathurst, J.C. (1993). Flow resistance through the channel network. In: Beven, K. and Kirkby, M.J. (Ed.), Channel Network Hydrology. Wiley, Chichester: 69-98.

Bathurst, J.C. (1996). Field measurement of boulder flow drag. *J. Am. Soc. Civ. Eng. Hydraul. Div.*, 122: 167-169.

Bathurst, J.C., Li, R.M. and Simons, D.B. (1981). Resistance equation for large scale roughness. *J. Am. Soc. Civ. Eng. Hydraul. Div.*, 107: 1593-1613.

Bayazit, M. (1976). Free surface flow in a channel of large relative roughness. *J. of Hydraul. Res.*, 14: 115-125.

Bayazit, M. (1983). Flow structure and sediment transport mechanics in steep channels. In: Sumer, B.M. and Muller, A (Ed.), Mechanics of sediment transport, proceedings of EURO-MECH 156 Colloquium. A.A. Balkema, Rotterdam, Netherlands, 197-206.

Beltaos, S. (1982). Dispersion in tumbling flow. . *J. Am. Soc. Civ. Eng. Hydraul. Div.*, 108: 591-612.

Beven, K., Gilman, K. and Newson, M. (1979). Flow and flow routing in upland channel networks. *Hyd. Sci.*, 24: 303-325.

Billi, P., D'Agostino, V., Lenzi, M.A., Marchi, L. (1995). Bed and suspended load measurements, slope and channel processes in a high altitude alpine torrent. *3rd International workshop on gravel-bed rivers*, 21-26 August 1995, Gold Bar, Washington, USA.

Bowman, D. (1977). Stepped-bed morphology in arid gravelly channels. *Geol. Soc. Am. Bull.*, 88: 291-298.

Bray, D.I. (1979). Estimating average velocity in gravel-bed rivers. *J. Am. Soc. Civ. Eng. Hydraul. Div.*, 105: 1103-1122.

Chadwick, A.J. and Morfett, J.C. (1986). Hydraulics in civil engineering. Allen and Unwin, London.

Chin, A. (1989). Step pools in stream channels. *Prog. in Phy. Geog.*, 13: 391-407.

Church, M. (1975). Electrochemical and flurometric tracer techniques for streamflow measurements. *BGRG Tech. Bull.*, 12, 72pp.

Church, M., Wolcott, J. and Maizels, J. (1990). Palaeovelocity: a parsimonious proposal. *Earth Surf. Proc. and Land.*, 15: 475-480.

Coleman, N.L. (1967). A theoretical and experimental study of drag and lift forces acting on a sphere resting on a hypothetical streambed. *Proceedings of the International Association of Hydraulic Research*, 3: 185-192.

Davies, T.R.H. and Sutherland, A.J. (1980). Resistance to flow past deformable boundaries. *Earth Surf. Proc.*, 5: 175-179.

Davies, T.R.H. (1980). Bedform spacing and flow resistance. *J. Am. Soc. Civ. Eng. Hydraul. Div.*, 106: 423-433.

Day, T.J. (1976). On the precision of salt dilution gauging. *J. Hydrol.*, 31: 293-306.

de Jong, C. (1992). Measuring changes in micro and macro roughness on mobile gravel beds. in Erosion and sediment transport monitoring programmes in river basins *IAHS Publ.* 210: 31-40.

El Khashab, A.M. (1986). Form drag resistance of two dimensional stepped steep open channels. *Canadian Journal of Civil Engineering*, 13: 523-527.

Elder, K., Kattelmann, R. and Ferguson, R. (1990). Refinements in dilution gauging for mountain streams. In: Lang, H and Musy, A (Ed.), Hydrology in Mountainous Regions, *IAHS-AIHS Publ.* 193, International Association of Hydrological Sciences, Wallingford: 247-254.

Ergenzinger, P. (1992). Riverbed adjustments in a step-pool system: Lainbach, Upper Bavaria. In: Billi, P. et al (Ed.), Dynamics of Gravel-bed rivers. Wiley, Chichester: 415-430.

Fenton, J. and Abbott, J.E. (1977). Initial movement of grains on a stream bed: the effect of relative protrusion. *Proc. Roy. Soc. Lond.*, A352, 523-537.

Ferguson, R.I. (1986). Hydraulics and hydraulic geometry. *Prog. in Phy. Geog.*, 10: 1-31.

Ferguson, R.I. (1994). Critical discharge for entrainment of poorly sorted gravel. *Earth Surf. Proc. and Land.*, 19: 179-186.

Flammer, G.H., Tullis, J.P., Mason, E.S. (1970). Free surface, velocity gradient flow past hemisphere. *J. Am. Soc. Civ. Eng. Hydraul. Div*, 96: 1485-1502.

Gilman, K. (1977). Dilution gauging on the recession limb: 2. The integration method. *Hydrol. Sci. Bull.* 22: 469-481.

Graf, W.H., Cao, H.H.and Suszka, L. (1983). "Hydraulics of steep, mobile-bed channels". *Proc. 20th Congress Intl. Ass. Hydraul. Res.*, Moscow, 7: 301-305.

Grant, G.E. (1994). Hydraulics and sediment transport dynamics controlling step-pool formation in high gradient streams: a flume experiment. In: Ergenzinger, P. and Schmidt, K.-H. (Ed.), Dynamics and Geomorphology of mountain rivers, Lecture notes in Earth Sciences 52, Springer-Verlag, Berlin: 241-250.

Grant, G.E., Swanson, F.J. and Wolman, M.G. (1990). Pattern and origin of stepped bed morphology in high gradient streams, Western Cascades, Oregon. *Geol. Soc. Am. Bull.*, 102: 340-352.

Grant, G.E. (1997). Critical flow constrains flow hydraulics in mobile-bed streams: A new hypothesis. *Wat. Resour Research*, 33: 349-358.

Griffiths, G.A. (1981). Flow resistance in coarse gravel bed rivers. *J. Am. Soc. Civ. Eng. Hydraul. Div.*, 107: 899-918.

Gustavson, T.C. (1974) Sedimentation on gravel outwash fans, Malaspina glacier foreland, Alaska. *J. of Sed. Petrol.*, 44: 374-389.

Hasegawa, K., Mori, A. and Ishikawa, S. (1990). Bed topographies and sediment transport during flood in mountainous rivers. In: White, W.R. (Ed.), International conference on river flood hydraulics: 327-336.

Heede, B.H. (1981). Dynamics of selected mountain streams in the Western United States of America. *Zeitschrift fur Geomorphology*, 25: 17-32.

Henderson, F. M. (1966). Open Channel Flow. Macmillan.

Hey, R.D. (1979). Flow resistance in gravel bed rivers. *J. Am. Soc. Civ. Eng. Hydraul. Div.*, 105: 365-379.

Iseya, F., and Ikeda, H. (1987). Pulsations in bedload transport rates induced by a longitudinal sediment sorting: a flume study using sand and gravel mixtures. *Geografiska Annaler* A(1) 69: 15-27.

Jarrett, R.D. (1984). Hydraulics of high gradient streams. *J. Am. Soc. Civ. Eng. Hydraul. Div.*, 110: 1519-1539.

Jarrett, R.D. (1988). Hydraulics and sediment transport in high gradient streams. *EOS*, 69: 1217.

Judd, H.E. (1964). A study of bed characteristics in relation to flow in rough, high-gradient, natural streams. Dissertation, presented to Utah State University, Logan, Utah in partial fulfilment of the requirements for the degree of Doctor of Philosophy.

Judd, H.E. and Peterson, D.F. (1969). Hydraulics of large bed element channels. Rep. PRWG 17-6, Utah Wat. Res. Lab., Utah State University, Logan, Utah.

Kellerhals, R. (1970). Runoff routing through steep natural channels. *J. Am. Soc. Civ. Eng. Hydraul. Div.*, 96: 2201-2217.

Kellerhals, R. (1972). Hydraulic performance of steep natural channels. In: Slaymaker,O and McPherson, H.J. (Ed.) Mountain Geomorphology: 131-140.

Kennedy, J.F. (1963). The mechanics of dunes and antidunes in erodible-bed channels. *J. of Fluid Mech.*, 16: 521-544.

Keulegan, G.H. (1938). Laws of turbulent flow in open channels. *Journal of Research of the National Bureau of Standards*, 21, Research Paper RP1151: 707-741.

Kite, G. (1993). Computerized streamflow measurement using slug injection. *Hydrol. Proc.*, 7: 227-233.

Knighton, D. (1984). Fluvial Forms and Processes. Edward Arnold, London.

Koster, E.H. (1978). Transverse ribs: their characteristics, origin, and paleohydraulic significance. In: Miall, A. (Ed.) Fluvial Sedimentology. Canadian Society of Petroleum Geologists, Calgary, Alberta: 161-186.

Leeder, M.R. (1982). Sedimentology: Process and Product. Harper Collins, London.

Li, R-M and Simons, D.B. (1982). Geomorphological and hydraulic analysis of mountain streams. In: Hey, R.D. et al (Ed.) Gravel-bed rivers. Wiley, Chichester: 425-442.

Lisle, T.E. (1986). Stabilization of a gravel channel by large streamside obstructions and bedrock bends, Jacoby Creek, northwestern California. *Geol. Soc. Am. Bull.* 999-1011.

Lisle, T.E. (1987). Channel morphology and sediment transport in steepland streams. In: Beschta, R.L. (Ed.) Erosion and sedimentation in the Pacific Rim, *IAHS Publ.* 165: 287-298.

Marchant, J.P., Jarrett, R.D. and Jones, L.L. (1984). Velocity profile, water-surface slope and bed material size for selected streams in Colorado. *Open-File Rep.* 84-773, U.S. Geological Survey, Washington, D.C.

McDonald, B.C. and Banerjee, I. (1971). Sediments and bed forms on a braided outwash plain. *Canadian Journal of Earth Sciences*, 8:1282-1301.

Middleton, G.V.(1965). Antidune cross-bedding in a large flume. *J. of Sed. Petrol.*, 35: 922-929

Montgomery, D.R., Buffington, J.M., Smith, R.D., Schmidt, K.M. and Pess, G. (1995) Pool spacing in forest channels. *Wat. Resour. Res.*, 31: 1097-1105

Newson, M.D. and Harrison, J.G. (1978). Channel studies in the Plynlimon experimental catchments. *Institute of Hydrology Report*, 47.

Nikuradse, J. (1933). Stromungsgesetze in rauhen Rohrne. VDI-Forschungsheft 361. (English translation: Laws of flow in rough pipes, NACA Tech. Memo, 1292, Natl. Advis. Comm. For Aeron., Washington D.C., 1950).

Noori, B.M.A. (1984). Form drag of two dimensional stepped steep open channel. In: Smith, K.V.H (Ed.), Proceedings of the 1st International Conference on Hydraulic Design in water resources Engineering, channels and channel control structures, Southampton, UK, Springer-Verlag, Berlin: 1133-1147.

Nowell, A.R.M. and Church, M. (1979). Turbulent flow in a depth-limited boundary layer. *Journal of Geophysical Research*, 84: 4816-4824.

Parker, G. and Klingeman, P.C. (1982). On why gravel bed streams are paved. *Wat. Resour. Res*. 18: 1409-1423.

Peterson, D.F. and Mohanty, P.K. (1960). Flume studies of flow in steep, rough channels. *J. Am. Soc. Civ. Eng. Hydraul. Div.*, 86: 55-76.

Ranga Raju, K.G. and Garde, R.J. (1970). Resistance to flow over two-dimensional strip roughness. *J. Am. Soc. Civ. Eng. Hydraul. Div.*, 96: 815-834.

Rattray, M. Jr and Mitsuda, E. (1974). Theoretical analysis of conditions in a salt wedge. *Estuarine Coastal Mar. Sci.*, 2: 373-394.

Rouse, H. (1965). Critical analysis of open-channel resistance. *J. Am. Soc. Civ. Eng. Hydraul. Div.*, 91: 1-26.

Schlichting, H. (1979). Boundary-layer theory. McGraw-Hill, New York.

Schmidt, K-H. and Ergenzinger, P. (1992). Bedload entrainment, travel lengths, step lengths, rest periods - studied with passive (iron, magnetic) and active (radio) tracer methods. *Earth Surf. Land. and Proc.*, 17: 147-165.

Schoklitsch, A. (1962). Handbuch des Wasserbaues, Springer, Wien.

Shaw, J. and Kellerhals, R. (1977). Paleohydraulic interpretation of antidune bedforms with applications to antidunes in gravel. *J. Sed. Petrol.*, 47 (1): 257-266.

Shields, A. (1936). Application of the theory of similarity and turbulent research to the bed load movement. *Mitt. Preuss. Vers. Wasser Schiff*, 26.

Shields, A. (1936). Application of the theory of similarity and turbulent research to the bed load movement. *Mitt. Preuss. Vers. Wasser Schiff*, 26.

Smart, J.M. and Jaeggi, M.N.R. (1983). Sediment transport on steep slopes. Mitteil. 64, Versuchsanstalt fur Wasserbau, Hydrologie und Glaziologie, ETH-Zurig, Switzerland.

Smart, G.M. (1984). Sediment transport formula for steep channels. *J. Am. Soc. Civ. Eng. Hydraul. Div.*, 110: 267-276.

Thompson, S.M. and Campbell, P.L. (1979). Hydraulics of a large channel paved with boulders. *J. Hyd. Res.*, 17: 341-354.

Warbuton, J. (1992). Channel bed changes in a proglacial mountain stream. *Arctic and Alpine research*, 24: 195-203.

Whiting, P.J., Dietrich, W.E. and Leopold, L.B. (1988). Bedload sheets in heterogeneous sediment. *Geology*, 16: 105-108.

Whittaker, J.C. and Jaeggi, M.N.R. (1982). Origin of step-pool systems in mountain streams. *J. Am. Soc. Civ. Eng. Hydraul. Div.*, 108: 758-773.

Whittaker, J.G. (1987a). Sediment transport in step-pool streams. In: Thorne, C.R. et al (Ed.) Sediment Transport in gravel bed rivers. Wiley, Chichester: 545-579.

Whittaker, J.G. (1987b). Modelling bed-load transport in steep mountain streams. In: Beschta, R.L. et al (Ed.) Erosion and Sedimentation in Pacific Rim. *IAHS Publ.* 165: 319-332.

Wiberg, P.L. and Smith, J.D. (1991). Velocity distribution and bed roughness in high-gradient streams. *Wat. Resour. Res.*, 27: 825-838.

Wiberg, P.L. and Smith, J.D. (1987). Initial motion of coarse sediment in streams of high gradient. In: Beschta,R.L. (Ed.), Erosion and Sedimentation in Pacific Rim . *IAHS Publ.*, 165: 299-308.

Wohl, E.E. and Grodek, T. (1994). Channel bed-steps along Nahal Yael, Negev Desert, Israel. *Geomorphology*, 9: 117-126.

Wohl, E.E., Anthony, D.J., Madsen, S.W. and Thompson, D.M. (1996). A comparison of surface sampling methods for coarse fluvial sediments. *Wat. Resour. Res.*, 32: 3219-3226.

Wohl, E., Madsen, S. and MacDonald, L. (1997). Characteristics of log and clast bed-steps in step-pool streams of northwestern Montana, USA. *Geomorphology*, 20: 1-10.

Yalin, M.S. (1992). River mechanics. Pergamon Press, Oxford.

Appendix 1
Reconnaissance survey sheet

Date: Stream Name: Flow:

Stream Characteristics:			**Reach:**		
Reach length (m)			Steps and pools(%)		
Width (m): 20th			Waterfalls (m)		
19th			Rapids (m)		
21st			Bends (no.)		
Slope: Clinometer			Other		
From map					
Max depth: steps (cm)					
Max depth: pools (cm)					
Sediment Characteristics:			**Site Characteristics:**		
Dmax(cm): 0-50			Distance from car		
50-75			Easy access?		
75-100					
100-125					
125-150			Photo number		
>150			Grid Reference		
Steps (number):					
Alluvial					
Bedrock					
Logs/wood present?					
Step Features:					
Spacing to 21st (m)					
Spacing to 19th (m)					
Oblique steps?					
Partial steps?					

Appendix 2
Fieldsite location map

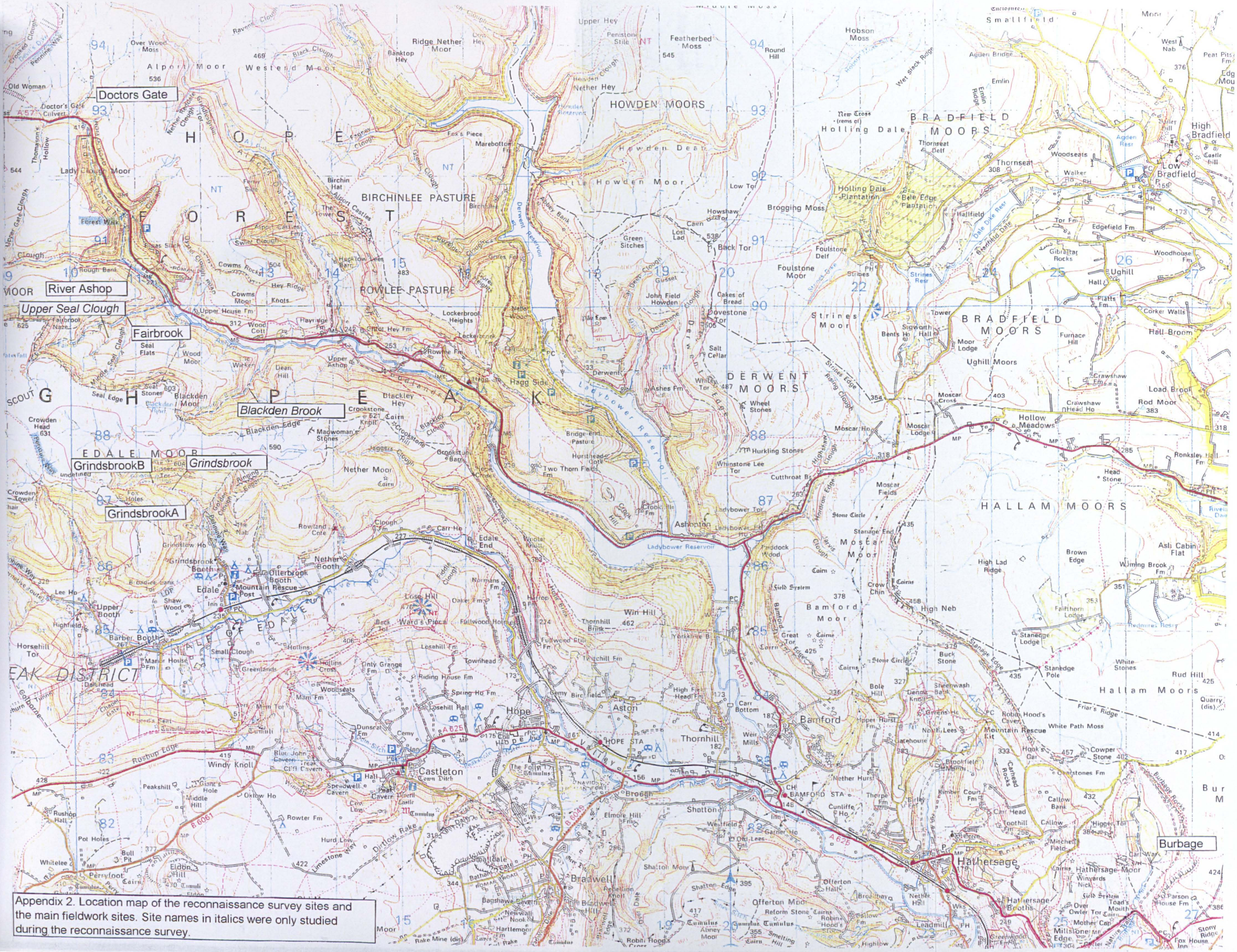

Appendix 2. Location map of the reconnaissance survey sites and the main fieldwork sites. Site names in italics were only studied during the reconnaissance survey.

Appendix 3
Reconnaissance survey data

Stream name	Bedrock steps (%)	Step water depth (m)	Pool water depth (m)	Step height (m)	Step Dmax (cm)	Oblique steps?	Partial steps?
Blackden	20	0.05	0.22	0.42	125-150	Y	Y
Blackden	30	0.04	0.13	0.33	75-100	Y	N
Blackden	15	0.1	0.33	0.53	50-75	Y	N
Blackden	5	0.08	0.23	0.43	0-50	N	Y
Blackden	25	0.1	0.14	0.34	50-75	Y	Y
Blackden	30	0.12	0.26	0.46	100-125	N	Y
Fairbrook	0	0.06	0.32	0.51	100-125	Y	Y
Fairbrook	0	0.05	0.17	0.45	75-100	Y	N
Fairbrook	40	0.05	0.24	0.45	100-125	Y	Y
Fairbrook	25	0.1	0.27	0.50	75-100	Y	Y
Fairbrook	25	0.09	0.16	0.42	100-125	Y	N
Fairbrook	25	0.03	0.26	0.55	>150	N	N
Fairbrook	15	0.05	0.18	0.38	50-75	N	Y
Upper Seal Clough	60	0.05	0.15	0.35	50-75	Y	N
Grindsbrook	0	0.01	0.17	0.42	75-100	N	N
Grindsbrook	30	0.03	0.16	0.40	50-75	Y	Y
Grindsbrook	10	0.02	0.23	0.53	100-125	Y	N
Grindsbrook	5	0.02	0.31	0.58	75-100	Y	N
Grindsbrook	30	0.05	0.26	0.61	125-150	Y	N
Grindsbrook	25	0.02	0.3	0.68	75-100	Y	N
Grindsbrook	20	0.04	0.17	0.43	50-75	N	N
River Ashop	0	0.04	0.03	0.25	75-100	Y	Y
River Ashop	0	0.36	0.45	0.60	50-75	Y	N
River Ashop	0	0.02	0.35	0.58	50-75	Y	N
Doctors Gate	0	0.01	0.07	0.34	50-75	N	N
Burbage	10	0.03	0.25	0.47	100-125	Y	N
Burbage	10	0.05	0.39	0.55	100-125	N	N
Burbage	0	0.08	0.4	0.52	100-125	Y	N
Burbage	10	0.03	0.14	0.31	>150	Y	N
Burbage	25	0.04	0.18	0.41	75-100	Y	N

Stream name	Channel width (m)	Av. step spacing (m) (asp)	asp / width	Measured step spacing (m) (msp)	msp / width
Blackden	1.93	3.43	1.77	6.55	3.39
Blackden	1.50	3.21	2.14	4.55	3.03
Blackden	1.97	6.58	3.35	6.75	3.43
Blackden	1.88	4.47	2.38	3.75	1.99
Blackden	1.93	4.63	2.40	3.15	1.63
Blackden	1.25	5.00	4.00	5.80	4.64
Fairbrook	2.88	5.16	1.79	5.55	1.93
Fairbrook	2.82	6.58	2.34	7.60	2.70
Fairbrook	2.75	4.76	1.73	4.68	1.70
Fairbrook	2.03	6.66	3.27	5.75	2.83
Fairbrook	2.93	7.16	2.44	3.15	1.07
Fairbrook	2.45	7.79	3.18	6.95	2.84
Fairbrook	1.65	6.84	4.15	6.55	3.97
Upper Seal Clough	0.85	3.33	3.92	5.18	6.09
Grindsbrook	3.92	5.39	1.38	2.90	0.74
Grindsbrook	2.81	6.10	2.17	3.30	1.17
Grindsbrook	1.81	4.38	2.42	3.38	1.86
Grindsbrook	3.88	5.01	1.29	3.85	0.99
Grindsbrook	1.98	6.00	3.03	7.45	3.76
Grindsbrook	2.96	6.55	2.21	3.50	1.18
Grindsbrook	2.83	5.56	1.96	2.05	0.72
River Ashop	4.78	12.18	2.55	9.05	1.89
River Ashop	4.68	14.42	3.08	24.48	5.23
River Ashop	4.08	16.92	4.14	14.78	3.62
Doctors Gate	0.86	5.14	6.00	2.45	2.86
Burbage	2.94	10.79	3.67	4.15	1.41
Burbage	3.98	5.61	1.41	6.35	1.59
Burbage	3.07	9.47	3.09	5.68	1.85
Burbage	2.73	16.63	6.09	5.80	2.12
Burbage	3.59	19.05	5.31	8.10	2.26

Stream name	Step number	Reach length (m)	Waterfalls and rapids (m)	Pools and riffles (m)	Adjusted reach length (m)	Gradient
Blackden	15	58	10	0	48	0.105
Blackden	15	61	16	0	45	0.141
Blackden	20	125	0	0	125	0.132
Blackden	20	85	0	0	85	0.176
Blackden	20	88	0	0	88	0.132
Blackden	20	115	20	0	95	0.096
Fairbrook	20	98	0	0	98	0.052
Fairbrook	20	125	0	0	125	0.035
Fairbrook	20	100.5	10	0	90.5	0.052
Fairbrook	20	141.5	15	0	126.5	0.061
Fairbrook	20	155	19	0	136	0.061
Fairbrook	20	200	52	0	148	0.061
Fairbrook	20	165	35	0	130	0.079
Upper Seal Clough	10	57	27	0	30	0.123
Grindsbrook	20	102.5	0	0	102.5	0.052
Grindsbrook	20	119.9	4	0	115.9	0.079
Grindsbrook	20	87.2	4	0	83.2	0.070
Grindsbrook	20	95.2	0	0	95.2	0.070
Grindsbrook	20	140	26	0	114	0.087
Grindsbrook	20	144.5	20	0	124.5	0.105
Grindsbrook	10	86	36	0	50	0.149
River Ashop	20	250.5	19	0	231.5	0.035
River Ashop	20	274	0	0	274	0.026
River Ashop	10	152.25	0	0	152.25	0.035
Doctors Gate	20	97.7	0	0	97.7	0.070
Burbage	20	228	4	19	205	0.105
Burbage	20	112.5	0	6	106.5	0.167
Burbage	20	200	0	20	180	0.044
Burbage	20	316	0	0	316	0.035
Burbage	20	362	0	0	362	0.070

Appendix 4
Field and flume data

Site	Discharge $m^3 s^{-1}$	Velocity $m s^{-1}$	Width m	Depth m	Friction factor	Relative roughness	Froude number
Ashop	0.175	0.256	4.33	0.16	4.7	1.11	0.21
Ashop	0.032	0.057	2.81	0.20	109.6	0.88	0.04
Ashop	0.042	0.086	3.53	0.14	36.3	1.26	0.08
Ashop	0.050	0.124	3.21	0.13	15.9	1.39	0.12
Ashop	0.046	0.116	3.15	0.13	18.2	1.39	0.11
Ashop	0.081	0.121	3.73	0.18	23.7	0.97	0.09
Ashop	0.056	0.090	3.44	0.18	41.8	0.97	0.07
Ashop	0.028	0.083	2.89	0.12	32.3	1.52	0.08
Ashop	0.528	0.517	5.12	0.20	1.4	0.88	0.38
Ashop	0.228	0.345	4.66	0.14	2.3	1.24	0.30
Ashop	0.416	0.421	5.12	0.19	2.1	0.91	0.32
Burbage	0.190	0.317	2.76	0.22	14.2	0.78	0.23
Burbage	0.011	0.062	1.73	0.10	175.9	1.69	0.07
Burbage	0.031	0.140	1.96	0.11	39.2	1.51	0.14
Burbage	0.005	0.045	1.25	0.09	294.8	1.90	0.05
Burbage	0.008	0.060	1.53	0.09	160.3	1.98	0.07
Burbage	0.009	0.074	1.65	0.08	98.2	2.20	0.09
Burbage	0.006	0.056	1.41	0.08	172.4	2.12	0.07
Burbage	0.005	0.046	1.34	0.08	250.9	2.17	0.06
Doctor's Gate	0.002	0.055	0.91	0.04	59.0	1.99	0.09
Doctor's Gate	0.036	0.230	1.29	0.12	8.8	0.72	0.23
Doctor's Gate	0.002	0.037	0.73	0.06	181.9	1.38	0.05
Doctor's Gate	0.079	0.456	1.61	0.11	2.1	0.80	0.47
Doctor's Gate	0.001	0.041	0.71	0.05	117.5	1.78	0.06
Doctor's Gate	0.002	0.044	0.79	0.07	135.7	1.28	0.06
Doctor's Gate	0.004	0.079	0.88	0.06	36.0	1.55	0.11
Doctor's Gate	0.001	0.028	0.66	0.08	362.7	1.15	0.04
Doctor's Gate	0.036	0.284	1.40	0.09	4.6	0.95	0.32
Doctor's Gate	0.035	0.286	1.40	0.09	4.5	0.95	0.32
Doctor's Gate	0.013	0.134	1.16	0.09	19.1	1.01	0.16
Doctor's Gate	0.014	0.133	1.16	0.09	20.1	0.96	0.15
Fairbrook	0.059	0.129	2.71	0.17	47.4	0.61	0.11
Fairbrook	0.077	0.189	2.71	0.15	19.7	0.68	0.16
Fairbrook	0.054	0.146	2.68	0.14	30.5	0.74	0.13
Fairbrook	0.047	0.156	2.61	0.11	22.6	0.90	0.15
Fairbrook	0.046	0.193	2.47	0.10	12.4	1.07	0.21
Fairbrook	0.052	0.135	2.65	0.15	37.6	0.70	0.12
Fairbrook	0.058	0.136	2.67	0.16	40.0	0.64	0.11
Fairbrook	0.038	0.106	2.51	0.14	58.7	0.72	0.09
Fairbrook	0.280	0.582	3.08	0.16	2.2	0.66	0.49
Fairbrook	0.136	0.286	2.98	0.16	9.2	0.64	0.24
Fairbrook	0.281	0.622	3.08	0.15	1.8	0.70	0.54
GrindsbrookA	0.035	0.090	3.05	0.13	143.1	1.60	0.08
GrindsbrookA	0.020	0.095	2.32	0.10	102.8	2.00	0.10
GrindsbrookA	0.020	0.096	2.32	0.10	99.2	2.00	0.10
GrindsbrookA	0.022	0.091	2.32	0.10	111.1	2.00	0.10
GrindsbrookA	0.056	0.159	3.06	0.12	41.9	1.76	0.15
GrindsbrookA	0.017	0.092	2.14	0.08	91.4	2.42	0.10
GrindsbrookA	0.014	0.080	2.09	0.08	121.2	2.40	0.09
GrindsbrookA	0.017	0.077	2.14	0.10	155.1	1.97	0.08
GrindsbrookA	0.015	0.080	2.08	0.09	125.8	2.29	0.09
GrindsbrookA	0.120	0.212	3.37	0.17	33.3	1.22	0.17

GrindsbrookA	0.302	0.325	3.37	0.28	22.1	0.74	0.21
GrindsbrookA	0.349	0.330	3.37	0.31	23.9	0.65	0.20
GrindsbrookA	0.239	0.288	3.37	0.25	25.4	0.83	0.20
GrindsbrookB	0.016	0.033	1.76	0.28	2759.7	0.66	0.02
GrindsbrookB	0.016	0.030	1.53	0.34	3682.3	0.82	0.02
GrindsbrookB	0.036	0.057	2.07	0.30	1053.7	0.73	0.04
GrindsbrookB	0.016	0.025	1.57	0.41	6416.8	0.99	0.02
GrindsbrookB	0.015	0.037	1.71	0.24	1927.0	0.58	0.03
GrindsbrookB	0.013	0.031	1.66	0.26	3070.3	0.63	0.02
GrindsbrookB	0.015	0.022	1.64	0.42	8522.7	1.01	0.01
GrindsbrookB	0.015	0.029	1.64	0.31	3889.6	0.75	0.02
GrindsbrookB	0.064	0.054	2.38	0.50	1760.9	1.21	0.03
GrindsbrookB	0.296	0.235	2.59	0.49	92.3	1.17	0.13
GrindsbrookB	0.303	0.229	2.59	0.51	100.3	1.23	0.12
GrindsbrookB	0.137	0.172	2.59	0.31	120.8	0.74	0.11
GrindsbrookB	0.149	0.146	2.59	0.39	204.1	0.95	0.08
Flume	0.0018	0.224	0.3	0.028	2.18	0.76	0.43
Flume	0.0035	0.357	0.3	0.033	1.21	0.71	0.63
Flume	0.0041	0.366	0.3	0.037	0.99	0.7	0.6
Flume	0.005	0.402	0.3	0.041	0.86	0.68	0.63
Flume	0.005	0.396	0.3	0.042	0.97	0.67	0.61
Flume	0.007	0.54	0.3	0.044	0.56	0.67	0.82
Flume	0.008	0.545	0.3	0.049	0.55	0.65	0.79
Flume	0.009	0.535	0.3	0.055	0.6	0.61	0.73
Flume	0.01	0.662	0.3	0.051	0.46	0.61	0.94
Flume	0.011	0.673	0.3	0.055	0.42	0.61	0.92
Flume	0.011	0.653	0.3	0.056	0.42	0.61	0.88
Flume	0.012	0.674	0.3	0.059	0.36	0.59	0.88
Flume	0.012	0.669	0.3	0.06	0.41	0.6	0.87

Appendix 5
Flume data

	Run date	Slope	Discharge $m^3 s^{-1}$	Velocity $m s^{-1}$	depth m	variance m	Rel. rough.	Friction factor	Froude number
Before steps	03/12/96	0.0588	0.012	0.659	0.061	0.0094	0.60	0.46	0.85
	16/01/97	0.0556	0.005	0.423	0.039	0.0266	0.70	0.76	0.69
	16/01/97	0.0556	0.012	0.697	0.057	0.0266	0.62	0.37	0.93
	28/01/97	0.0625	0.007	0.534	0.044	0.0100	0.67	0.60	0.81
	28/01/97	0.0625	0.011	0.666	0.055	0.0100	0.63	0.44	0.91
	06/02/97	0.0588	0.0041	0.389	0.036	0.0110	0.71	0.96	0.66
	06/02/97	0.0588	0.008	0.563	0.048	0.0110	0.65	0.55	0.82
	06/02/97	0.0588	0.011	0.666	0.055	0.0110	0.63	0.42	0.91
	06/03/97	0.0560	0.00183	0.226	0.027	0.0088	0.77	1.95	0.44
	06/03/97	0.0563	0.005	0.450	0.037	0.0088	0.71	0.65	0.75
	06/03/97	0.0564	0.009	0.583	0.051	0.0088	0.63	0.50	0.82
	25/02/97	0.0667	0.00346	0.357	0.033	0.0093	0.73	1.15	0.63
	25/02/97	0.0667	0.01	0.621	0.054	0.0093	0.64	0.56	0.85
After run	03/12/96	0.0491	0.012	0.674	0.059	0.0139	0.59	0.36	0.88
	16/01/97	0.0546	0.005	0.402	0.041	0.0096	0.68	0.86	0.63
	16/01/97	0.0546	0.012	0.669	0.060	0.0096	0.60	0.41	0.87
	28/01/97	0.0590	0.007	0.540	0.044	0.0141	0.67	0.56	0.82
	28/01/97	0.0590	0.011	0.673	0.055	0.0141	0.61	0.42	0.92
	06/02/97	0.0554	0.0041	0.366	0.037	0.0139	0.70	0.99	0.60
	06/02/97	0.0554	0.008	0.545	0.049	0.0139	0.65	0.54	0.79
	06/02/97	0.0553	0.011	0.653	0.056	0.0139	0.61	0.42	0.88
	06/03/97	0.0560	0.00183	0.224	0.028	0.0175	0.76	2.17	0.43
	06/03/97	0.0563	0.005	0.396	0.042	0.0175	0.67	0.97	0.61
	06/03/97	0.0562	0.009	0.535	0.055	0.0175	0.61	0.60	0.73
	25/02/97	0.0657	0.00346	0.357	0.033	0.0157	0.71	1.21	0.63
	25/02/97	0.0660	0.01	0.662	0.051	0.0157	0.61	0.46	0.94